HETEROPHILIC INTERACTION BETWEEN BCH DOMAINS OF BNIP-2 AND BPGAP1 REGULATES RHOA SIGNALING

CHIN FEI LI JASMINE

NATIONAL UNIVERSITY OF SINGAPORE

2011

HETEROPHILIC INTERACTION BETWEEN BCH DOMAINS OF BNIP-2 AND BPGAP1 REGULATES RHOA SIGNALING

CHIN FEI LI JASMINE

(B.Sc. (Life Sciences) (Hons.), National University of Singapore)

A THESIS SUBMITTED

FOR THE DEGREE OF DOCTOR OF PHILOSOPHY

DEPARTMENT OF BIOLOGICAL SCIENCES

NATIONAL UNIVERSITY OF SINGAPORE

2011

ACKNOWLEDGEMENTS

I would like to express my sincere gratitude and appreciation to my supervisor, Associate Professor Low Boon Chuan, for his dedicate supervision and guidance throughout the years of my graduate studies. I sincerely thank him for his patience, knowledge and advice whilst allowing me the room to work in my own way.

I would also like to convey my heartfelt thanks to my mentor, Dr. Zhou Yiting, for his patient guidance as well as imparting to me invaluable knowledge and experimental skills during the course of my research. Special thanks to Dr. Chew Li Li for her generous advice on my project that aid me in overcoming the many hiccups encountered. I deeply appreciate and am grateful to both of them for being so generous with their time.

I am delightful to have worked alongside with members of the laboratory, past and present, including Uncle Zhou (Dr Zhou Yi Ting), Dr Chew Li Li, Dr Soh Jim Kim Unice, Dr Liu Lihui, Tan Jee Hian Allan, Dr Zhong Dan Dan, Dr Aarthi Ravichandran, Dr Sharmy Jennifer James, Dr Pan Qiurong Catherine, Chew Ti Weng, Kenny Lim Gim Keat, Pearl Toh Pei Chern, Denise Wong Ming Zhi, Dr Anjali Bansal Gupta, Archna Ravi, Shelly Kaushik, Sun Jichao, Huang Lu, Akila Surendran and Zhang Zhenghua. Many thanks for all the support and help, not forgetting of course the countless moments of fun and laughter. I would also like to specially thank Guo Kunyao Alvin for helping me always in whatever ways possible.

I hereby acknowledge National University of Singapore for awarding me four years of research scholarship.

Above all, I owe my dearest thanks to my parents for their unconditional love, encouragement and kind understanding always. I am truly indebted to my family and friends who have walked me through the trying period of my life.

Thank you all very much.

Chin Fei Li Jasmine

TABLES OF CONTENTS

SUMMARY

BPGAP1 (BNIP-2 and Cdc42GAP Homology [BCH] domain-containing, Proline-rich and Cdc42GAP-like protein 1) is a multi-domain GTPase-activating protein (GAP) that exerts catalytic activity specifically towards RhoA. By coordinating induction of morphological changes via BCH and GAP domains, and translocation of cortactin to cell periphery through the proline-rich region, BPGAP1 functions to promote cell migration. Interaction of this RhoGAP protein with EEN/endophilin II through also its proline-rich region further enhances EGF receptor endocytosis upon EGF stimulation, thereby activating ERK1/2 signaling.

Apart from mediating cellular functions, association of BPGAP1 with other interacting partners could also serve regulatory purposes. For instance, release of auto-inhibition within BPGAP1 by active MEK2 that targets the proline-rich region allows Pin1 to suppress BPGAP1-induced acute ERK activation, and promote attenuation of Rho signaling. On-going research on BPGAP1 interacting partners identified in proteomics pull-down further reveal that both SmgGDS and human LanCL1 negatively regulate the effect of BPGAP1 on Ras activation. In earlier work, BNIP-2 (Bcl-2 and E1B Nineteen kDa Interacting Protein-2) has been shown to interact with BPGAP1. However, the significance of their interaction has yet to be uncovered.

To elucidate the functional significance of BNIP-2-BPGAP1 interaction, BNIP-2 was first confirmed as a *bona fide* interacting partner of BPGAP1 through semi-endogenous immunoprecipitation study. Intriguingly, BNIP-2 BCH domain not only forms heterophilic interaction with the corresponding BCH domain of BPGAP1 but associates also with its GAP module, probably to stabilize the structure of BPGAP1 for its catalytic function. Furthermore, both BNIP-2 and BPGAP1 harbor

Rho binding motifs within their BCH domains that are capable of binding RhoA. Despite both RhoA and BPGAP1 share overlapping interaction sites on BNIP-2 BCH domain, these three proteins could possibly form a triple complex from immunofluorescence study. Interestingly, a greater degree of active RhoA downregulation by BPGAP1 was observed in the presence of BNIP-2, an effect that was no longer evident once the RhoGAP activity of BPGAP1 was abolished with a catalytic inactive mutant. Consistently, this synergistic effect on RhoA inactivation also led to a further loss of stress fiber, an increase in GAP-induced cell rounding, and an overall decrease in cellular proliferation.

Our present study hereby establishes the role of BNIP-2 as a regulator of BPGAP1 that serves to synergistically enhance the RhoGAP activity of BPGAP1 towards RhoA. This effect could possibly be achieved by the relieve of auto-inhibition within BPGAP1 by BNIP-2 through heterophilic interactions of their BCH domains and possible stabilization of the altered conformation via binding to the GAP module to bring about more efficient catalysis of RhoA GTP hydrolysis. These results further substantiate earlier findings of BCH domain as a regulatory module for Rho proteins and their immediate regulators, as well as indicate a possible role as a scaffold.

(449 words)

LIST OF TABLES

LIST OF FIGURES

LIST OF ABBREVIATIONS

Units and Measurements

A	Ampere
bp	basepair
^{o}C	Degree Celsius
Da	Dalton
g	gram
hr	hour
k	kilo
l	liter
m	milli
μ	micro
min	minute
M	Molar
MW	Molecular Weight
n	nano
nm	nanometer
OD	Optical Density
rpm	revolutions per minute
s	second
U	Unit

Others

ADP	Adenosine diphosphate
Arf	ADP-ribosylation factor
Arg	Abl-related gene
APC	Adenomatous polyposis coli
APS	Ammonium persulphate
ARAP1	ArfGAP and RhoGAP with ankyrin repeat and PH domains
ARP2/3	Actin-related proteins 2/3
Asef	APC-stimulated guanine nucleotide exchange factor
BAR	Bin/amphiphysin/Rvs
BCH	BNIP-2 and Cdc42GAP Homology

Bcl	B-cell lymphoma
bHLH	basic helix-loop-helix
BNIP-2	Bcl-2 and E1B Nineteen kDa Interacting Protein 2
BNIP-H	BNIP-2 Homology
BNIP-S	BNIP-2 Similar
BNIP-XL	BNIP-2 extra long
BPGAP1	BCH domain-containing, proline-rich and Cdc42GAP-like protein 1
BrdU	5-bromo-2'-deoxyuridine
Brk	Breast tumor kinase
BSA	Bovine Serum Albumin
CCMB	Calcium/manganese based buffer
Cdc42	Cell division cycle 42
Cdk	Cyclin-dependent kinase
CMV	Cytomegalovirus
CRIB	Cdc42/Rac-Interacting Binding
CZH	CDM and Zizimin Homology
C1	Cysteine-rich phorbol ester
C2	Calcium-dependent lipid binding
DAG	Diacylglycerol
Dbl	Diffuse B-cell lymphoma
DEP	Dishevelled/Egl-10/pleckstrin
DH	Dbl Homology
DHR	Downstream of CRK (Dock) Homology Region
DIC	Differential Interference Contrast
DLC1	Deleted in Liver Cancer 1
DMEM	Dulbecco's Modified Eagle's Medium
DNA	Deoxyribonucleic acid
dNTP	Deoxynucleoside triphosphate
DTT	Dithiothreitol
Duo	Huntingtin-associated protein-interacting protein
ECM	Extracellular matrix
EDTA	Ethylenediaminetetra-acetic acid
EEN	Extra Eleven Nineteen

EGF	Epidermal Growth Factor
EMT	Epithelial to Mensenchymal Transition
ERK	Extracellular signal-regulated kinase
ERM	erzin-radixin-moesin
E2F	E2 promoter binding factor
FGF	Fibroblast Growth Factor
FH	Formin Homology
FRET	Fluorescence Resonance Energy Transfer
GAP	GTPase Activating Protein
GBD	GTP Binding Domain
GDF	GDI Dissociation Factor
GDI	Guanine nucleotide Dissociation Inhibitor
GDP	Guanine nucleotide diphosphate
GEF	Guanine nucleotide Exchange Factor
GFP	Green Fluorescence Protein
GST	Glutathione-S-transferase
GTP	Guanine nucleotide triphosphate
GTPase	Guanosine triphosphatase
HA	Hemagglutinin
HEPES	N-2-hydroxyethylpiperazine-N'-2-2ethanesulfonic acid
HV	Hypervariable
Ig	Immunoglobulin
IP	Immunoprecipitates
IPTG	Isopropyl Thio-β-D-Galactoside
JNK	Jun NH_2-terminal Kinase
LB	Luria-Bertani
Lbc	Lymphoid blast crisis
LIMK	(Lin11, Isl1 and Mec3) Kinase
LMW-PTP	Low molecular weight protein-tyrosine phosphatase
LPA	Lysophosphatidic acid
MAPK	Mitogen-activated protein kinase
MBS	Myosin Binding Subunit
MCS	Multiple cloning sites
MEF	Mouse Embryonic Fibroblast

MEK	MAP kinase kinase
mDia	Mammalian Diaphanous proteins
MgcRacGAP	Male germ cell RacGAP
Miro	Mitochondria Rho
MLCK	(Myosin Light Chain) Kinase
MMP	Metalloproteinase
MOTC	Microtubule-organizing center
M-RIP	Myosin phosphatase-Rho Interacting Protein
Nap1	Nck-associated protein 1
NFκB	Nuclear Factor κB
NF1	Neurofibromatosis type 1
NMR	Nuclear Magnetic Resonance
PAGE	Polyacrylamide Gel Electrophoresis
PAK	p21-associated protein kinase
Par	Partitioning-defective
PBS	Phosphate buffered saline
PCR-SSCP	Polymerase Chain Reaction-single strand conformation polymorphism
PCNA	Proliferating Cell Nuclear Antigen
PD	Pull-down
PDGF	Platelet Derived Growth Factor
PDZ	Post synaptic density protein PSD 95, Discs-Large, ZO-1
PH	Pleckstrin Homology
PIP_2	Phosphatidylinositol-4,5-bisphosphate
PIP_3	Phosphatidylinositol-3,4,5-triphosphate
PI3K	Phosphatidylinositol 3-kinase
PIP5K	Phosphatidylinositol-4-phosphate 5-kinase
PITP	PtdIns transfer protein
PIX	PAK-interacting exchange factor
PKC	Protein Kinase C
PKN	Protein Kinase N
PRC1	Protein Regulating Cytokinesis 1
PS	Phaosphatidylserine
PtdIns	Phosphatidylinositol

PtdCho	Phosphatidylcholine
PTEN	Phosphatase and tensin homolog
PTK	Protein Tyrosine Kinase
PVDF	Polyvinylidene difluoride
RA	Ras association
Rab	Ras-like protein in brain
Rac	Ras-related C3 botulinum toxin substrate
Ran	Ras-like nuclear protein
Ras	Ras sarcoma
RBD	Rho Binding Domain
RIPA	Radio Immunoprecipitation Assay
Rif	Rho in filopodia
Rho	Ras homologous
RhoBTB	Rho Broad complex, Tramtrack and Bric-a-brac
Rnd	Round
ROCK	Rho-associated protein kinase
ROS	Reactive Oxygen Species
RPMI	Roswell Park Memorial Institute
SAM	Sterile Alpha Motif
SDS	Sodium Dodecyl Sulphate
SH	Src Homology
siRNA	small interfering Ribonucleic acid
SRE	Serum Response Element
SRF	Serum Response Factor
PCR-SSCP	PCR-single strand conformation polymorphism
STAT	Signal Transducer and Activation of Transcription
SV40	Simian virus 40
TAE	Tris Acetate EDTA
TEMED	N,N,N’,N’-tetramethylethylenediamine
Tiam1	T-cell lymphoma invasion and metastasis 1
TIMP	Tissue Inhibitors of metalloproteinases
TNFα	Tumor necrosis factor alpha
UV	Ultraviolet
WASP	Wiscott-Aldrich syndrome protein

WAVE	WASP-family Verprolin-homologous protein
WB	Western Blotting
WCL	Whole cell lysate
Wrch	Wnt1-responsive cdc42 homolog

LIST OF SYMBOLS

^{o}	degree
Δ	deletion

Chapter 1

Introduction

1 INTRODUCTION

1.1 The Ras superfamily of small GTPases – Master regulators of cellular dynamics

The Ras (Ras sarcoma) superfamily of monomeric small (20-25 kDa) guanosine triphosphatases (GTPases) are guanosine diphosphate/guanosine triphosphate (GDP/GTP)-regulated proteins (Vetter and Wittinghofer, 2001) that coordinate a diverse array of fundamental cellular processes. These proteins, with a human repertoire of 154 members, are evolutionarily conversed with orthologs present in insects (*Drosophila*), nematodes (*Caenorhabditis elegans*), fungi (*Saccharomyces cerevisiae*; *Schizosaccharomyces pombe*), amoeba (*Dictyostelium discoideum*) and plants (Colicelli, 2004; Wennerberg et al., 2005).

Based on sequence identity, structure and functional similarities (Wennerberg et al., 2005), members of the Ras superfamily have typically been classified into five major subfamilies comprising of Ras, Rho (Ras homologous), Rab (Ras-like proteins in brain), Ran (Ras-like nuclear protein) and Arf (ADP-ribosylation factor). However, this classification is less than definitive due to the lack of functional data especially for the less-studied proteins, thereby leaving some of them unclassified (Wennerberg et al., 2005). In addition, the atypical GTPases Miro (Mitochondria Rho), previously marginally classified under Rho subfamily, are redefined as a distinct subgroup due to the lack of a characteristic Rho insert domain and their distinct phylogenetic origin (Figure 1.1) (Boureux et al., 2007; Wennerberg et al., 2005).

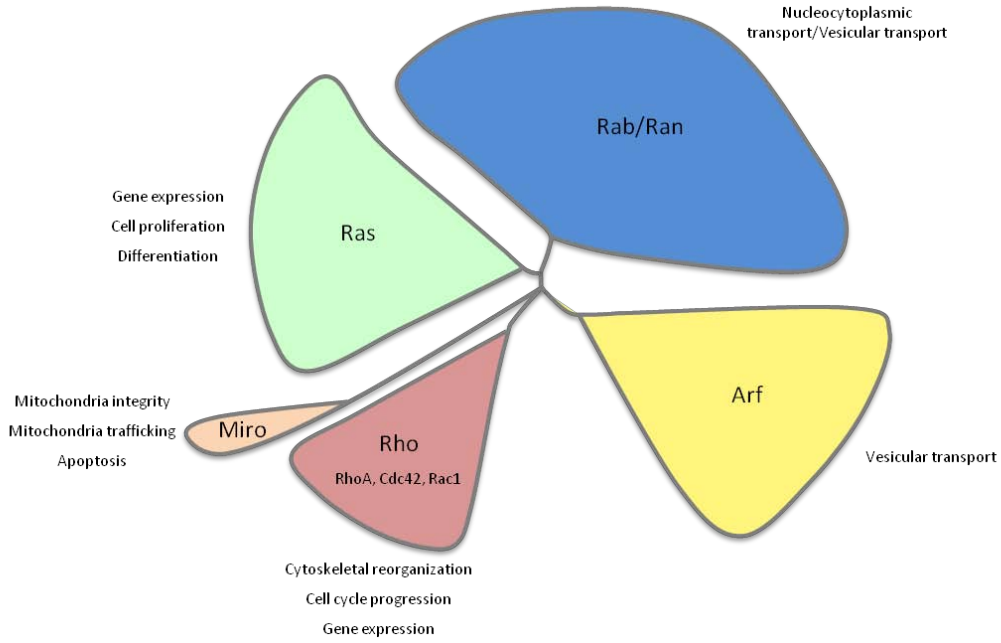

Figure 1.1 The human Ras superfamily of small GTPases. The five major subfamilies are indicated by the coloured branches: Ras (green), Rho (pink), Rab (blue), Ran (blue) and Arf (yellow). Atypical GTPases – Miro (orange), is presented as a separate subgroup from Rho. [Adapted from Colicelli, 2004].

GTPases of the Ras superfamily serve as nucleotide-regulated binary molecular switches through their basic biochemical activity of GTP binding and hydrolysis (Colicelli, 2004; Vetter and Wittinghofer, 2001). This activity is mediated by the conserved ~20 kDa core G domain comprising of five G-box GDP/GTP-binding motifs: G1 [GXXXXGKS/T], G2 [T], G3 [DXXGQ/H/T], G4 [T/NKXD] and G5 [C/SAK/L/T], that bind phosphate and Mg^{2+} or guanine (Bourne et al., 1991; Wennerberg et al., 2005). Within the G domain are two loop regions, Switch I and II, that re-orientate during the GDP/GTP-cycling process. These changes in conformation allow the effectors to bind preferentially to GTP-bound GTPase via the core effector domain (Figure 1.2) (Vigil et al., 2010).

Besides the basic biochemical activity, majority of the small GTPases are also subjected to post-translational modifications by lipids at either the amino-terminal (N-terminal) (for example Arf) or carboxyl-terminal (C-terminal) hypervariable regions of different terminating Cysteine-containing motifs (Ras, Rho, Rab) (Figure 1.2) (Vigil et al., 2010). These modifications are essential for their targeting to distinct membrane compartments and subcellular localizations for interactions with different regulators and effectors (Wennerberg et al., 2005). Together, these properties confer small GTPases the ability to modulate diverse cellular processes such as proliferation (Ras), differentiation (Ras), gene expression (Ras and Rho), cytoskeletal reorganization (Rho), polarity (Rho), nucleocytopasmic transport (Ran) and intracellular vesicle transport and protein trafficking (Rab and Arf).

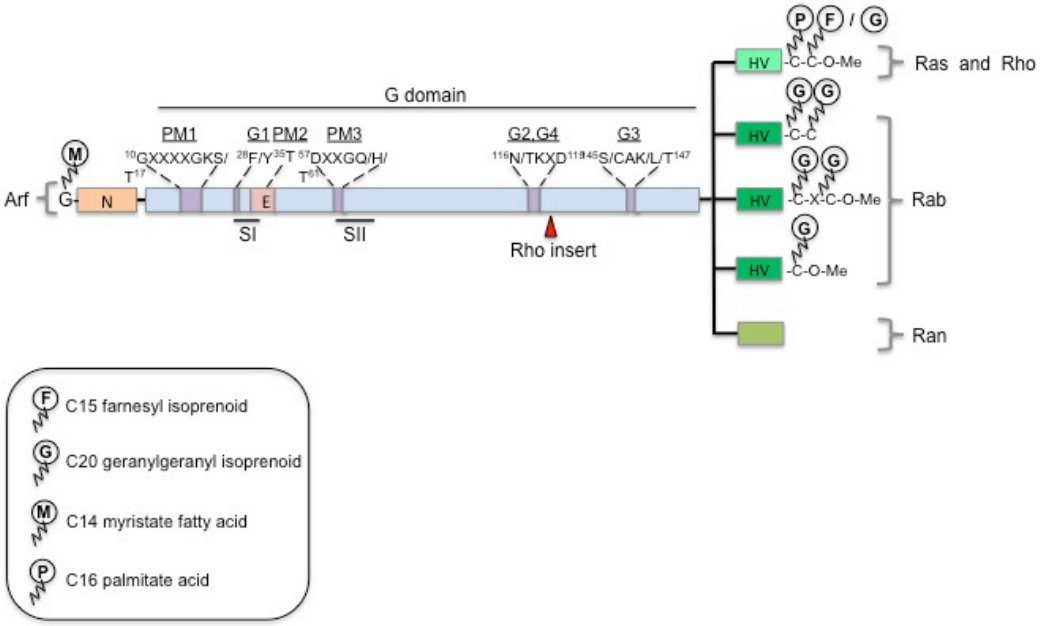

Figure 1.2 Domain architecture of Ras superfamily GTPases. The conserved ~20 kDa core G domain consists of five guanine nucleotide consensus sequence motifs (G boxes). These G boxes bind to phosphate and Mg^{2+} (PM) or guanine (G) as indicated. Switch I (SI; Ras residues 30-38) and switch II (SII; Ras residues 59-76) in the two loop regions undergo conformation changes during the nucleotide cycling process. These re-orientations allow preferential binding of the effectors to the core effector domain in the GTP-bound state (E; Ras residues 32-40). Post-translational lipid modifications (farnesylation or geranylgeranylation and/or palmitoylation of cysteine residues) occur at the C termini hypervariable (HV) regions of Ras, Rho and Ran GTPases. Arf GTPases, on the other hand, have an N-terminal extension that is also myristoylated for some members. These lipid modifications and extensions are essential for membrane targeting and for mediating associations. While Ran GTPases are not lipid modified, they too harbor a C-terminal extension that is required for its function. The 'Rho Insert' sequence of Rho GTPases lies between Ras residues 122 and 123. [Adapted from Vigil et al., 2010].

1.2 The Rho family GTPase – Intermediaries of signaling networks

1.2.1 The Rho family GTPases

The Rho gene was first identified from the sea-slug *Aplysia* in 1985 (Madaule and Axel, 1985) with Rac proposed as the evolutionary founder of the Rho family (Boureux et al., 2007). All members of the Rho family are characterized by a 13-amino acid helical insertion (Rho insert) positioned between G4 and G5 boxes of the canonical G domain (Boureux et al., 2007).

To date, the human Rho GTPase family comprises 20 members and is redefined into eight subfamilies based on primary amino acid sequence identity, structural motifs and biological functions. These subfamilies include Rho-like [RhoA-C], Rac (Ras-related C3 botulinum toxin substrate)-like [Rac1-3; RhoG], Cdc42 (Cell division cycle 42)-like [Cdc42; TC10; TCL], RhoD/RhoF [RhoD; Rif], RhoH, RhoUV [Wrch-1 (Wnt1-responsive cdc42 homologue-1); Chp], Rnd (Round) [Rnd1-3] and RhoBTB (Broad complex, Tramtrack and Bric-a-brac) [RhoBTB1-2] (Boureux et al., 2007; Heasman and Ridley, 2008). In addition, splice isoforms of Rac1 and Cdc42 have been identified (Wennerberg and Der, 2004).

While classical Rho GTPases are subjected to GDP/GTP-regulation, eight proteins within the Rho family exist predominantly in GTP-bound form and are termed atypical Rho GTPases (Figure 1.3) (Heasman and Ridley, 2008; Vega and Ridley, 2008). This exception arises due to either mutations at amino acid residues critical for GTP hydrolysis and GDP binding (for example Rnd proteins and RhoH) or increased nucleotide exchange in the case of Wrch-1 (Aspenstrom et al., 2007; Chardin, 2006; Heasman and Ridley, 2008).

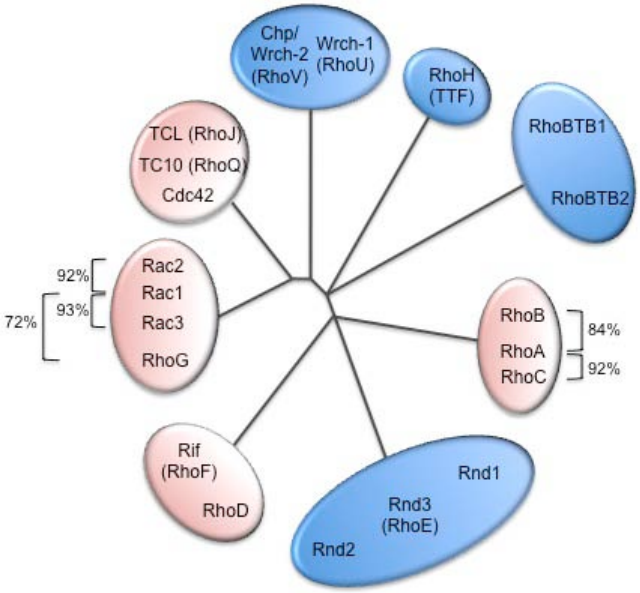

Figure 1.3 The mammalian Rho family GTPases. The 20 Rho GTPase members are categorized into eight subfamilies: Rho-like (RhoA-C), Rac-like (Rac1-3; RhoG); Cdc42-like (Cdc42; TC10; TCL), RhoD/RhoF (RhoD; Rif), RhoH, RhoUV (Chp, Wrch-1), Rnd (Rnd1-3) and RhoBTB (RhoBTB1-2). Classical Rho GTPases (pink) undergo GDP/GTP cycling while the atypical Rho GTPases (blue) are not subjected to this mode of regulation. Amino acid identities between proteins in the same subfamily are the highest for Rho-like and Rac-like subfamilies [Adapted from Heasman and Ridley, 2008].

1.2.2 Rho GTPases function as binary molecular switches

To fulfill the fundamental role as signal transducers, Rho GTPases operate as molecular switches that can be turned on and off. This on/off mechanism is dependent on the nucleotide status of Rho GTPases such that they become active when in GTP-bound state and are inactive when in GDP-bound form (Vetter and Wittinghofer, 2001). The underlying basis of this universal mechanism lies in the conformation changes during GDP/GTP cycling that occur primarily in the two loop regions - Switch I and II (Hakoshima et al., 2003; Wennerberg and Der, 2004). During the exchange of GDP for GTP, hydrogen bonds formed between the γ-phosphate and conserved threonine and glycine residues (Thr^{37}/Gly^{62} in RhoA) in Switch I and II,

respectively (Wei et al., 1997), stabilize the structure of GTPases and thus allows for high affinity binding to downstream effectors. Conversely, such interactions are abolished upon GTP-hydrolysis. Once in the relax state, the switch regions can assume variable structural forms and this reduces the affinity for effector proteins, leading to their rapid dissociations (Colicelli, 2004; Hakoshima et al., 2003).

Although classical Rho GTPases possess high binding affinity for GDP and GTP, they function ineffectively as molecular switches. This is attributed to their slow intrinsic GDP/GTP exchange and GTP hydrolysis activities (Wennerberg et al., 2005). As such, the GDP/GTP cycling process is tightly regulated by three classes of regulatory proteins, namely, guanine nucleotide exchange factors (GEFs), GTPase-activating proteins (GAPs) and guanine nucleotide dissociation inhibitors (GDIs).

In the absence of stimuli, Rho GTPases in GDP-bound form are sequestered in the cytosol by GDIs, hence disallowing any association with the plasma membrane or interaction with regulators. Upon the arrival of a stimulus, this triggers the dissociation of GTPases from the inhibitory complexes. Following their release, these proteins translocate to the plasma membrane where the GEFs catalyze the dissociation of GDP. By virtue of the much higher intracellular GTP concentration, GTP is spontaneously incorporated into the GTPase. Binding of GTP to the GTPase promotes GTPase-effector interaction, thus activating the appropriate downstream signaling. Rho GTPase signaling is attenuated by the recruitment of GAPs that function to inactivate the GTPases by accelerating their intrinsic GTPase activity. Once in the GDP-bound form, these GTPases can no longer interact with the effectors and are sequestered by GDIs till the next activating stimulus (Tcherkezian and Lamarche-Vane, 2007). This GDP/GTP-cycling process is summarized in Figure 1.4.

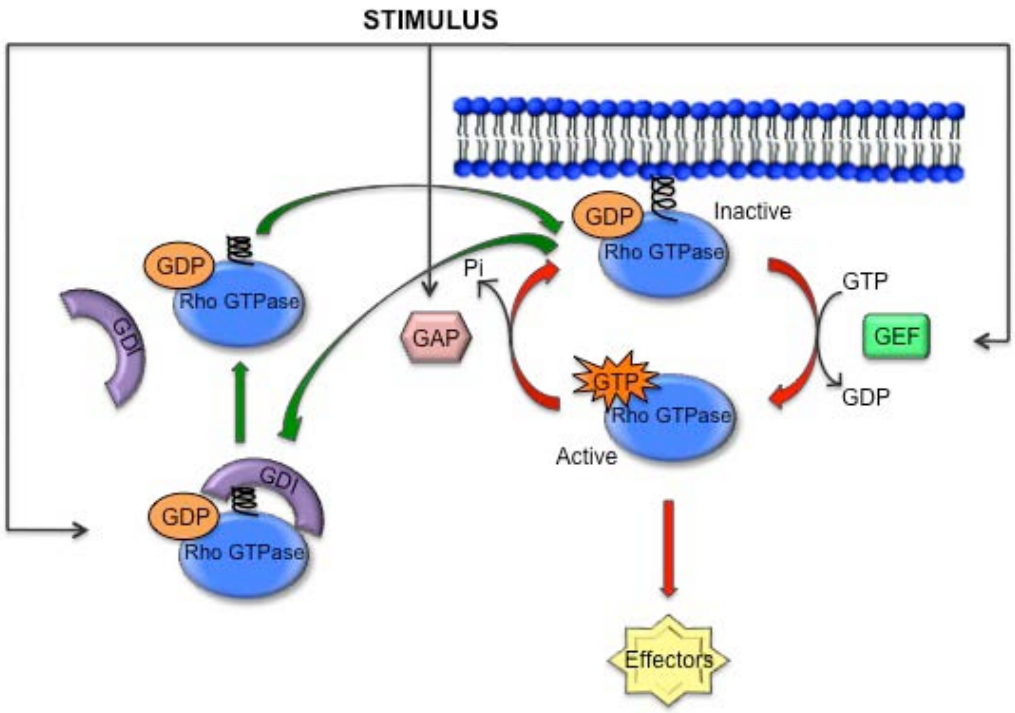

Figure 1.4 The Rho GTPases cycling process. Rho GTPases function as nucleotide-regulated binary switches that exist in either inactive GDP-bound or active GTP-bound state. Three main classes of regulators: GDIs, GEFs and GAPs, orchestrate this cycling process. GDIs serve to sequester and regulate the intracellular location of the GTPases, while GEFs and GAPs function to catalyze the activation (exchange of GDP for GTP) and inactivation (intrinsic GTP hydrolysis) of Rho GTPases, respectively.

1.2.3 Post-translational modification and subcellular targeting of Rho GTPases

Apart from the highly conserved switch apparatus that govern the fundamental GTPase activity, majority of the Rho GTPases are subjected to a series of post-translational modifications characterized by the covalent attachment of a prenyl group to the cysteine residue of the C-terminal CAAX tetrapeptide. The lipid modifications, together with immediate upstream hypervariable regions, mediate associations of Rho GTPases with the membrane and dictate their subcellular localization such as to the plasma membrane or endosomes (Roberts et al., 2008; Wennerberg et al., 2005). Variations in subcellular locations create microenvironments that facilitate

interactions of the Rho GTPases with distinct upstream activators and downstream effectors, thus allowing them to perform their divergent functions (Wennerberg and Der, 2004).

1.2.3.1 Rho GTPase CAAX-dependent post-translational lipid modifications

Of the 20 members in the Rho GTPase family, 16 Rho proteins terminate with the canonical CAAX tetrapeptide motif (where C = cysteine, A = aliphatic amino acid and X = any amino acid) except Wrch-1, Chp/Wrch-2, RhoBTB1 and RhoBTB2 (Roberts et al., 2008). CAAX-dependent post-translational modifications of the Rho GTPases occur in a three-step process beginning with covalent attachment of either a 15-carbon (C15)-farnesyl or a C20-geranylgeranyl isoprenoid to the cysteine residue. Geranylgeranyl attachment predominates among the classical Rho GTPases, whereas majority of the atypical Rho proteins are modified by farnesylation (Roberts et al., 2008).

In general, the lipid moiety added is determined by the identity of the last amino acid residue in the tetrapeptide. Though not exclusive, knowledge derived from previous studies has proposed that Rho GTPase is subjected to farnesylation where X is hydrophobic (Met), polar (Gln) or small (Cys, Ser, Thr or Ala). On the other hand, geranylgeranylation occurs if X is Leu and less specifically for Met, Phe, Ile or Val (Roberts et al., 2008; ten Klooster and Hordijk, 2007). Although the more hydrophobic geranylgeranyl isoprenoid confers a stronger membrane association, there is no evidence of direct translation to any functional distinctions, probably with the exception of RhoB, which is either farnesylated or geranylgeranylated (Michaelson et al., 2001; Wennerberg and Der, 2004).

In subsequent lipid modifications, AXX residues are cleaved from the carboxyl end of the protein, followed by addition of a methyl group to the prenylated cysteine residue. Together, these three modifications increase the overall hydrophobicity of the Rho GTPases and function as a lipid anchor to enable membrane association (Ellenbroek and Collard, 2007; Roberts et al., 2008).

1.2.3.2 Rho GTPase targeting via hypervariable regions

Besides post-translational modifications, all Rho proteins exhibit diverse sequences mainly at their C-termini and this hypervariable region comprises approximately ten amino acid residues that precede the CAAX motif (ten Klooster and Hordijk, 2007). This region may include cysteine residue(s) immediately before the tetrapeptide or is rich in lysine and/or arginine residues (polybasic region) or have a combination of both features. The presence of extra cysteine residue(s) enables another type of lipid modification whereby a palmitate fatty acid is covalently attached to cysteine. This form of lipidation constitutes an additional targeting signal for some Rho family members, for example RhoB and TC10 (Roberts et al., 2008). Palmitoylation of Rho GTPases may also affect recognition and hence their interaction with RhoGDIs (Michaelson et al., 2001).

Apart from subcellular targeting, the hypervariable region may also play a role in enhancing membrane associations by facilitating interaction of the GTPases with acidic membrane-associated lipids through the net positively charged polybasic region (Roberts et al., 2008). In summary, these variations at the C-terminal region allow otherwise highly similar Rho GTPases (eg. Rho-related proteins) to be differentially targeted (ten Klooster and Hordijk, 2007) for interactions with their diverse effectors.

1.2.4 Rho GTPases and their effector proteins

Considering the diversity of cellular functions associated with merely 20 members of the Rho family, it is not surprising that approximately 100 downstream targets have been identified thus far (Hall, 2009). While each Rho GTPase may exhibit binding affinity towards multiple effectors, some effector proteins are recognized by multiple Rho GTPases. Rho GTPase-effector interaction is mediated mainly through Switch I loop region, also known as the effector domain. Specificity in interaction is possible due to differences in amino acid residues at sites critical for interaction. For instance, PKN serine/threonine kinases act downstream of RhoA through interactions at Glu^{40}, Ala^{44} and Asp^{49}, but not Cdc42 with corresponding residues Asp^{38}, Val^{42} and Asp^{47} (Maesaki et al., 1999). Besides Switch I loop region, α-helical Rho insert and sequences outside the effector domain can also contribute to effector binding (Bishop and Hall, 2000; Karnoub et al., 2004).

Most of the effectors of Rho GTPases are either scaffold proteins or kinases such as serine/threonine, tyrosine and lipid kinases (Ellenbroek and Collard, 2007; Jaffe and Hall, 2005). Common serine/threonine kinases include Rho-associated protein kinases (ROCK I and II) and p21-activated kinase (PAK), which activate their target proteins via phosphorylation to initiate the signaling cascades. On the other hand, non-kinase effector proteins such as neuronal Wiscott-Aldrich syndrome protein (N-WASP) function as scaffold proteins to mediate interactions with other proteins (Ellenbroek and Collard, 2007). Commonly, Rho GTPases activate their effectors by disrupting autoinhibition present within these proteins to free up the catalytic or functional domain, thus allowing activation of downstream signaling (Bishop and Hall, 2000; Jaffe and Hall, 2005).

1.2.5 Functions of Rho family GTPases

RhoA, Rac1 and Cdc42 are among all, the three best-characterized mammalian Rho GTPases. Early studies on Rho GTPases have established their fundamental yet major role in regulating actin cytoskeleton organization. Since cytoskeletal remodeling form the basis of many cellular events, Rho GTPases are hence involved in regulating many cytoskeleton-dependent events including changes in cell shape, cell adhesion, spreading events, motility, polarity, cytokinesis and vesicle trafficking (Wennerberg et al., 2005). In addition, they are implicated in a plethora of other functions such as cell cycle progression, gene transcription and cell survival (Burridge and Wennerberg, 2004; Ellenbroek and Collard, 2007; Etienne-Manneville and Hall, 2002). Rho GTPases therefore function primarily as molecular switches at signaling nodes, where diverse extracellular stimuli converge, to control the transmission of signaling events to their extensive pool of downstream effectors (Karnoub et al., 2004) (Figure 1.5). A subset of their functions pertaining to actin cytoskeleton reorganization, cell motility and proliferation are further discussed in the following sections.

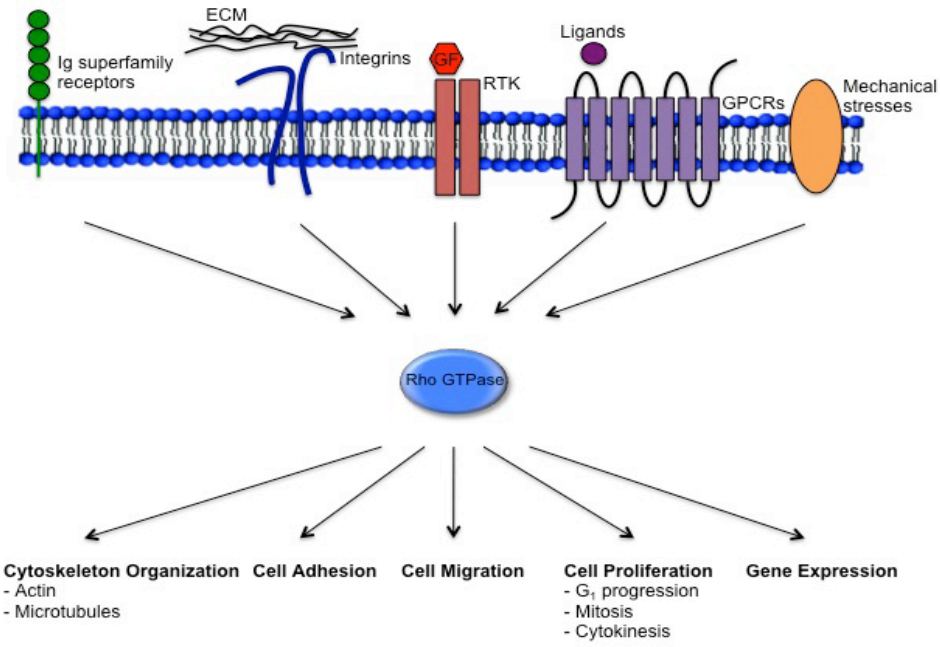

Figure 1.5 Functions of Rho GTPases. Rho GTPases function as intermediaries at signaling nodes to receive signals from various extracellular stimuli and elicit a plethora of downstream cellular functions.

1.2.5.1 Rho GTPases and actin cytoskeleton dynamics

First descriptions of the major function of Rho GTPases, mainly Rho, Rac and Cdc42, as key signal transducers linking cell surface receptors to the organization of actin cytoskeleton emerged in the early 1990s (Hall, 1998). It was described in quiescent Swiss3T3 fibroblast, in which serum starvation results in a very low level of organized F-actin structures, that Rho regulates the assembly of contractile actin-myosin stress fiber and of associated focal adhesions (Ridley and Hall, 1992). This observed effect is induced by lysophosphatidic acid (LPA) and inhibited by exoenzyme C3 transferase. In the same system, Rac triggers the formation of a dynamic meshwork of actin filaments at the cell periphery known as lamellipodia and membrane ruffles (Ridley et al., 1992). Formation of these thin curtain-like extensions associated with integrin-based adhesion complexes is stimulated by growth factors such as platelet-derived growth factor (PDGF), insulin or epidermal growth factor (EGF). On the other hand, Cdc42 induces the formation of periphery microspikes or filopodia in bradykinin-treated fibroblast (Kozma et al., 1995; Nobes and Hall, 1995). Similarly, these actin-rich finger-like cytoplasmic protrusions are found to be in association with focal contacts. Together, these three morphologically distinct actin structures induce by the respective GTPases, constitute the actin component of the entire cytoskeletal network, alongside with intermediate filaments and microtubules.

Rho GTPases modulate the dynamics of actin organization by coordinating various signal transduction pathways that involve actin polymerization or depolymerization, and organization (filament bundling) of the actin filaments (Jaffe

and Hall, 2005). Formation of stress fibers is elicited by the concreted actions of two major effectors downstream of Rho signaling, namely mDia and ROCK. Mammalian Diaphanous protein (mDia) belongs to one of the seven formin subfamilies and is characterized by the presence two formin homology (FH) domains: FH2 domain and the variable-length profilin-binding FH1 domain. These two domains cooperatively mediate actin filament assembly such that upon the relief of autoinhibitory interactions through association with activated Rho, mDia continually associates with the barbed end of an actin filament via its FH2 domain, while the FH1 domain containing multiple proline-rich motifs interacts with the profilin/G-actin complex. These interactions facilitate filament elongation, which in turn provides the driving force for membrane extension (Bishop and Hall, 2000; Jaffe and Hall, 2005; Sit and Manser, 2011).

ROCK, another of the Rho effectors, is a serine/threonine kinase. It acts downstream of Rho by regulating the phosphorylation states of a variety of substrates (Riento and Ridley, 2003). Mainly, ROCK phosphorylates the myosin-binding subunit (MBS) of myosin light chain phosphatase and by doing so inhibits its phosphatase activity. ROCK is also able to directly phosphorylate myosin light chain (MLC) and contributes to an overall increase in the amount of phosphorylated MLC, either through its direct action on MLC or indirectly via the inhibition of MLC phosphatase activity. MLC, when phosphorylated mainly at Ser^{19}, stimulates the actin-activated ATPase activity of myosin II to cross-link actin filaments and thus enhances actomyosin contractility (Bishop and Hall, 2000; Sit and Manser, 2011).

Besides the above-mentioned targets, ROCK can also phosphorylate LIM kinase (LIMK) and initiate another signaling cascade in which activated LIMK phosphorylates its substrate cofilin at Ser^{3}, rendering it inactive (Schwartz, 2004; Sit

and Manser, 2011). Cofilin is an actin-depolymerizating molecule which has been suggested to act by promoting actin monomer dissociation from the pointed end of actin filament or by functioning as a severing factor for filamentous actin, thereby hindering barbed-end elongation. Thus, the Rho-ROCK-LIM pathway contributes to the stability of existing filamentous actin structures via negative regulation of cofilin (Sit and Manser, 2011). The concerted actions of both mDia and ROCK leading to stress fiber formation are depicted in Figure 1.6.

While the expression of constitutively active ROCK alone generates actin bundles that are disorganized due to random bundling and cell contraction, co-expressing active forms of mDia abolishes this phenomenon, thereby producing thinner and less-bundled stress fibers. These results therefore suggest that mDia may serve to modulate the action of ROCK (Narumiya et al., 2009). Indeed, it is later revealed that Rac is activated downstream of Rho-mDia signaling through Src activation and subsequent phosphorylation-dependent formation of Cas/Crk/DOCK180 complex (Tsuji et al., 2002). Intriguingly, this Rho-dependent mDia-Rac pathway is inhibited by ROCK activity, which is in turn suppressed by active Rac. Therefore, distinct stress fiber pattern and cell shape may be achieved by establishing an equilibrium between the antagonistic Rho-mDia and Rho-ROCK signaling events (Narumiya et al., 2009). This form of modulation is clearly evident during the neurite-extension process in cultured cerebellular granule neurons such that in the presence of high level of active Rho, ROCK pathway is predominantly active, promoting enhanced actomyosin contraction and subsequently induces neurite retraction. Conversely, mDia is preferentially activated at low levels of active Rho to enhance neurite elongation (Figure 1.7) (Arakawa et al., 2003; Narumiya et al., 2009).

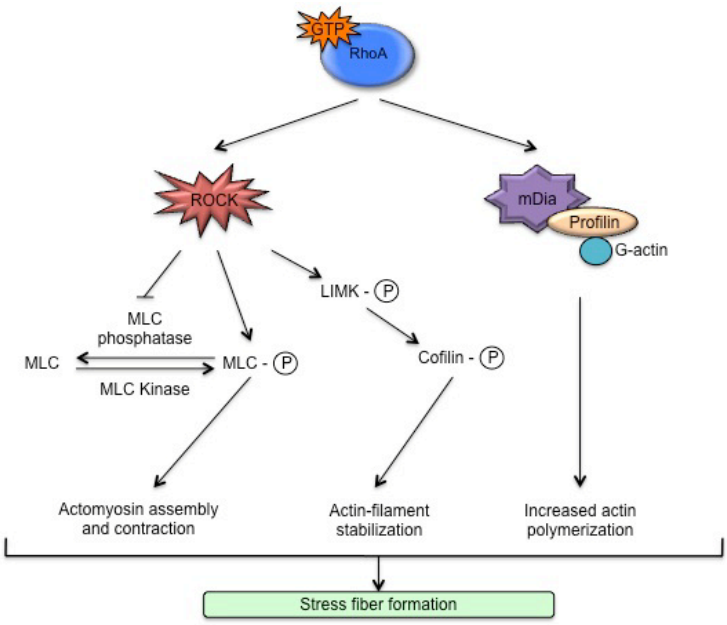

Figure 1.6 RhoA-induced signal transduction pathways for stress fiber formation. Active Rho promotes contractile actin:myosin filament assembly through concerted actions of mDia and ROCK, the two major effectors downstream of Rho signaling. [Adapted from Bishop and Hall, 2000].

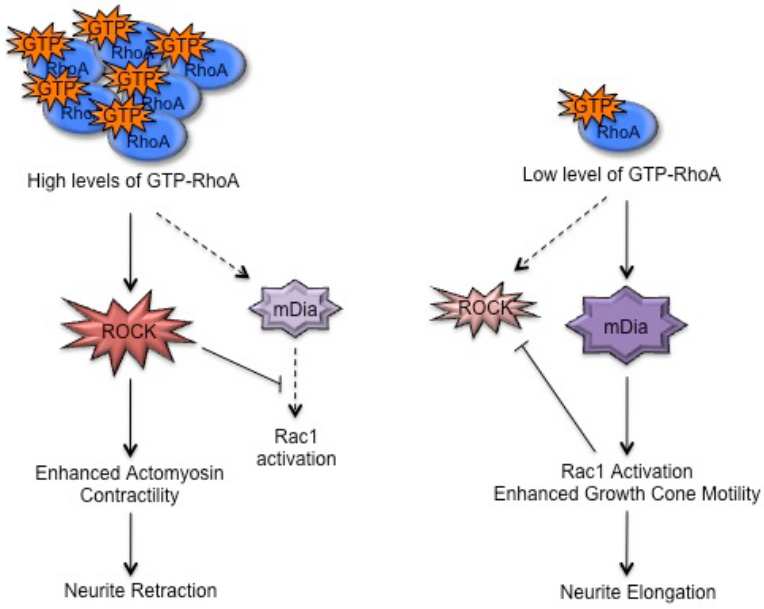

Figure 1.7 Antagonistic actions of RhoA-mDia and RhoA-ROCK signaling pathways in mediating neurite outgrowth. Local level of active RhoA determines the preferential activation of a particular Rho signaling pathway. In neuron cells, high level of active RhoA predominantly activates the RhoA-ROCK pathway, leading to enhanced actomyosin contractility and hence neurite retraction. Conversely, selective activation of RhoA-mDia signaling under low level of active RhoA results in Rac1 activation that enhances growth cone motility and finally neurite elongation. A similar mechanism may function in other cell types under different contexts. [Adapted from Narumiya, 2009].

Lamellipodia and filopodia are two types of protrusions often seen generated at the leading edge of a migrating cell. Rac1 and Cdc42 initiate their formation through several downstream effectors, some of which are common amongst the two. Both Rac1 and Cdc42 signal to nucleation actin-related protein 2/3 (Arp2/3) complex to initiate filamentous actin branching and increase the number of free barbed ends via the scaffold proteins, WASP-family Verprolin-homologous (WAVE) family proteins and WASP, respectively (Burridge and Wennerberg, 2004; Ellenbroek and Collard, 2007). Cdc42 initiates actin polymerization and formation of filopodia through the recruitment of N-WASP that functions primarily as a scaffold protein for the assembly of components required for actin polymerization, including actin monomers/profilin and Arp2/3 complex (Bishop and Hall, 2000). Although similar in structure to N-WASP, WAVE family proteins do not interact directly with active Rac1. Instead, their interactions occur through a heteropentameric WAVE complex containing WAVE protein, Rac1-binding protein PIR121, Nck-associated protein 1 (Nap1), Abl-interacting protein (Abi) 1, 2 and 3, and HSPC300. However, both Rac1-induced activation of WAVE complex via PIR121 and Cdc42-mediated WASP activation might occur through a similar mechanism (Sit and Manser, 2011).

PAK – a serine/threonine kinase, is another effector common to both Rac1 and Cdc42. Similar to ROCK, PAK acts along the same pathway via LIMK to negatively regulate cofilin, thereby maintaining the stability of actin filaments. In addition, it also participates in the regulation of MLC, leading to a corresponding reduction in actomyosin contractility by phosphorylating and inhibiting MLCK, a direct activator of MLC ATPase activity (Bishop and Hall, 2000). Filamin, another downstream target of PAK, is a major actin binding protein at the cell cortex. It is enriched in

membrane ruffles and serves to crosslink filamentous actin, hence stabilizing this meshwork of actin filaments (Burridge and Wennerberg, 2004).

Amongst the effectors of Rho GTPases are also lipid kinases, indicating the involvement of these GTPases in lipid signaling pathways that contribute to actin cytoskeleton dynamics. For instance, both Rho (via ROCK activity) and Rac signal to lipid kinase phosphatidylinositol-4-phosphate 5-kinase (PIP5K) that is involved in the production of phosphatidylinositol-4,5-bisphosphate (PIP_2). PIP_2 increases actin polymerization by stimulating the release of capping proteins such as gelsolin (Bishop and Hall, 2000). It also participates in the activation of erzin-radixin-moesin (ERM) family proteins through phosphorylation by ROCK for their function as linkers between actin and multiple transmembrane proteins to stabilize the cortical actin network (Schwartz, 2004; Sit and Manser, 2011).

Taken together, Rho GTPases coordinate a complex network of signaling events to regulate actin cytoskeleton dynamics, thereby forming the basis for many other cytoskeleton-dependent cellular events.

1.2.5.2 Rho GTPases and cell motility

Cell migration is an orchestrated process in organisms that is essential for driving embryonic morphogenesis during development, tissue repair and regeneration, immune surveillance and also contributes to pathological processes such as cancer (Ridley et al., 2003). Directed migration of cells occur in response to extracellular cues including growth factors or chemokines gradients, extracellular matrix (ECM) proteins for instance collagen and fibronectin, as well as mechanical forces (Parsons et al., 2010). To initiate a migration cycle, the cell first polarizes and extends protrusions to form a leading edge towards the direction of migration. These

protrusions adopt distinct morphological features with large, broad lamellipodia and finger-like filopodia driven by actin polymerization. While newly formed nascent adhesions that link actin cytoskeleton to the underlying substratum aids in stabilizing these protrusions, the mature focal adhesions connected to the ends of actin stress fibers serve as traction sites for migration as the cell body contracts and moves over them. Finally, disassembly of focal adhesions at the cell rear follows to allow for detachment and forward movement of the cell. These iterative cycles of protrusion and retraction therefore enable the cell to migrate in a highly directed manner in response to environmental changes (Parsons et al., 2010; Ridley et al., 2003).

Cell migration, a well-coordinated multistep process, is mediated by a number of highly integrated signaling events regulated by the Rho GTPases. Dissecting the roles of Rho GTPases in cell migration has led to the understanding that Cdc42 establishes cell polarity to ensure directed migration and Rac1 is localized to the leading edge to induce lamellipodia formation towards the stimulus; whereas RhoA activity is required for focal complex maturation into focal adhesions, cell body contraction to pull the cell body forward, rear end retraction (Raftopoulou and Hall, 2004) and surprisingly at the leading edge, probably to promote actin polymerization via mDia. In spite of their distinct roles, crosstalks exist among the Rho GTPases. For instance, Cdc42 signals to activate Rac1 locally whereas Rac1 and RhoA act either in a cooperative or antagonistic manner to spatially define their activities and effects (Machacek et al., 2009; Ridley et al., 2003).

1.2.5.2.1 Cdc42: A master regulator of cell polarity in cell migration

In general, migrating cells observed in tissue culture displayed a unique polarized morphology with a broad, flat lamellum extending in the direction of migration with a ruffling lamellipodium at the leading edge and a narrow retracting tail at the cell rear (Wittmann and Waterman-Storer, 2001). Cdc42 influences actin cytoskeleton polarity by defining the spatial region within the cell in which Rac1 is active and hence determine the location where lamellipodia are formed (Cau and Hall, 2005; Ridley et al., 2003). Such signaling specificity is achieved through selective accumulation of an activating RacGEF βPIX at the leading edge of the migrating cell as induced by PAK, which acts downstream of Cdc42 (Cau and Hall, 2005). With Rac1 only activated at the leading edge, this ensures that the formation of lamellipodia is efficiently restricted towards the direction of migration.

Besides altering actin cytoskeleton polarity, microtubules in slower migrating cells are reorganized such that the microtubule-organizing center (MTOC) and golgi apparatus are positioned in front of the nucleus, oriented towards the direction of migration. Realignment of these organelles may serve to enhance directed migration by facilitating microtubule growth and hence the transport of golgi-derived vesicles to the leading edge to provide the membrane components and associated proteins essential for generating forward protrusions (Ridley et al., 2003). Cytoskeletal network polarization is mediated mainly by Cdc42, which is active towards the front of a migrating cell (two microns behind the leading edge) as observed with fluorescent resonance energy transfers (FRET)-based studies (Machacek et al., 2009). Since directed migration can be abolished with either inhibition or global activation of Cdc42, this further supports the role of Cdc42 as a master regulator of cell polarity (Etienne-Manneville and Hall, 2002).

1.2.5.2.2 Rac1: Driving the protrusive machinery in cell migration

Similar to Cdc42, Rac1 is activated at 2 microns behind the leading edge of a migrating cell (Machacek et al., 2009), in part due to the coupling of local Rac1 activity to Cdc42 signaling. Localized Rac1 activity is crucial for the extension of a protrusive leading edge in the direction of migration by inducing lamellipodia formation via Arp2/3. In addition to Cdc42-induced Rac1 activation, this differential spatial localization of Rac1 is also mediated by an increase in concentration of phosphatidylinositiol 3,4,5 triphosphate (PIP_3) at a similar region. PIP_3 accumulation is positively regulated by PI3K that catalyzes its formation whereas PTEN, a PIP_3 phosphatase that inhibits PI3K activity, down-regulates this accumulation. Indeed, such tight regulation is achieved via mutually exclusive distribution of PI3K and PTEN, where PI3K is found only at the cell front and PTEN is restricted to regions where PI3K is absent (Hall, 2009; Raftopoulou and Hall, 2004; Ridley et al., 2003). Besides stimulating Rac1 activity through localization of PIP_3-sensitive RacGEFs, PIP_3 also function as signaling molecules to locally amplify even a very shallow gradient of difference in concentrations of chemoattractants, thus triggering directional migration (Raftopoulou and Hall, 2004; Ridley et al., 2003).

1.2.5.2.3 RhoA: Multiple roles of RhoA in cell migration

Although it has previously been widely accepted that RhoA activity is not required at the cell front for protrusions as RhoA and Rac1 are mutually antagonistic, this notion has been challenged by experimental evidences that shown otherwise. In FRET-based analysis of Rho GTPase activities during cell protrusion, it was found that RhoA is activated at the leading edge synchronous with edge advancement whereas both Cdc42 and Rac1 are activated slightly behind with a delay of

approximately 40 s (Machacek et al., 2009; Pertz et al., 2006). The presence of RhoA at the migrating forefront is further supported by observations that RhoA co-localizes with mDia in this region (Goulimari et al., 2005). Multiple roles of RhoA at the leading edge pertaining to its signaling to mDia have been suggested.

First, it is proposed that RhoA initiates the iterative cycles of protrusion and retraction in migration. mDia, when activated at the cell front, promotes actin polymerization to generate the initial actin filaments that are required for Arp2/3-mediated dendritic polymerization. It can also attach an actin barbed end to the membrane for subsequent polymerization (Machacek et al., 2009). Other studies have suggested that RhoA-mDia signaling contributes to migration via two separate pathways, either microtubule-dependent or actin-dependent (Narumiya et al., 2009). In the microtubule-dependent pathway, RhoA-mDia signaling promotes accumulation of Cdc42 and APC recruitment at the cell front for migration. This signaling pathway in turn induces actin-dependent translocation of Src to focal complexes to stimulate adhesion turnover, hence facilitating migration.

As the cell migrates, RhoA activity is also required for focal complex maturation, cell body contraction and rear end retraction. RhoA activation promotes the process of focal adhesion maturation through activation of myosin II, which brings about adhesion maturation and stability (Parsons et al., 2010). Contraction of actin-myosin bundles anchored at the adhesion sites then provides the traction force for cell body contraction and retraction of the lagging tail (Raftopoulou and Hall, 2004; Ridley et al., 2003). This contractility is mediated by RhoA-ROCK signaling pathway that triggers subsequent downstream phosphorylation cascades, leading to eventual phosphorylation and hence inactivation of MLC phosphatase and cofilin. Through inactivation of these negative regulators, this sustains the level of actin

filaments cross-linked by phosphorylated myosin, thereby generating the contractile force required for forward movement and rear end retraction. RhoA-ROCK signaling is also essential for negatively regulating integrin adhesions in the tail region for retraction (Narumiya et al., 2009). In summary, RhoA functions as an initiator of protrusion (RhoA-mDia) and a mediator of contractility (RhoA-ROCK) by signaling through different pathways.

1.2.5.3 Rho GTPases and cell proliferation

Uncontrolled cell proliferation is a hallmark of cancer. Proliferation of eukaryotic cells is an elegantly coordinated yet tightly regulated process in which cells undergo a round of cell division only when both extracellular and intracellular conditions are met (Villalonga and Ridley, 2006). Amongst environmental factors such as cell density, both availability of mitogenic growth factors and cell anchorage to extracellular matrix are critical determinants for entry into cell cycle (Welsh, 2004). With the ability of Rho GTPases to function as signal transducers to transmit upstream signals from the plasma membrane receptors to other components within the cells, it is not surprising that they are involve in cell cycle regulation. Rho GTPases modulate the activity of cyclin-dependent kinases (Cdks) during G_1 phase and subsequently the organization of microtubules and actin cytoskeleton during mitosis (Jaffe and Hall, 2005).

1.2.5.3.1 Rho GTPases in G_1 phase cell cycle regulation

The first evidence indicating the involvement of Rho GTPases in cell cycle came from an early study whereby exoenzyme C3 transferase blocks G_1 progression in Swiss3T3 fibroblasts (Yamamoto et al., 1993). Subsequently, microinjection

studies using dominant negative or constitutive active mutants of RhoA, Rac1 and Cdc42 further proved their involvement in mitogen-stimulated G_1 to S phase progression (Olson et al., 1995). However, the exact roles of Rho GTPases and the underlying mechanisms by which they coordinate the progression are complex and cell-type dependent (Jaffe and Hall, 2005), thus requiring further investigations. By far, Rho GTPases have been shown to modulate G_1 to S phase progression primarily by regulating cyclin D expression and levels of p21 and p27 (Hall, 2009).

Mitogenic growth factors stimulate the expression of cyclin D via the canonical Ras-MEK-ERK pathway. However, ERK activation must be sustained in order to achieve both optimal timing and levels of cyclin D expression (Hall, 2009). In NIH3T3 fibroblasts, RhoA mediates prolonged ERK activation via integrin-mediated adhesion and hence referred to as anchorage-dependent proliferation. RhoA activation leads to the formation of stress fibers that are required for the clustering of integrins. Here a positive feedback loop exists whereby these integrin focal complexes further promote RhoA activation by recruiting RhoGEFs to these sites. RhoA, when activated by integrins, signals through RhoA-ROCK-LIMK pathway to induce sustain ERK activation and thus maintain the expression of cyclin D for G_1 progression (Hall, 2009). Interestingly, inhibition of RhoA activity not only leads to an abolishment of prolonged ERK activity but also results in an earlier rapid increase in cyclin D level through a Rac-dependent mechanism that is normally suppressed by LIMK activity in the cell nucleus (Coleman et al., 2004; Roovers et al., 2003). As such, RhoA may function as an anchorage-dependent cell cycle checkpoint to regulate the timing and cytoskeletal dependence of cyclin D expression during G_1 phase via RhoA-ROCK-LIMK pathway (Coleman et al., 2004; Villalonga and Ridley, 2006). In general, ectopic expression of Rho, Rac and Cdc42 can promote transcription of

cyclins D and E via various pathways including nuclear factor-κB (NFκB), reactive oxygen species (ROS), PAK, c-Jun N-terminal kinase (JNK) or p38, depending on the cell type (Hall, 2009; Villalonga and Ridley, 2006).

Rho and Ras GTPases function in synergism in the regulation of cell cycle. Apart from their combined effect in prolonging cyclin D expression through G_1 phase, such synergism is also observed through their effect on CDK inhibitor p21. In a non-transformed mitogen-stimulated cell, p21 expression increases in response to ERK activation, probably due to its function as an assembly factor for cyclinD/cdk4,6 complex. This increase, however, is followed by a gradual decrease from the mid to late G_1 phase that is adhesion-dependent but ERK-independent. RhoA may contribute to this decrease via p53-independent suppression of p21 transcription. Taken together, RhoA acts as an anchorage-dependent cell cycle checkpoint and mediates G_1 progression in non-transformed cells. Conversely, RhoA facilitates oncogenic Ras-induced cell cycle progression in transformed cells through its inhibitory effect on p21 expression, thus accounting for the role of Rho GTPases in Ras-induced transformation (Coleman et al., 2004; Welsh, 2004). Activated Rac and Cdc42, induced by either mitogenic factors or by integrin-mediated cell attachment, may also decrease p21 through activation of its ubiquitin-independent proteosome-mediated degradation (Coleman et al., 2004).

1.2.5.3.2 Rho GTPases in mitosis and cytokinesis

Besides G_1 progression, Rho GTPases have also been implicated in G_2 to M progression and mitosis (Villalonga and Ridley, 2006). During mitosis, the effect of Rho GTPases are observed mainly on cytoskeletal changes that accompanied this process; from the rounding of cell at the onset of mitosis driven by RhoA-ROCK

pathway (Maddox and Burridge, 2003), to the attachment of microtubules to kinetochores during metaphase for proper chromosome alignment regulated by mDia3 downstream of Cdc42 (Yasuda et al., 2004) and the positioning of spindle mediated by Cdc42-induced assembly of Par6/αPKC polarity complex at the membrane (Hall, 2009). Lastly, RhoA plays a crucial role in cytokinesis due mainly to its ability to promote actomyosin-based contractility (Villalonga and Ridley, 2006).

Cytokinesis is characterized by the formation of a cleavage furrow consisting of a ring of contractile actin-myosin II filaments at the cortex and subsequent ingression of the ring to constitute the midbody, resulting in the separation into two daughter cells (abscission) (Hall, 2009). During this process, active RhoA accumulates at a narrow zone in the cortex to initiate actomyosin contractile ring formation and subsequent ring ingression via stimulation of mDia, ROCK and citron kinase. ROCK promotes furrow ingression by phosphorylating MLC at Ser^{19} and inhibiting MLC phosphatase, while citron kinase that di-phosphorylate MLC at Thr^{18} and Ser^{19} mediates the completion of cytokinesis (Piekny et al., 2005; Wadsworth, 2005). RhoA activity is therefore crucial for cytokinesis and is regulated spatiotemporally specifically by RhoGEF Ect2 and RhoGAPs including MgcRacGAP (male germ cell RacGAP) and p190RhoGAP (D'Avino and Glover, 2009; Manchinelly et al., 2010; Su et al., 2009; Werner and Glotzer, 2008). Various roles of Rho GTPases in the cell cycle are depicted in Figure 1.8.

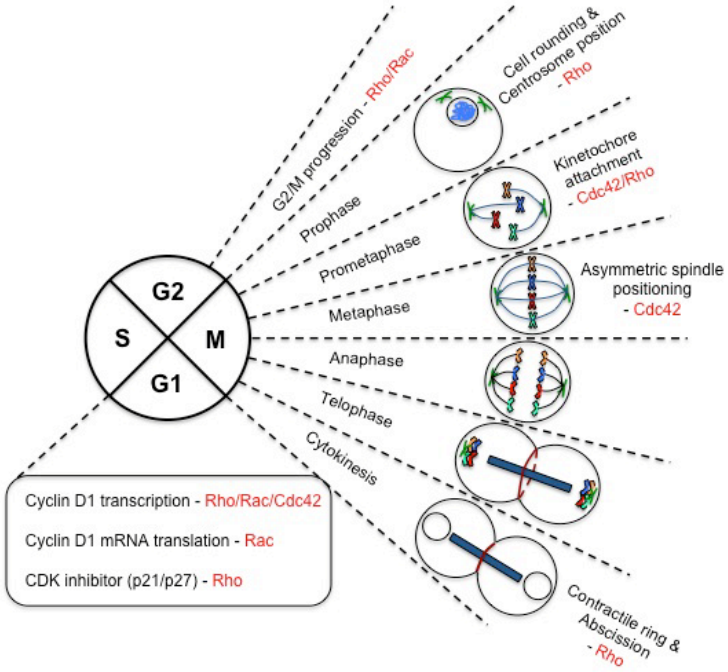

Figure 1.8 Roles of Rho family GTPases in the cell cycle. Rho GTPases play pivotal role in the regulation of cell cycle, particularly G_1 phase and mitosis. In G_1 phase, Rho GTPases promote Cyclin D1 transcription or translation and inhibit the CDK inhibitors, p21 or p27. During mitosis, they are involved in various processes at different stages including cell rounding and centrosome positioning in prophase, kinetochore attachment and asymmetric spindle positioning in metaphase and lastly contractile ring formation and abscission in cytokinesis [Adapted from Hall, 2009].

1.2.5.4 Rho GTPases and gene transcription

Of the many cellular effects associated with Rho GTPases, some are the result of alterations in gene transcription induced downstream of Rho GTPases signaling. Many transcription factors have been identified as targets of Rho GTPases signaling including SRF, NFκB, Stat3, Stat5, E2F and many more (Aznar and Lacal, 2001). Among them, serum response factor (SRF) is a well-known RhoA-induced transcription factor stimulated by mitogenic factors such as serum, LPA and PDGF. Activity of SRF can be modulated by changes in actin dynamics such that depletion of G-actin in response to RhoA-induced treadmilling and increase in actin

polymerization can induce gene transcription (Sotiropoulos et al., 1999). This actin-dependent SRF activation requires nuclear translocation of its myocardin-related co-activator MAL triggered downstream of RhoA (Miralles et al., 2003). Once activated, SRF binds to the serum response element (SRE) that is present in many gene promoters and induces transcription of distinct genes respective to the upstream stimuli. Although SRF activity has been associated with the transcription of diverse gene targets including those specific for embryonic development, proliferation and differentiation, it is an essential transcription factor in RhoA-induced morphological changes contributing to cell motility (Benitah et al., 2004; Merdek et al., 2008). Therefore, RhoA-dependent induction of SRF may confer the invasive phenotype of tumor cells since SRF activity is present only in tumor cells that have undergone epithelial to mesenchymal transition (EMT) in a mouse skin carcinogenesis model (Benitah et al., 2004).

Stat transcription factors constitute a family of latent cytoplasmic transcription factors (Benitah et al., 2003) and the activities of some of which are also modulated by Rho GTPases. For instance, RhoA and Rac1 can activate Stat3 in human cells by inducing its simultaneous dual tyrosine and serine phosphorylation, though via different mechanisms. Stat3 activity is necessary for RhoA-induced anchorage independent growth of human cells, as well as RhoA- and Rac1-induced transformation of murine fibrobasts. It is therefore possible that Rho GTPases promote transformation via transcriptional activity of Stat3, in particular through the regulation of cell cycle-related genes such as cyclin D1 or c-Myc (Benitah et al., 2004). The requirement of Stat3 activity for RhoA-induced NFκB and cyclin D1 transcription, cell proliferation, transformation, stress fiber formation and migration is further demonstrated in mouse embryonic fibroblasts (MEF) (Debidda et al., 2005),

thereby reinforcing the importance of Stat3 as a transcription factor functioning downstream of RhoA. Apart from Stat3, RhoA, Rac1, Cdc42 and RhoC can also signal to Stat5a, which has been demonstrated to be essential for both EMT and enhanced motility of RhoA-transformed MDCK cells, but suppresses proliferation in these cells (Benitah et al., 2003). Taken together, RhoA modulates activity of Stat3 for cell proliferation and Stat5a for processes contributing to a motile phenotype including migration and EMT.

1.2.6 Rho GTPases and cancer

Rho GTPases regulate a plethora of cellular functions and their deregulations contribute to most if not all stages of cancer development ranging from tumor initiation to cancer progression and metastasis (Figure 1.10). During initial tumor growth, cells acquire the ability for uncontrolled proliferation, accompanied by increased survival signals and evasion from apoptosis (Vega and Ridley, 2008). As evident from the requirement of Rho GTPases for oncogenic Ras transformation, RhoA and Rac1 contribute to carcinogenesis by promoting G_1 phase progression through induction of cyclin D1 expression and also inhibition of cdk inhibitors p21 and p27 by RhoA. Moreover, Rho GTPases can signal to transcription factors to alter the expression of genes for survival and prevention of apoptosis (Vega and Ridley, 2008). For instance, RhoA promote Stat3 activity for proliferation, while Rac1 suppresses Ras-induced apoptosis via NFκB (Ellenbroek and Collard, 2007).

EMT, a process which transformed cells transit into a more motile phenotype through disruption of adherens junctions, is a major event in cancer development. Multiple studies have linked RhoA signaling to reduced formation and destabilization of E-cadherin-mediated cell-cell adhesion, leading to EMT (Chang et al., 2009).

Conversely, E-cadherin can also negatively regulate active RhoA level via p190RhoGAP (Ellenbroek and Collard, 2007).

In malignant cancers, tumor cells that have acquired an invasive phenotype become more aggressive and can undergo metastasis. These invasive tumor cells can migrate in two different modes, either via proteolysis-guided mesenchymal movement or actomyosin-driven amoeboid movement (Narumiya et al., 2009). In mesenchymal migration, invasion of tumor cells into the surrounding tissues require degradation of ECM by enzymes matrix metalloproteinases (MMPs) and Rho GTPases have been shown to modulate the expression and secretion of these proteases (Bryan and D'Amore, 2007; Ellenbroek and Collard, 2007). Furthermore, Rho GTPases can regulate tissue inhibitors of metalloproteinases (TIMPs), thus enhancing the remodeling of ECM for invasion (Ellenbroek and Collard, 2007). On the other hand, tumor cells migrating via protease-independent amoeboid movement adopt a spherical form for squeezing through the fibrillar network and such movement is mediated primarily by the Rho-ROCK pathway (Narumiya et al., 2009). While availability of MMPs is a determining factor for utilization of different migratory mechanisms, Rho GTPases can also dictate the mode of migration through selective inhibition of either RhoA or Rac1 activity (Narumiya et al., 2009; Sanz-Moreno et al., 2008).

Lastly, angiogenesis is an essential step in supplying nutrients to support the growth of solid tumors. Rho GTPases participate in this process through regulation of proliferation, survival and migration of endothelial cells, as well as lumen formation and capillary branching (Bryan and D'Amore, 2007). RhoC, in addition, promotes this process by inducing the production of angiogenic factors in inflammatory breast cancer (Merajver and Usmani, 2005).

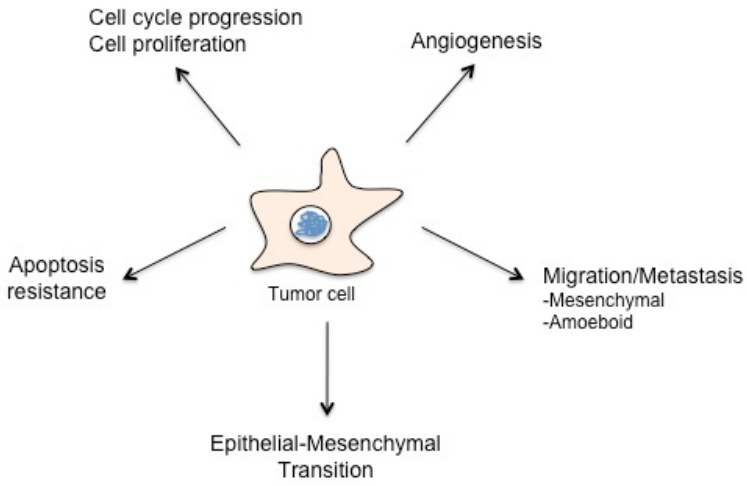

Figure 1.9 Possible involvement of Rho family GTPases in various stages during cancer progression.

Given the wide implications that Rho GTPases have on multiple stages in tumorigenesis, it is surprising that genetic mutations that may result in gain- or loss-of-functions rarely exist in these proteins in human cancers. A few exceptions include Rac1, of which mutations have been found to affect the effector domain (Hwang et al., 2004), and RhoH that has been found to undergone gene rearrangement in non-Hodgkin's lymphomas and myeloma, with also reports of hypermutations in the non-coding regions in diffuse large-cell lymphoma that may affect its expression (Karlsson et al., 2009). This rarity is in contrast with Ras GTPases that are mutated in about 30 % of human cancers of different origins (Ellenbroek and Collard, 2007). On the contrary, deregulations of Rho GTPase signaling in human cancers are often associated with perturbed expression of these proteins as shown in Table 1.1 or of their regulators.

Table 1.1 Altered Rho GTPases (Rho, Rac and Cdc42) expression in human cancers. [Adapted from Karlsson et al., 2009].

Rho GTPase	Alteration	Malignancies
RhoA	Overexpression	Invasion of hepatocellular carcinoma
		Metastasis of hepatocellular carcinoma
		Invasion and metastasis of bladder cancer
		Progression of esophageal squamous cell carcinoma
		Head and neck squamous cell carcinoma
		Progression of ovarian carcinoma
		Progression of gastric carcinoma
		Progression of testicular cancer
		Colon and lung cancer and progression of breast cancer
RhoB	Loss of expression	Progression of lung cancer
	Reduced expression	Head and neck squamous cell carcinoma
	Overexpression	Presence and progression of breast cancer
RhoC	Overexpression	Invasion of non-small cell lung carcinoma
		Inflammatory breast cancer
		Presence and progression of breast cancer
		Metastasis of breast cancer
		Invasion of breast carcinoma
		Metastasis of gastric cancer
		Progression and metastasis of hepatocellular carcinoma
		Progression of pancreatic ductal adenocarcinoma
		Metastasis of prostate cancer
		Metastasis of melanoma
		Head and neck squamous cell carcinoma
		Squamous cell carcinoma of skin
		Invasion and metastasis of bladder cancer
		Progression of esophageal squamous cell carcinoma
		Progression of ovarian carcinoma
Rac1	Overexpression	Progression and metastasis of breast tumors
		Oral squamous cell carcinoma
		Progression of prostate cancer
		Progression of gastric carcinoma
		Progression of testicular cancer
		Breast cancer
	Hyperactivity	Chronic myelogenous leukemia
	Alternative splicing to Rac1b	Colorectal tumors
Rac2	Overexpression	Head and neck squamous cell carcinoma
		Squamous cell carcinoma and basal cell carcinoma of skin
	Hyperactivity	Chronic myelogenous leukemia
Rac3	Hyperactivity or overexpression	Breast cancer
Cdc42	Overexpression	Progression of testicular cancer
		Breast cancer

1.2.7 Regulators of Rho GTPase activity

1.2.7.1 Rho family Guanine Nucleotide Dissociation Inhibitors (RhoGDIs) inhibits Rho GTPase signaling

Functions of Rho GTPases are dependent fundamentally on their cycling between active and inactive states, and their membrane associations at distinct subcellular compartments (Wennerberg and Der, 2004). Although RhoGDIs are not directly involved in the cycling process, they are pivotal regulators of Rho GTPases and function to maintain equilibrium between the cytosolic and membrane pools of Rho GTPases. In contrast to RhoGEFs and RhoGAPs, there are currently only three identified mammalian RhoGDIs, namely RhoGDIα (RhoGDI-1), RhoGDIβ (RhoGDI-2 or Ly/D4GDI) and RhoGDIγ (RhoGDI-3). RhoGDIα is ubiquitously expressed whereas both RhoGDIβ and RhoGDIγ display tissue-specific expression. In addition, these three GDIs also have differential Rho-binding specificity, with RhoGDIα showing the widest substrate spectrum (DerMardirossian and Bokoch, 2005; Dovas and Couchman, 2005).

RhoGDIs are cytosolic proteins and form complexes with prenylated Rho proteins in a 1:1 stoichiometry (DerMardirossian and Bokoch, 2005). Binding of RhoGDI to the GTPase requires both its N-terminal flexible domain and C-terminal domain with an immunoglobulin-like fold through protein-protein and protein-lipid interactions, respectively, which are essential to the inhibitory function of RhoGDI (Dovas and Couchman, 2005). When in association with GDP-bound GTPase, RhoGDI prevents the dissociation of GDP and GEF-mediated GDP/GTP exchange. Alternatively, RhoGDI can also interact with GTP-bound GTPase to inhibit both the intrinsic and GAP-catalyzed GTP hydrolysis, and its interactions with downstream effectors. Taken together, RhoGDI functions to prevent the GDP/GTP cycle and

subsequent activation of Rho GTPase-mediated biological activities by inhibiting GDP dissociation and interactions with regulatory and effector molecules (DerMardirossian and Bokoch, 2005).

Apart from the above mentioned, RhoGDI also mediates the extraction of Rho GTPase from the membrane via a biphasic mechanism in which a rapid association of RhoGDI and Rho protein precedes a slow transfer of the lipid moiety from the membrane to RhoGDI (Nomanbhoy et al., 1999). Insertion of the isoprenyl moiety of Rho protein into the hydrophobic pocket of immunoglobulin-like β-sandwich of RhoGDI increases the solubility of GTPase. Therefore, through formation of RhoGDI-GTPase complexes, RhoGDIs replenish and maintain a cytosolic pool of soluble lipid-modified Rho GTPases by contributing to the recycling of Rho proteins (DerMardirossian and Bokoch, 2005).

Although the intracellular amount of RhoGDIs exceeds that of any single Rho GTPase, it is comparable to the total amount of Rho GTPases (Michaelson et al., 2001). This stoichiometry strongly indicates that majority of the Rho proteins are in complex with RhoGDIs and maintained as inactive form in the cytosol. Formation of RhoGDI-GTPase complex therefore constitutes an important mechanism for the tight regulation of Rho GTPase signaling (Wennerberg and Der, 2004).

1.2.7.2 Rho family Guanine Nucleotide Exchange Factors (RhoGEFs) activate Rho GTPase signaling

Function to accelerate GDP/GTP exchange, RhoGEFs constitute a large family of multi-domain proteins that confer not only speed but also specificity to the activation of Rho GTPases. Since the discovery of the first mammalian GEF – Dbl, isolated as a transforming gene in human diffuse B-cell lymphoma cells (Eva and

Aaronson, 1985), more than 70 human RhoGEFs have been identified (Garcia-Mata and Burridge, 2007). Based on the type of catalytic domain, RhoGEFs can be further classified into either Dbl or CZH/DOCK180 (CDM and Zizimin homology/Dedicator of cytokinesis 180) family. Canonical RhoGEFs in the former group contain a minimal module composed of the catalytic Dbl homology (DH) domain and a pleckstrin homology (PH) domain adjacent and C-terminal to the DH domain, whereas the newly defined members in the latter are characterized by the presence of two Dock homology regions (DHR) for mediating nucleotide exchange in replace of the DH-PH module (Ellenbroek and Collard, 2007; Garcia-Mata and Burridge, 2007). Beyond the basic structural requirement for nucleotide exchange activity, these otherwise highly diversified RhoGEFs may also contain additional functional domains including protein-protein or protein-lipid interaction domains such as Src homology 2 (SH2), SH3, PDZ (PSD95/Discs-large/ZO-1) and PH, or catalytic domains such as Ser/Thr or Tyr kinase, RasGEF and RhoGAP domains, which confer additional means for regulation (Schmidt and Hall, 2002).

Although structurally unrelated, both types of RhoGEF catalytic module function biochemically via a generalized mechanism in which interaction between RhoGEF and its target Rho GTPase deforms the nucleotide-binding site and results in a reduced affinity for GDP (Bos et al., 2007). In detail, conformation changes that occur within the GTPase upon binding of RhoGEF introduce a steric hindrance from either residues of the GEF itself or the repositioned alanine side chain of the conserved DTAG motif in switch II region of Rho GTPase. This steric occlusion of the magnesium-binding site, together with perturbation of the phosphate-binding surface, disrupt high-affinity binding of the nucleotide and promote its release from the Rho protein (Renault et al., 2003; Thomas et al., 2007). On the other hand, the

nucleotide base-binding region remains undisturbed and this allows the spontaneous binding of GTP, whose intracellular concentration is approximately ten times higher than that of GDP (Bos et al., 2007). This action re-orientates the essential threonine residue in the effector loop and displaces RhoGEF (ten Klooster and Hordijk, 2007), leaving the GTP-bound Rho GTPase ready to bind to its effectors.

Intriguingly, the number of RhoGEFs present in human far exceeds their cognate targets (Schmidt and Hall, 2002). No doubt this reflects specificity of some RhoGEFs for a single Rho GTPase such as p190RhoGEF for RhoA, Tiam1 for Rac1 and Tuba for Cdc42, others including Vav can activate multiple Rho GTPases (Ellenbroek and Collard, 2007). Conversely, multiple RhoGEFs can act on the same Rho GTPase. Therefore, the large number of RhoGEFs provides a level of complexity and control to Rho GTPase signaling. Since majority of the RhoGEFs are ubiquitously expressed (Schmidt and Hall, 2002), additional means of regulation are required to modulate their activities to ensure precise control of Rho GTPase activation and subsequent downstream signaling. Indeed, this extra level of control is conferred by the multi-domain nature of RhoGEFs. For instance, PH domain though not required for RhoGEF catalytic activity, is essentially present in all Dbl family members with a few exceptions. This approximately 100-residue PH domain has been associated with both positive and negative regulatory roles pertaining to membrane targeting, interactions with phospholipids and proteins, and nucleotide exchange efficiency (Buchsbaum, 2007; Rossman et al., 2005).

Multiple combinations of different functional domains therefore provide the basis for modulation of RhoGEF activity via different modes including protein-protein or protein-lipid interactions, binding of second messengers and post-translation modifications (Bos et al., 2007). Apart from regulation, these characterized

modules also allow the RhoGEFs to serve an additional function of dictating Rho GTPase downstream signaling pathways, either by direct associations with immediate effectors or by functioning as a scaffold to integrate components of other signaling pathways (Buchsbaum, 2007; Ellenbroek and Collard, 2007).

1.2.7.3 Rho family GTPase Activating Proteins (RhoGAPs) terminate Rho GTPase signaling

In the GDP/GTP cycle, RhoGAPs act in antagonism to RhoGEFs to accelerate deactivation of Rho GTPases by stimulating their weak intrinsic GTPase activity, thereby leading to enhanced GTP hydrolysis. Characterized by the presence of an approximately 150-residue RhoGAP domain, the human RhoGAP family is predicted to encompass up to 80 members from human genome analysis (Moon and Zheng, 2003). Although members of the RhoGAP family may share as little as 20 % sequence identity in the RhoGAP domain, they form a distinct class of their own among other GAPs for the Ras superfamily (Moon and Zheng, 2003), similar to that observed for RhoGEFs. In addition to the RhoGAP domain, which constitutes a minimal module sufficient for binding GTP-bound Rho GTPase and catalyzing its GTPase activity, RhoGAPs are also multi-domain proteins that contain various combinations of additional functional modules. While some RhoGAPs may be specific to a single Rho GTPase, others display a broad substrate specificity and it remains to be determined how this variation is established (Tcherkezian and Lamarche-Vane, 2007).

Inherently low GTPase activity of Rho GTPases contributes to slow GTP hydrolysis and prolongs signal transductions. In the presence of RhoGAP, GTP hydrolysis rate is enhanced by several orders of magnitude and allows for rapid

termination of Rho GTPase signaling. Though diverse in sequence, the RhoGAP domain adopts a similar tertiary folding pattern and functions via a fundamental GTPase-activating mechanism as that of RasGAP (Zheng and Quilliam, 2003). In principle, RhoGAP facilitates the hydrolysis process by stabilizing the intrinsically mobile catalytic machinery of the GTPase and via the insertion of a catalytic residue *in trans* to stabilize the transition state (Bos et al., 2007). Indeed, structure analysis of p50RhoGAP shows that the GAP domain comprises nine α-helices and binds to both Switch I and II and P-loop of Rho GTPase to stabilize them (Hakoshima et al., 2003). Furthermore, a structural comparison of the transition state mimic, consisting of RhoGAP in complex with RhoA bound to GDP and aluminum fluoride, to that of RhoGAP-RhoA bound to GMPPNP which is a non-hydrolysable GTP analog, reveals a 20 ^{o} rotation between the two structures (Hakoshima et al., 2003; Moon and Zheng, 2003; Nassar et al., 1998).

Taken together, binding of RhoGAP domain to Rho GTPase stabilizes the glutamine residue that coordinates the orientation of the attacking water molecule. In addition, insertion of a highly conserved catalytic residue known as the arginine finger by the RhoGAP *in trans* to interact directly with the glutamine residue neutralizes the negative charge at the γ-phosphate, thereby stabilizes the transition state. Through stabilization of this glutamine residue, the freedom of water molecule is restricted and this in turn may reduce the energy barrier for GTP hydrolysis (Bos et al., 2007; Rittinger et al., 1997; Scheffzek et al., 1997). While mutational analysis has confirmed the importance of this arginine finger in catalyzing Rho GTP hydrolysis, additional amino acids may also play secondary role in orientating the GTPase machinery for efficient hydrolysis (Moon and Zheng, 2003; Peck et al., 2002).

Intriguingly, the presence of a large number of regulators that exceeds the Rho GTPases by two to three folds and the diverse multi-domain architecture of these regulators are two striking features common to both RhoGEFs and RhoGAPs - regulators of the GDP/GTP cycle. The vast number, coupled with multiple combinations of different functional domains, provides the basis for tight modulation of the activities of these regulators (Moon and Zheng, 2003; Tcherkezian and Lamarche-Vane, 2007). This is not surprising given the diverse spectrum of cellular activities under the control of Rho GTPases and dysfunctions of these proteins and their regulators have been implicated in various diseases. Similar to RhoGEFs, the multi-domain nature of many RhoGAPs allows the convergence of different signaling pathways through interactions with other molecules, as dictated by the domains present (Moon and Zheng, 2003). Alternatively, these domains may interact with different effectors of the Rho GTPases to specify activation of distinct pathways. Given the importance of the regulatory role that RhoGAPs have on switching off the Rho proteins, it is therefore imperative to understand how these regulators may in turn be modulated.

1.2.8 Mechanisms of RhoGAP regulation

RhoGAP activity is subjected to stringent regulation via multiple mechanisms. These regulatory mechanisms include protein-protein interaction, lipid binding, phosphorylation and proteolytic degradation (Tcherkezian and Lamarche-Vane, 2007) that may serve to modulate the GAP activity, mediate translocation to specific intracellular location, relieve autoinhibition or bring about protein degradation (Bos et al., 2007).

Firstly, the presence of different protein interaction domains such as SH2, SH3, PDZ and SAM (Sterile Alpha Motif) facilitates regulation via protein-protein interactions. For instance, interaction of CdGAP through probably its proline-rich motif with SH3 domain of intersectin, an endocytic scaffolding protein, may induce a conformation change in CdGAP that leads to the inhibition of its GAP activity (Jenna et al., 2002). Moreover, direct binding of PRC1 (protein regulating cytokinesis 1) to GAP domain of MgcRacGAP downregulates its GAP activity during metaphase (Ban et al., 2004). Interaction of Rap1 with RA (Ras association) domain of RA-RhoGAP, on the other hand, activates the RhoGAP via relief of intramolecular autoinhibition imposed by the RA domain (Yamada et al., 2005).

Besides protein interaction domains, some RhoGAPs may contain lipid binding domains such as BAR (Bin/amphiphysin/Rvs), DEP (Dishevelled/Egl-10/pleckstrin), C1 (cysteine-rich phorbol ester) and C2 (calcium-dependent lipid binding) that may participate in membrane targeting and mediate subcellular localization (Kandpal, 2006). For example, binding of phorbol ester or diacylglycerol (DAG) to the cysteine-rich region of chimaerin, a Rac-specific GAP, stimulates its GAP activity and induces its translocation from the cytosol to perinuclear region and golgi (Moon and Zheng, 2003). In addition, there have been reports on the regulation of GAP activity of p190RhoGAPs (p190-A and p190-B) by phospholipids such that several phospholipids including phosphatidylserine (PS), PIP_2 and phosphatidic acid inhibit their GAP activity *in vitro*, whereas PS and PIP_2 can promote the GAP activity of p190RhoGAPs towards Rac1 (Ligeti et al., 2004).

Next, protein kinases can modulate RhoGAP activity via phosphorylation and p190RhoGAP is one such example that may be targeted by various kinases. Src-induced phosphorylation of p190RhoGAP at two tyrosine residues near the RhoGAP

domain recruits p120RasGAP through a SH2 domain-phosphotyrosine interaction and this activates the GAP activity of p190RhoGAP (Moon and Zheng, 2003). Conversely, activation of low molecular weight protein-tyrosine phosphatase (LMW-PTP) upon phosphorylation by c-Src in response to PDGF receptor signaling allows direct interaction of this protein with p190RhoGAP. This interaction facilitates the dephosphorylation of p190RhoGAP by LMW-PTP phosphatase activity, thus negatively regulate Src-induced activation of p190RhoGAP (Moon and Zheng, 2003). Furthermore, p190RhoGAP can be phosphorylated on Ser/Thr residues by PKC, which promotes the translocation of p190RhoGAP from the cytosol to membrane ruffles upon Src activation (Brouns et al., 2000).

Lastly, the protein level of RhoGAPs can be controlled intrinsically by targeting the protein for degradation. It is demonstrated that expression of p190ARhoGAP is transiently downregulated via ubiquitin-mediated degradation during late mitosis for successful completion of cytokinesis (Su et al., 2003). Given the modular complexity of RhoGAPs, it presents many possibilities on how these RhoGAPs can be modulated and are awaiting to be discovered. It is therefore through further characterization of members of the RhoGAP family that new insights can be gained and one such RhoGAP is further discussed in the following section.

1.3 BCH (BNIP-2 and Cdc42GAP Homology) domain-containing, proline-rich and Cdc42GAP-like protein 1 (BPGAP1)

As discussed, the human RhoGAP family comprises many multi-domain proteins characterized by the presence of a conserved RhoGAP domain, coupled with additional functional signaling modules. Many RhoGAPs, termed as ARHGAP1-12, have been identified from the human genome. BPGAP1 is a novel RhoGAP that was first discovered through bioinformatics analysis and it harbors an unique domain architecture similar to that of p50RhoGAP/ARHGAP1 (Shang et al., 2003). Together, p50RhoGAP and BPGAP1 constitute a distinct subgroup within the RhoGAP family (Johnstone et al., 2004) as defined by a N-terminal BCH (BNIP-2 and Cdc42GAP Homology)/Sec14p-like domain, followed by a proline-rich region and a C-terminal RhoGAP domain (Figure 1.10) (Shang et al., 2003).

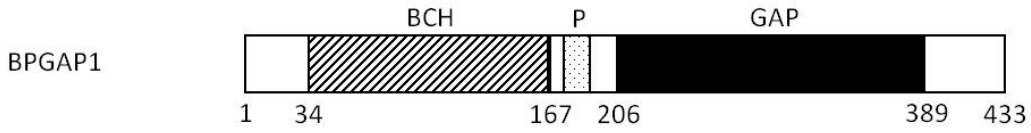

Figure 1.10 Domain architecture of BPGAP1. BPGAP1 harbors a N-terminal BCH domain followed by a proline-rich motif (P) and a C-terminal RhoGAP domain with a highly conserved arginine residue at position 232. [Adapted from Shang et al., 2003].

BPGAP1, also known as ARHGAP8, is encoded by 12 exons in the *ARHGAP8* gene mapped to human chromosome 22q13.31 (Johnstone et al., 2004). Composed of 433 amino acids, BPGAP1 lacks a 31-amino acid insertion in the BCH domain due to the removal of exon 5 by alternative splicing (Johnstone et al., 2004; Shang et al., 2003). Thus far, transcripts of two other isoforms have been detected, with one encoded by all 13 exons of *ARHGAP8* gene (BPGAP2) and the other has

five amino acids – YWDYR missing from the BCH domain as a consequence of a final 15 bp deletion from exon 5. However, both these transcripts are present at a much lower level as compared to BPGAP1 in normal breast and colon tissues tested (Johnstone et al., 2004). A mouse ortholog has also been detected and is encoded by the *Arhgap8* gene located on mouse chromosome 15, region E2, in a region syntenic with human chromosome 22q13. Although mouse *Arhgap8* gene shares an identical exon/intron organization to human *ARHGAP8*, it lacks an exon 5 equivalent and the 541 bp CpG island in its 5' region (Johnstone et al., 2004).

1.3.1 BPGAP1 and p50RhoGAP

BPGAP1 and p50RhoGAP are amongst the smallest RhoGAP proteins in the family and are most closely related to each other (Johnstone et al., 2004; Peck et al., 2002). With an identical domain organization, these two proteins share an overall approximate 54 % amino acid identity and 52 % identity within the RhoGAP domain itself. Conversely, BPGAP1 differs from p50RhoGAP such that it has a 44-amino acid extension C-terminal to the RhoGAP domain, whereas p50RhoGAP harbors extra 50 amino acids N-terminal to the BCH domain (Shang et al., 2003). While p50RhoGAP is ubiquitously expressed in the adult tissues tested including brain, colon, heart, kidney, liver, lung, placenta, small intestine, spleen, stomach and testis, albeit at a lower level in skeletal muscle; BPGAP1 is also present in all except brain, liver and spleen, with highest expression in kidney and placenta (Johnstone et al., 2004). Since both RhoGAP proteins possess the same genome organization with correspondingly identical domain architecture and a high overall amino acid identity, it is likely that these two genes have evolved from a common ancestor via gene duplication (Johnstone et al., 2004).

1.3.2 Expression of BPGAP1 is upregulated in colorectal and cervical cancers

The mapping of *ARHGAP8* to a region in human chromosome 22q13.31 that frequently exhibits loss-of-heterozygosity in colorectal and breast tumors (Castells et al., 2000; Castells et al., 1999) suggests that BPGAP1 may be implicated in these cancers. In mutational analysis of colorectal and breast tumors by PCR-SSCP (Polymerase chain reaction-single strand conformation polymorphism), six germline missense variants were identified, whereas no somatic mutation have been detected (Johnstone et al., 2004). Even though epigenetic silencing of *ARHGAP8* in tumors may occur through hypermethylation of the 5' CpG island, this is not the case and surprisingly, ARHGAP8 mRNA is found to be overexpressed in the majority of colorectal tumors. This upregulation occurs irrespective of tumor location, stage or level of differentiation (Johnstone et al., 2004). Recently, increased transcription of *ARHGAP8* is also detected in cervical cancer (Song et al., 2008). While upregulation of *ARHGAP8* may potentially constitute a negative feedback loop to counteract overexpression of Rho GTPases in these cancers (Johnstone et al., 2004), it is also possible that BPGAP1 may play a role in cancer progression, in accordance to studies which demonstrate that BPGAP1 has the ability to promote prolonged ERK activation and cell migration (Lua and Low, 2004; Lua and Low, 2005a; Shang et al., 2003).

1.3.3 Multi-domain nature of BPGAP1 mediates its functions

BPGAP1 harbors a domain organization characterized by a N-terminal protein-protein interaction domain - BCH/Sec14p-like domain that also possess lipid binding properties, followed by a proline-rich motif that potentially contain more than one consensus sequence PXXP for binding to SH3 and lastly a C-terminal RhoGAP domain with a highly conserved arginine residue (Figure 1.10) (Shang et al., 2003).

This multi-domain nature of BPGAP1 therefore presents a new array of potential functions in association with these functional modules that may serve to regulate its primary function as a RhoGAP, dictate its subcellular localization or integrate multiple signaling pathways. These domains may act either independently or in unison to bring about their designated cellular effects. Thus far, studies on BPGAP1 have implicated it with enhancing cell migration (Lua and Low, 2004; Shang et al., 2003) and induction of ERK activation (Lua and Low, 2005a; Pan et al., 2010), mediated through interactions with the various identified partners. Functions of BPGAP1 brought about by its domains will be described in the following sections.

1.3.3.1 BPGAP1 functions biochemically as a RhoA GAP and regulates cell morphology via its BCH and GAP domains

To fulfill its role as a negative regulator of Rho GTPase function, the GAP domain of BPGAP1 harbors an invariant arginine residue at position 232. Mutation of this conserved arginine residue to alanine (R232A mutant) abolishes its RhoGAP activity (Shang et al., 2003), consistent with the critical role of a canonical arginine finger in the GAP domain for catalyzing GTP hydrolysis. *In vitro* analysis of the activity level of RhoA, Rac1 and Cdc42 reveals that BPGAP1 is active towards RhoA and Cdc42, with a significant preference for the latter. Such activity, however, is not observed for Rac1 (Shang et al., 2003). While it has been demonstrated for some RhoGAPs that the *in vitro* substrate profile may not truly reflect the *in vivo* substrate selectivity (Ridley et al., 1993), *in vivo* analysis has indeed indicated that BPGAP1 exerts its GAP activity solely on RhoA despite the ability of BPGAP1 to also form complexes with Rac1 and Cdc42 (Shang et al., 2003).

As a mainly cytosolic protein, ectopic expression of BPGAP1 induces the formation of distinctive short and long protrusions (pseudopodia) via its BCH and GAP domains, respectively. These unique cellular morphological changes are mediated through a GAP-dependent mechanism that attenuates RhoA signaling and also via an unknown mechanism that involve signaling downstream of active Cdc42 and Rac1, as demonstrated by the use of constitutive active and dominant negative mutants of these Rho GTPases (Shang et al., 2003). Therefore, inactivation of RhoA by the GAP domain generates long protrusions, whereas active Cdc42 or Rac1 contributes to the induction of short, branched extensions.

1.3.3.2 BPGAP1 facilitates cell migration via concerted interplay of its functional modules for cell morphological changes and translocation of cortactin to the cell periphery

In line with the generation of cellular protrusions, BPGAP1 also serves to promote cell migration. Despite omission of the need for proline-rich region in inducing cellular morphological changes, its presence is required to trigger cell motility (Shang et al., 2003). This absolute requirement of the proline-rich region in BPGAP1-induced cell migration could potentially imply the involvement of other interacting partners since this motif may mediate binding to SH3, WW and Enabled/VASP homology domains (Zarrinpar et al., 2003). As predicted, cortactin, which contains a C-terminal SH3 domain and functions as a molecular scaffold protein that mediates actin cytoskeleton assembly and organization (Lua and Low, 2005b), is identified as an interacting partner of BPGAP1 along with many others as revealed by proteomics.

Further analyses demonstrate that cortactin is indeed a *bona fide* target of BPGAP1 and their interaction occurs through the consensus PXXP motif within the proline-rich region of BPGAP1, with proline residues 184 and 186 being the critical residues (Lua and Low, 2004). In addition, cortactin is shown to translocate to the cell periphery, accompanied by an increase in filamentous actin assembly in the presence of BPGAP1 but does not require growth factor stimulation. Cooperatively, BPGAP1 and cortactin enhance cell migration in epithelial cells, an effect that is not seen with increased expression of either protein alone (Lua and Low, 2004). As such, BPGAP1 may function to integrate cortactin and Rho GTPase signaling by facilitating the translocation of cortactin to the cell periphery, coupling changes in cell morphology to enhancement of cell migration (Figure 1.11).

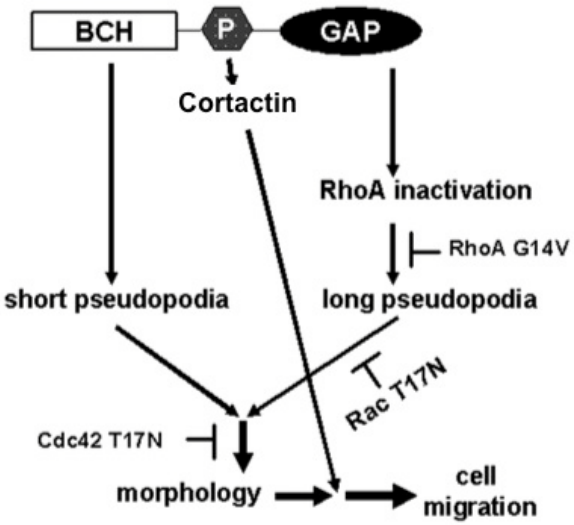

Figure 1.11 Model for BPGAP1-induced cell morphological changes and migration. BPGAP1 elicits the formation of unique short and long protrusions via its BCH and GAP domains, respectively, while the proline-rich region targets cortactin and facilitates its translocation to the cell periphery, thereby coupling changes in cell morphology to enhancement of cell migration. [Adapted from Shang et al., 2003; Lua and Low, 2004].

1.3.3.3 BPAGP1 activates EGF receptor endocytosis and ERK signaling, mediated by its functional RhoGAP domain and interaction with EEN/endophilin II

Identification of novel BPGAP1-interacting partners by proteomics has introduced an exciting means by which cellular functions of BPGAP1 can be uncovered. Following the characterization of cortactin, another protein known as extra eleven-nineteenth (EEN)/Endophilin II that belongs to the endocytic endophilin family has also been extensively studied for its interaction with BPGAP1. This family of proteins has been associated with regular cellular processes such as endocytosis and cell cycle, as well as implicated in pathological diseases including human leukemia and Huntington's disease (Lua and Low, 2005a).

Similar to cortactin, BPGAP1 interacts with the C-terminal SH3 domain of EEN via its proline-rich region through the canonical EEN-binding motif PPXRP in this instance, with Pro^{184} and Pro^{186} being the critical residues. While both BPGAP1 and EEN individually promote EGF receptor internalization, they function synergistically to augment this endocytic effect. Integration of signaling pathways of these two proteins has been demonstrated through utilization of a BPGAP1 mutant that is incapable of mediating direct interaction with EEN (PP mutant) or a dominant mutant of EEN that lacks its C-terminal SH3 domain (NT fragment), which shows that similar augmentation effect on EGF receptor endocytosis cannot be achieved when either mutant is coexpressed with the wild-type protein of the other. Moreover, use of the RhoGAP catalytic inactive mutant (R232A) is sufficient to cause a reduction in either BPGAP1-induced or EEN- and BPGAP1-induced EGF receptor internalization. Taken together, these results indicate that BPGAP1 enhances EGF

receptor endocytosis via concerted action of its interaction with EEN and its RhoGAP activity (Lua and Low, 2005a).

Although internalization of growth factor-bound receptors can serve either to initiate or terminate signaling (Le Roy and Wrana, 2005), the former applies to both BPGAP1- and EEN-induced EGF receptor endocytosis, leading to activation of MAPK pathway and ERK1/2 phosphorylation (Lua and Low, 2005a). The corresponding increase in levels of phosphorylated ERK1/2, as induced by BPGAP1 and EEN individually or collectively, is in accordance with their effect on EGF receptor endocytosis. While the dominant negative mutant of EEN exerts an inhibitory effect on BPGAP1-induced ERK1/2 phosphorylation in a similar manner to its effect on BPGAP1-induced endocytosis, both the non-interactive and RhoGAP inactive mutants still promote ERK1/2 phosphorylation while still exerting their inhibitory effect on EEN-induced ERK1/2 phosphorylation. Therefore, there exists an alternative mechanism by which BPGAP1 can facilitate phosphorylation of ERK1/2, independent of its direct interaction with EEN and the functional GAP domain. Indeed, BPGAP1 can activate MAPK pathway separately via its BCH domain, leading to ERK1/2 phosphorylation (Lua and Low, 2005a). In short, BPGAP1 and EEN function cooperatively to facilitate EGF receptor endocytosis through integration of RhoGAP and endophilin-mediated signaling pathways, thereby regulating Ras/MAPK pathway to promote ERK1/2 phosphorylation (Figure 1.12) (Lua and Low, 2005a).

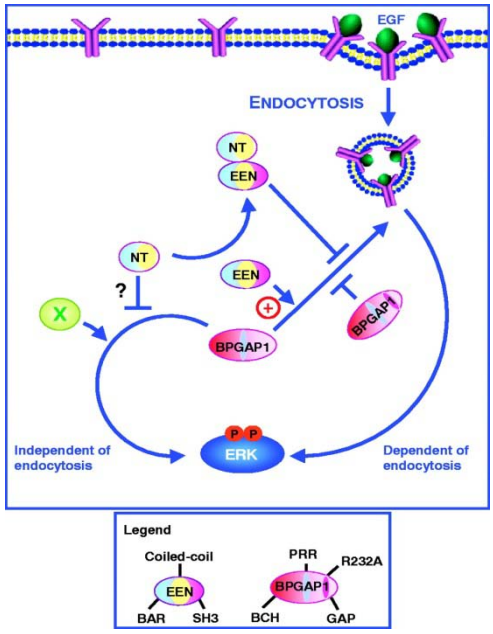

Figure 1.12 Model for BPGAP1- and EEN-mediated EGF receptor endocytosis and ERK1/2 phosphorylation. EGF receptor undergoes internalization upon EGF stimulation and triggers ERK1/2 phosphorylation. These processes are mediated by both BPGAP1 and EEN, either individually or synergistically through interaction between BPGAP1 proline rich region and SH3 domain of EEN. EEN devoid of its SH3 domain (NT) functions as a dominant negative mutant and completely inhibit the effects of BPGAP1 on receptor internalization and ERK1/2 phosphorylation. On the other hand, both non-interactive (PP) and GAP inactive (R232A) mutants reduce BPGAP1-, EEN-mediated, as well as BPGAP1- and EEN-coinduced endocytosis, indicating the requirement of GAP activity in this process. Since ERK1/2 phosphorylation can still occur in the presence of these mutants, this suggests that BPGAP1 can enhance ERK1/2 phosphorylation via an endocytosis independent pathway through its BCH domain. [Adapted from Lua and Low, 2005a].

1.3.3.4 Interaction between Pin1 and BPGAP1 mediated by active MEK2 suppresses BPGAP1-induced acute ERK activation and cell migration

While earlier work has established that BPGAP1 modulates cell migration dynamics and promotes ERK activation, a recent study identifies Pin1 as a negative regulator of BPGAP1 signaling at least in cell migration. Pin1 is a WW domain-containing peptidyl-propyl *cis*/*trans* isomerase and functions to modify protein conformations via its isomerase activity. Although the WW domain of Pin1 generally

recognizes and binds to its targets via a core motif containing a phosphorylated Ser/Thr followed by a proline residue (Lu et al., 1999), BPGAP1 and Pin1 interact through the type II WW domain-binding PPXP motif within the proline-rich region of BPGAP1, while the PPI domain of Pin1 targets the DDYGD motif of RhoGAP domain. Such interactions require the presence of active MEK2 as a scaffold (Pan et al., 2010).

When present in the cell, Pin1 can suppress BPGAP1-induced acute ERK activation in a GAP-independent manner, and attenuate Rho signaling by stimulating its RhoGAP activity. In addition, Pin1 is found to exert a negative effect on cell migration induced by BPGAP1 and active MEK2. Taken together, it is possible that Pin1 simultaneously downregulates both ERK and Rho signaling, hence suppressing BPGAP1- and MEK2-coinduced cell motility (Pan et al., 2010).

Thus far, understanding on the regulation and functions of BPGAP1 has arisen from the associations between proline-rich motif of BPGAP1 and its interacting partners. Analysis on properties of the protein-protein interaction domain - BCH domain, may therefore provide the basis for further exploration of BPGAP1 functions and regulation.

1.4 Family of BCH domain-containing proteins

First identified as a novel functional module more than a decade ago, BCH domain is discovered as a region of homology shared by both BNIP-2 and Cdc42GAP/p50RhoGAP, and hence termed as BNIP-2 and Cdc42GAP homology (BCH) (Figure 1.13) (Low et al., 1999; Low et al., 2000a; Low et al., 2000b). This unique protein domain comprises approximately 150 amino acids and is evolutionarily conserved among many organisms such as *Saccharomyces cerevisiae*, *Caenorhabditis elegans*, *Homo sapiens* and *Aradidopsis thaliana*, indicative of an important physiological function confers by this domain (Low et al., 2000a). Early studies have shown that BCH domain is a protein-protein interaction domain capable of mediating homophilic and heterophilic interactions between same and different proteins harboring this domain, respectively (Low et al., 2000a; Shang et al., 2003). In addition, this domain contains specific motifs that allow binding to Rho GTPases (Low et al., 2000b; Zhou et al., 2010; Zhou et al., 2005), confer non-canonical GAP activity *in vitro* (Low et al., 1999; Low et al., 2000b) or for establishing autoinhibitory intramolecular interaction (Moskwa et al., 2005).

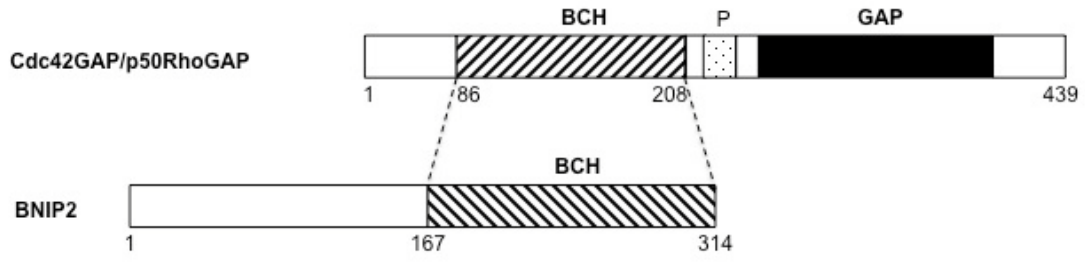

Figure 1.13 Schematic diagram of homologous BCH domains in Cdc42GAP/p50RhoGAP and BNIP-2. BCH domains within BCH domain-containing proteins mediate protein-protein interactions. [Adapted from Low et al., 1999; 2000a].

1.4.1 BCH domain: a distinct subset of Sec14 superfamily

Intriguingly, bioinformatics analysis has revealed that BCH domain shares subtle homology of less than 20 % with a lipid binding module known as Sec14 domain, thereby bringing BCH domain-containing proteins under the wing of Sec14 superfamily (Low et al., 2000a). The yeast Sec14p is the prototypic representative of this superfamily and functions as a transport protein for phosphatidylinositol (PtdIns) and phosphatidylcholine (PtdCho) (Mousley et al., 2007; Saito et al., 2007; Schaaf et al., 2008). This same domain is also known as CARL_TRIO domain in the mammalian counterparts, named after the two proteins containing this module – cellular retinaldehyde binding protein and Trio protein (Saito et al., 2007). However, this PtdIns transport function of Sec14p in higher eukaryotes has been assumed by another group of structurally unrelated family of PtdIns transfer proteins (PITPs). Nevertheless, Sec14 domain still retains lipid-binding ability and some may have evolved for carrying out more specialized transport functions that are vital for the maintenance of organelle physiology (Saito et al., 2007). Indeed, the biological significance of members in the Sec14 superfamily in mammals is reflected by the association of human diseases with dysfunctions of Sec14 domain in these proteins, which include autosomal-dominant cancers linked to reduced level of neurofibromin, ataxia due to loss of function of caytaxin/BNIP-H and retinal degeneration syndromes as a consequence of CRALBP deficiencies (Bankaitis et al., 2010).

Annotated in the NCBI database are approximately 1550 Sec14 domain-containing proteins (Bankaitis et al., 2010) of which some are Sec14-like, while others are multi-domain proteins including those that can function as protein tyrosine phosphatases (PTP-MEG2), RhoGAP (p50RhoGAP), RhoGEFs (Trio, Dbl, Duo) and RasGAP (NF1) (Bankaitis et al., 2010; Saito et al., 2007). Given the limited

homology of BCH domain with Sec14 domain and the ability of BCH domain to mediate protein-protein interactions in addition to lipid binding properties, it is possible that BCH domain-containing proteins have diverged sufficiently from the Sec14 superfamily to constitute a distinct subset (Low et al., 2000a). Two different domain organizations with respect to BCH domain have been described such that proteins with their BCH domain located at the C-terminal are of type I distribution, whereas those of type II distribution have a N-terminal BCH domain that precedes a GAP domain at the C terminus (Low et al., 2000a).

1.4.2 BNIP-2 is the prototype of BNIP-2 family of BCH domain-containing protein

Termed as Bcl-2 and E1B Nineteen kDa Interacting Protein 2, BNIP-2 is first cloned and identified as a cellular interacting partner of adenovirus E1B 19 kDa protein using yeast two-hybrid screen (Boyd, 1994). By utilizing the same screening system, this protein is later found to be a putative substrate of fibroblast growth factor (FGF) receptor and can be tyrosine phosphorylated upon growth factors stimulation, which negatively regulates its interaction with other proteins (Low et al., 1999). BNIP-2, which consists of 314 amino acids, has a simple molecular architecture comprising of a single EF-hand calcium-binding motif at the N-terminal region and a then newly described BCH domain at its C-terminal. Strikingly, this protein localizes in the cytosol in a punctate manner and concentrates at the leading edge of cell protrusions (Zhou et al., 2005), as well as in the nuclear envelope/endoplasmic recticulum region (Boyd, 1994).

1.4.2.1 BNIP-2 induces cell elongation and membrane protrusions via Cdc42 signaling

With only a single recognizable domain, much attention has been focused on the BCH domain when characterizing BNIP-2. Indeed, it has been demonstrated that through the BCH domain, BNIP-2 is capable of forming homodimer with itself and heterodimer with p50RhoGAP/Cdc42GAP via the region ^{217}RRKMP^{221} (Low et al., 2000a). Apart from p50RhoGAP, BNIP-2 also binds to Cdc42 using a separate region within the BCH domain that corresponds to residues 285 to 292 (Low et al., 2000b).

Interestingly, while transient expression of BNIP-2 or its BCH domain alone was able to elicit cellular morphological changes, distinctively cell elongation and membrane protrusions, non-interacting BNIP-2 mutant devoid of the Cdc42-interacting motif and mutants lacking the immediate upstream sequence of 34 amino acids failed to promote such changes. Furthermore, since BNIP-2-induced morphological changes can be abolished by inhibiting the Cdc42 signaling pathway using Cdc42 dominant negative mutants T17N and PAK-CRIB (Cdc42 and Rac1 Interacting Binding) domain but not by blockage of the association of BNIP-2 with Cdc42GAP using a non-interacting BNIP-2 mutant, this establishes that the observed effect of BNIP-2 on cell morphology is mediated by Cdc42 signaling without the involvement of Cdc42GAP (Figure 1.14) (Zhou et al., 2005).

With the inhibition of BNIP-2-induced cell elongation and membrane protrusions, the unique distribution of BNIP-2 in punctate spots and its concentration at the leading edge of membrane protrusions was replaced by a more diffused appearance. As such, it is possible that cell protrusions elicited by BNIP-2 are coupled to its translocation (Zhou et al., 2005). Of note, although BNIP-2 displays *in vitro* catalytic GAP activity towards Cdc42 via a non-canonical arginine patch within its

BCH domain (Low et al., 2000b), such enhancement of Cdc42 GTPase activity is not detected *in vivo* and is not conferred by the BCH domain of Cdc42GAP (Zhou et al., 2005).

a

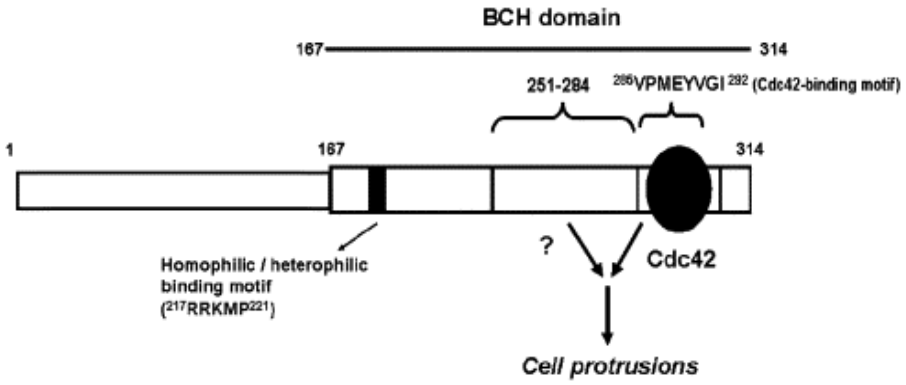

b

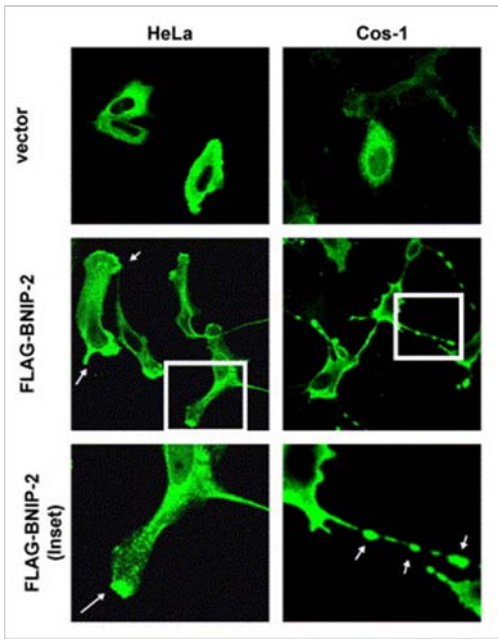

Figure 1.14 BNIP-2 induces cell elongation and membrane protrusions. (a) BNIP-2 BCH domain mediates homophilic interaction to itself, heterophilic interaction to Cdc42GAP, and signals to Cdc42 to induce membrane protrusions via distinct motifs. (b) Cells transfected with BNIP-2 display unique BNIP-2 distribution in punctate spots and also concentrates at the leading edge of membrane protrusions. [Adapted from Zhou et al., 2005].

1.4.2.2 BNIP-2 functions as a scaffold to facilitate integration of Cdc42 signaling and p38α/β MAPK activity during myogenic and neuronal differentiation

In more recent studies, use of siRNA has demonstrated the requirement of BNIP-2 in both myogenic and neuronal differentiation, downstream of receptor Cdo (Kang et al., 2008; Oh et al., 2009). Cdo is a cell surface receptor belonging to Immunoglobulin (Ig) superfamily and is highly expressed in both myoblast and neuronal progenitors (Oh et al., 2009). It has previously been established that during myogenesis, Cdo binds via its intracellular region to JLP, a scaffold protein for p38α/β MAPK pathway, which in turn binds p38α/β (Takaesu et al., 2006). Through downstream activation of p38α/β MAPK pathway mediated by these interactions, this leads to the phosphorylation of E proteins that are heterodimeric partners of lineage-specific bHLH (basic helix-loop-helix) transcription factors, and other proteins that regulate myogenesis. Subsequent heterodimerization of specific E protein and bHLH transcription factor thereby induces gene expression essential for myogenic differentiation (Kang et al., 2008; Oh et al., 2009).

Independent of JLP, Cdo also associates with BNIP-2 through a 31-amino acid region (residues 261-292) in the BCH domain. In C2C12 cells, induction of BNIP-2 expression promotes myotube formation and increases the level of muscle-specific protein markers, whereas downregulation of BNIP-2 proteins by siRNA leads to an opposite effect. Such positive effect on myogenic differentiation induced by BNIP-2 is dependent on its interaction with both Cdc42 and Cdo as demonstrated with the respective non-interacting mutants. In addition, Cdc42 activity level, which is required for myogenesis, varies correspondingly with the protein levels of BNIP-2 and Cdo in differentiating C2C12 cells and myoblasts in a positive manner. Consistently, alteration of Cdc42 activity through expression of Cdc42GAP or

BPGAP1 impairs myogenesis, whereas introduction of siRNA against Cd42GAP promotes myogenesis. With the activation of p38α/β MAPK downstream of Cdc42 signaling, this implies that Cdo by coordinating mutual interactions with both BNIP-2 and JLP, integrates signaling of Cdc42 to p38α/β as mediated by Cdo-BNIP-2-Cdc42 and Cdo-JLP-p38α/β interactions (Kang et al., 2008). A similar mechanism is also involved in neuronal differentiation (Oh et al., 2009). Taken together, BNIP-2 may function as a scaffold protein for dynamic regulation of Cdc42 signaling (Figure 1.15) (Kang et al., 2008).

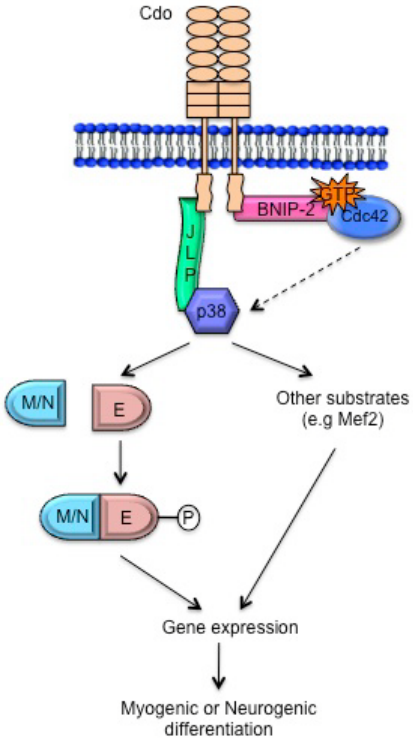

Figure 1.15 Model of Cdo-mediated p38α/β activation leading to myogenic or neurogenic differentiation. Cdo induces myogenic or neurogenic differentiation in lineage-specific cells via concerted action of scaffold proteins JLP and BNIP-2 that bind p38α/β and Cdc42, respectively, thereby promoting activation of p38α/β downstream of active Cdc42. Heterodimerization of phosphorylated E protein with myogenic or neurogenic basic helix loop helix (bHLH) factors (M/N) subsequently triggers expression of genes necessary for myogenic or neurogenic differentiation. [Adapted from Kang et al., 2008; Oh et al., 2009].

1.4.2.3 BNIP-2 is a potentially pro-apoptotic protein

Following the discovery of BNIP-2 as an interacting partner of Bcl-2 and p19 E1B pro-survival factors, several studies have implicated BNIP-2 as a pro-apoptotic protein. For instance, *BNIP-2* gene is found to be downregulated in SK-ER3 neuroblastoma cells upon 17 beta-estradiol treatment which confers neuroprotection. On the other hand, overexpression of BNIP-2 in these neuroblastoma cells triggers massive cell death, which can be counteracted by cotransfection of Bcl-2, indicating that BNIP-2 and Bcl-2 act in an opposing manner. The anti-apoptotic effect of estrogen in decreasing *BNIP-2* expression also delays TNFα-induced apoptosis in non-neuronal cells such as MCF-7 epithelial cells and U937 monoblastoid cells (Belcredito et al., 2001). Similarly, a decrease in *BNIP-2* expression is detected in murine lung adenomas and carcinomas, suggesting a decrease in apoptotic signaling during cancer development (Bonner et al., 2004).

Furthermore, cleavage of BNIP-2 by caspases during apoptosis induced in MCF-7 cells has also been reported, with the region I^{80}DLDGLDT identified as the putative cleavage site. This motif harbors two potential cleavage sites including D^{83}GLD$^{\downarrow}$T that can be recognize by caspase-3 and I^{80}DLD$^{\downarrow}$G which can be recognized by caspase-6 and caspase-8 (Valencia et al., 2007). More recently, a candidate granzyme B cleavage site has also been proposed using bioinformatics analysis. While it is demonstrated that BNIP-2 can be cleaved by granzyme B *in vitro*, cleavage of endogenous BNIP-2 is also detected in tumor cells that are subjected to killing by nature killer cells (Scott et al., 2010). Although majority of the studies have implicated *BNIP-2* as a pro-apoptotic gene whose upregulation is associated with apoptosis, downregulation of this gene has also been reported in neutrophils, coincident with their apoptosis (Kobayashi et al., 2005).

1.4.3 BCH domain-containing proteins regulate various aspects of cellular dynamics

Amongst the many BCH domain-containing proteins, a few including BNIP-2, BNIP-H (BNIP-2 Homology), BNIP-Sα (BNIP-2 Similar), BNIPXL (BNIP-2 extra long), p50RhoGAP and BPGAP1 have been extensively characterized by members in our laboratory. These BCH domain-containing proteins, whose functions are elicited mainly by their respective BCH domains, are implicated in a spectrum of cellular processes as shown in Figure 1.16. Although different BCH domains can mediate diverse aspects of cellular dynamics, many of them are involved in the regulation of Rho GTPase signaling, which will be further discussed in the following section.

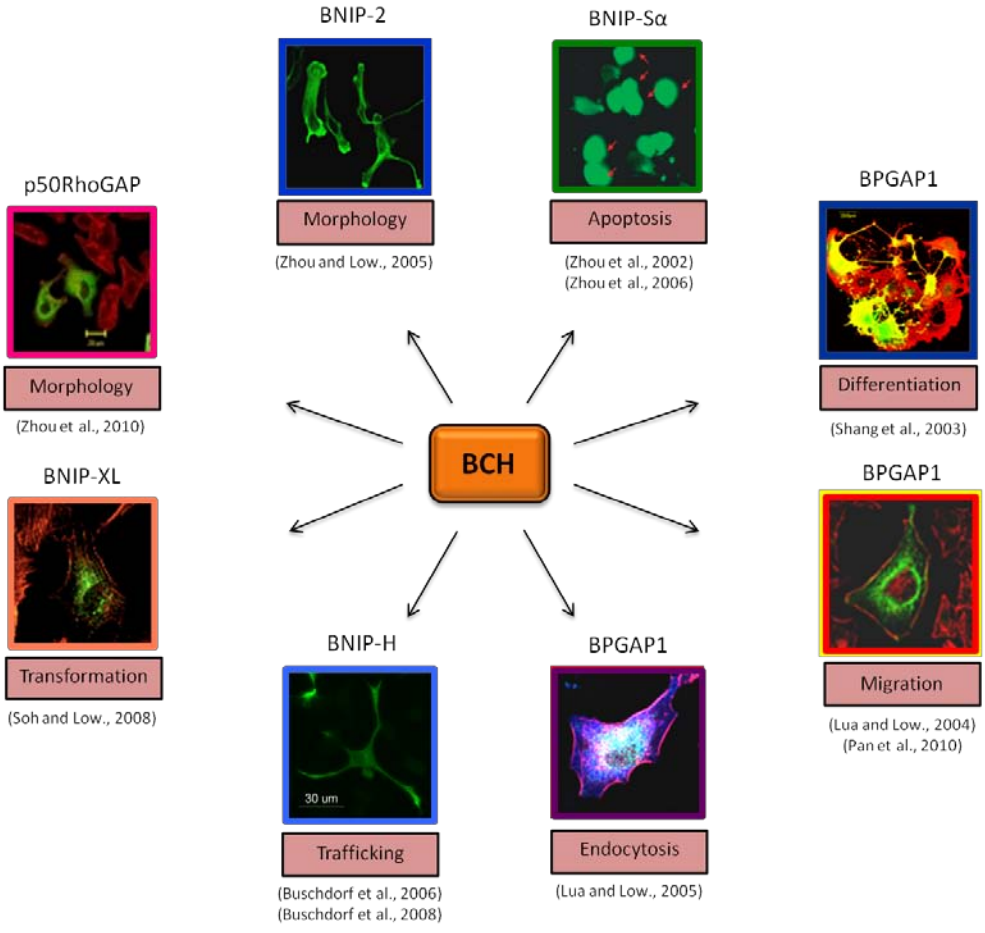

Figure 1.16 BCH domain-containing proteins and their functions. Members of the BNIP-2 and p50RhoGAP families of BCH domain-containing proteins mediate diverse aspects of cellular dynamics, mainly via the highly conserved BCH domain.

1.4.4 BCH domain functions as a new class of regulatory domain for GTPases signaling

From the numerous studies on BCH domain-containing proteins, there are increasing evidences that these different BCH domains participate in mediating and regulating Rho GTPases signaling, thereby leading to their designated cellular effects. As discussed previously, BNIP-2 BCH domain elicits cell elongation and membrane protrusions by signaling to Cdc42, and promote myogenic and neurogenic differentiation downstream of Cdo receptor by coupling Cdc42 signaling to activation of p38α/β. Other members of the BNIP-2 family, such as BNIP-Sα and BNIPXL, have also been shown to regulate RhoA signaling in concert with their cognate regulators, p50RhoGAP and Lbc (Lymphoid blast crisis) RhoGEF, respectively.

For BNIP-Sα, its BCH domain harbors a RhoA binding region that interacts specifically with RhoA and another overlapping region that mediates heterophilic interaction with BCH domain of p50RhoGAP, an inactivator of RhoA signaling. These overlapping yet specific binding motifs result in a tripartite competition whereby BNIP-Sα competes with and sequesters p50RhoGAP from binding to RhoA, hence preventing RhoA inactivation. Separately, BNIP-Sα can induce RhoA activation through its BCH domain. Therefore, BNIP-Sα acts by displacing p50RhoGAP and facilitating RhoA activation to promote cell rounding and apoptosis through its BCH domain (Figure 1.17a) (Zhou et al., 2006).

In another example, BNIPXL reduces the level of active RhoA through its ability to associate with both RhoA and a RhoA-specific RhoGEF – Lbc, via its BCH domain, thus preventing RhoA activation by competing away Lbc. Moreover, the N-terminal region of BNIPXL without its BCH domain can also associate with the proline-rich motif of Lbc to exert an inhibitory effect on cellular transformation.

Taken together, BNIPXL inhibits RhoA activation via its BCH domain by sequestering Lbc, thereby suppressing Lbc-induced cellular transformation (Figure 1.17b) (Soh and Low, 2008).

While there are ample examples of BCH domain functioning as a regulatory domain for Rho GTPases signaling that it is likely to act in concert with other immediate regulators such as RhoGAP and RhoGEF, a few studies also show that BCH domain can serve as a regulatory module when present *in cis* within the molecule. p50RhoGAP, which has a BCH domain at its N terminus and a C-terminal RhoGAP domain, exists in an autoinhibited state as mediated in part by an intramolecular interaction region within its BCH domain (Moskwa et al., 2005). A recent study further demonstrates that this BCH domain-mediated inhibition of the adjacent RhoGAP activity requires an essential RhoA-binding moiety within the BCH domain, without which the RhoGAP domain is free to target RhoA for inactivation. This absolute requirement of the RhoA-binding moiety in BCH domain for regulating RhoGAP activity is complemented by the previously identified intramolecular interaction region. Intriguingly, the BCH domain of p50RhoGAP exerts its inhibitory effect only when *in cis* but not *in trans*. Taken together, BCH domain of p50RhoGAP binds RhoA through its RhoA-binding motif and sequesters it from inactivation by the adjacent RhoGAP domain (Figure 1.17c) (Zhou et al., 2010).

a

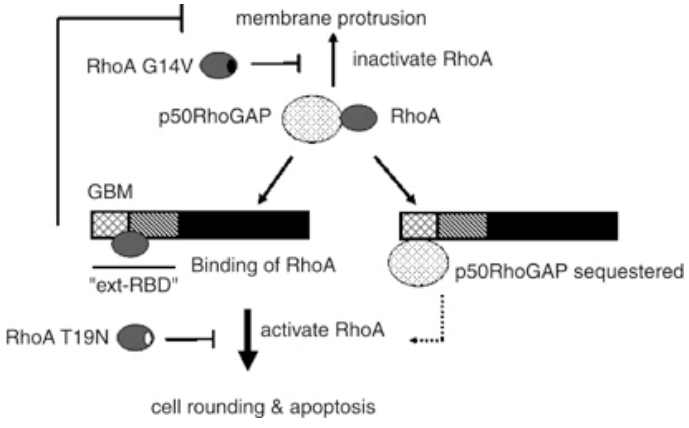

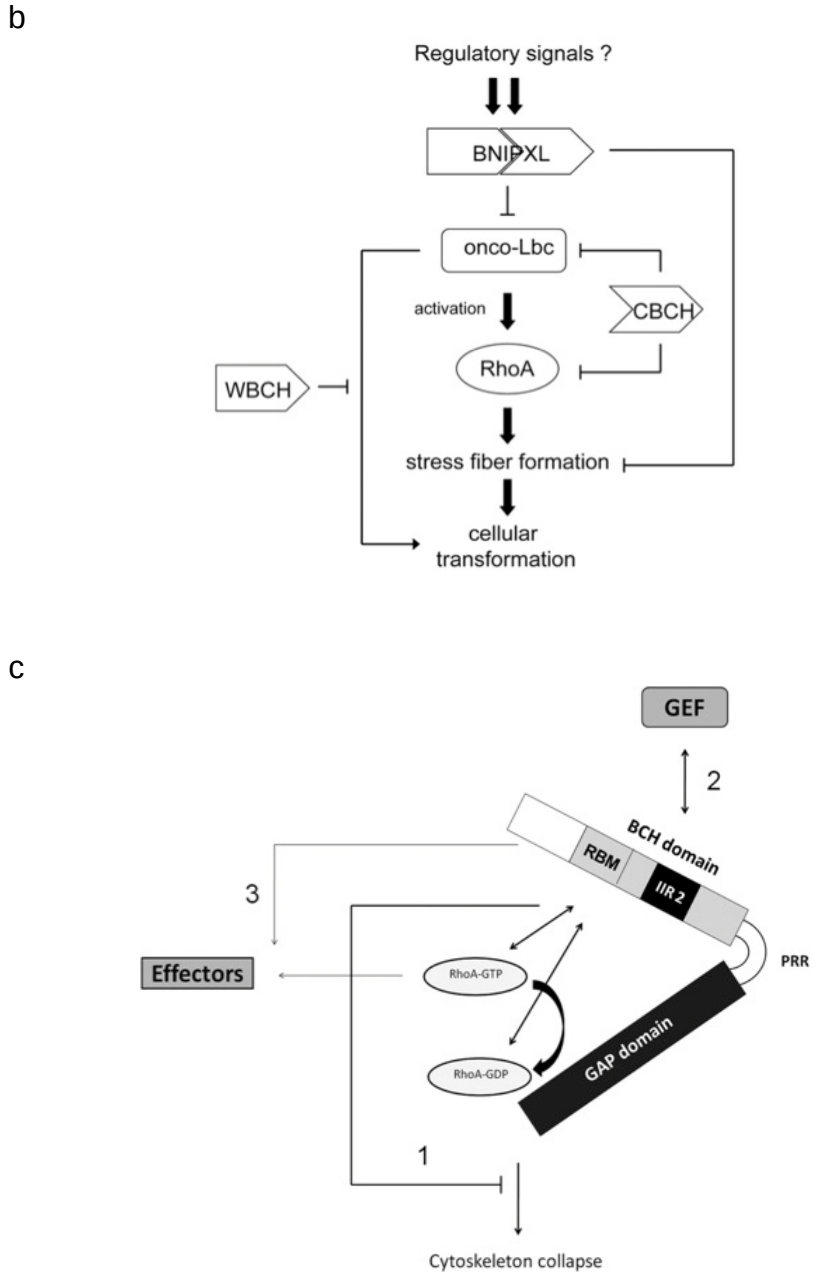

Figure 1.17 BCH domain functions as a regulatory module for Rho GTPases signaling. (a) BNIP-Sα, through overlapping regions in its BCH domain, interacts with both RhoA and p50RhoGAP in a mutually exclusive manner. As such, BNIP-Sα facilitates RhoA inactivation to promote cell rounding and apoptosis in part by sequestering p50RhoGAP and by displacing p50RhoGAP from RhoA. (b) Similar to BNIP-Sα, BNIP-XL BCH domain mediates interaction with RhoA and sequesters another of its immediate regulator, Lbc RhoGEF. These interactions suppress RhoA activation and lead to stress fibers disruptions and inhibition of cellular transformation triggered by oncogenic Lbc. (c) BCH domain of p50RhoGAP inhibits the activity of its adjacent GAP domain *in cis* by associating with RhoA via the RhoA-binding motif, which is further complement by intramolecular interactions existing within the BCH and GAP domains [Adapted from Zhou et al, 2006; Soh and Low, 2008; Zhou et al., 2010].

1.5 Hypothesis and objectives

Along with the identification of BCH as the conserved region of homology between BNIP-2 and p50RhoGAP/Cdc42GAP and a novel protein-protein interaction domain that is capable of mediating homophilic interaction with itself and heterophilic interaction with other homologous BCH domains, it is established that BNIP-2 with type I BCH domain distribution has the ability to interact with p50RhoGAP that is of type II BCH domain organization (Low et al., 1999), as suggested by Boyd et al. (1994). In terms of function, association of BNIP-2 and p50RhoGAP is required neither in BNIP-2-induced cell elongation and membrane protrusions (Zhou et al., 2005), nor in BNIP-2-facilitated myogenic and neuronal differentiation (Kang et al., 2008). Heterophilic interactions between these two forms of BCH domain-containing proteins might therefore be involved in regulatory functions.

Indeed, mounting evidences from different studies on BCH domain-containing proteins have ascertained that BCH domains together form a class of regulatory module that mediates Rho GTPases signaling, which in turn govern multiple aspects of cellular dynamics. Notably, the regulatory effect of BCH domain extends not only to the Rho GTPases, but also to their immediate regulators - RhoGAPs and RhoGEFs. For instance, BNIP-Sα BCH domain mediates RhoA activation to induce cell rounding by displacement and sequestration of p50RhoGAP (Zhou et al., 2006), while BNIP-XL prevents RhoA activation by Lbc RhoGEF and inhibits cellular transformation via a similar mechanism (Soh and Low, 2008). Intriguingly, apart from regulation by accessory proteins, GAP activity of p50RhoGAP is also governed by intramolecular interactions and the adjacent BCH domain *in cis* (Zhou et al.,

2010), clearly demonstrating the importance of BCH domain as a regulatory module for BCH domain-containing proteins-mediated Rho GTPase signaling.

Apart from p50RhoGAP, BPGAP1 is another BCH domain-containing protein with a RhoGAP domain (Shang et al., 2003) and is held also by intramolecular interactions (Ravichandran and Low, unpublished). While this protein has been extensively characterized in terms of its functions, recent studies focus on its regulation by other interacting partners. In this regard, earlier work using immunoprecipitation studies with overexpressed proteins has shown that BNIP-2 interacts with BPGAP1. When introduced separately into cells, both BNIP-2 and BPGAP1 induced cellular protrusions (Shang et al., 2003; Zhou et al., 2005), indicating the possibility of their involvement in common downstream pathways or processes. Taken together and via a candidate approach, we hypothesize that BNIP-2 could potentially exert a regulatory function towards BPGAP1 through its BCH domain. With the ability of BCH domain-containing proteins to modulate RhoGAP activity and Rho GTPases signaling, we aim to decipher what impact does BNIP-2 and BPGAP1 interaction have in these aspects. Furthermore, is/are there any effect(s) on cell physiology that is/are conferred by BNIP-2-BPGAP1 signaling? To this end, this thesis work aims to:

i) ascertain that BNIP-2 and BPGAP1 interact endogenously;
ii) investigate the involvement of BNIP-2-BPGAP1 interaction in Rho GTPase signaling;
iii) determine the impact of BNIP-2 on BPGAP1 RhoGAP activity;
iv) delineate the domain(s) and specific region(s) essential for their binding; and
v) examine the cellular effect(s) mediated by BNIP-2-BPGAP1 interaction

By identifying regulators of BPGAP1 and along with the understanding on the mechanisms underlying its regulation, it is hoped that a greater insight on the modulation of BPGAP1-associated processes can be achieved.

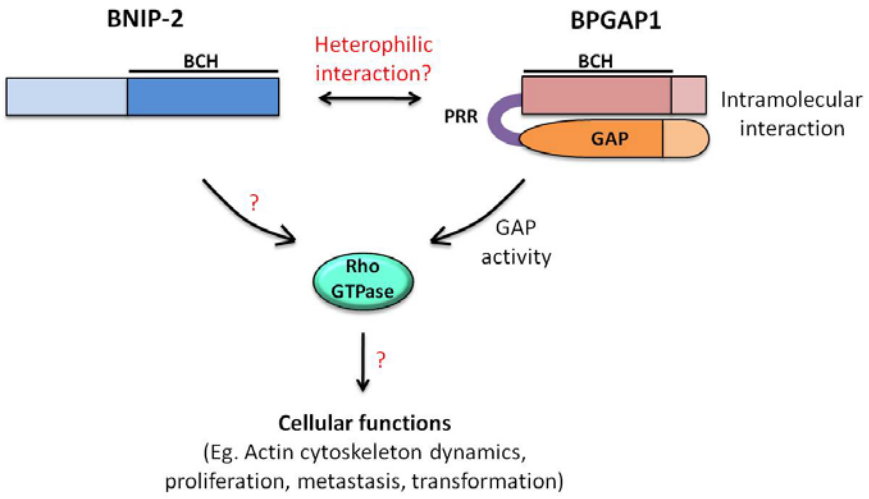

Figure 1.18 Schematic representation of the objectives in the study of BNIP-2 and BPGAP1 interaction.

Chapter 2

Materials and Methods

2 Materials and Methods

2.1 Generation of expression plasmids

2.1.1 Cloning and expression vectors

Constructs used in this study were kindly provided by colleagues for re-transformation and subsequent usage, cloning into expression vectors using Polymerase Chain Reaction (PCR) or sub-cloning. Identities of the cloned constructs were confirmed by DNA sequencing and their expressions in the mammalian cells were verified. For generation of internal deletion and domain truncation mutants, secondary structure analyses of BNIP-2 and BPGAP1 were carried out using Jpred, a secondary structure prediction server (available at http://www.compbio.dundee.ac.uk/www-jpred/), to avoid disruption of any recognizable secondary structure motifs such as α-helices and β-sheets. Two types of expression vector, pXJ40 and pGEX-4T-1, were utilized for inducing protein expression in mammalian and bacterial systems, respectively.

2.1.1.1 pXJ40 expression vector series

pXJ40 expression vector (courtesy of Dr. E. Manser, Institute of Molecular and cell Biology, Singapore), a 4.3 kb plasmid vector, can be differentially tagged to insert a FLAG epitope (DYKDDDDK), a hemagglutinin (HA) epitope (YPYDVPDYA) or other fluorescence protein sequences such as green fluorescence protein (GFP) at the N-terminal of the expressed protein. A pXJ40-mCherry vector encoding for fluorescence protein mCherry was generated for the purpose of this study. Expression of the target genes was driven by cytomegalovirus (CMV) promoter and enhancer flanking the multiple cloning sites (MCS). The vector also

harbors a β-globin intron to improve gene expression in mammalian cells and an ampicillin-resistance gene to facilitate selection of the plasmids in bacteria.

2.1.1.2 pGEX-4T-1 expression vector

pGEX-4T-1 (Amersham Biosciences) is a 4.95 kb vector plasmid that contains a Glutathione S-Transferase (GST) gene immediately upstream of the MCS and this feature allows generation of a N-terminal GST-tagged fusion protein. Within the vector, there is an ATG start site in the GST gene, a ribosome-binding site controlled by *tac* promoter and inducible by 1 to 5 mM Isopropyl Thio-β-D-Galactoside (IPTG), an ampicillin-resistance gene, as well as a thrombin cleavage site that allows removal of the GST protein.

2.1.2 Polymerase Chain Reaction

For designing of primers used in PCR, online program NEBcutter V2.0 (http://tools.neb.com/NEBcutter2/) was utilized to search for restriction enzymes that do not cut the sequence in query and BioMath Calculators available on Promega website (http://www.promega.com/biomath/) was employed to calculate the melting temperatures (T_m) of oligonucleotides. PCR was performed using plasmid constructs as templates and the respective designed primers as listed in Table 2.1. In general, a 50 µl reaction was set up to contain the template, 0.2 nM of dNTPs, 0.2 µM each of forward and reverse primers, 1 x DyNAzyme EXT buffer and 1 U of high fidelity DyNAzyme EXT DNA polymerase (Finnzymes). For templates longer than 1 kb, 2.5 U of Pfu Turbo DNA polymerase (Stratagene) and its corresponding 1 x buffer were used instead. PCR reaction was carried out in a thermal cycler (BioRad) under the following cycling conditions: an initial denaturation step at 94 ^{o}C for 2 mins, followed

by 30 iterative cycles of denaturation at 94 ^{o}C for 30 s; annealing at the appropriate T_m for 30 s and extension at 72 ^{o}C for 40 s/kb, and a last step of final extension at 72 ^{o}C for 10 mins before maintaining the mixture at 4 ^{o}C.

Table 2.1 Primer sequences used for cloning. The template and primer sequences used for cloning the various constructs are listed as follow. **F**: Forward; **R**: Reverse.

Construct name	**Template**	**Primer Sequence**
BNIP-2 Δ167-184	FLAG-BNIP-2	**F**: 5' CCC CTC GAG TAC CTG ATG GAC AAT CTT TTT AAA 3'
		R: 5' CCC CTC GAG GGC ATT TAA TCC ATC CCC ATA ATA 3'
BNIP-2 Δ185-211	FLAG-BNIP-2	**F**: 5' CCC CTC GAG AAT GGT GCA ACA ACT CGA AGA AAA 3'
		R: 5' CCC CTC GAG TCT ATA GTT AGG CTG ACT ACT TTC 3'
PGAP (168-281)	FLAG-BPGAP1	**F**: 5' CCC AAG CTT CAG AGC CTG CAC GAG GGC 3'
		R: 5' CCC C TC GAG CTA GGT CAG AAG CGG CTG 3'
PGAP (168-310)	FLAG-BPGAP1	**F**: 5' CCC AAG CTT CAG AGC CTG CAC GAG GGC 3'
		R: 5' CCC CTC GAG CTA GAG GCT CCG TAA GAT CTG 3'
pXJ40-mCherry vector	pmCherry-C1 vector (Clonetech Laboratories)	**F**: 5' AAA GAA TTC ACC ATG GTG AGC AAG GGC GAG GAG G 3'
		R: 5' AAA GGA TCC CTT GTA CAG CTC GTC CAT GC 3'
pXJ40-mCherry-BPGAP1	FLAG-BPGAP1	**F**: 5' CCC AAG CTT CG ACC ATG GCT GGC CAG GAT CCT 3'
		R: 5' CCC GGT ACC CTA GAG ACG TCT TCT GGC TGC CAT 3'
pXJ40-mCherry-BPGAP1(R232A)	FLAG-BPGAP1(R232A)	**F**: 5' CCC AAG CTT CG ACC ATG GCT GGC CAG GAT CCT 3'
		R: 5' CCC GGT ACC CTA GAG ACG TCT TCT GGC TGC CAT 3'

2.1.3 Agarose gel electrophoresis

Agarose gels of 1 to 2 % (w/v) were first casted by dissolving agarose (1st Base) in 1 x TAE buffer and SYBR®Safe DNA gel stain (Invitrogen Life Technologies) was added at a dilution of 1:50 000 for visualization of DNA bands under ultraviolet (UV) radiation. Separation of DNA fragments mixed with 6 x Loading Dye (Fermentas), alongside with either GeneRuler™ 100bp DNA ladder Plus or 1 kb DNA ladder (Fermentas), was carried out using agarose gel electrophoresis in 1 x TAE buffer [40 mM Tris-base; pH 8.0 with glacial acid, 10 mM EDTA].

2.1.4 Gel extraction

Images of the size-fractioned DNA bands after gel electrophoresis were captured using Quantity One 1-D analysis software of Molecular Imager Gel Doc XR system (BioRad). Alternatively, for gel extraction, DNA bands were visualized under the ultraviolet transilluminator at 50 % UV radiation and the desired bands were excised quickly using a sterile blade. DNA was extracted and purified using QIAquick gel extraction kit (Qiagen) in accordance with manufacturer's protocol.

2.1.5 Restriction enzyme digestion

Gel purified PCR products were digested at 37 ^{o}C for 4 to 8 hrs with 25 U each of the respective restriction enzymes predetermined during primer design. Each μg of vector plasmid was similarly digested with 4 U each of the restriction enzymes. All reactions were carried out in 1 x reaction buffer and/or BSA as recommended by manufacturer's instructions and with total enzyme composition not exceeding 10 % of the reaction volume. Restriction enzymes were selected base on their presence in the

MCS of vectors but yet do not cut within the sequence of interest. In general, the cloning sites used for generation of BNIP-2 constructs were *Hind III* and *Sma I,* while those used for BPGAP1 constructs were *Hind III* and *Xho I*. After digestion, the released fragments were separated using gel electrophoresis and the desired products were extracted and purified.

2.1.6 Ligation

Next, a ligation mixture comprising 200 U of T4 DNA Ligase (New England Biolabs), 1 x Ligase buffer, as well as insert DNA and vector DNA at a molar ratio of 3:1 was set up. For generation of internal deletion mutants, the insert and vector DNA were replaced by single restriction enzyme digested PCR product for self-ligation. The ligation reaction was carried out either at room temperature for 4 hrs or overnight at 4 ^{o}C.

2.1.7 Preparation of competent cells (*Escherichia coli* strain DH5α)

E. coli DH5α is a strain of bacteria commonly used for cloning due to presence of a mutation in the *endA* gene that reduces the level of endonuclease activity, thereby allowing production of high yield and high purity DNA. To prepare competent *E. coli* DH5α, bacteria cells were first streaked onto antibiotics-free Luria Bertani (LB) agar plate for overnight incubation at 37 ^{o}C. A single colony was then picked, inoculated into 5 ml of antibiotics-free LB broth and cultured overnight at 37 ^{o}C with constant agitation at 250 rpm. On the following day, starter culture was added into 50 ml of antibiotics-free LB broth at a dilution ratio of 1:500 and grown at 37 ^{o}C with shaking at 250 rpm until the optical density (OD) measured at 600 nm fell within the range of 0.3 to 0.6. Next, the bacteria culture was kept on ice for 10 mins and

centrifuged at 5500 rpm for 15 mins at 4 ^{o}C to pellet the cells. The cell pellet was reconstituted by gentle vortexing in 17 ml (approximately 1/3 of original culture volume) of ice-cold calcium/manganese based buffer (CCMB) [80 mM $CaCl_2 \cdot 2H_2O$, 20 mM $MnCl_2 \cdot 4H_2O$, 10 mM $MgCl_2 \cdot 6H_2O$, 10 mM KoAc, 10 % (v/v) glycerol; final pH 6.4] before further incubating on ice for 20 mins. Lastly, the bacteria suspension was centrifuged at 3000 rpm for 10 mins at 4 ^{o}C, after which the pellet was again resuspended in 4 ml (approximately 1/12 of original culture volume) of chilled CCMB. Aliquots of competent cells were snap-frozen in liquid nitrogen and stored at -80 ^{o}C.

2.1.8 Plasmid transformation into bacteria

2.1.8.1 Heat shock transformation

For cloning, ligated products were introduced into competent *E. coli* DH5α by heat shock transformation. A 100 µl aliquot of frozen competent cells was thawed on ice into which the ligated product was added and mixed gently by tapping. Next, the mixture was kept on ice for 30 mins and subjected to a brief heat-shock at 42 ^{o}C for 90 s. After heat shock, the mixture was immediately incubated on ice for 2 mins and 900 µl of antibiotics-free LB broth was added. The bacteria cells were then allowed to recover by incubating at 37 ^{o}C for 1 hr with constant shaking at 250 rpm. After recovery, these cells were briefly centrifuged at 800 rpm for 1 min. Excess LB broth was removed to concentrate the cells into 100 µl for plating onto LB agar containing 100 µg/ml of ampicillin. The plates were then incubated overnight at 37 ^{o}C.

2.1.8.2 Re-transformation by KCM

To propagate the plasmid DNA, DNA uptake into competent *E. coli* DH5α was facilitated by KCM method. A small volume of DNA of approximately 0.2 to 0.5 µl was added into 15 µl of pre-chilled KCM solution [100 mM KCl, 30 mM $CaCl_2$, 50 mM $MgCl_2$] and mixed with an equal volume of freshly thawed *E. coli* DH5α competent cells. The mixture was left on ice for 30 mins and plated on LB agar containing 100 µg/ml of ampicillin. The plates were then incubated overnight at 37 ^{o}C.

2.1.9 Plasmid extraction and purification

Single colonies of plasmid-containing bacteria grown successfully on ampicillin-containing LB agar plate were individually picked and inoculated into 5 ml of ampicillin-containing LB broth for growing overnight at 37 ^{o}C with constant agitation at 250 rpm. Subsequently, the bacteria culture may be used directly for plasmid DNA isolation and purification using Miniprep kit (Axygen or Qiagen) or as a starter culture for overnight culturing of a larger volume (50 ml) of bacteria to be used for extraction of plasmid DNA by Midiprep (Axygen or Qiagen), both according to manufacturer's instructions.

2.1.10 Quantification of plasmid DNA by spectrophotometry

After DNA extraction, the quantity and purity of plasmid DNA was assessed by spectrophotometry. Concentration of DNA can be calculated from the absorbance value at 260 nm, while a ratio of absorbance values at 260 nm and 280 nm (ratio 260/280) of within 1.8 to 2.0 indicates that the DNA is of high purity with minimum contamination. To determine DNA concentration, the plasmid DNA was diluted 200

times in deionized water, the same type of solvent used for DNA elution, and its absorbance was measured at 260 nm. Actual DNA concentrated was then calculated with the following formula: DNA concentration (μg/ml) = OD_{260nm} x dilution factor x 50 μg/ml.

2.1.11 Colony screening by PCR

Single colonies of bacteria grown on ampicillin-containing LB plate after heat shock transformation were screen using colony PCR for positive clones containing the desired plasmid constructs. In brief, single colonies were individually picked and resuspended in 10 μl of sterile deionized water for use as template in PCR. Reaction mixtures were set up as outlined in section 2.1.2 for DNA amplification with DyNAzyme II DNA polymerase (Finnzymes) under the following cycling conditions: an initial denaturation step at 94 ^{o}C for 2 mins, followed by 25 iterative cycles of denaturation at 94 ^{o}C for 30 s; annealing at 55 ^{o}C for 30 s and extension at 72 ^{o}C for 40 s/kb, and a last step of final extension at 72 ^{o}C for 10 mins. The amplified products were then resolved by agarose gel electrophoresis and visualized under UV. Positive colonies that contain the desired plasmid constructs were inoculated into 5 ml of antibiotics-containing LB broth and cultured overnight at 37 ^{o}C with shaking at 250 rpm for subsequent plasmid extraction and quantification as described in sections 2.1.9 and 2.1.10.

2.1.12 DNA sequencing

To confirm the identity and to determine the exact nucleotide sequence of the cloned plasmids, DNA sequencing reactions of 5 μl were set up to contain the following components: 50 to 125 ng plasmid, 0.8 μM each of T7 promoter forward

(5' TAATACGACTCACTAT 3') or pXJ40 reverse (5' GAGCGCAGCGAGTCAGTGAG 3') sequencing primers in separate reactions, 1 µl Big-Dye Terminator Ready Reaction Mix and 1 µl of 5 x sequencing buffer. Sequencing products were generated in 25 iterative cycles with each cycle composed of denaturation at 96 ^{o}C for 30 s, annealing at 55 ^{o}C for 15 s and extension at 60 ^{o}C for 4 mins. During ethanol precipitation of the products, 5 µl of PCR sample was added to 80 µl of precipitating solution [3 µl of 3 M Sodium acetate; pH 4.6, 62.5 µl of 95 % ethanol, 14.5 µl of deionized water] and incubated at room temperature for 10 mins. Precipitated DNA was centrifuged at 14 000 rpm for 10 mins and the DNA pellet was washed once with 500 µl of 75 % ethanol before centrifuging for another 5 mins at 14 000 rpm. Lastly, the DNA pellet was dried on 85 ^{o}C heat block for 1 to 2 min to remove any residual ethanol. To perform DNA sequencing, dried DNA pellet was reconstituted in 10 µl of HiDi formamide by vortexing and processed using the automated ABI PRISM 3130 Genetic Analyzer (Applied Biosystems). Sequencing results obtained were analyzed using DNAMAN sequence analysis software and BLAST (Basic Local Alignment Search Tool) program available on NCBI (National Center for Biotechnology Information) website (http://blast.ncbi.nlm.nih.gov/Blast.cgi).

2.1.13 Expression check of cloned constructs

Before carrying out experiments with the sequenced constructs, expression of proteins as encoded by these plasmids were first verified by transient transfection of the plasmid DNA into 293T cells as described in section 2.3.1 to obtain whole cell lysates for Western blot analysis as outlined in section 2.5.

2.2 Cell culture – Cell lines and maintenance

2.2.1 293T

Human embryonic kidney 293T epithelial cell (American Type Cell Culture), hereby referred as 293T, is a highly transfectable clonal derivative of 293 adherent cell line stably expressing simian virus 40 (SV40) large T-antigen. These cells were cultured as monolayer on surface treated tissue culture dishes (Nunc) in RPMI (Roswell Park Memorial Institute)-1640 medium (Hyclone Laboratories) supplemented with 10 % (v/v) defined fetal bovine serum (PAA Cell Culture), as well as 2 mM L-glutamine, 10 mM HEPES, 2 g/L sodium bicarbonate, 100 U/ml penicillin and 100 U/ml streptomycin (all from Hyclone Labratories) and maintained in humidified 5 % CO_2 incubator at 37 ^{o}C. For subculturing, the cell monolayer was trypsinized with 0.25 % trypsin-EDTA (Hyclone Laboratories) and harvested in serum-containing medium. An appropriate number of cells was seeded for subsequent experiments or general maintenance.

2.2.2 CHO and CV-1

Epithelial-like CHO (Chinese Hamster Ovary) is a cell line derived from the ovary of an adult Chinese Hamster (*Cricetulus griseus*), while CV-1 is propagated as fibroblast initiated from the kidney of a male adult African green monkey (*Cercopithecus aethiops*) (American Type Cell Culture). Both cell types were grown as monolayer on surface treated tissue culture dishes (Nunc) in high glucose DMEM (Dulbecco's modified Eagle's medium) supplemented with 10 % (v/v) defined fetal bovine serum (PAA Cell Culture), as well as 3.7 g/L sodium bicarbonate, 1 mM sodium pyruvate, 100 U/ml penicillin and 100 U/ml streptomycin (all from Hyclone Labratories) and maintained in humidified 5 % CO_2 incubator at 37 ^{o}C. To passage

the cells, cell monolayer was trypsinized using 0.25 % trypsin-EDTA (Hyclone Laboratories) and harvested in serum-containing medium. An appropriate number of cells was then seeded for subsequent experiments or general maintenance.

2.3 Transient transfection

2.3.1 293T and CHO

Transient introduction of plasmid DNA into 293T or CHO cells was performed using TransIT®-LT1 Transfection Reagent (Mirus Bio) in accordance to manufacturer's protocol. Cells were grown for 18 to 24 hrs to achieve a confluency of approximately 50 % to 80 % and the culture medium was replaced with fresh complete growth medium just prior to transfection. As recommended, 3 µl of transfection reagent was diluted in 100 µl of serum-free medium and let stand for 5 mins at room temperature. Care was taken to avoid any contact of the transfection reagent with walls of the plastic tubes. Next, 1 µg of high purity plasmid DNA was introduced into the pre-mixed solution and let stand for 20 mins at room temperature before being added drop-wise to the cells. The plates were swirled gently to ensure uniform distribution of transfection complexes and the cells were cultured for 18 to 24 hrs at 37 ^{o}C in a humidified 5 % CO_2 incubator.

2.3.2 CV-1

A confluency of approximately 50 % at the time of transfection was desired for CV-1 and these cells were grown in antibiotics-free medium for 18 to 24 hrs on 13-mm microscope cover glasses (EINST Technology) placed in 6-well cell culture dishes (Nunc). Just before transfection, the culture medium was replaced with serum-free medium without any antibiotics and Lipofectamine^{TM} 2000 (Invitrogen Life

Technologies) was used for transfection according to manufacturer's instructions. In brief, 2 μg of high purity plasmid DNA was added to 100 μl of Opti-MEM® I reduced serum medium (Gibco), while 4 μl of Lipofectamine transfection reagent was similarly diluted in 100 μl of Opti-MEM® medium and let stand for 5 mins at room temperature. Both solutions were later combined and further incubated for 20 mins at room temperature, after which it was added drop-wise to the cells. The plates were then swirled gently to ensure uniform distribution of transfection complexes and returned to 37 ^{o}C incubator with humidified 5 % CO_2. To reduce toxicity to cells due to transfection reagent, medium containing the transfection complexes was replaced with fresh growth medium without antibiotics 4 hrs post-transfection.

2.4 Immunoprecipitation studies

2.4.1 Preparation of mammalian whole cell lysates

293T cells plated on 6-well cell culture dishes were transfected with construct-containing expression plasmids or empty vectors as control as described in section 2.3.1. At time of harvest, medium was aspirated from each well and cells were lysed with 250 μl of chilled RIPA (Radio Immuno Precipitation Assay) lysis buffer [50 mM Tris-HCl; pH 7.3, 150 mM sodium chloride, 0.25 mM EDTA, 1 % (w/v) sodium deoxycholate, 0.2 % (w/v) sodium fluoride, 1 % (v/v) Trition X-100] freshly supplemented with 5 mM sodium orthovanadate, 25 mM glycerol phosphate and protease inhibitors cocktail (Roche Applied Science). Harvested lysates were vortexed briefly and centrifuged at 14 000 rpm for 15 mins at 4 ^{o}C. Without disturbing the cell debris pellet, the supernatant was transferred into fresh tubes for subsequent experiments.

2.4.2 Semi-endogenous pull down and immunoprecipitation

For semi-endogenous detection of protein-protein interaction, 5 µl of Glutathione Sepharose 4B beads (Amersham Biosciences) was added to a fraction of the whole cell lysates harvested from control cells or 293T cells transfected with either mammalian GST-tagged BPGAP1 or empty expression vector and incubated at 4 ^{o}C for 3 hrs with constant rotation to facilitate binding of GST-tagged protein complexes to the beads. Semi-endogenous immunoprecipitation was performed in a similar manner using harvested whole cell lysates of 293T cells transfected with FLAG-tagged plasmids and protein complexes were immunoprecipitated with 5 µl of anti-FLAG® M2 Affinity Gel (Sigma-Aldrich) instead. After incubation, the beads were washed thrice, each with 1 ml of chilled RIPA lysis buffer. Bound proteins were then denatured in Laemmli loading buffer [0.1 M Tris-HCl; pH 6.8, 15 % (v/v) glycerol, 3 % (v/v) SDS, 7.5 % (v/v) β-mercaptoethanol, 0.005 % (w/v) bromophenol blue] at 85 ^{o}C for 5 mins and separated by gel electrophoresis for Western blot analysis.

2.4.3 Co-immunoprecipitation

In co-immunoprecipitation studies, whole cell lysates of 293T cells co-transfected with FLAG- and HA-tagged expression plasmids were prepared as outlined in section 2.4.1. Similarly, 5 µl of anti-FLAG M2 beads was added to a portion of the supernatant and subjected to 3 hrs of immunoprecipitation at 4 ^{o}C with constant rotation. The beads were subsequently washed with ice-cold RIPA lysis buffer and heated in Laemmli loading buffer at 85 ^{o}C for 5 mins before running the samples on denaturing polyacrylamide gels for Western blot analysis.

2.5 Western blot analysis

2.5.1 SDS-PAGE (Sodium Dodecyl Sulphate - Polyacrylamide Gel Electrophoresis) and electrophoretic transfer

Protein samples were resolved for analysis using varying percentages of SDS polyacrylamide gels according to molecular weight (MW) of the proteins. Different percentages of resolving SDS-containing polyacrylamide gels containing the following components: 10 % to 15% (v/v) acrylamide solution [40 % acrylamide/bis solution, 29:1 (3.3 % cross-linker concentration)] (Biorad), 0.375 mM Tris-HCl; pH 8.8, 0.1 % (w/v) SDS, 0.0075 % (w/v) ammonium persulphate (APS) (Sigma) and 0.05 % (v/v) N, N, N', N'-tetramethylethylenediamine (TEMED) (Sigma) were first casted and allowed to polymerize. Next, stacking gel solution comprising 5% (v/v) acrylamide, 0.125 mM Tris-HCl; pH 6.8, 0.1 % (w/v) SDS, 0.0075 % (w/v) APS and 0.08 % (v/v) TEMED was prepared and overlaid on the solidified resolving gel.

Sets of protein samples were loaded alongside the Precision Plus pre-stained protein standards (BioRad) and gel electrophoresis was carried out in Mini-PROTEAN 3 electrophoresis system (BioRad) with 1 x electrophoresis buffer [25 mM Tris-base (1^{st} Base), 0.19 M glycine; pH 8.3, 0.1 % (w/v) SDS] at a constant current of 50 mA for 1 hr. After electrophoresis, the size-fractioned proteins were transferred onto PVDF membrane (Polyvinylidene fluoride Immobilon-P transfer membrane) (Millipore) in 1 x transfer buffer [33.7 mM Tris-HCl, 0.256 nM glycine, 20 % (v/v) methanol, 0.1 % (w/v) SDS] at 100 V for 1 to 1.5 hrs in 4^{o}C using Mini Trans-Blot electrophoretic transfer cell (BioRad).

2.5.2 Western blot detection

After completion of electrophoretic transfer process, the membranes were immersed in blocking buffer [1 x PBS (phosphate-buffered saline), 0.1 % (v/v) Tween 20, 1 % (w/v) Bovine serum albumin (BSA) (Sigma)] and placed on an orbital shaker for blocking either 1 hr at room temperature or overnight at 4 ^{o}C. Next, the membranes were incubated in primary antibodies diluted in blocking buffer for 1 hr at room temperature or overnight at 4 ^{o}C, with gentle shaking. To remove any non-specifically-bound antibodies, the membranes were rinsed 4 times with wash buffer (PBST) [1 x PBS, 0.1 % (v/v) Tween 20], each with 5 mins of constant agitation, before incubating with appropriate secondary antibodies diluted in wash buffer for an hour at room temperature on the orbital shaker. Similarly, these blots were rinsed in wash buffer after secondary antibody incubation to remove any non-specifically-bound antibodies and treated with Supersignal West Pico chemiluminiscent substrate (Thermo Scientific) to visualize the protein bands using either Kodak X-ray medical films (Eastman Kodak Company) or Fuji Super RX Blue medical X-Ray films (FUJIFILM Medical Systems USA).

For re-probing of membrane with other primary antibodies, the original membrane was first stripped off of the bound antibodies in the presence of stripping buffer (pH 2) [25 mM glycine, 1 % (v/v) SDS] and constant agitation. Subsequently, the membrane was washed multiple times to remove any residual stripping buffer and blocked in blocking buffer before repeating the entire process beginning from primary antibody incubation.

Common primary antibodies used for detection of tagged proteins in this study include polyclonal anti-FLAG (Sigma) [1:10 000] and polyclonal anti-HA (Zymed) [1:2500]. Other protein-specific primary antibodies such as anti-RhoA and anti-

PCNA (Santa Cruz Biotechnologies), anti-BNIP-2 and anti-BPGAP1 (purified in our laboratory), anti-phospho-Histone H3 (Millipore), anti-Histone H3 (Abcam) and anti-β-tubulin (Invitrogen Life Technologies) were also used. Common secondary antibodies used were anti-mouse IgG and anti-rabbit IgG (Sigma) [1:2500].

2.6 Antibody purification

Frozen sera of rabbits injected with His-tagged BNIP-2, obtained from one of our collaborators Dr. Lin Sheng-cai (Xiamen University, Xiamen, Fujian, China), or frozen sera of rabbits immunized with GST-tagged BPGAP1 by our colleague Dr. Lua B.L., were used for antibodies purification. To extract the respective antibodies, bacterially produced purified GST-BNIP2 proteins or His-tagged PGAP (proline-rich region and GAP domain of BPGAP1) fragment was resolved by SDS-PAGE gel electrophoresis and immobilized onto PVDF membrane as described in section 2.5.1. A single long band corresponding to the approximate size of the protein was excised from the membrane and further cut into smaller pieces of dimension 1 mm by 1 mm. These small pieces of membrane were transferred to a tube containing 1 ml of serum and incubated overnight at 4^{o}C with constant rotation. After removal of serum, the membrane pieces were washed repeatedly, each with 1.5 ml of TTBS [20 mM Tris-Cl; pH 7.8, 0.1 % (v/v) Tween-20, 0.01% NaN_3] supplemented with 0.5 M NaCl, until the measured absorbance at 280 nm dropped below 0.02. Antibodies were then eluted with 100 µl of 0.2 M glycine at pH 2.8 containing 0.02 % NaN3, and vortexed to release the bound antibodies. Following elution, the antibody solution was neutralized with 5 µl of 1 M Tris; pH 8.5 and stored at -80 ^{o}C in small aliquots. The antibody titre and specificity were tested subsequently.

2.7 *In vivo* RBD (Rho-binding domain) assay

2.7.1 Expression and purification of GST-fusion proteins in bacteria

Plasmid vector pGEX-4T-1 containing the gene construct for GST fusion with Rho-binding domain of Rhotekin (GST-RBD) or the empty vector was re-transformed into *E. coli* DH5α competent cells and streaked onto LB agar plate containing 100 μg/ml of ampicillin for overnight incubation at 37 ^{o}C. Single colonies for the respective plasmids were picked, inoculated into 5 ml of LB broth containing ampicillin and cultured overnight at 37 ^{o}C with constant agitation at 250 rpm. The starter culture was diluted into 100 ml of LB broth with ampicillin at a ratio of 1:500 and grown at 37 ^{o}C, 250 rpm until the measured OD_{600nm} fell within the range of 0.3 to 0.6 before adding 10 μM of IPTG for overnight induction of protein production. Subsequently, the culture was centrifuged at 5500 rpm for 15 mins at 4 ^{o}C to pellet the cells and bacteria pellets were stored at -80 ^{o}C after supernatant was discarded.

2.7.2 Preparation of beads

Frozen pellets of GST-RBD and GST alone were thawed and reconstituted in 10 ml of chilled lysis buffer [1 x PBS, 1 % (v/v) Triton X-100] freshly supplemented with 100 mM dithiothreitol (DTT) and protease inhibitors cocktail. The bacteria suspension was sonicated on ice using Sonicator XL 2020 (Misonix Incorporated) at 20 % amplitude for 3 mins, with iterative cycles of 3 s pulses followed by 6 s of lag time. Lysed sample was then centrifuged at 5500 rpm for 1 hr at 4 ^{o}C to remove the cell debris. For binding, the supernatant was transferred to a fresh 15 ml falcon tube for overnight incubation with 300 μl of Glutathione Sepharose 4B beads at 4 ^{o}C with constant rotation. Next, the beads were washed thrice with 10 ml of chilled lysis buffer and twice with chilled 1 x PBS, each wash with centrifugation at 500 rpm for 1

min at 4 ^{o}C. After the last wash, the beads were resuspended in an equal volume of 1 x PBS.

To check for protein expression, 5 and 10 µl of beads suspension, together with 10, 25 and 50 µg of BSA, were separately prepared by denaturing the samples in Laemmli loading buffer at 85 ^{o}C for 5 mins. These samples were then resolved via SDS-PAGE, stained with Coomassie Brilliant Blue solution [0.2 % (w/v) Coomassie blue R250, 40 % (v/v) methanol, 10 % acetic acid] for an hour and destained with water.

2.7.3 RhoA activity assay

Level of active RhoA in cells can be examined by using Rho-binding domain of Rhotekin - an effector of RhoA, which binds only to RhoA in the GTP-bound form. When bound, Rhotekin RBD inhibits both intrinsic and GAP-induced GTP hydrolysis, thereby giving a reflection on the amount of GTP-RhoA present (Ren and Schwartz, 2000). Cell transfected with the appropriate plasmids were lysed as outlined in section 2.4.1 and serial dilutions were performed to achieve 5 x, 10 x and 20 x dilutions of the whole cell lysates. Subsequently, 10 µg of either GST-RBD or GST proteins bound to glutathione sepharose beads was added to 200 µl each of the diluted whole cell lysates and subjected to gentle rotation for 45 mins at 4 ^{o}C to allow binding. The beads were then washed thrice, each with 1 ml of RIPA buffer, before heating in Lamelli buffer to prepare for SDS-PAGE and Western blot analysis. The level of active RhoA was detected using either polyclonal anti-HA or monoclonal anti-RhoA [1:1000]. After detection, the blots were stained with amido black to ascertain equal loading of the GST-fusion proteins.

2.7.4 Statistical analysis

To enable quantitative comparison of active RhoA level in the presence or absence of proteins of interest, densitometry analysis of the protein bands on X-ray films was performed using gel analyzer function in ImageJ software (http://rsbweb.nih.gov/ij/). In brief, the bands of interest within a data set were outlined separately using the rectangular selection tool to generate lane profile plots, which reflect the mean intensity and number of pixels of each sample. Output of each dataset was presented on a spreadsheet as relative percentage of each band amongst all the bands analyzed.

In the data analysis, densitometry profiles of active RhoA pulldown by Rhotekin-RBD were normalized against corresponding level of total RhoA present within the cells before comparing the relative amount present in each sample with the control sample. Means of 3 or more independent sets of experiments were tabulated and standard error mean was derived from division of the standard deviation by square root of sample size. The p-value was then generated using two-tailed Student's t-test with unequal variance available in Microsoft Excel to determine the statistical significance across pairs of samples.

2.8 Immunofluorescence studies

2.8.1 Immunostaining

CV-1 cells seeded on coverslips and transfected as described in section 2.3.2 were washed twice with 1 x PBS and fixed with pre-warmed 3.7 % paraformaldehyde for 15 mins at room temperature. After fixation, the coverslips were washed twice with 1 x PBS, followed by another 2 washes with 1 x PBS containing 50 mM ammonium chloride and washed twice again with 1 x PBS. To permeabilize the cells

for immunostaining, the coverslips were incubated with 1 x PBS containing 0.2 % (v/v) triton X-100 for 15 mins at room temperature and blocked for an hour at room temperature with blocking buffer [1 x PBS, 2 % (w/v) BSA, 2 % (v/v) defined fetal bovine serum].

During primary antibody staining, the coverslips were incubated face-down for an hour at room temperature in 50 µl of blocking buffer containing diluted primary antibodies at the respective dilutions: monoclonal mouse anti-FLAG M2, clone M2 (Sigma) [1:200], polyclonal rabbit anti-HA (Zymed) [1:100]. Filamentous actin was examined using Alexa Fluor® 633 phalloidin (Invitrogen) [1:200]. After incubation, the coverslips were washed thrice in 1 x PBS containing 0.2 % (v/v) triton X-100 and twice with 1 x PBS, with each wash lasting for 2 mins with constant shaking to remove any unbound primary antibodies. The cells were then stained with fluorophore-conjugated secondary antibodies by incubating the coverslips face-down in 50 µl of diluted secondary antibodies for 1 hr at room temperature. Common secondary antibodies used include Alexa Fluor® 488 donkey anti-mouse IgG, 568 donkey anti-mouse IgG, 568 donkey anti-rabbit IgG, 633 goat anti-mouse IgG, 633 goat anti-rabbit IgG and pacific-blue goat anti-mouse IgG (all from Invitrogen) [1:100]. After secondary antibody staining, the coverslips were similarly washed to remove any unbound antibodies and mounted onto glass slides using FluorSave reagent (Calbiochem) before leaving to dry overnight at room temperature.

2.8.2 Immunofluorescence detection

For immunofluorescence analysis by confocal fluorescence microscopy, cells fixed and stained as outline in section 2.8.1 were viewed and imaged on Carl Zeiss Laser Scanning Microscope (LSM) 510 Meta at 63 x magnifications (Plan-

Apochromat 63 x/1.4 NA oil objective lens). The captured images were merged using the LSM 510 software (Carl Zeiss).

To examine cell morphology and integrity of filamentous actin in CV-1 cells in the absence or presence of BNIP-2 and/or BPGAP1, fluorescence images of filamentous actin stained with Alexa Fluor® 633 phalloidin were captured using wide-field fluorescence Delta Vision Core at 10 x magnifications (PL FL 10 x/0.40 NA air objective lens) and viewed with softWoRx software (Applied Precision).

2.8.3 Statistical analysis

In statistical analysis on the significance of observed changes in cell morphology and integrity of stress fibers, at least 3 independent sets of experiments were performed and a minimum of 150 transfected cells per sample were evaluated. Transfected cells were scored for either rounding or shrinkage as one category and neither of the observed effects for the other. Similarly, for analysis of stress fiber integrity, transfected cells were divided into two groups based on the presence or absence of stress fiber. The data obtained were expressed as percentages of total number of transfected cells counted and mean values were computed from data derived from at least 3 independent sets of experiments. Standard error mean was expressed as division of standard deviation by square root of sample size. Statistical significance (p-value) across pairs of samples was analyzed using two-tailed Student's t-test with unequal variance (Microsoft Excel).

2.9 Proliferation studies

2.9.1 Preparation of samples

CHO cells were seeded on 6-well cell culture dishes and transfected with various expression constructions as described in section 2.3.1. After 24 hrs of transfection, cells in the individual wells were washed once with 1 x PBS and treated with 0.25 % trypsin-EDTA before harvesting in equal volume of serum-containing medium. Cells in each sample were reseeded at 50 % into 10-cm tissue culture dishes (Nunc) each containing a 13-mm microscope cover glass and allowed to grow for the next 24 hrs post-transfection at 37 ^{o}C in a humidified 5 % CO_2 incubator to achieve a confluency of approximately 50 % on the following day.

2.9.2 BrdU (5-bromo-2'-deoxyuridine) cell proliferation assay

BrdU cell proliferation assay was performed using *In Situ* Cell Proliferation Kit, FLUOS (Roche Applied Science) according to manufacture's protocol. At 24 hrs post-reseeding of the cells after transfection, the coverslip in each tissue culture dish was transferred using a sterile forceps into 12-well multi-dishes (Nunc) containing fresh growth medium. The cells were then incubated in 10 μM BrdU labeling solution diluted in fresh growth medium for an hour at 37 ^{o}C in a humidified 5 % CO_2 incubator to allow for incorporation of BrdU into the DNA of proliferating cells.

After incubation, the cells were washed thrice in 1 x PBS and fixed with ethanol fixative solution [30 % (v/v) glycine solution (50 mM glycine; pH 2.0), 70 % (v/v) absolute ethanol] for 45 mins at room temperature. The coverslips were then washed twice with 1 x PBS and incubated in 4 M HCl for 10 to 20 mins at room temperature to denature the DNA. Next, the coverslips were washed thrice in 1 x PBS at 5 mins per wash with constant shaking to neutralize the acid before incubating in

blocking buffer [1 x PBS, 0.5 % (w/v) BSA, 0.1 % (v/v) Tween 20] at room temperature for 10 mins. To detect the incorporated BrdU by immunofluorescence, the coverslips were incubated face-down in 50 µl of immunolabelling solution containing flurophore-conjugated anti-BrdU antibody (anti-BrdU-FLUOS) diluted in blocking buffer at a ratio of 1:10, as well as monoclonal mouse anti-FLAG [1: 200]. After 1 hr of incubation at room temperature, the coverslips were wash thrice in 1 x PBS at 5 mins per wash with constant shaking.

For identification of transfected cells, the coverslips were incubated face-down in 50 µl of diluted Alexa Fluor® 633 goat anti-mouse IgG [1:100] for 1 hr at room temperature. Coverslips were washed to remove any unbound secondary antibodies and mounted onto glass slides using FluorSave reagent before leaving to dry overnight at room temperature. The cells were imaged using wide-field fluorescence Delta Vision Core at 10 x magnifications (PL FL 10 x/0.40 NA air objective lens) and viewed with softWoRx.

2.9.3 Western blot analysis of proliferation markers

2.9.3.1 Bradford assay

Cells seeded in 10-cm plates (Section 2.9.1) were lysed and harvested in RIPA buffer as described in section 2.4.1. Protein concentration of each sample was quantified using spectrophotometry analysis of the absorbance values of Bradford reagent measured at 595 nm after its addition to the samples. Protein standards of 0, 2, 4, 6, 8 and 10 µg of BSA in 20 µl solutions were prepared from BSA stock solution (10 mg/ml) and these samples were prepared by diluting 1 µl of whole cell lysate into 19 µl of deionised water. Next, 980 µl of freshly diluted Bradford reagent (1:5) was added to each of the 20 µl standards as well as samples and incubated for 15 mins at

room temperature before measuring their absorbance at 595 nm. A Bradford standard curve was plotted for calculating the concentrations of samples, which were then diluted accordingly to achieve equal protein concentration in each sample for Western blot analysis.

2.9.3.2 Western blot analysis

Whole cell lysates of samples with equal protein concentration were denatured in Lamelli buffer and heated at 85 ^{o}C for 5 mins before separation by gel electrophoresis and immobilization onto membranes as outlined in section 2.5.1. Western blot analysis was carried out by incubating the cut membranes in the following primary antibodies diluted in blocking buffer: rabbit polyclonal anti-PCNA [1:1000], rabbit polyclonal anti-phospho-Histone H3 (Ser10) [1:3000] or mouse monoclonal anti-β-tubulin [1:1000], followed by incubation in the respective secondary antibodies for detection by chemiluminiscence as described in section 2.5.2.

2.9.4 Statistical analysis

Proliferation level of cells differentially transfected with various expression constructs was evaluated by BrdU and Western blot analysis of different proliferation markers in 3 independent sets of experiments. In BrdU cell proliferation assay, at least 100 transfected cells per sample were imaged, scored for the presence or absence of BrdU, and expressed as relative percentages of total number of transfected cells counted. For analyzing the level of proliferation markers in each experimental set, levels of PCNA (Proliferating cell nuclear antigen) and phospho-Histone H3 (Ser10) in different samples were determined by densitometry analysis using ImageJ software

as detailed in section 2.7.4. Densitometry profiles of PCNA and phospho-Histone H3 (Ser10) were then normalized against corresponding level of loading control β-tubulin before comparing the values of samples with vector control. Similarly, to assess statistical significance of the data obtained, means values and standard error mean were tabulated for calculation of p-values across pairs of samples using two-tailed Student's t-test with unequal variance (Microsoft Excel).

Chapter 3

Results

3 RESULTS

3.1 BNIP-2 is a *bona fide* endogenous interacting partner of BPGAP1

Using an overexpression system in immunoprecipitation study, BNIP-2 has previously been shown to bind BPGAP1 (Shang et al., 2003). To ascertain that BNIP-2 is indeed an endogenous interacting partner of BPGAP1, lysates of control cells and 293T cells transfected with mammalian GST-tagged BPGAP1 or empty vector were used in pull-down experiments with glutathione sepharose beads and probed with BNIP-2 antibodies. Endogenous BNIP-2 was detected in pull-downs from lysates of cells transfected with mammalian GST-BPGAP1 but not in those from cells expressing empty vector or untransfected cells (Figure 3.1b), thereby confirming that BNIP-2 is indeed a *bona fide* interaction partner of BPGAP1. BNIP-2 was resolved as multiple bands when analyzed by SDS-PAGE, which could represent either alternatively spliced isoforms or phosphorylated forms of BNIP-2 (Kang et al., 2008; Low et al., 1999). Neither reciprocal semi-endogenous immunoprecipiation studies involving overexpressed BNIP-2 and endogenous BPGAP1, nor immunoprecipitation studies of endogenous BNIP-2 and BPGAP1 were carried out due to the lack of specific antibodies for BPGAP1.

Given that harvesting of cell lysates yields a mixture of proteins regardless of their cellular localization, we next examined where BNIP-2 and BPGAP1 interactions occur within the cells by co-expressing these two proteins in fibroblast CV-1 and analyzed their localization using confocal immunofluorescence microscopy. These cells have an extensive cytoplasmic area that allows for suitable analysis of protein localization within the cytoplasm and also for analysis of actin cytoskeleton network.

Consistent with earlier observations in other cell types including HeLa and Cos-1 cells (Zhou et al., 2005), BNIP-2, when expressed alone, localized in the cytoplasm as punctate structures with distinct regions of concentration at the edges of cellular protrusions (Figure 3.2, first row). In comparison, BPGAP1 appeared more diffused within the cytosol (Figure 3.2, second row). However, when co-expressed, these two proteins co-localized at areas within the cytoplasm, as well as at the edges of cellular protrusions (Figure 3.2, third row merged image and inserts, white arrows), which further supports the finding that BNIP-2 interacts with BPGAP1 *in vivo*, at specific localities that might be important for certain cellular functions.

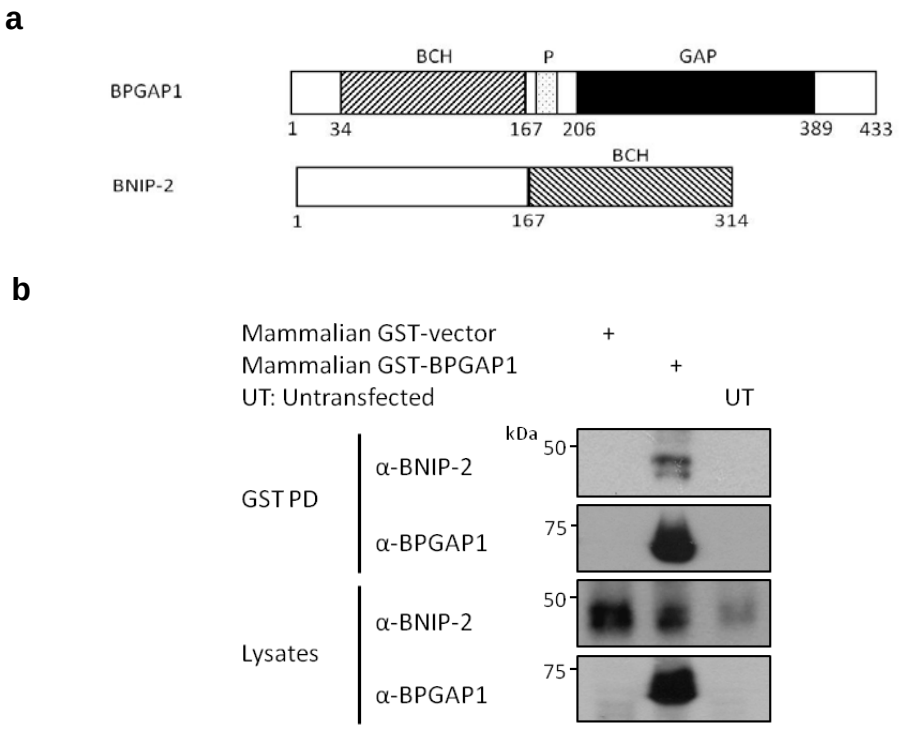

Figure 3.1 BPGAP1 interacts with endogenous BNIP-2. (a) Schematic diagram of domain architecture of full-length BPGAP1 and BNIP-2. Domain boundaries were as indicated by the respective amino acid residue numbers. (b) 293T cells were transfected with either mammalian GST-tagged BPGAP1 or expression vector for 20-24 hrs. Lysates of control or transfected cells were incubated with glutathione sepharose beads and the proteins pulled down were separated using SDS-PAGE, blotted and probed with anti-BNIP-2 antibodies to detect any bound endogenous BNIP-2 (first panel) and with anti-BPGAP1 antibodies to verify the presence of mammalian GST-BPGAP1 (second panel). Cell lysates were similarly analyzed by Western blot for detection of endogenous BNIP-2 (third panel) and overexpressed BPGAP1 (fourth panel). PD: Pull-down.

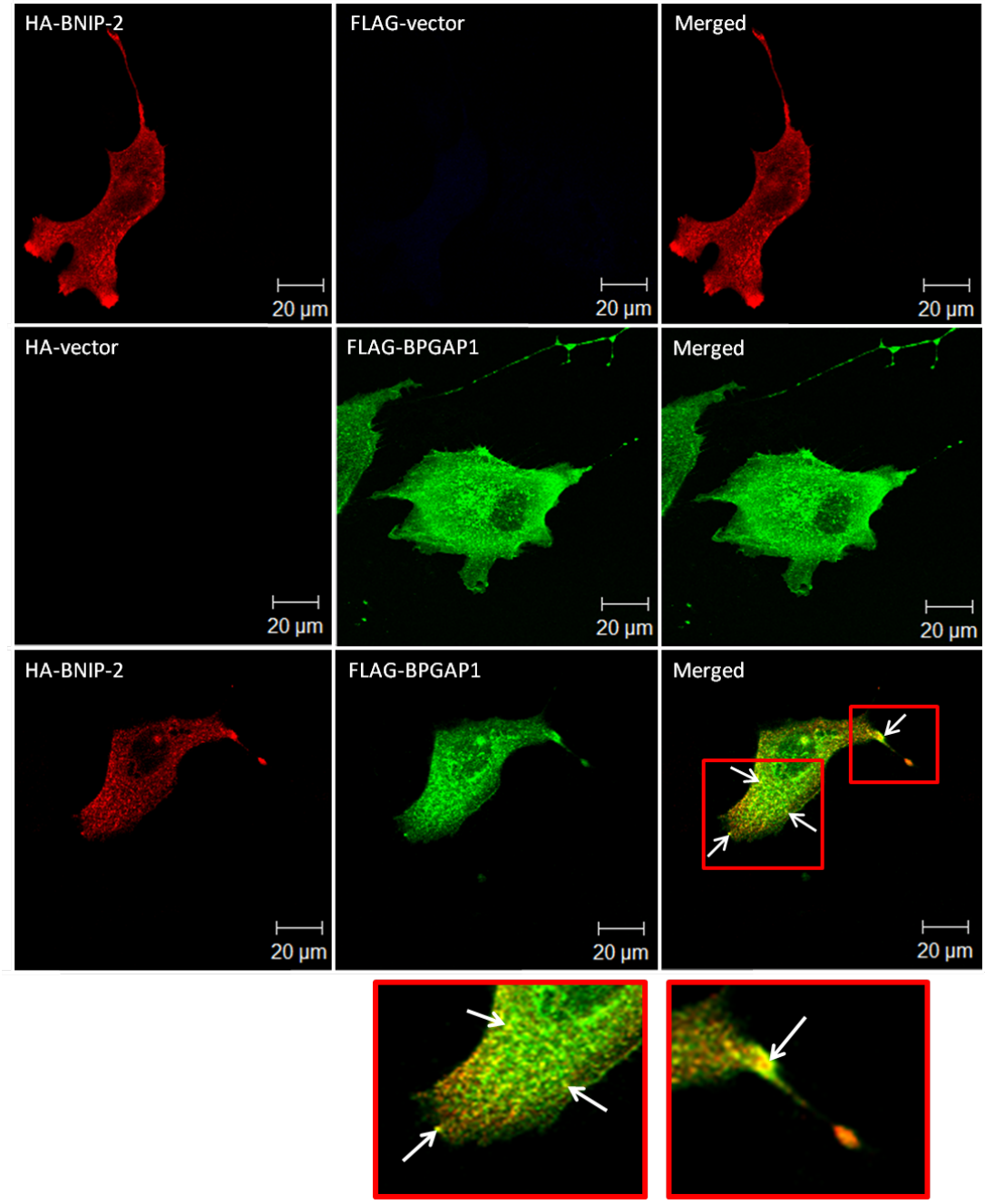

Figure 3.2 BNIP-2 and BPGAP1 co-localized within the cytoplasm and at the edges of membrane protrusions. CV-1 cells were transfected with plasmids encoding HA-BNIP-2, FLAG-BPGAP1 or in combination as indicated for 20 hrs. After which, the cells were fixed, permeabilized and stained for indirect immunofluorescence detection by confocal fluorescence microscopy as described in *Materials and Methods*. HA-BNIP-2 and FLAG-BPGAP1 were labeled with polyclonal rabbit anti-HA and monoclonal mouse anti-FLAG antibodies, respectively, followed by the appropriate fluorophore-conjugated secondary antibodies. Regions of co-localization between HA-BNIP-2 (red) and FLAG-BPGAP1 (green) were represented by yellow spots in the merged image and inserts, indicated by white arrows. Scale bar, 20 µm.

3.1.1 BCH domains mediate heterophilic interaction between BNIP-2 and BPGAP1

BCH domain-containing proteins can form homo or heterodimers through their BCH domains (Low et al., 2000a; Shang et al., 2003). Therefore, it is plausible that interaction between BNIP-2 and BPGAP1 is mediated by their respective BCH domains. To test this possibility, transient transfection of two BPGAP1 mutants, each harboring a distinct moiety of either BCH domain or GAP domain with the proline-rich region (PGAP) as depicted in Figure 3.3ai, was carried out to examine their ability to interact with endogenous BNIP-2 that has only a single recognizable BCH domain. Similar to full-length BPGAP1, its BCH domain was capable of binding to endogenous BNIP-2 (Figure 3.3b) and this demonstrates that the BCH domains mediate heterophilic interaction between BNIP-2 and BPGAP1. To our surprise, PGAP region of BPGAP1 was also able to capture endogenous BNIP-2. Although the faster migrating band of BNIP-2 was weaker, it could be detected after longer exposure. This association between PGAP region and BNIP-2 therefore indicates that interaction between BNIP-2 and BPGAP1 is not due simply to heterophilic interaction of the BCH domains but also involves the PGAP region, which plays a role that is currently yet unclear.

In order to confirm that interaction between BNIP-2 and BPGAP1 occurs via BNIP-2 BCH domain and not its N-terminal region, mutant constructs corresponding to either of these regions (Figure 3.3aii) were co-transfected with full-length BPGAP1, BCH domain (BPGAP1) or PGAP region in immunoprecipitation studies. Figure 3.3c shows that while both BNIP-2 and its BCH domain alone were able to bind full-length and various domains of BPGAP1, no interaction was detected with

the N-terminal region, thereby confirming that BCH domain is indeed important for mediating heterophilic interaction between BNIP-2 and BPGAP1.

ai

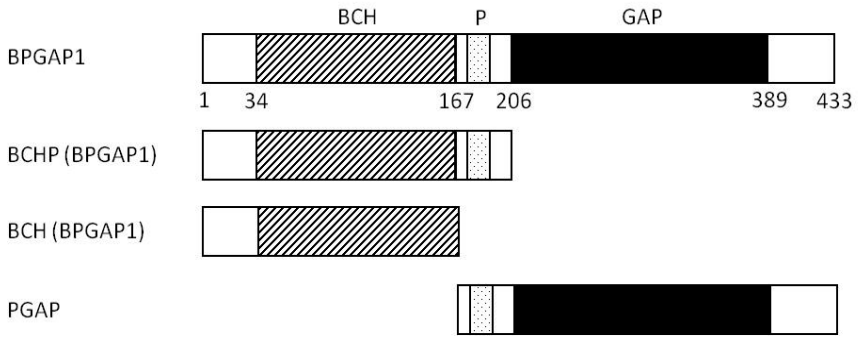

aii

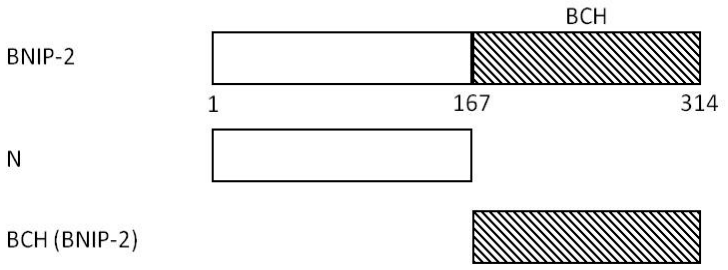

b

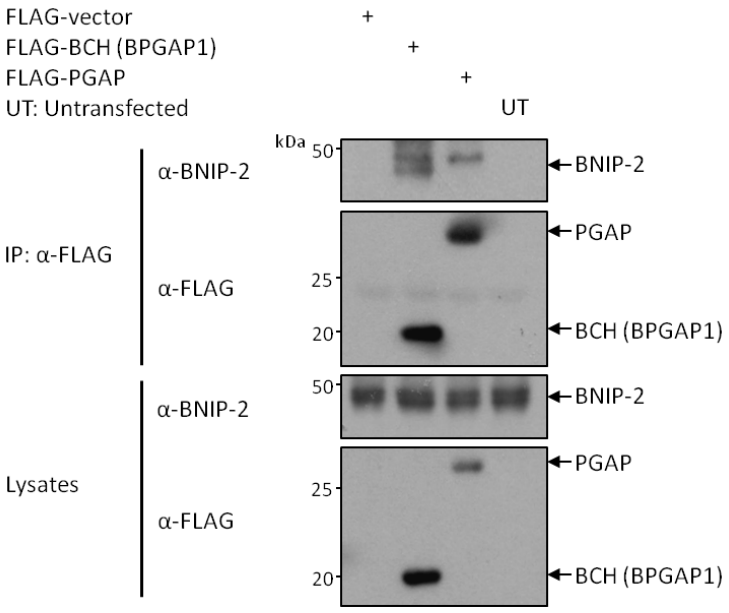

c

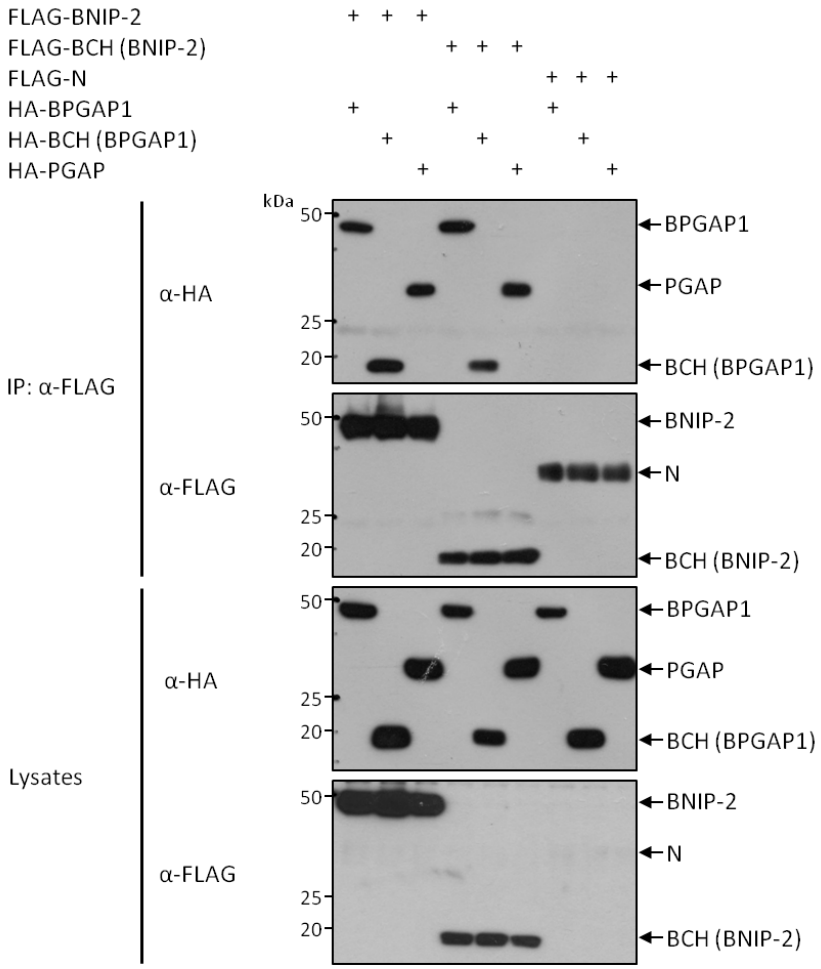

Figure 3.3 BCH domains are important for heterophilic interaction between BNIP-2 and BPGAP1. (a) Schematic representations of full-length and truncation mutants of (i) BPGAP1: BCHP (BCH domain with proline-rich region; amino acids 1-206), BCH (BCH domain; amino acids 1-167), PGAP (C terminus without BCH domain; amino acids 168-433) and of (ii) BNIP-2: N (N terminus without BCH domain, amino acids 1-166), BCH (BCH domain; amino acids 167-314). (b) 293T cells were transfected with FLAG-tagged BPGAP1 truncation mutants or expression vector as indicated for 20-24 hrs. Harvested lysates of control or transfected cells were subjected to immunoprecipitation with anti-FLAG M2 beads. Bound proteins, along with cell lysates, were separated by SDS-PAGE, blotted and probed with anti-BNIP-2 antibodies for detection of endogenous BNIP-2 (first and third panel) and with anti-FLAG antibodies to verify the presence of overexpressed FLAG-tagged BCH (BPGAP1) and PGAP (second and fourth panel). (c) Transfected cells expressing HA-tagged BPGAP1 or its domains in the presence of FLAG-tagged BNIP-2 or its truncation mutants were harvested and lysates were subjected to immunoprecipitation with anti-FLAG M2 beads. Associated proteins and cell lysates were analyzed by Western blot and probed with anti-HA and anti-FLAG antibodies for detection of bound proteins (first and second panel), as well as expression of the constructs introduced (third and fourth panel). IP: Immunoprecipitates.

3.1.2 Possible associations of BNIP-2, BPGAP1 and RhoA in a tripartite complex

Having established the interaction between BNIP-2 and BPGAP1, we sought to decipher the relationship between these two proteins and RhoA as previous work in our laboratory has shown that BPGAP1 functions biochemically as a GAP towards RhoA *in vivo* (Shang et al., 2003). Through individual interactions of BPGAP1 with BNIP-2 and RhoA, it is possible that these associations could result in the formation of a tripartite complex. Alternatively, BNIP-2 might compete against BPGAP1 for binding to RhoA, hence preventing their interaction. To test these possibilities, immunoprecipitation studies were performed by co-expressing BPGAP1 with BNIP-2 and RhoA, either together or separately as indicated, to determine if BPGAP1 could associate with both BNIP-2 and RhoA in the presence of each other. Subsequent analyses by Western blot revealed that RhoA was captured by BPGAP1 in the presence of BNIP-2 or vice versa (Figure 3.4). This result indicates the possible existence of a tripartite complex or in another instance; separate pools of BPGAP1 could exist to interact with BNIP-2 and RhoA independently.

On the basis that proteins forming interacting complexes exist in close proximity in the same subcellular region to carry out specific functions, confocal immunofluorescence study was also carried out to explore the relationship between BNIP-2, BPGAP1 and RhoA. Interestingly, analyses of confocal microscopy images demonstrate that BNIP-2 together with BPGAP1, stained red and blue respectively, exhibit partial co-localization with GFP-RhoA (green) at regions within the cytoplasm and at the cell periphery. These areas of co-localization appeared white in the merged image and inserts as indicated by the white arrows (Figure 3.5). Taken together, it is

therefore possible that BNIP-2, BPGAP1 and RhoA could exist in a tripartite complex within the cells.

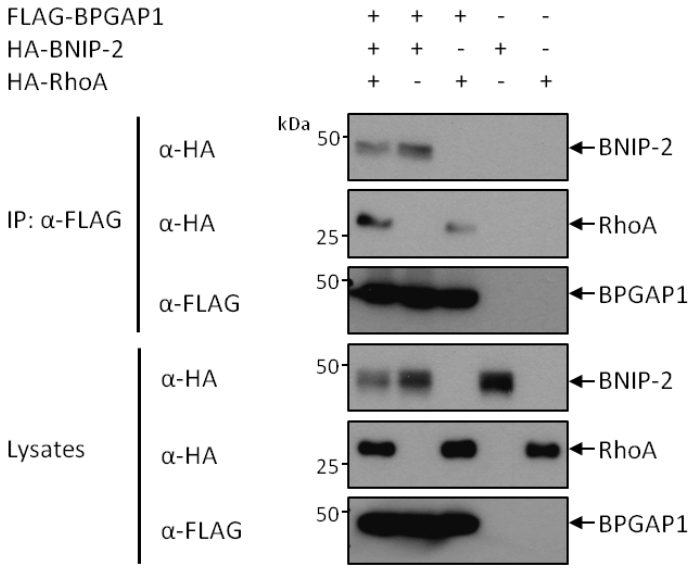

Figure 3.4 BPGAP1 associates with both BNIP-2 and RhoA in the presence of each other. 239T cells were transfected with FLAG-BPGAP1, HA-tagged BNIP-2 or RhoA as indicated by the + sign or with an equivalent amount of similarly tagged expression vector control, indicated by the – sign. Harvested lysates were subjected to immunoprecipitation with anti-FLAG M2 beads and associated proteins were separated on SDS-PAGE, blotted and detected with anti-HA (first and second panel) and anti-FLAG antibodies (third panel). Protein expression was verified by Western blot analyses of cell lysates using anti-FLAG (bottom panel) and anti-HA antibodies (fourth and fifth panel).

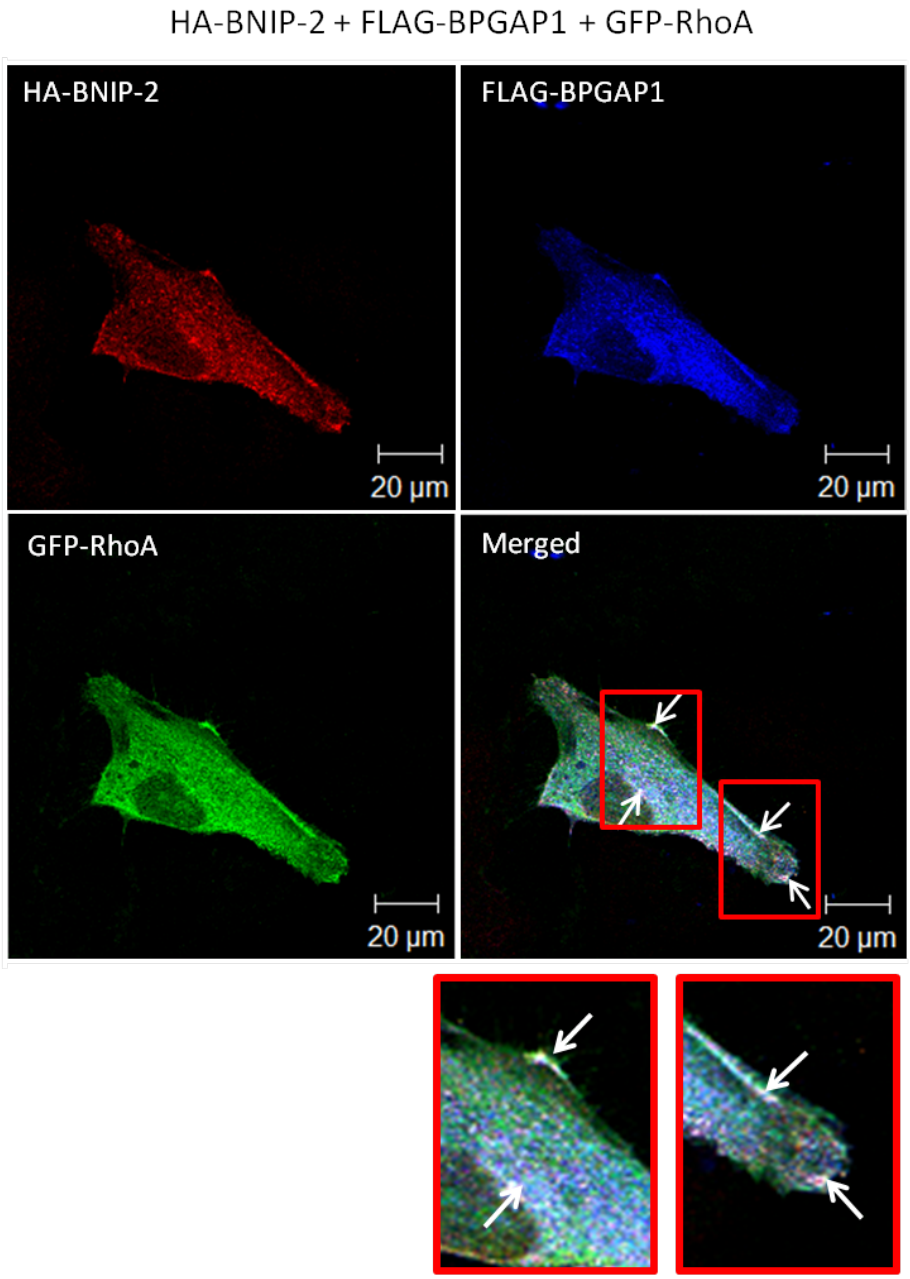

Figure 3.5 BNIP-2, BPGAP1 and RhoA co-localize at regions within the cytoplasm and at the cell periphery. HA-BNIP-2, FLAG-BPGAP1 and GFP-RhoA were expressed in CV-1 cells, fixed after 20 hrs, permeabilized and stained for immunofluorescence detection by confocal fluorescence microscopy as described in *Materials and Methods*. The expressed HA-BNIP-2 and FLAG-BPGAP1 were labeled with polyclonal rabbit anti-HA and monoclonal mouse anti-FLAG antibodies, respectively, followed by the appropriate fluorophore-conjugated secondary antibodies. Co-localization of BNIP-2 (red), BPGAP1 (blue) and RhoA (green) at regions in the cytoplasm and cell periphery were represented by white spots in the merged image and inserts, indicated by white arrows. Scale bar, 20 µm.

3.2. BNIP-2 associates with Rho-like family of Rho GTPases, and the BCH domain mediates interaction of BNIP-2 or BPGAP1 with RhoA

Next, to further examine the possibility of tripartite complex formation between BNIP-2, BPGAP1 and RhoA using immunoprecipitation study, in which each of these three proteins was used separately to capture the remaining two proteins; one important prerequisite of this method is that there must not be any direct interaction between one pair of these proteins and in this case, BNIP-2 and RhoA. As such, this study was continued by first assessing whether BNIP-2 itself associates with RhoA.

3.2.1 BNIP-2 interacts with RhoA

Within the Rho GTPase family, the three most well-characterized Rho GTPases – RhoA, Cdc42 and Rac1, were expressed in HA-epitope and tested for their ability to interact with BNIP-2 using immunoprecipitation study. Western blot analyses revealed that RhoA, as compared to Rac1 and Cdc42, was selectively co-immunoprecipitated by BNIP-2 (Figure 3.6), suggesting that BNIP-2 may potentially function to regulate RhoA signaling as demonstrated for other BCH domain-containing proteins including BNIP-Sα, BNIP-XL and p50RhoGAP (Soh and Low, 2008; Zhou et al., 2010; Zhou et al., 2006).

Interestingly, though BNIP-2 has previously been shown in 293T cells to bind Cdc42 in GST pull-down and conferred GAP activity towards Cdc42 via a non-canonical arginine patch motif (Low et al., 1999; Low et al., 2000a; Low et al., 2000b), interaction between these two proteins has not been directly observed when co-expressed for immunoprecipitation studies in this case. On the other hand, other studies have indicated that Cdc42 signaling was indeed necessary for BNIP-2 induced

cell elongation and membrane protrusions in MCF-7 (Zhou et al., 2005), and BNIP-2 functions as a scaffold for Cdo signaling to Cdc42 during myogenic and neuronal differentiation in C2C12 and C17.2 neural precursor cells, respectively (Kang et al., 2008; Oh et al., 2009). While the importance of functional association between BNIP-2 and Cdc42 in some cell types could not be undermined, interaction between these proteins might vary under different cellular conditions and in different cell types.

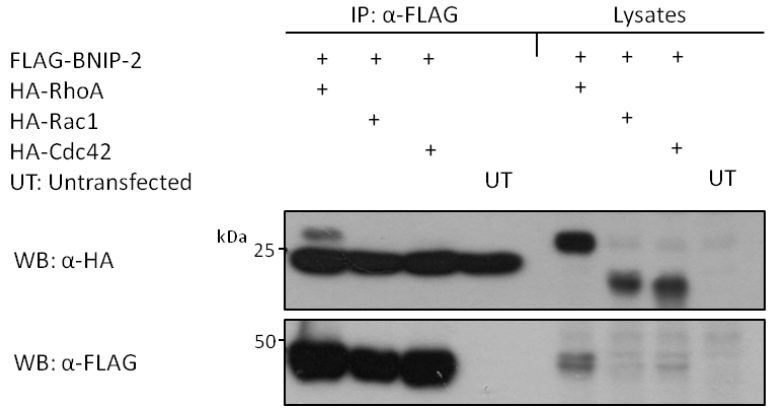

Figure 3.6 BNIP-2 binds specifically to RhoA in 293T cells. Lysates of control cells and cells transfected with FLAG-BNIP-2, along with HA-tagged RhoA, Cdc42 or Rac1, were incubated with anti-FLAG M2 beads. Bound proteins were separated on SDS-PAGE, blotted and probed with anti-HA antibody. Similarly, whole cell lysates were analyzed by Western blot to verify expression of proteins using anti-HA and anti-FLAG antibodies as indicated. IP: Immunoprecipitates; WB: Western blotting.

Consistent with previously reported observations (Roberts et al., 2008), RhoA proteins, as observed in immunofluorescence studies, were distributed in the cytoplasm, as well as localized to the plasma membrane of the cell (Figure 3.7, second row). Intriguingly, when BNIP-2 and RhoA were co-expressed, they exhibited regions of co-localization within the cell and in particular at area near the tips where BNIP-2 was found to be concentrated (Figure 3.7, third row merged image and inserts, white arrows). This observed co-localization at specific localities reinforces

earlier finding that BNIP-2 interacts with RhoA as shown by immunoprecipitation studies and their interaction could potentially play an important role in cell physiology.

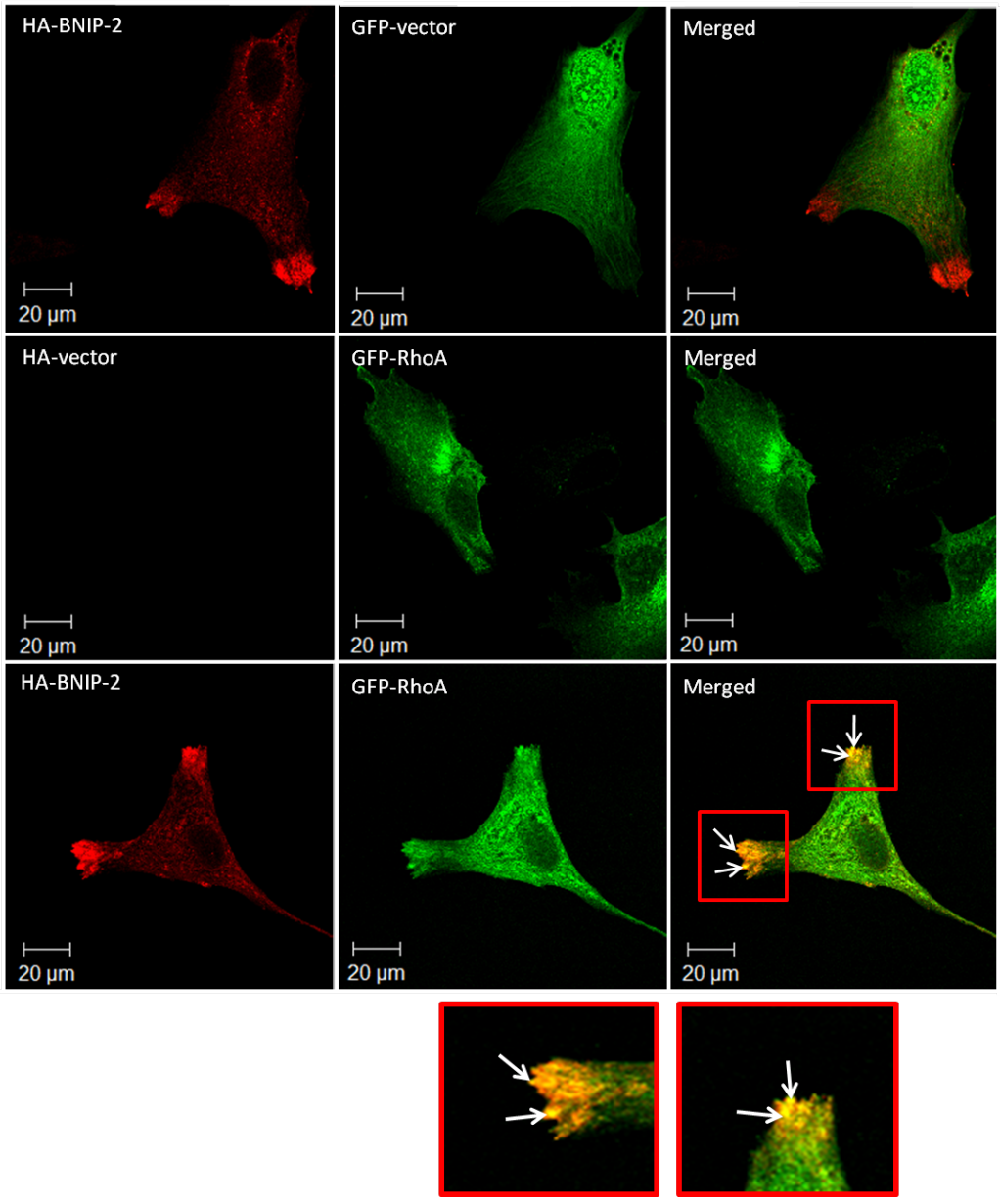

Figure 3.7 BNIP-2 and RhoA co-localize at specific areas of cellular tips. HA-BNIP-2, GFP-RhoA or in combination were expressed in CV-1 cells as indicated. The cells were fixed after 20 hrs, permeabilized and stained for immunofluorescence detection by confocal fluorescence microscopy as described in *Materials and Methods*. HA-BNIP-2 was first labeled with polyclonal rabbit anti-HA antibody, followed by the fluorophore-conjugated secondary antibody. BNIP-2 (red) and RhoA (green) co-localized within the cell, in particular at tips of cellular extensions, as represented by yellow spots in the merged image and inserts, indicated by white arrows. Scale bar, 20 µm.

3.2.2 RhoA and RhoC are enriched by BNIP-2 in immunoprecipitation

RhoA, RhoB and RhoC, despite sharing a high sequence identity of 85 % and induce stress fibers in cells, are functionally different in several aspects. RhoA, which has been studied extensively for its major role in regulating actomyosin contractility, promotes oncogenic transformation, whereas RhoC is involved in cell migration and tumor metastasis. RhoB, on the other hand, participates mainly in endosomal trafficking and delivery of signaling proteins (Vega and Ridley, 2008; Wheeler and Ridley, 2004). These variations in functionalities may be attributed to differential localization, specific interactions or unequal affinities for regulators or target proteins. For instance, GEF XPLN (eXchange factor found in platelets, leukemic and neuronal tissues) acts solely on RhoA and RhoB, excluding RhoC (Arthur et al., 2002), while BCH domain of BNIP-XL, a regulator of RhoA and its positive regulator Lbc RhoGEF, associates specifically with RhoA and RhoC (Soh and Low, 2008). By acting through different targets, RhoA and RhoC perform distinct roles in processes such as migration and invasion (Vega et al., 2011). Associations with specific Rho isoforms may therefore provide an indication on the functional roles of interacting proteins. Thus, we sought to find out if BNIP-2 displays such differences in affinity towards these three Rho GTPases.

BNIP-2, together with RhoA, RhoB or RhoC, were introduced into 293T cells and the lysates subjected to co-immunoprecipiation were analyzed by Western blot. Though BNIP-2 interacted with all three Rho isoforms, RhoA and RhoC were enriched in immunoprecipitation by BNIP-2, suggesting a preference towards these two proteins (Figure 3.8a). To confirm these selective interactions, reciprocal co-immunoprecipitation was carried out and similarly, a comparatively weaker band corresponding to interaction between RhoB and BNIP-2 was observed (Figure 3.8b).

However, it is possible that weaker binding occurred as a result of differential localization but not due to variations in affinity towards the different Rho isoforms.

a

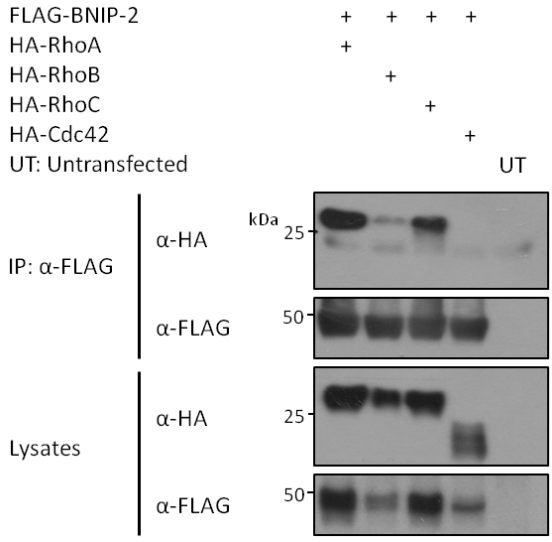

b

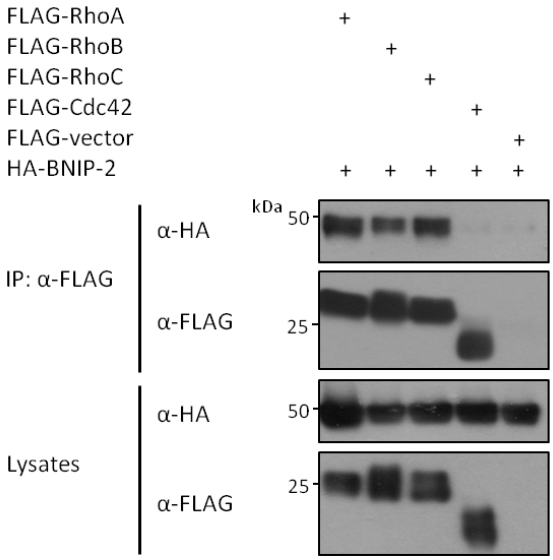

Figure 3.8 BNIP-2 associates preferentially with RhoA and RhoC. Expression constructs of (a) FLAG-BNIP-2 and HA-tagged RhoA, RhoB or RhoC; (b) HA-BNIP-2 with each of the FLAG-tagged Rho isoforms, were introduced into the cells as indicated. Co-transfections of reciprocally tagged BNIP-2 and Cdc42 were included as negative control. Control and transiently transfected cells were lysed after 20-24 hrs, immunoprecipitated with anti-FLAG M2 beads and associated proteins were analyzed using Western blot by probing with anti-HA (first panel) and anti-FLAG antibodies (second panel). WCL were similarly resolved by SDS-PAGE and probed with anti-HA and anti-FLAG antibodies to verify the presence of overexpressed proteins (third and fourth panel).

3.2.3 BPGAP1 displays similar interaction profile to Rho isoforms as BNIP-2

Next, we examined whether BPGAP1, a previously identified GAP for RhoA, could also interact with specific Rho isoforms. To investigate this through immunoprecipitation study, FLAG-BPGAP1 and HA-tagged RhoA, RhoB or RhoC were co-expressed in the cells and incubated with anti-FLAG M2 beads. Interestingly, BPGAP1 clearly demonstrated specificity towards RhoA and RhoC, as shown by their enrichment in the immunoprecipitates (Figure 3.9a). These preferential interactions were recapitulated in reciprocal immunoprecipitation studies in which HA-BPGAP1 was selectively captured by FLAG-tagged RhoA and RhoC (Figure 3.9b). In contrast, only a weak interaction could be detected for BPGAP1 and RhoB. These results therefore indicated that BPGAP1 acts specifically towards RhoA and RhoC, in a profile similar to BNIP-2.

a

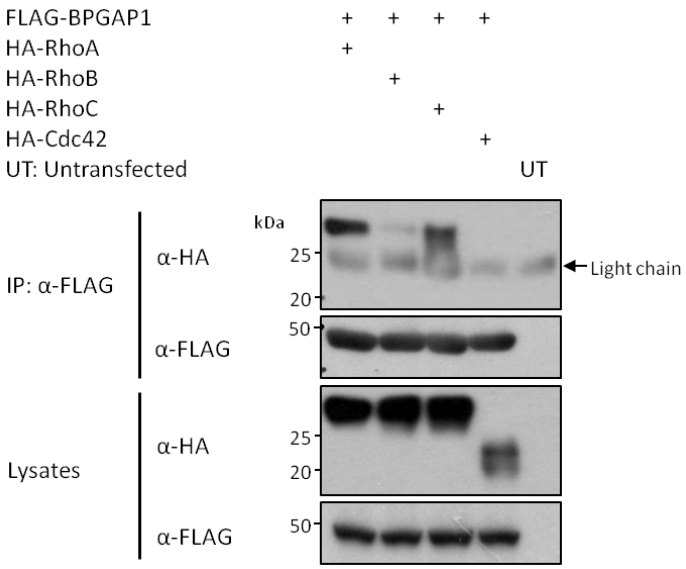

b

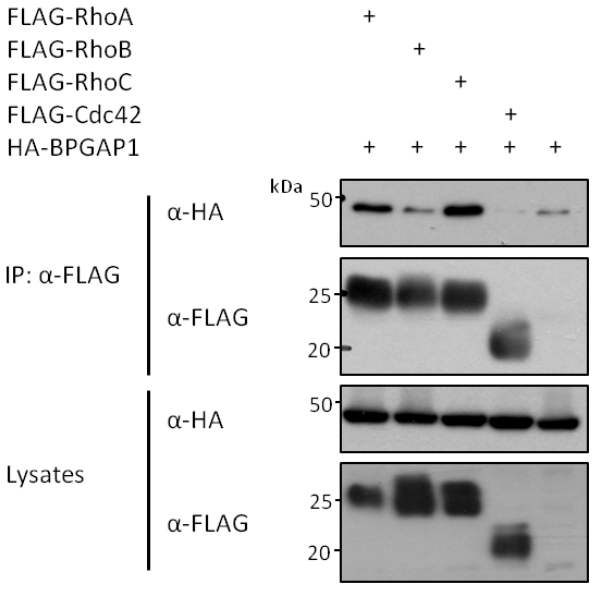

Figure 3.9 BPGAP1 binds selectively to RhoA and RhoC. Immunoprecipitation studies were performed using lysates from control cells and cells co-expressing (a) FLAG-BPGAP1 and HA-tagged RhoA, RhoB or RhoC; (b) HA-BPGAP1 with each of the FLAG-tagged Rho isoforms. To detect the bound proteins, lysates were resolved on SDS-PAGE, blotted and probed with anti-HA (first panel) and anti-FLAG antibodies (second panel). WCL were also analyzed by Western blot to verify the expression of these proteins by anti-HA and anti-FLAG antibodies as indicated (third and fourth panel).

3.2.4 Both BNIP-2 and BPGAP1 target RhoA via the BCH domain

Previous work has established that the respective BCH domain of BNIP-Sα, BNIP-XL and p50RhoGAP modulates RhoA signaling through direct binding of the protein and including its direct regulators in some instances (Soh and Low, 2008; Zhou et al., 2010; Zhou et al., 2006). Focusing on the associations of BNIP-2 and BPGAP1 with RhoA, we aimed to determine if these interactions are mediated by their respective BCH domains. To do so, RhoA was expressed in the cells together with expression vector control, BNIP-2, BPGAP1 or their truncation mutants as depicted in Figure 3.3a for immunoprecipitation studies. Of the two BNIP-2 truncation mutants, only BCH (BNIP-2) could bind readily to RhoA, whereas no

binding was observed for the N-terminal alone (Figure 3.10). Hence, this indicates that the BCH domain is indeed responsible for the interaction of BNIP-2 with RhoA.

Furthermore, both truncation mutants of BPGAP1 harboring the BCH domain, namely BCH (N terminus with BCH domain) and BCHP (BCH domain with proline-rich region), were able to immunoprecipitate HA-RhoA (Figure 3.10). However, only a weak interaction could be detected between PGAP (C terminus without BCH domain) and RhoA despite BPGAP1 having GAP activity towards RhoA. This could be due to the high turnover, as well as transient nature of enzyme-substrate interaction. Collectively, these data demonstrate that BCH domains are essential for binding of RhoA by both BNIP-2 and BPGAP1, further raising the possibility that BCH domains of these two proteins might also function as regulatory modules for GTPase signaling.

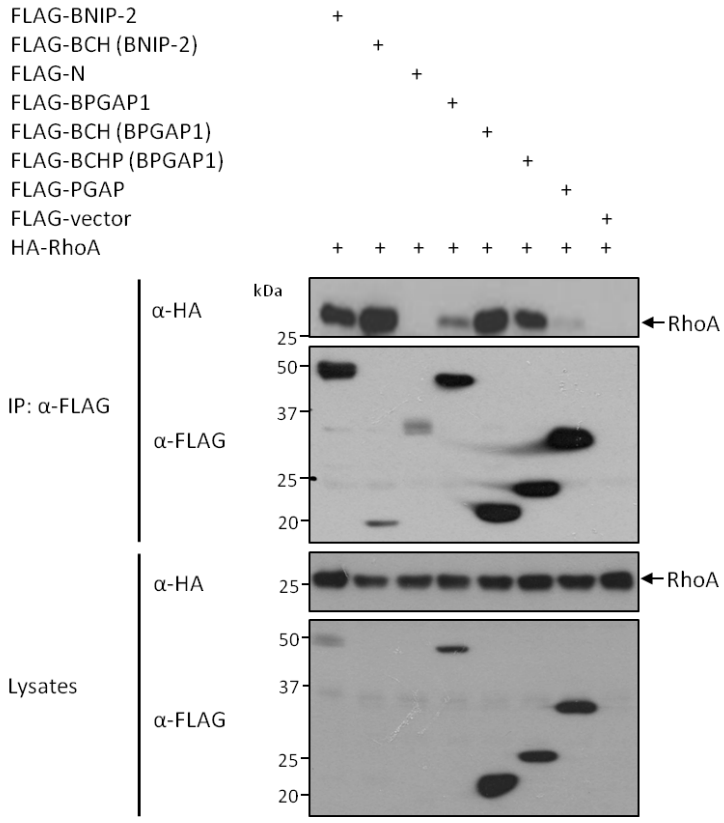

Figure 3.10 BCH domains of BNIP-2 and BPGAP1 are important for RhoA binding. 293T cells were transfected with HA-RhoA, in the presence of expression vector control, full-length BNIP-2, BCH (BNIP-2), N terminal (N), full-length BPGAP1 or the respective domains as indicated, all expressed in FLAG-epitope. For immunoprecipitation studies, cell lysates were harvested after 20-24 hrs, incubated with anti-FLAG M2 beads and associated proteins were analyzed by Western blot. Bound and expressed proteins resolved by SDS-PAGE were probed with anti-HA (first and third panel) and anti-FLAG antibodies (second and fourth panel).

3.2.4.1 RhoA binding motif of BNIP-2 lies within residues 167-211 of BCH domain

In the study of RhoA signaling regulation by BNIP-Sα, a unique RhoA binding motif has been identified to reside within BNIP-Sα BCH domain (residues 133-177) (Zhou et al., 2006). Since BCH domains of BNIP-2 and BNIP-Sα share a high degree of sequence homology (85 %) (Zhou et al., 2002), it is possible that BNIP-2 may also contain a site for RhoA interaction. To identify the potential RhoA binding motif, sequence alignment of primary amino acid sequences of BNIP-2 and BNIP-Sα BCH domains was performed and residues within BNIP-2 BCH domain that correspond to RhoA binding motif of BNIP-Sα BCH domain were identified as the putative RhoA binding motif (courtesy of Dr. Zhou Y.T.) (Figure 3.11a).

Next, to further examine if the putative RhoA binding motif of BNIP-2 modulates binding to RhoA, a series of internal deletion mutants generated based on secondary structure predictions were tested for their ability to interact with RhoA using co-immunoprecipitation studies. Analyses of lysates of cells transfected with HA-RhoA and mutants expressed in FLAG-epitope (Figure 3.11b) by Western blot revealed that BNIP-2 mutant that is devoid of amino acid residues 167 to 211 of BCH domain could no longer associate with RhoA while the remaining internal deletion mutants all retained binding to RhoA (Figure 3.11c). Taken together, the region

comprising residues 167 to 211 of BNIP-2 BCH domain indeed constitutes a unique RhoA binding motif, suggesting that there may be a consensus sequence within BCH domain for mediating interaction with RhoA.

a

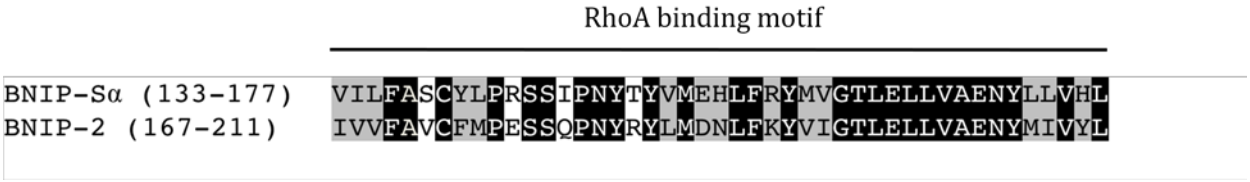

b

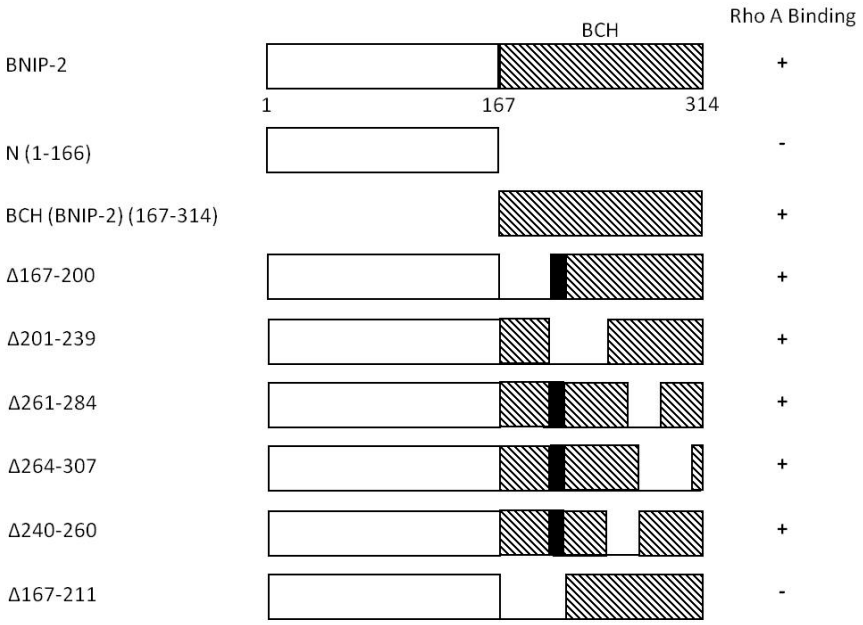

c

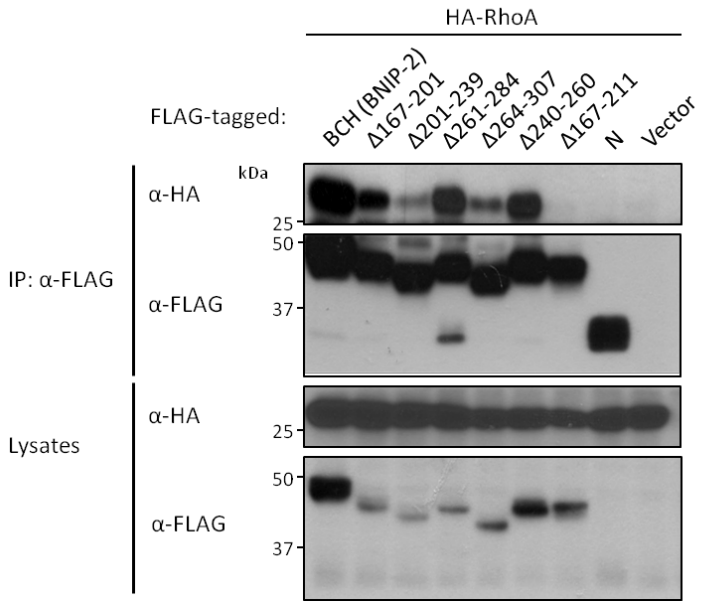

Figure 3.11 Residues 167-211 of BNIP-2 BCH domain constitute a unique RhoA binding motif. (a) Amino acid sequence alignment of BNIP-Sα (AY078983) RhoA binding motif and BNIP-2 (U15173) BCH domain using BLASTp and formatted with BOXSHADE. (b) Schematic representation of expression plasmids encoding BNIP-2 and its deletion mutants. Interaction of each protein with RhoA is denoted by either the positive (+) or negative (–) sign. (c) Lysates of cells co-transfected with FLAG-tagged BNIP-2 BCH domain deletion mutants and HA-RhoA were subjected to immunoprecipitation by anti-FLAG M2 beads. Co-expression of HA-RhoA with FLAG-tagged full length BNIP-2, N terminal or expression vector control was included as controls. To detect associated proteins, immunoprecipitated lysates were separated using SDS-PAGE, blotted and probed with anti-HA (first panel) and anti-FLAG antibodies (second panel). WCL were also analyzed by Western blot to verify the presence of overexpressed proteins.

3.2.4.2 B1 region (residues 34-74) of BPGAP1 BCH domain is important for RhoA binding

From the results of immunoprecipitation studies shown in Figure 3.10, it was found that RhoA was enriched by the BCH domain of BPGAP1, implying the existence of a RhoA binding region within this domain. To further define the specific region required for interaction with RhoA, immunoprecipitation studies as described

earlier were similarly employed to examine the RhoA binding abilities of various internal deletion and truncation mutants of BPGAP1 BCH domain (Figure 3.12a). As summarized in Figure 3.12a, mutants lacking amino acid residues 34 to 74 including ΔB1 and B23P, failed to interact with RhoA. Although deletion mutants ΔB1A (Δ34-47) and ΔB1B (Δ48-74) were able to associate with RhoA, their interactions were very weak and sometimes undetectable, suggesting that residues 34 to 74 constitute the full region necessary for forming stable associations with RhoA (Figure 3.12b). Indeed, sequence alignment of p50RhoGAP and BPGAP1 BCH domains revealed that RhoA binding motif of p50RhoGAP (Zhou et al., 2010) corresponds to residues 35 to 75 within BCH domain of BPGAP1 (Figure 3.12c). This further supports that B1 region is important for RhoA binding.

a

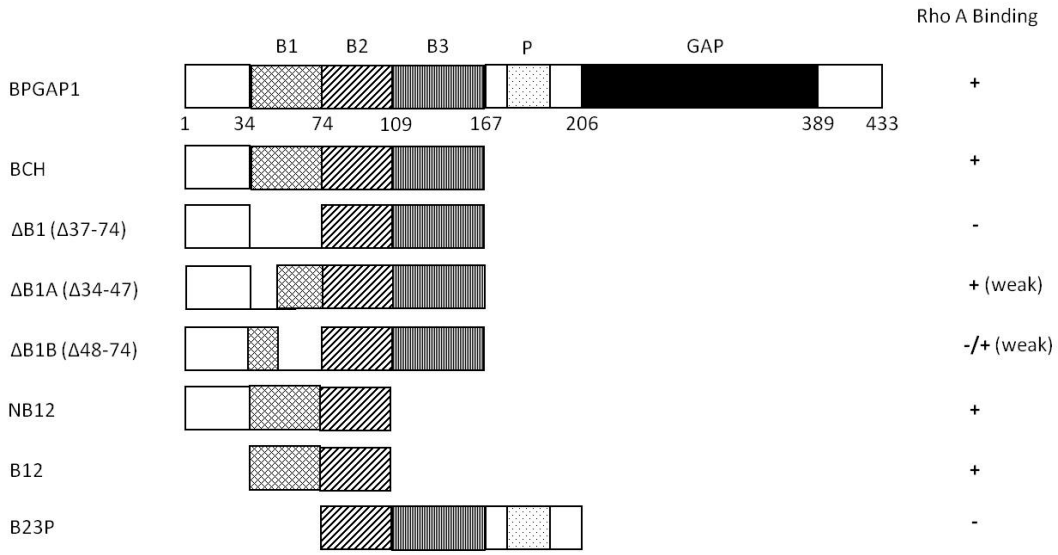

b

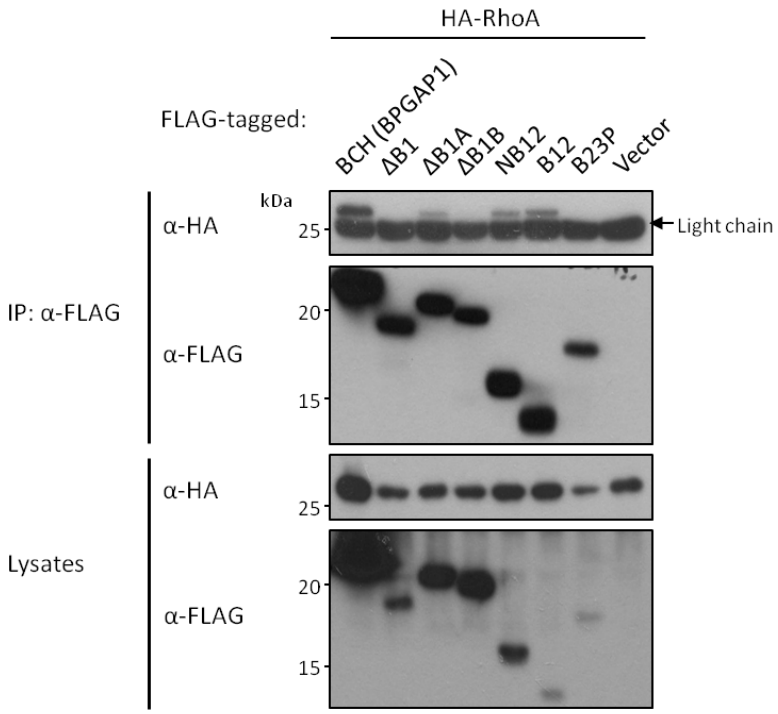

c

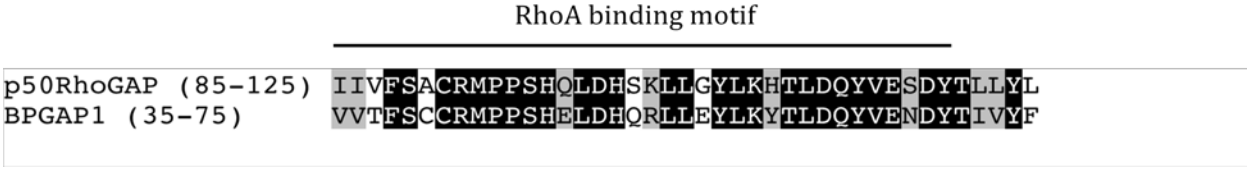

Figure 3.12 RhoA binding motif of BPGAP1 lies within B1 region (residues 34-74) of its BCH domain. (a) Schematic representation of BPGAP1 and its BCH domain mutants. The positive (+) or negative (–) sign denotes the ability of each protein to bind RhoA. (b) Lysates of cells co-expressing each of the BPGAP1 BCH domain mutants and HA-RhoA as indicated were immunoprecipitated with anti-FLAG M2 beads. BCH domain (BPGAP1) and expression vector were used as controls. For analyses, immunoprecipitates and cell lysates were resolved on SDS-PAGE, blotted and probed with anti-HA (first and third panel) and anti-FLAG antibodies (second and fourth panel). IP: Immunoprecipitates. (c) Protein sequence alignment of p50RhoGAP (Q07960) RhoA binding motif and BPGAP1 (AAN40769) BCH domain using BLASTp and formatted with BOXSHADE.

3.2.4.3 BCH domains of BNIP-2 and BPGAP1 recognize specific forms of RhoA

Small GTPases can exist in either active GTP-bound or inactive GDP-bound state. BNIP-XL, a member of BNIP-2 family of BCH domain-containing proteins that regulates RhoA signaling via its BCH domain, has been shown to bind specific RhoA conformers *in vivo* (Soh and Low, 2008). Thus, we investigated whether BNIP-2 and BPGAP1, and their respective BCH domains, could also recognize specific RhoA conformers by examining their interactions with various RhoA constitutively active or dominant negative mutants. Constitutively active mutants G14V and Q63L are locked in an active conformation mimicking GTP-RhoA and thus rendering them constitutively active, whereas the mutant F30L behaves like wild-type RhoA but with an accelerated GDP to GTP exchange. Conversely, dominant negative mutant T19N could possibly hinder RhoA activation by sequestering multiple RhoGEFs, suggesting the presence of a higher GDP-RhoA level.

From the results of immunoprecipitation studies, RhoA mutants F30L and T19N displayed enhanced interactions with both BNIP-2 and BPGAP1, as well as their BCH domains. In contrast, these proteins failed to associate with the constitutively active mutants G14V and Q63L (Figure 3.13a and b). Since both BNIP-2 and BPGAP1 recognize RhoA that can cycle between active and inactive states but not to the constitutively active forms, it is likely that these proteins can detect RhoA conformation changes through their BCH domains as similar to BNIP-XL BCH domain (Soh and Low, 2008), and play regulatory roles in RhoA signaling.

ai

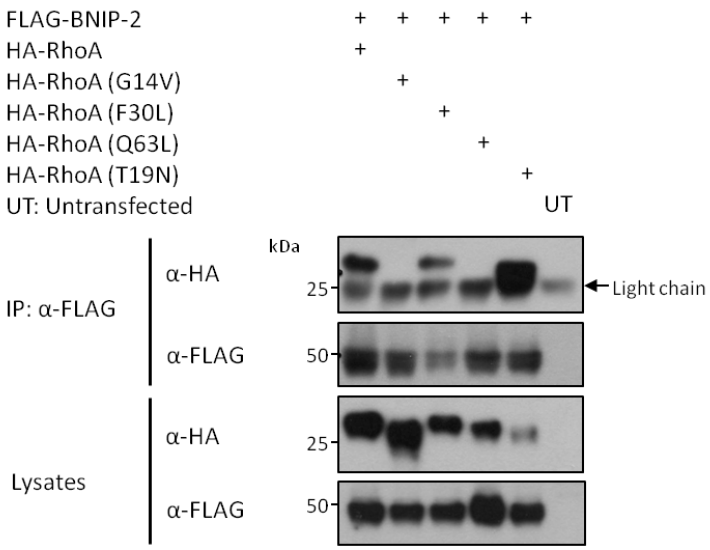
FLAG-BNIP-2 + + + + +
HA-RhoA +
HA-RhoA (G14V) +
HA-RhoA (F30L) +
HA-RhoA (Q63L) +
HA-RhoA (T19N) +
UT: Untransfected UT
kDa
IP: α-FLAG
α-HA
α-FLAG
25
50
Light chain
Lysates
α-HA
α-FLAG
25
50

aii

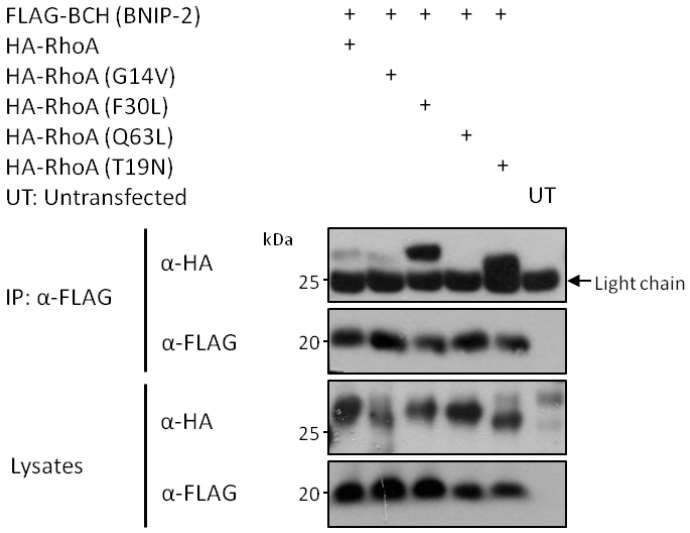
FLAG-BCH (BNIP-2) + + + + +
HA-RhoA +
HA-RhoA (G14V) +
HA-RhoA (F30L) +
HA-RhoA (Q63L) +
HA-RhoA (T19N) +
UT: Untransfected UT
kDa
IP: α-FLAG
α-HA
α-FLAG
25
20
Light chain
Lysates
α-HA
α-FLAG
25
20

bi

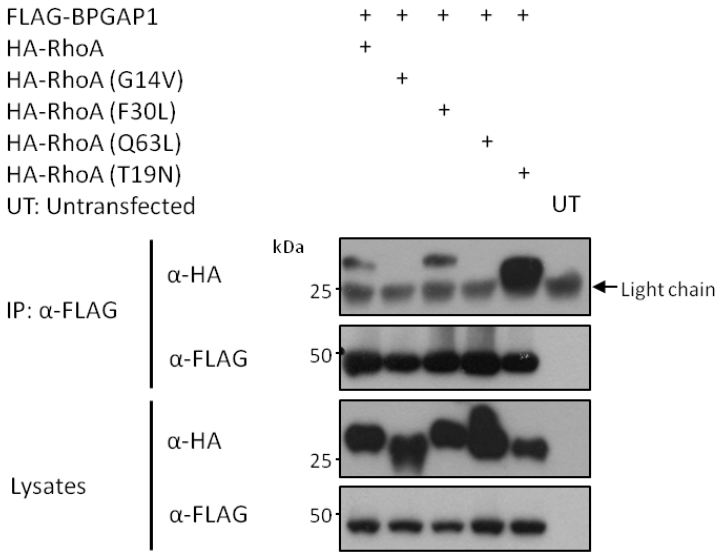

bii

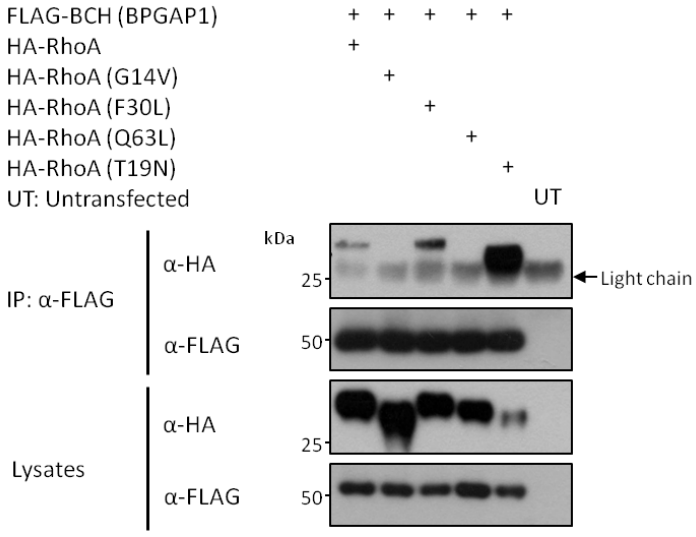

Figure 3.13 BCH domains of BNIP-2 and BPGAP1 mediate associations with specific forms of RhoA. FLAG-tagged (ai) BNIP-2; (aii) BNIP-2 BCH domain; (bi) BPGAP1 and (bii) BPGAP1 BCH domain was each tested for their interactions with different RhoA mutants, including constitutive active mutants G14V and Q63L, fast cycling mutant F30L and dominant negative mutant T19N, all expressed in HA-epitope. After incubation of the cell lysates with anti-FLAG M2 beads, bound proteins were analyzed by Western blot and probed with anti-HA and anti-FLAG antibodies to detect the immunoprecipitated (first and second panel) and overexpressed proteins (third and fourth panel).

3.3 BNIP-2 functions in synergism with BPGAP1 to promote RhoA inactivation *in vivo*

So far, it is established that interaction between BNIP-2 and BPGAP1 occurs through their BCH domains, as well as PGAP region of BPGAP1, and both proteins associate with RhoA via distinct RhoA binding motifs within their BCH domains. On the basis that BPGAP1 exerts its GTPase activating activity towards RhoA *in vivo* to reduce active RhoA level (Shang et al., 2003) and BNIP-2 is able to associate with both BPGAP1 and RhoA via its BCH domain, RhoA activity assay was next carried out to explore the functional effect of BNIP-2 and BPGAP1 on RhoA activity. The results of this assay are presented in the following sections.

3.3.1 BNIP-2 promotes the reduction of RhoA activity by BPGAP1 *in vivo*

While it has been established that BPGAP1 functions as a RhoGAP specifically towards RhoA *in vivo* (Shang et al., 2003), the role of BNIP-2 in regulating Rho GTPase activity remains unclear. Although BNIP-2 has previously been reported to display *in vitro* GAP activity towards Cdc42 via a non-canonical arginine patch in its BCH domain (Low et al., 2000b), this increment in Cdc42 GTPase activity was not detected *in vivo* (Zhou et al., 2005). After assessing the interactions between BNIP-2, BPGAP1 and RhoA, we proceeded to investigate whether the individual proteins, as well as when present together, have any effect on RhoA activity *in vivo*.

To do so, cells were transfected with expression plasmids of RhoA, along with either BNIP-2 or BPAGP1, or both. Harvested lysates were subjected to pull-down using pre-prepared GST-RBD- or GST-bound glutathione sepharose beads and the amount of active RhoA present in the cells was reflected by the magnitude of

interaction with RBD of Rho effector, Rhotekin, as described in *Materials and Methods*. Both GST-RBD- and GST-bound beads were first tested for their specificity towards GTP-RhoA such that the GST-RBD-bound beads were able to capture Q63L that mimicks GTP-RhoA but not T19N, whereas GST-bound beads function as control and could bind neither of the expressed proteins (Figure 3.14a).

Results of RhoA activity assay demonstrate that in the presence of BPGAP1, the amount of active RhoA was reduced as compared to control cells that were overexpressing only RhoA proteins (Figure 3.14b, first panel, lane 3 and 4). This decrease is likely attributed to the enhancement of GTP hydrolysis stimulated by GAP activity of BPGAP1. Co-expression of BNIP-2 and RhoA, on the other hand, led only to a minimal decrease in RhoA activity (Figure 3.14b, first panel, lane 2). More importantly, introduction of BPGAP1 and RhoA in the presence of BNIP-2 further augmented the reduction in active RhoA amount to approximately half the magnitude of the control cells (Figure 3.14b, first panel, lane 1 and 4). Collectively, data from three independent sets of experiments reflect that BNIP-2 and BPGAP1, when co-introduced into the cells, cooperate to induce a greater degree of suppression on RhoA activity (Figure 3.14c). This observation raises the possibility that BNIP-2 might function in synergism with BPGAP1 to enhance its GAP activity towards RhoA, thereby promoting RhoA inactivation.

In assessing the binding specificity of BNIP-2 and BPGAP1, as well as their domains, to different RhoA mutants, a greater amount of mutant F30L was detected in the immunoprecipitates as compared to wild-type RhoA (Figure 3.13). Since the fast cycling mutant retains regular GTP hydrolysis, RhoA activity assay was similarly carried out with mutant F30L, in replace of wild-type RhoA, to corroborate the synergistic effect of BNIP-2 and BPGAP1 in decreasing active RhoA level. Indeed,

similar activity profile (Figure 3.14d) and trend (Figure 3.14e) were obtained for mutant F30L, thereby supporting the earlier observations obtained with wild-type RhoA that BNIP-2 and BPGAP1 function in synergism to reduce RhoA activity.

a

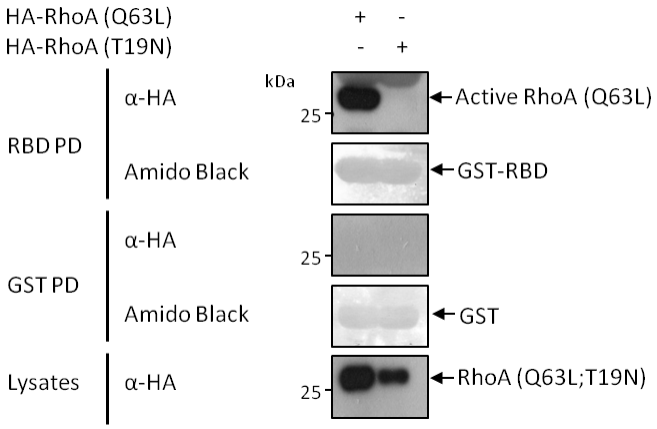

b

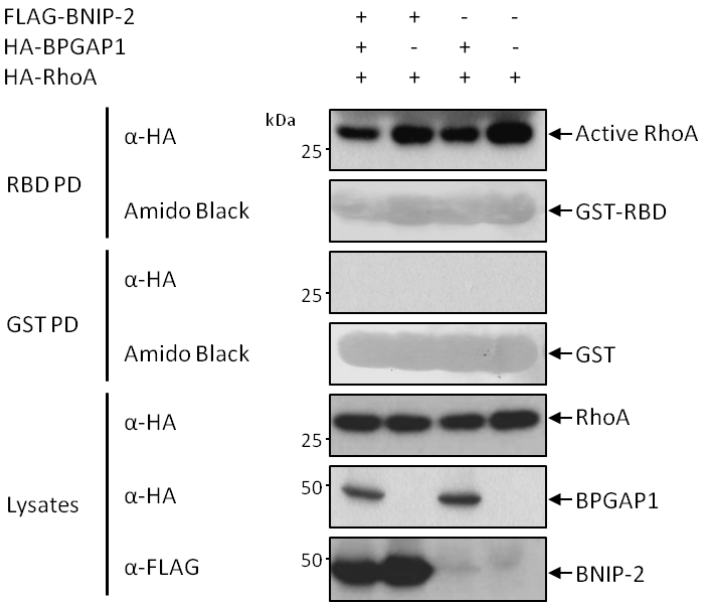

c

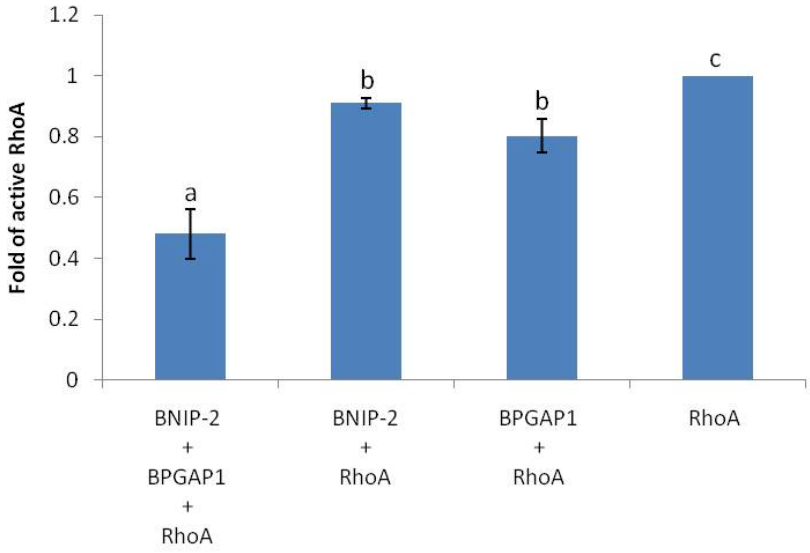
Fold of active RhoA
1.2
1
0.8
0.6
0.4
0.2
0
a
b
b
c
BNIP-2 + BPGAP1 + RhoA
BNIP-2 + RhoA
BPGAP1 + RhoA
RhoA

d

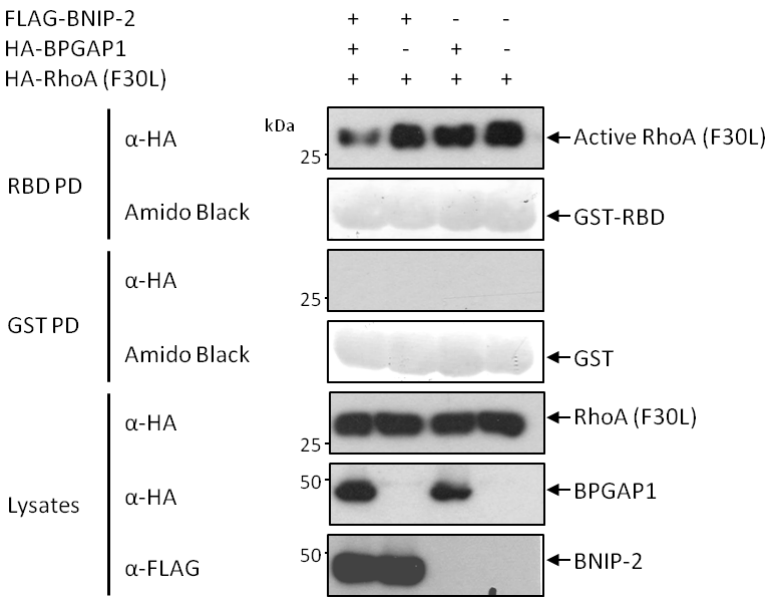
FLAG-BNIP-2 + + - -
HA-BPGAP1 + - + -
HA-RhoA (F30L) + + + +
kDa
RBD PD
α-HA
Amido Black
Active RhoA (F30L)
GST-RBD
GST PD
α-HA
Amido Black
GST
Lysates
α-HA
α-HA
α-FLAG
RhoA (F30L)
BPGAP1
BNIP-2
25
25
25
50
50

e

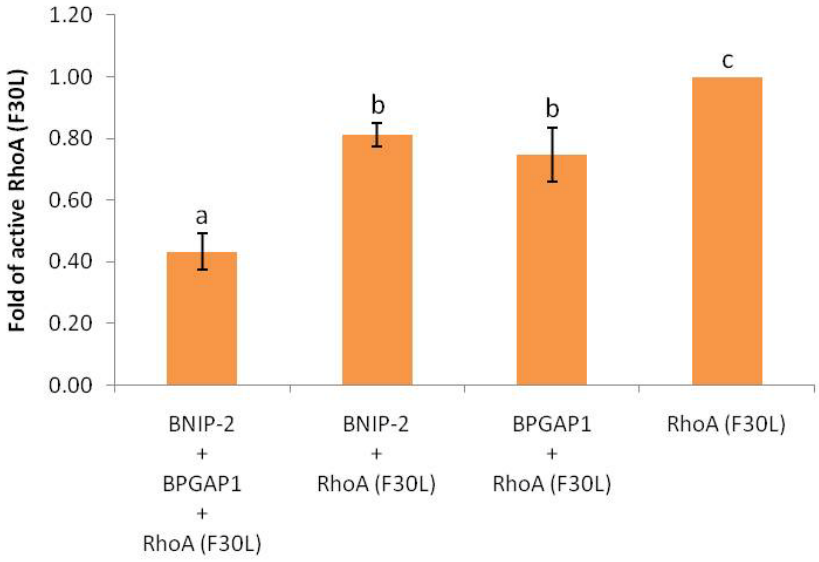

Figure 3.14 BNIP-2 promotes reduction of RhoA activity by BPGAP1 *in vivo*. (a) Lysates of 293T cells transfected with HA-tagged RhoA mutants Q63L or T19N were incubated with GST-RBD- or GST-bound beads to confirm the specificity of GST-RBD. Associated active RhoA mutant Q63L and WCL were subjected to Western blot analyses using anti-HA antibody (first, third and bottom panel) and amido black staining was used to show equal loading of the beads (second and fourth panel). To measure Rho GTPase activity, (b) wild-type HA-RhoA with either HA-BPGAP1 or FLAG-BNIP-2 or both; (d) fast cycling mutant HA-RhoA (F30L) with either HA-BPGAP1 or FLAG-BNIP-2 or both, were expressed in 293T cells as indicated for 20-24 hrs, lysed and incubated with GST fusion of RBD of Rhotekin immobilized on glutathione sepharose beads as described in *Materials and Methods*. GST proteins were used as negative control (third panel). Bound active RhoA or RhoA (F30L) proteins were resolved on SDS-PAGE, blotted and probed with anti-HA antibody (first panel). Protein expression of RhoA or RhoA (F30L), BPGAP1 and BNIP-2 in the cell lysates was confirmed by Western blotting using the respective anti-HA or anti-FLAG antibodies (fifth, sixth and bottom panel). Equal loading of GST fusion proteins and GST proteins were shown using amido black staining in second and fourth panel, respectively. PD: Pull-down. For quantitative analysis, amount of active (c) wild-type RhoA; (e) RhoA (F30L), was normalized to total RhoA or RhoA (F30L) present in the cell lysates, respectively, and represented as fold of active RhoA or RhoA (F30L) relative to cells transfected with the respective forms of RhoA (set as 1), as described in *Materials and Methods*. Data derived from three independent sets of experiments are expressed as mean $\pm$ standard error mean and differences between values that are statistically significant at $p < 0.05$, measured by two-tailed Student's t-test with unequal variance, are represented by different letters.

3.3.2 Synergistic effect of BNIP-2 and BPGAP1 on RhoA inactivation is coupled to the GAP activity of BPGAP1

As a RhoGAP, BPGAP1 harbors an invariant arginine residue at position 232, which when mutated to alanine (R232A), results in the abolishment of its GAP activity (Shang et al., 2003). To further validate the hypothesis that BNIP-2 augments RhoA inactivation through enhancement of BPGAP1 GAP activity, RhoA activity assay was carried out using GAP inactive mutant BPGAP1(R232A) in the presence or absence of BNIP-2, together with RhoA as indicated. Certainly, Western blot analyses reveal that BPGAP1(R322A) alone failed to induce a significant decrease in active RhoA level as compared to the control consisting of overexpressed RhoA alone (Figure 3.15a, first panel, lane 3 and 4). Although there was a slight reduction in RhoA activity when BNIP-2 and BPGAP1(R232A) were co-transfected with RhoA in comparison to the control (Figure 3.15a, first panel, lane 1 and 4), no significant difference in active RhoA level was observed for cells co-expressing BPGAP1(R232A) and RhoA with or without BNIP-2 (Figure 3.15a, first panel, lane 1 and 3).

From the results of three independent sets of experiments, it is evident that BNIP-2 did not induce any significant decrease in active RhoA level when RhoA activity assay was performed with BPGAP1(R232A) mutant (Figure 3.15b), as opposed to the augmentation effect observed for wild-type BPGAP1 (Figure 3.14c). Taken together, these data therefore suggest that synergistic effect of BNIP-2 and BPGAP1 in promoting reduction of active RhoA level is coupled to the GAP activity of BPGAP1.

a

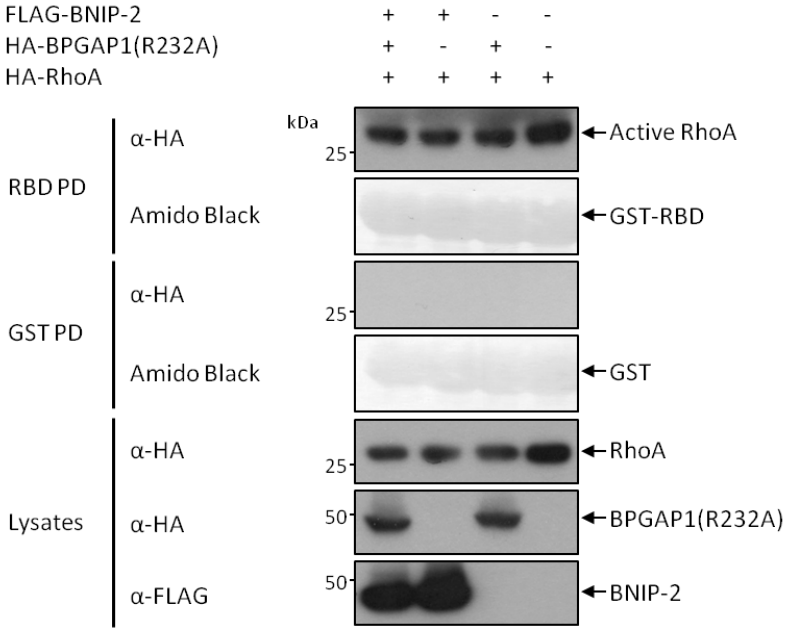
FLAG-BNIP-2 + + - -
HA-BPGAP1(R232A) + - + -
HA-RhoA + + + +
kDa
RBD PD
α-HA
Amido Black
GST PD
α-HA
Amido Black
Lysates
α-HA
α-HA
α-FLAG
25
25
25
50
50
Active RhoA
GST-RBD
GST
RhoA
BPGAP1(R232A)
BNIP-2

b

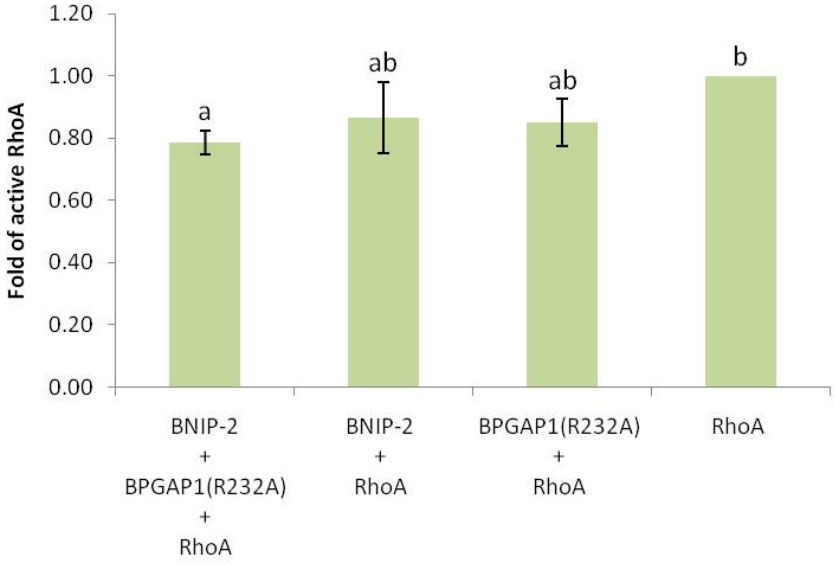
Fold of active RhoA
1.20
1.00
0.80
0.60
0.40
0.20
0.00
a
ab
ab
b
BNIP-2 + BPGAP1(R232A) + RhoA
BNIP-2 + RhoA
BPGAP1(R232A) + RhoA
RhoA

Figure 3.15 Synergistic effect of BNIP-2 and BPGAP1 on RhoA inactivation is coupled to the GAP activity. (a) 293T cells expressing wild-type HA-RhoA with either HA-BPGAP1(R232A) or FLAG-BNIP-2 or both were lysed 20-24 hrs post-transfection and incubated with GST-RBD or GST immobilized on glutathione sepharose beads as described in *Materials and Methods*. GST proteins were used as negative control (third panel). Active RhoA proteins captured by the beads were analyzed by western blotting using anti-HA antibody (first panel), while expression of RhoA, BPGAP1(R232A) and BNIP-2 in the cell lysates were verified with the respective anti-HA or anti-FLAG antibodies (fifth, sixth and bottom panel). Equal loading of GST fusion proteins and GST proteins were shown by amido black staining in the second and fourth panel, respectively. PD: Pull-down. (b) For quantitative analysis, the amount of active RhoA was normalized to total RhoA present in cell lysates and represented as fold of active RhoA relative to cells overexpressing RhoA alone (set as 1), as described in *Materials and Methods*. Data derived from three independent sets of experiments are expressed as mean $\pm$ standard error mean and differences between values that are statistically significant at $p < 0.05$, as measured by two-tailed Student's t-test with unequal variance, are represented by different letters.

To ascertain that the lack of synergistic effect between BNIP-2 and GAP mutant BPGAP1(R232A) in reducing RhoA activity is not attributed to any lost of interaction between these proteins, immunoprecipitation studies were performed to verify their associations. Cells co-expressing BNIP-2 or RhoA with either BPGAP1 or BPGAP1(R232A) were harvested for immunoprecipitation and subsequently analyzed by Western blot. As observed in Figure 3.16a, comparable amounts of bound BPGAP1 and BPGAP1(R232A) proteins were captured by BNIP-2, indicating that interaction between BNIP-2 and the GAP mutant was not affected. Similarly, BPGAP1(R232A) retains the ability to associate with RhoA (Figure 3.16b). Furthermore, investigations on the interaction between GAP mutant BPGAP1(R232A) and RhoA in the presence and absence of BNIP-2 did not reveal any differences (Figure 3.16c), similar to the interaction profiles for wild-type BPGAP1.

Consistent with results of the immunoprecipitation studies, regions of co-localization were also observed for BNIP-2, BPGAP1(R232A) and RhoA in confocal immunofluorescence studies. These areas of co-localization appeared white in the merged image and inserts, as indicated by white arrows (Figure 3.17). It is therefore unlikely that the lack of synergistic effect between BNIP-2 and GAP mutant BPGAP1(R232A) in reducing RhoA activity is caused solely by any lost in interactions, but rather involves a mechanism that is coupled to the GAP activity.

a

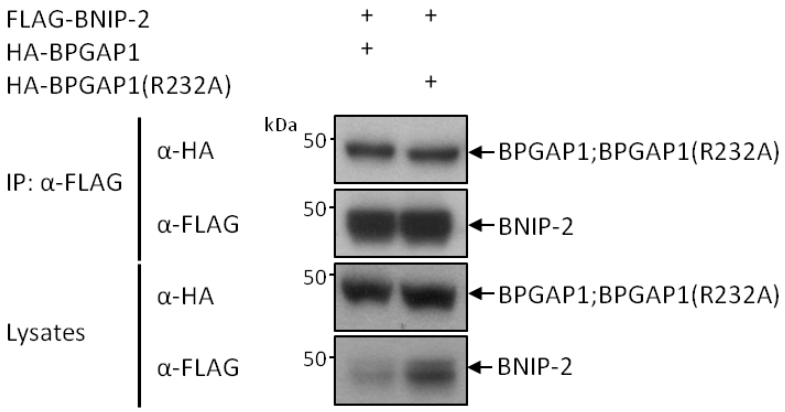

b

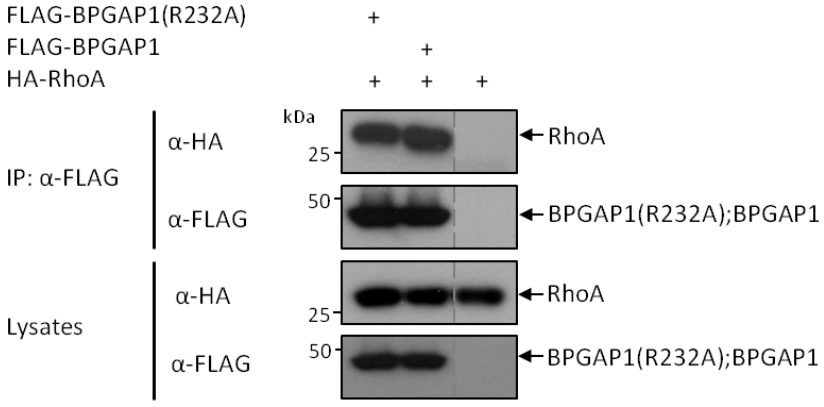

c

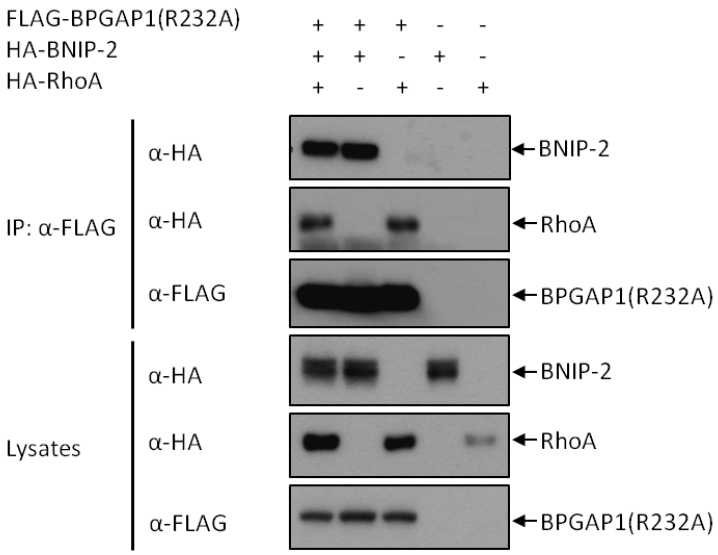

Figure 3.16 BPGAP1(R232A) displays similar interaction profile with BNIP-2 and RhoA with respect to BPGAP1. 293T cells transiently transfected with FLAG-tagged BPGAP1 or BPGAP1(R232A) were tested for their interaction with (a) HA-BNIP-2 and (b) HA-RhoA, respectively. Harvested lysates were immunoprecipitated with anti-FLAG M2 beads and the bound proteins were resolved on SDS-PAGE, blotted and probed using anti-HA antibody (first panel). Expression of proteins was verified by Western blot analyses of cell lysates using anti-FLAG (fourth panel) and anti-HA antibodies (third panel). Blots separated by the dotted lines are from the same blot with same exposure time. (c) FLAG-BPGAP1(R232A), HA-tagged BNIP-2 or RhoA as indicated by the + signs or an equivalent amount of correspondingly tagged expression vector control indicated by the – signs, were introduced into 239T cells and the harvested lysates were subjected to immunoprecipitation with anti-FLAG M2 beads. Associated proteins and WCL were analyzed by Western blot and probed with anti-HA and anti-FLAG antibodies to detect the bound proteins (first to third panel), as well as expression of the introduced constructs (fourth, fifth and bottom panel).

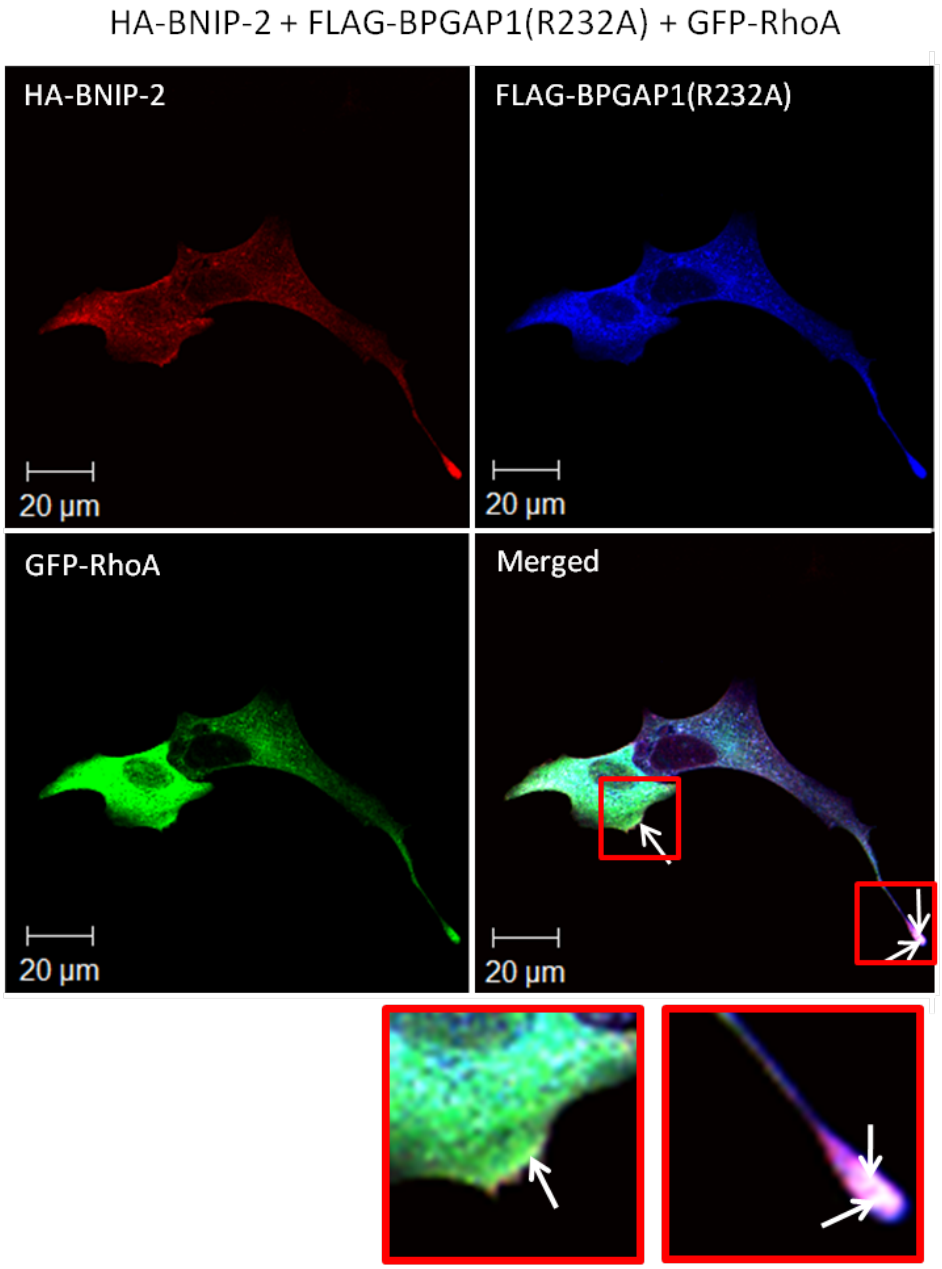

Figure 3.17 BNIP-2, BPGAP1(R232A) and RhoA exhibit regions of co-localization. HA-BNIP-2, FLAG-BPGAP1(R232A) and GFP-RhoA were expressed in CV-1 cells, fixed after 20 hrs, permeabilized and stained for immunofluorescence detection by confocal fluorescence microscopy as described in *Materials and Methods*. For visualization of the expressed proteins, HA-BNIP-2 and FLAG-BPGAP1 were labeled with polyclonal rabbit anti-HA and monoclonal mouse anti-FLAG antibodies respectively, followed by the appropriate fluorophore-conjugated secondary antibodies. Co-localization of BNIP-2 (red), BPGAP1(R232A) (blue) and RhoA (green) at regions within the cell were represented by white spots in the merged image and inserts, indicated by white arrows. Scale bar, 20 µm.

3.3.3 BNIP-2 augments BPGAP1 RhoGAP activity to suppress endogenous RhoA activity *in vivo*

The results obtained so far from RhoA activity assays using overexpressed RhoA have suggested that BNIP-2 functions in concert with BPGAP1 to promote GTP hydrolysis, thereby further reducing the amount of active RhoA present. As such, it is of interest to determine if such concerted action occurs endogenously to regulate RhoA activity. To do so, RhoA activity assay as described previously was performed using lysates of cells transfected with expression plasmids of BNIP-2, BPGAP1 or BPGAP1(R232A), either alone or together as indicated and the endogenous level of active RhoA was detected using monoclonal anti-RhoA antibody.

Consistent with the results from RhoA activity assays performed with overexpressed RhoA, expression of BPGAP1 alone led to a decrease in the amount of active endogenous RhoA with respect to vector control (Figure 3.18a, first panel, lane 3 and 4). The magnitude of RhoA inactivation in cells transfected with BNIP-2 alone was slightly lesser in comparison after normalization to total endogenous RhoA level (Figure 3.18b). When co-expressed, BNIP-2 and BPGAP1 concertedly suppress RhoA activity to a greater extent (Figure 3.18a, first panel, lane 1 and 4), similar to the results obtained with overexpressed RhoA. In contrast, inactivation of the RhoGAP activity of BPGAP1 abolished the synergism between BNIP-2 and BPGAP1 in suppressing RhoA activity (Figure 3.18a, first panel, lane 1 and 5). A significant reduction in RhoA activity was observed only when the effect of BNIP-2 was coupled to BPGAP1, but not with the GAP mutant (Figure 3.18b, $p < 0.05$). In all, these data indicate that BNIP-2 functions in synergism with BPGAP1 to promote endogenous RhoA inactivation, likely through the enhancement of RhoGAP activity of BPGAP1.

a

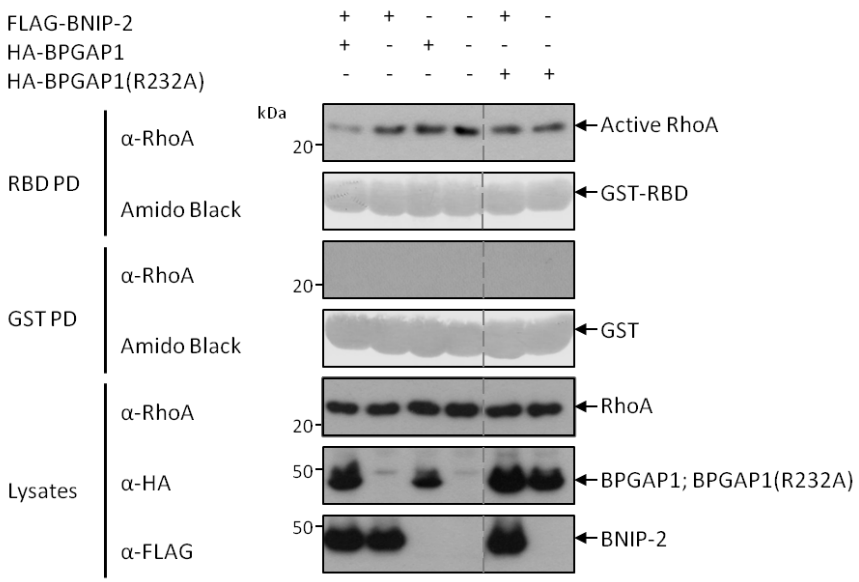
FLAG-BNIP-2
HA-BPGAP1
HA-BPGAP1(R232A)
+ + - - + -
+ - + - - -
- - - - + +
kDa
RBD PD
α-RhoA
Amido Black
GST PD
α-RhoA
Amido Black
Lysates
α-RhoA
α-HA
α-FLAG
20
20
20
50
50
Active RhoA
GST-RBD
GST
RhoA
BPGAP1; BPGAP1(R232A)
BNIP-2

b

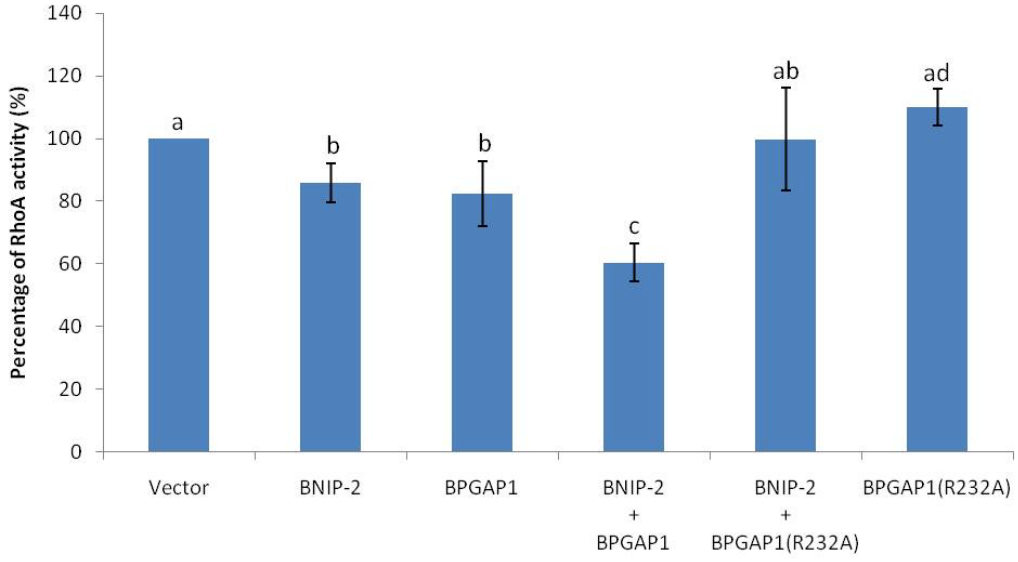
Percentage of RhoA activity (%)
140
120
100
80
60
40
20
0
a
b
b
c
ab
ad
Vector
BNIP-2
BPGAP1
BNIP-2 + BPGAP1
BNIP-2 + BPGAP1(R232A)
BPGAP1(R232A)

Figure 3.18 BNIP-2 functions in concert with BPGAP1 to suppress endogenous RhoA activity. (a) To assay endogenous level of active RhoA, FLAG-BNIP-2, HA-tagged BPGAP1 or BPGAP1(R232A) was expressed in 239T cells either alone or together. An equivalent amount of correspondingly tagged expression vector control denoted by the – sign was co-transfected as indicated to maintain a constant amount of DNA introduced into the cells. After 20-24 hrs, cell lysates were collected and incubated with either GST fusion of Rhotekin RBD immobilized on glutathione sepharose beads or with GST proteins as controls, as described in *Materials and Methods*. Subsequently, active RhoA proteins captured on GST-RBD beads and cell lysates were resolved on SDS-PAGE, blotted and probed with anti-RhoA antibody to detect the bound RhoA proteins (first panel) and endogenous total RhoA proteins (fifth panel). Similarly, protein expression of HA-tagged BPGAP1, BPGAP1(R232A) and FLAG-BNIP-2 was verified by Western blot analyses of WCL using anti-HA (sixth panel) or anti-FLAG antibodies (bottom panel). Equal loading of GST fusion proteins and GST proteins were shown using amido black staining in second and fourth panel, respectively. Blots separated by dotted line are from the same blot with same exposure time. PD: Pull-down. (b) For quantitative analysis, the amount of active RhoA captured by GST-RBD beads was normalized to total endogenous RhoA level in the cell lysates and represented as fold of active RhoA relative to vector-expressing control cells (set as 1), as described in *Materials and Methods*. Data derived from three or more independent sets of experiments are expressed as mean $\pm$ standard error mean and the different letters represent differences between values that are statistically significant at $p < 0.05$, measured by two-tailed Student's t-test with unequal variance.

3.4 Delineation of BNIP-2-BPGAP1 interacting regions

Since BNIP-2 promotes the RhoGAP activity of BPGAP1 to downregulate active RhoA level and these two proteins associate through their BCH domains, as well as via the PGAP region of BPGAP1, we aim to examine whether this synergism between BNIP-2 and BPGAP1 on RhoA inactivation is indeed brought about by the functional interaction of these proteins. To address this query, the binding regions between BNIP-2 and BPGAP1 are determined in an attempt to generate non-interacting mutants for assessing the significance of their interaction on the synergistic effect observed.

3.4.1 Residues 167-211 of BNIP-2 BCH domain constitutes the likely interacting region for BPGAP1

Results from co-immunoprecipitation studies performed earlier have demonstrated that BNIP-2 associates with BPGAP1 solely via its BCH domain (Figure 3.3c). To further delineate the region required for interaction, BNIP-2 BCH domain deletion mutants used previously for identifying the RhoA binding motif were tested for their ability to interact with BPGAP1 using immunoprecipitation studies. Subsequent western blot analyses of the lysates of cells co-expressing HA-BPGAP1 and BNIP-2 mutants expressed in FLAG-epitope reveal that interaction with BPGAP1 was much reduced when amino acid residues 167-211 were deleted from BNIP-2 BCH domain, though not completely abolished. On the other hand, associations of BPGAP1 with other mutants remained intact (Figure 3.19bi).

Interestingly, the region within BNIP-2 BCH domain that is important for binding to BPGAP1 overlaps with the previously identified RhoA binding motif. To further delineate the region necessary for interaction with BPGAP1, two internal deletion mutants, each comprising of a subdivision of the region from residues 167-211, were generated based on secondary structure predictions to avoid disruption of any major secondary structures such as α-helices and β-sheets (Appendix, Figure S1a). Both of these constructs Δ167-184 and Δ185-211, expressed in FLAG-epitope, were used in immunoprecipitation studies together with BPGAP1. While deletion of the entire region ranging from residues 167 to 211 weakens the binding to BPGAP1 considerably, removal of smaller sub-regions did not disrupt the interactions to a similar extent comparatively (Figure 3.19bii). A summary of the binding profile of full-length BPGAP1 to various BNIP-2 deletion mutants is shown in Figure 3.19a. Earlier, it has been demonstrated that BNIP-2 associates with both BCH domain and

PGAP module of BPGAP1. Therefore, immunoprecipitation studies were also carried out to examine if these associations are mediated by separate regions within BNIP-2 BCH domain. However, no apparent differences were seen in the interaction profiles of BNIP-2 mutants with BCH domain or PGAP region as compared to full-length BPGAP1 (Appendix, Figure S2).

Taken together, the interacting region between BNIP-2 and BPGAP1 comprises at least residues 167 to 211 of BNIP-2 BCH domain and may extent to the neighbouring residues beyond this region or consist of another secondary interacting site.

a

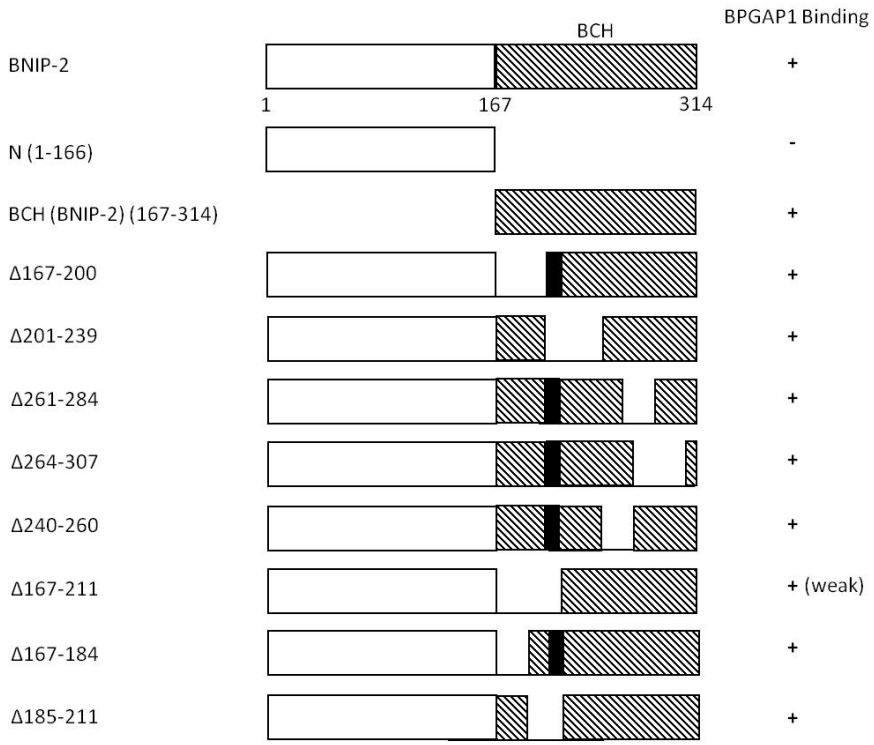

bi

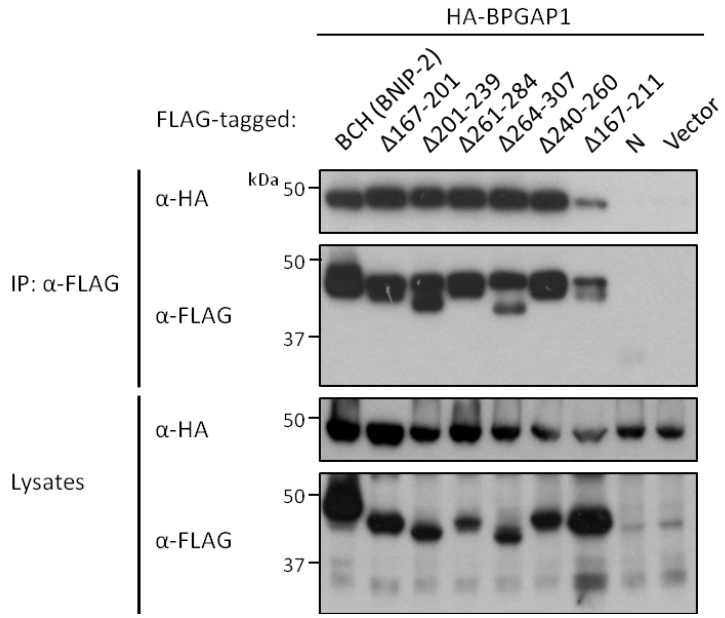

bii

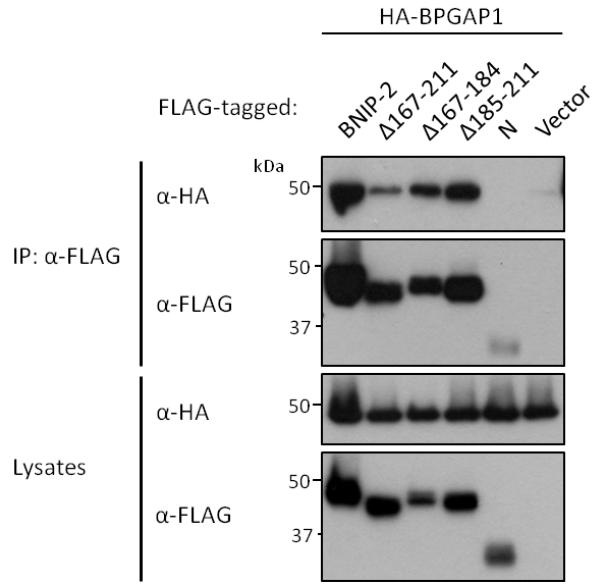

Figure 3.19 Residues 167 to 211 of BNIP-2 BCH domain are required for interaction with BPGAP1. (a) Schematic diagram of BNIP-2 and its deletion mutants. Binding abilities of BPGAP1 to the various mutants were summarized and as indicated by the positive (+) or negative (-) sign. (bi) and (bii) Lysates of cells co-transfected with each of the FLAG-tagged BNIP-2 BCH domain deletion mutants and HA-BPGAP1 as indicated were subjected to immunoprecipitation by anti-FLAG M2 beads. Co-expression of FLAG-tagged full length BNIP-2, N terminal or expression vector control with HA-BPGAP1 was included as controls. To detect the associated proteins, immunoprecipitated lysates were separated using SDS-PAGE, blotted and probed with anti-HA (first panel), before stripping and re-probing with anti-FLAG antibodies (second panel). WCL were also analyzed by Western blot to verify the expression of proteins (third and fourth panel).

A further examination of BNIP-2 mutant Δ167-211 by confocal immunofluorescence microscopy reveals that in opposed to the unique distribution of wild-type BNIP-2 that concentrates at the edges of cellular protrusions, such distinctive accumulations were rarely observed in cells transfected with this mutant. BNIP-2, when devoid of residues 167 to 211, appeared more localized within the main body of the cell and away from peripheral regions (Figure 3.20), suggesting that this region might be involved in the trafficking of this protein. A noticeable amount of floating cells were also seen following the transfection of 293T cells with this mutant. In addition, since deletion of this region affects the binding of BNIP-2 to both RhoA and BPGAP1, use of this mutant to examine whether the synergistic effect is brought about by association between BNIP-2 and BPGAP1 is not possible.

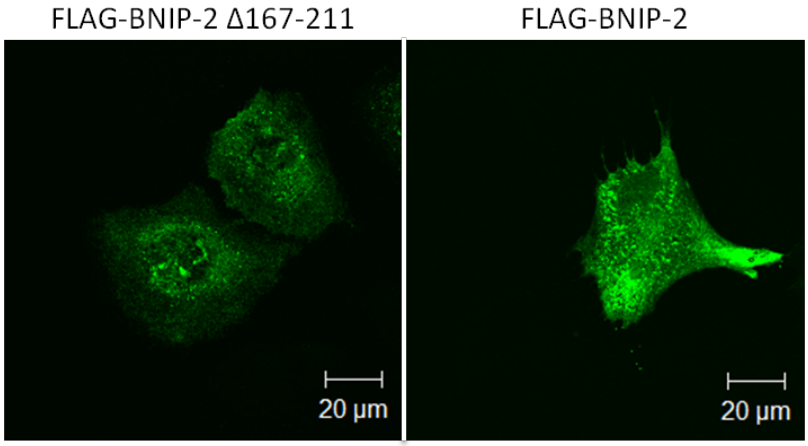

Figure 3.20 BNIP-2 mutant Δ167-211 fails to display the characteristic localization of wild-type BNIP-2. To study cellular distribution of FLAG-BNIP-2 mutant Δ167-211, CV-1 cells were transfected with the expression plasmid encoding this mutant. Cells were fixed after 20 hrs, permeabilized and labeled first with monoclonal mouse anti-FLAG antibody, followed by Alexa Fluro 488 donkey anti-mouse IgG. After which, the labeled cells were visualized by confocal fluorescence microscopy as described in *Materials and Methods*. Scale bar, 20 µm.

3.4.2 Multiple regions within BPGAP1 mediate interaction with BNIP-2 BCH domain

In Figure 3.3, the immunoprecipitation results demonstrate that both BCH domain and PGAP module of BPGAP1 mediate interactions with BNIP-2. In order to define the specific interaction motifs, two different sets of mutants, each encompassing different regions within BCH or GAP domain, were assessed separately for their ability to associate with full-length BNIP-2. The interaction profiles are shown in the following sections.

3.4.2.1 B1 region (residues 34-74) of BPGAP1 BCH domain is important for binding BNIP-2

To find out the residues within BPGAP1 BCH domain that are required for binding to BNIP-2, the set of deletion mutants used previously for identification of BPGAP1 RhoA binding motif was tested for interaction with BNIP-2 using co-immunoprecipitation studies. As revealed by Western blot analyses of the immunoprecipitated lysates, BNIP-2 displays a similar interaction profile to BPGAP1 BCH domain deletion mutants as RhoA (Figure 3.21a). In summary, deletion mutants that lack amino acid residues 34 to 74, including ΔB1 (Δ34-74) and B23P, failed to bind BNIP-2, while mutants ΔB1A (Δ34-47) and ΔB1B (Δ48-74) that encompass only part of B1 region associate weakly with this protein. Conversely, enrichment of BNIP-2 protein was observed selectively with mutants containing the full B1 region. Taken together, these data suggest that residues 34 to 74 are required for mediating interaction with BNIP-2 (Figure 3.21b), in addition to binding RhoA.

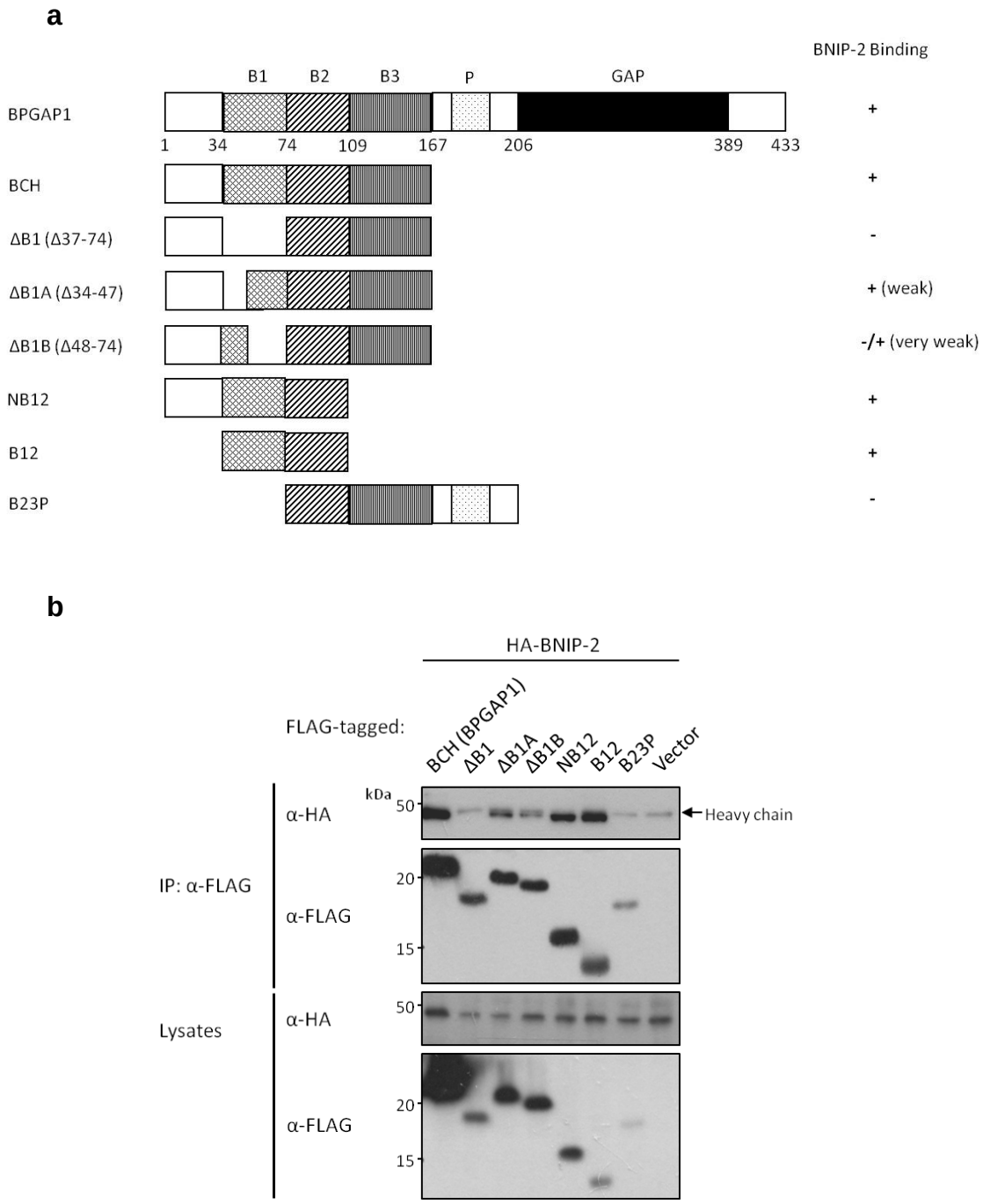

Figure 3.21 B1 region (residues 34-74) of BPGAP1 BCH domain mediates interaction with BNIP-2. (a) Schematic representation of BPGAP1 and its BCH domain deletion mutants. Binding abilities of different mutants to BNIP-2 were summarized and as indicated by the positive (+) or negative (-) sign. (b) Plasmids encoding HA-BNIP-2 and each of the FLAG-tagged BPGAP1 deletion mutants or vector control were introduced into 293T cells as indicated. Transiently transfected cells were lysed, incubated with anti-FLAG M2 beads and immunoprecipitated proteins were analyzed using Western blot by probing with anti-HA (first panel) and anti-FLAG antibodies (second panel). WCL were similarly resolved by SDS-PAGE and detected with anti-HA and anti-FLAG antibodies to verify the presence of overexpressed proteins (third and fourth panel).

3.4.2.2 A full composite GAP domain confers binding to BNIP-2

We next proceeded to map the BNIP-2 binding region on PGAP module. In addition to the current set of PGAP mutants available, two more GAP domain truncation mutants covering residues 168-281 and 168-310 were generated based on secondary structure predictions (Appendix, Figure S1b). To define the residues that are involved in mediating interaction with BNIP-2, immunoprecipitation studies were carried out using a series of PGAP truncation mutants (Figure 3.22a). Interestingly, deletion of different sub-regions of PGAP module failed to disrupt the interaction with BNIP-2 (Figure 3.22b), unlike the presence of a unique BNIP-2 interacting motif within BPGAP1 BCH domain. These results therefore suggest that the full composite PGAP region confers binding to BNIP-2.

a

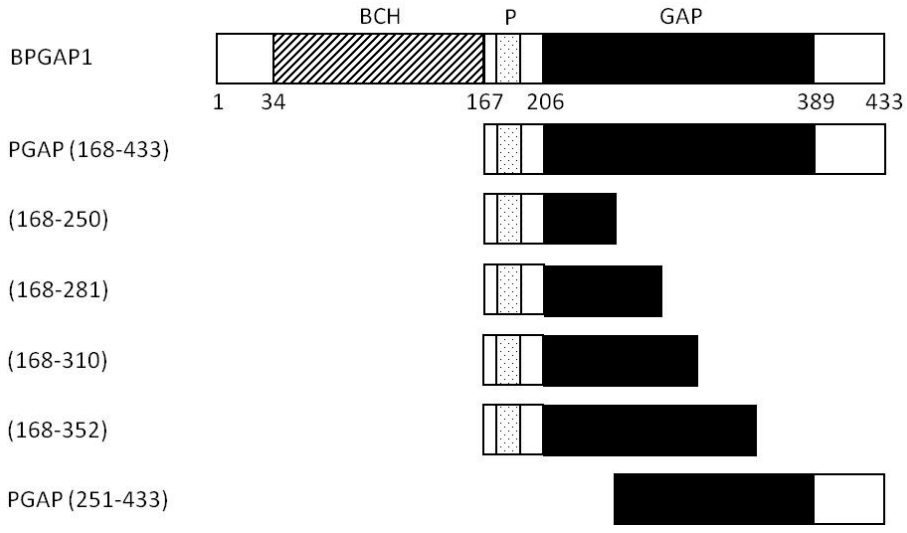

b

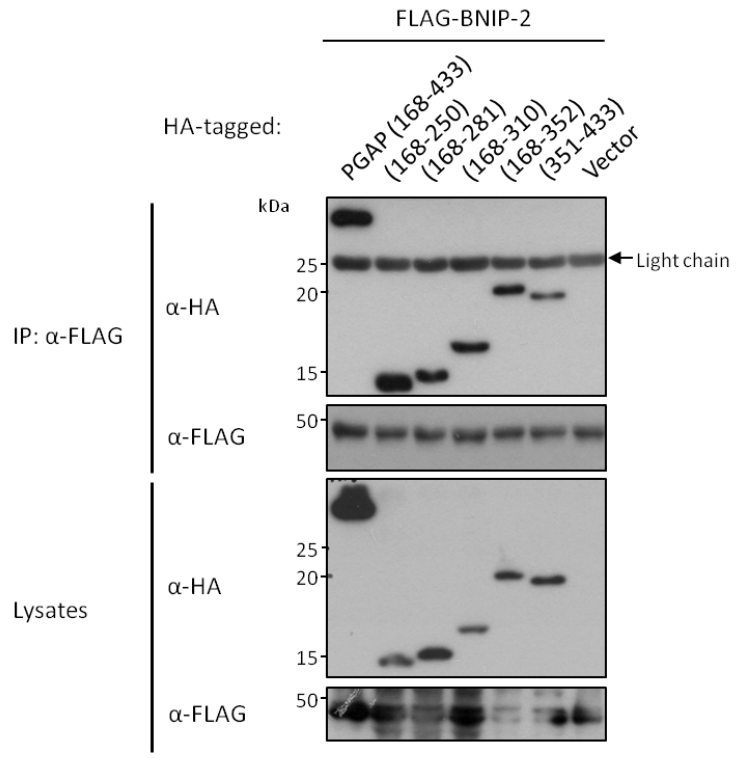

Figure 3.22 A full composite PGAP region confers binding to BNIP-2. (a) Schematic diagram of BPGAP1 and its PGAP truncation mutants. (b) Lysates of cells co-expressing FLAG-BNIP-2 and each of the HA-tagged PGAP mutants or expression vector control were subjected to immunoprecipitation with anti-FLAG M2 beads. Associated proteins and cell lysates were resolved on SDS-PAGE and analyzed by Western blot using anti-HA and anti-FLAG antibodies for detecting the bound proteins (first and second panel), as well as for verifying protein expression (third and fourth panel).

In the context of this study, deletion of both B1 region within BCH domain and the entire GAP domain to generate a non-interacting mutant is experimentally not feasible due to the requirement of the GAP domain for assessment of GAP activity in subsequent functional assays. Since synergistic effect between BNIP-2 and BPGAP1 can be abolished with the use of the GAP inactive mutant BPGAP1(R232A) as shown by RhoA activity assay (Figure 3.15), this mutant was employed in subsequent studies to further investigate the physiological effect(s) of BNIP-2-BPGAP1 interaction on RhoA inactivation.

3.5 BNIP-2 promotes the ability of BPGAP1 to induce loss of stress fiber via its GAP domain *in vivo*

Earlier results from RhoA activity assays on both overexpressed and endogenous RhoA have demonstrated that BNIP-2 functions in synergism with BPGAP1 to promote RhoA inactivation via the GAP activity of BPGAP1. To further determine the physiological function of BNIP-2 and BPGAP1 interaction on RhoA inactivation, we proceeded to examine the effects of these two proteins on stress fiber formation downstream of RhoA as it is well established that activation of RhoA induces formation of stress fibers within the cells (Hall, 1998). CV-1 cells, used earlier for confocal immunofluorescence microscopy in this study, display an extensive actin cytoskeleton network that allows for analysis of stress fibers. To visualize the stress fibers, CV-1 cells expressing the proteins-of-interest or expression vector controls as indicated were stained with Alexa Fluor 633 phalloidin to label the filamentous actin as described in *Materials and Methods*. Vector control and transfected cells expressing the intended proteins were analyzed using wide-field fluorescence microscopy and scored for the number of transfected cells exhibiting phalloidin staining which indicates presence of stress fibers. Representative fields of cells are shown in Figure 3.23a.

Consistent with the reduction of RhoA activity as demonstrated in RhoA activity assay, 70 % of the cells co-expressing BNIP-2 and BPGAP1 did not show any phalloidin staining. This percentage is higher in comparison to single expression of either BNIP-2 or BPGAP1 alone. On the other hand, presence of BNIP-2 did not appear to affect the percentage of cells that are without phalloidin staining in cells expressing the GAP mutant BPGAP1(R232A), with respect to cells transfected with BPGAP1(R232A) alone (Figure 3.23b). A comparison of single expression of the

GAP mutant with wild-type BPGAP1 shows a 20 % difference in the loss of stress fibers. This finding implies that the observed effect on stress fibers are in part due to a reduction in RhoA activity brought about by the GAP activity of BPGAP1. Intriguingly, 40% of the transfected cells still exhibit loss of stress fiber even when the RhoGAP activity was abolished, suggesting the presence of an alternative pathway mediated by BPGAP1 that might affect stress fiber.

Taken together, introduction of BNIP-2 along with BPGAP1 resulted in a small but statistically significant increase in the loss of stress fibers as compared to the extent induced by BPGAP1 alone. However, BNIP-2, when present together with BPGAP1(R232A), failed to induce a concerted effect on the loss of stress fiber with respect to expression of the GAP mutant alone. These results therefore imply that synergism between BNIP-2 and BPGAP1 on RhoA inactivation affects stress fiber formation and is in part linked to the RhoGAP activity.

a

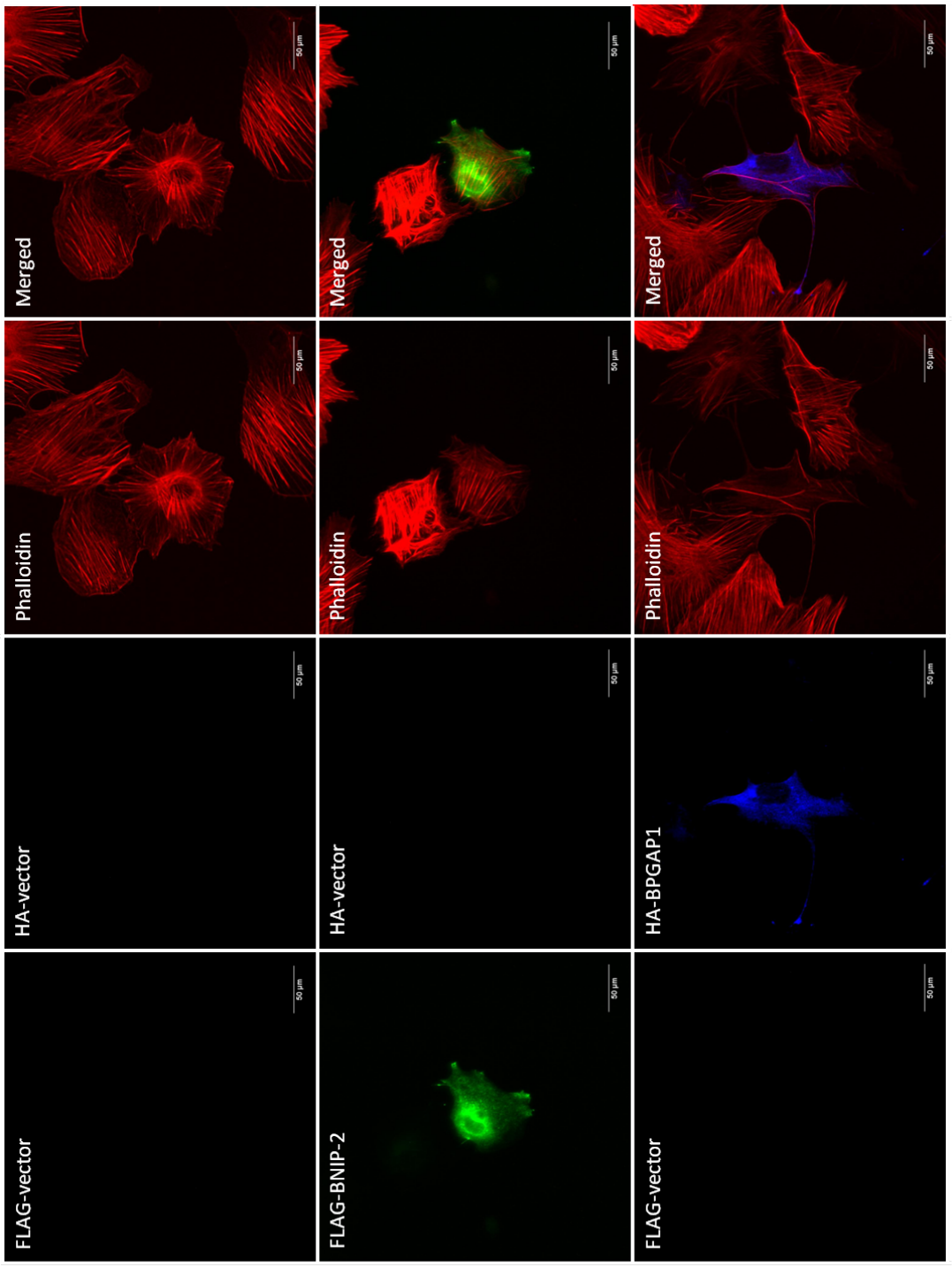
FLAG-vector
HA-vector
Phalloidin
Merged
FLAG-BNIP-2
HA-vector
Phalloidin
Merged
FLAG-vector
HA-BPGAP1
Phalloidin
Merged
Vector
FLAG-BNIP-2
HA-BPGAP1

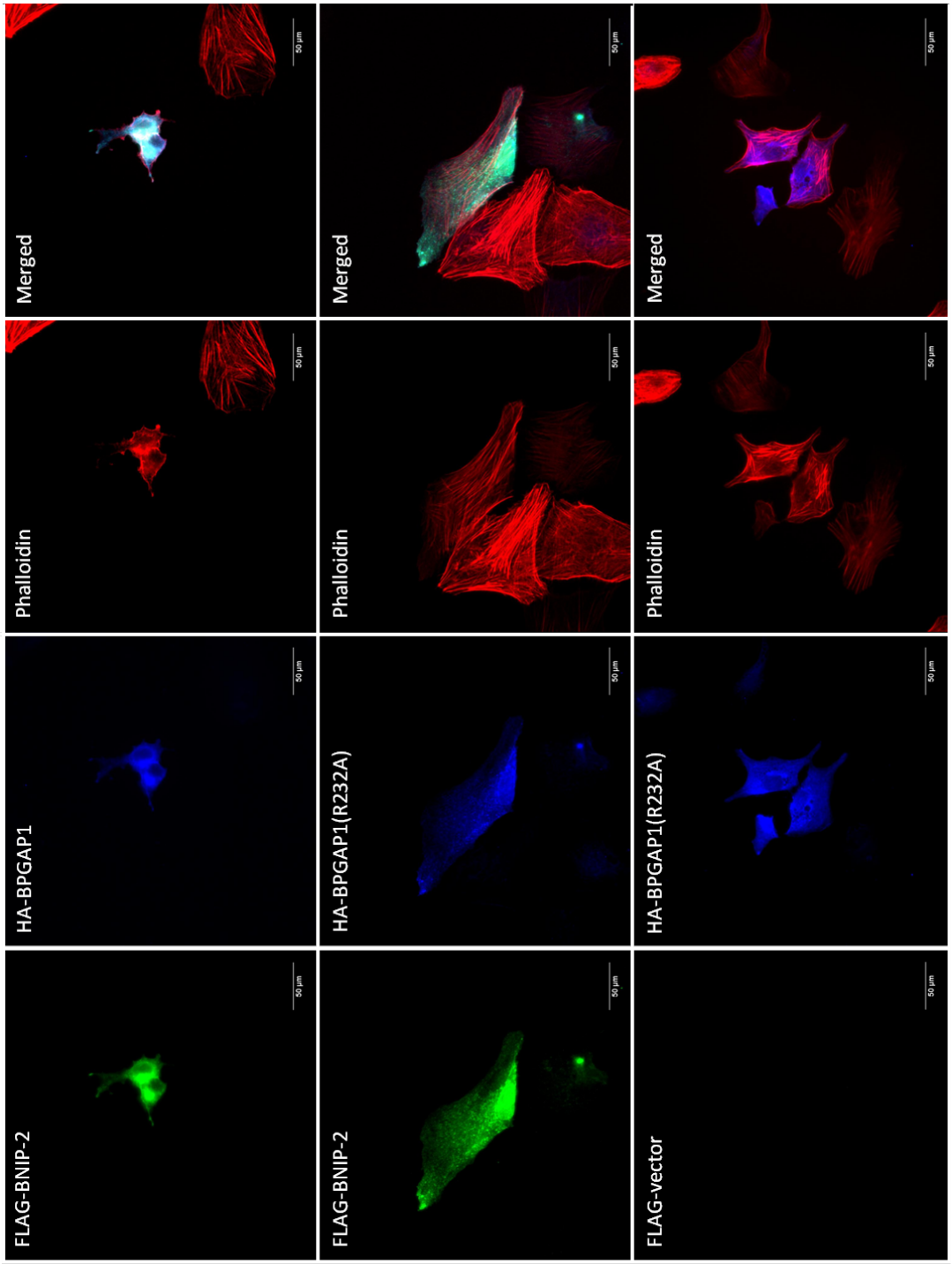
FLAG-BNIP-2
HA-BPGAP1
Phalloidin
Merged
FLAG-BNIP-2
HA-BPGAP1(R232A)
Phalloidin
Merged
FLAG-vector
HA-BPGAP1(R232A)
Phalloidin
Merged
FLAG-BNIP-2
+
HA-BPGAP1
FLAG-BNIP-2
+
HA-BPGAP1(R232A)
HA-BPGAP1(R232A)

b

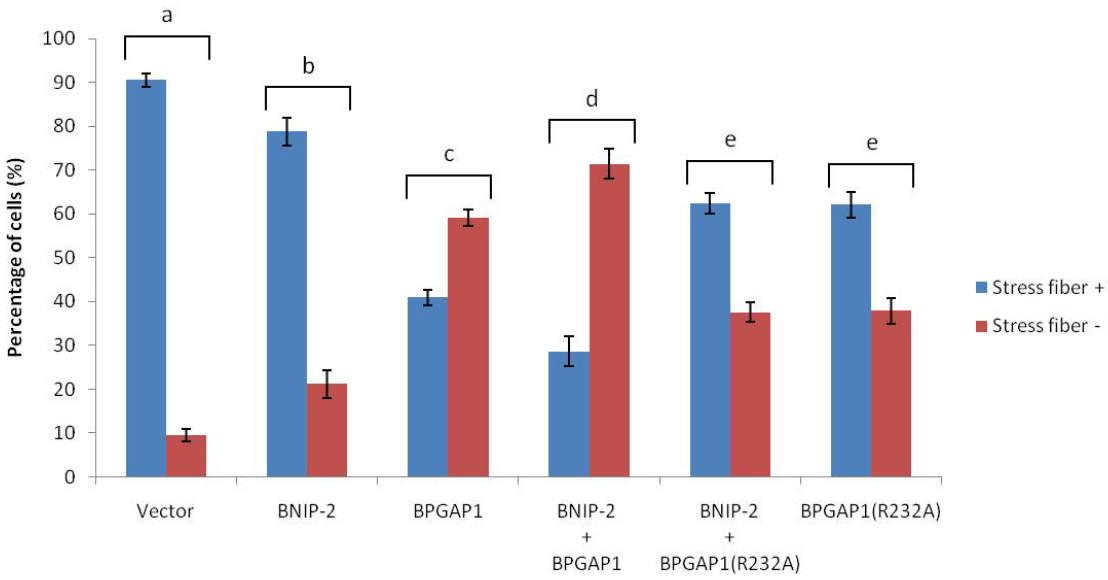

Figure 3.23 BNIP-2 promotes BPGAP1-induced loss of stress fiber *in vivo*. (a) Representative fields of CV-1 cells expressing vector control, FLAG-BNIP-2, HA-tagged BPGAP1 or BPGAP1(R232A) or in various combination as indicated. Cells were fixed after 20 hrs, permeabilized and stained for immunofluorescence detection. Stress fibers were labeled with Alexa Fluor 633 phalloidin for visualization by wide-field fluorescence microscopy and the expressed proteins were detected with polyclonal rabbit anti-HA and monoclonal mouse anti-FLAG antibodies, followed by the appropriate fluorophore-conjugated secondary antibodies. Scale bar, 50 μm. (b) For quantitative analysis, at least 150 transfected cells per sample per experiment were scored for with or without stress fiber and expressed as percentages. Data derived from three or more independent sets of experiments are expressed as mean ± standard error mean and the different letters represent differences between values that are statistically significant at $p < 0.02$, as measured by two-tailed Student's t-test with unequal variance.

3.6 BNIP-2 augments RhoGAP activity of BPGAP1 leading to enhanced cell rounding *in vivo*

During the examination of stress fibers, it was noticed that a population of the cells transfected with BPGAP1 or together with BNIP-2 exhibited rounding or drastic cell retraction/shrinkage. Indeed, alterations in actin cytoskeleton are often associated with corresponding changes in cellular morphology. In a recent study on p50RhoGAP

– a close relative of BPGAP1, it is established that the GAP domain of p50RhoGAP triggers cell rounding though inactivation of RhoA (Zhou et al., 2010). Working on this basis, we proceeded to investigate the individual and combined effects of BNIP-2, BPGAP1 or GAP inactive mutant BPGAP1(R232A) on the morphology of transfected cells. As described in the previous section for examination of stress fiber, transfected cells were scored for changes in cellular morphology including those that were round or exhibit drastic cell retraction/shrinkage. Representative fields of cells are shown in Figure 3.24a.

Similar to vector control, introduction of BNIP-2 alone did not result in any rounding or drastic retraction/shrinkage of the cells. When BPGAP1 was expressed, approximately 30 % of the transfected cells became round or show drastic retraction/shrinkage. In contrast to cells transfected with BNIP-2 alone, co-expression of BNIP-2 together with BPGAP1 resulted in cell rounding and retraction/shrinkage in 42 % of the transfected cells, implying that these two proteins function in synergism to induce changes in cellular morphology. More importantly, introduction of BNIP-2 and the GAP mutant BPGAP1(R232A) did not further promote the extent of morphological changes that were already observed in cells transfected with BPGAP1(R232A) alone. In addition, abolishment of the catalytic RhoGAP activity of BPGAP1 with the use of GAP inactive mutant BPGAP1(R232A) attenuates cell rounding or retraction/shrinkage, thereby indicating that such morphological changes are indeed a consequence of the GAP activity of BPGAP1. Collectively, these data confirm that BNIP-2 functions in synergism with BPGAP1 to enhance GAP-induced cell rounding via RhoA inactivation.

a

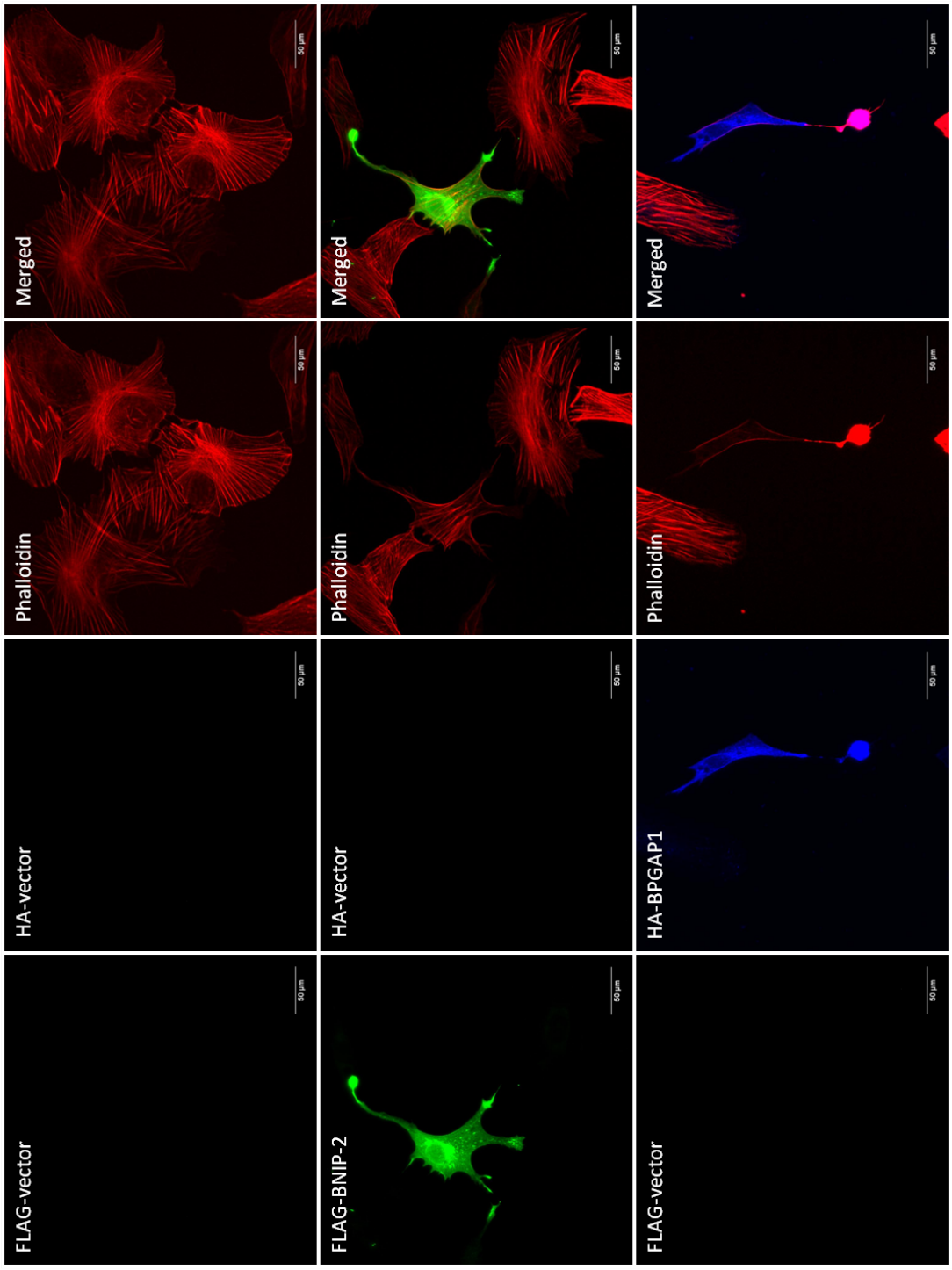
FLAG-vector
HA-vector
Phalloidin
Merged
FLAG-BNIP-2
HA-vector
Phalloidin
Merged
FLAG-vector
HA-BPGAP1
Phalloidin
Merged
Vector
FLAG-BNIP-2
HA-BPGAP1

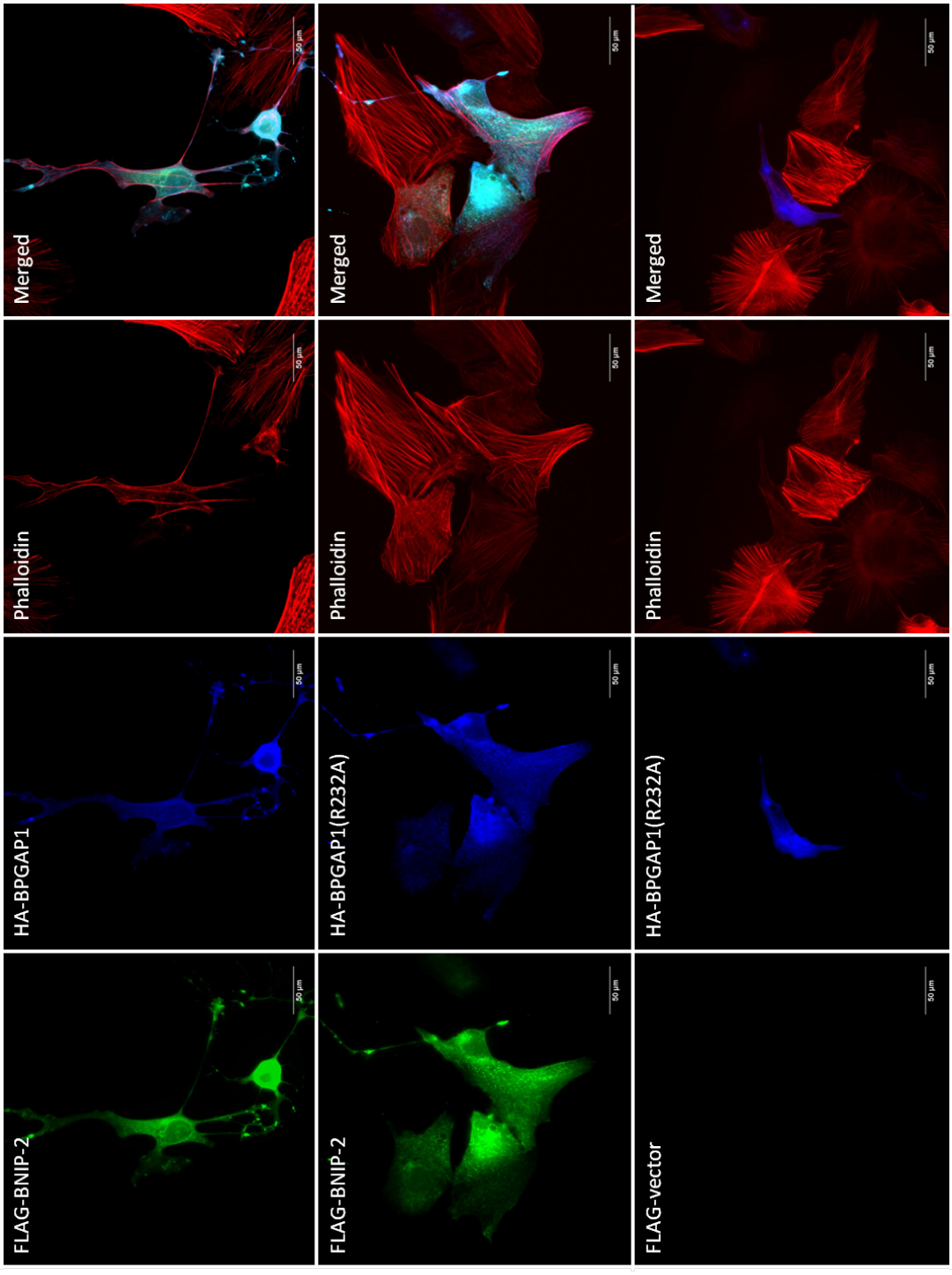
FLAG-BNIP-2
+
HA-BPGAP1
FLAG-BNIP-2
+
HA-BPGAP1(R232A)
HA-BPGAP1(R232A)
FLAG-BNIP-2
HA-BPGAP1
Phalloidin
Merged
FLAG-BNIP-2
HA-BPGAP1(R232A)
Phalloidin
Merged
FLAG-vector
HA-BPGAP1(R232A)
Phalloidin
Merged

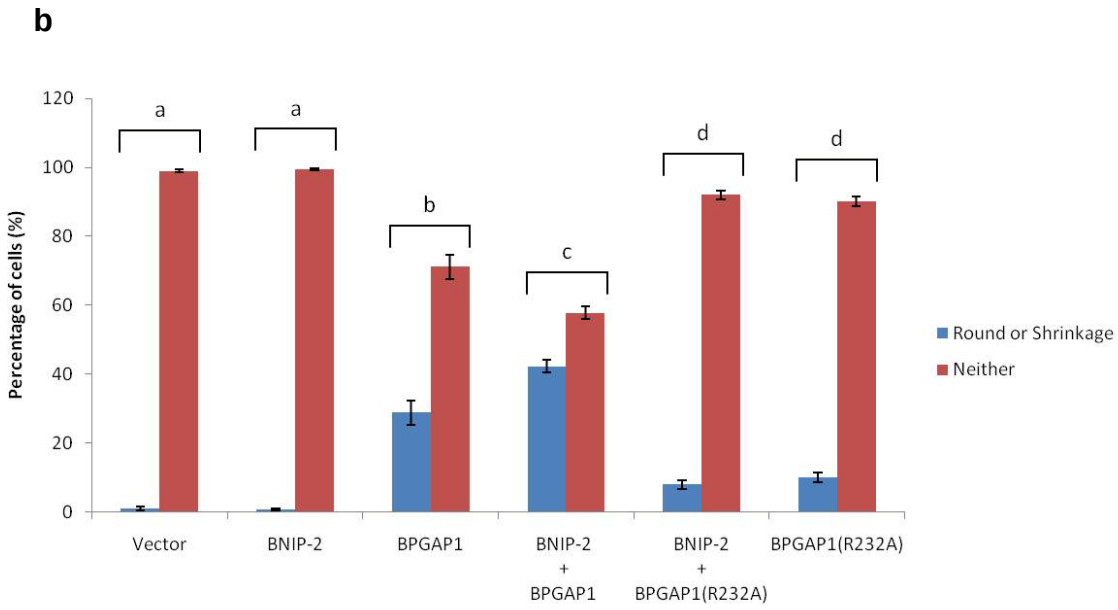

Figure 3.24 BNIP-2 augments BPGAP1 RhoGAP activity leading to enhanced cell rounding *in vivo*. (a) Representative fields of CV-1 cells expressing vector control, FLAG-BNIP-2, HA-tagged BPGAP1 or BPGAP1(R232A) or in various combination as indicated. Transiently transfected cells were fixed after 20 hrs, permeabilized and stained for immunofluorescence detection. Stress fibers were labeled with Alexa Fluor 633 phalloidin for visualization by wide-field fluorescence microscopy and the expressed proteins were detected with polyclonal rabbit anti-HA and monoclonal mouse anti-FLAG antibodies, followed by the appropriate fluorophore-conjugated secondary antibodies. Scale bar, 50 μm. (b) For quantitative analysis, at least 150 transfected cells per sample per experiment were scored for cells that were round or exhibit drastic retraction/shrinkage and expressed as percentages. Data derived from three or more independent sets of experiments are presented as mean ± standard error mean. Differences between values that are statistically significant at $p < 0.02$, measured by two-tailed Student's t-test with unequal variance, are labeled with different letters.

3.7 BNIP-2 and BPGAP1 concertedly suppress cell proliferation

Apart from the classical role of Rho GTPases in regulating actin cytoskeleton, RhoA is also implicated in the regulation of cell cycle progression and its overexpression has been reported in many cancer types (Karlsson et al., 2009). Although BPGAP1 functions as a GAP towards RhoA, its upregulation has surprisingly been detected in colorectal tumors irrespective of tumor location, stage or

level of differentiation (Johnstone et al., 2004), as well as in cervical cancer (Song et al., 2008). In addition, studies on BNIP-2 family of BCH domain-containing proteins have also revealed that these proteins are involved in processes associated with cancer, for instance apoptosis in the case of BNIP-2 and BNIP-Sα and transformation for BNIP-XL (Belcredito et al., 2001; Bonner et al., 2004; Scott et al., 2010; Soh and Low, 2008; Zhou et al., 2006). To explore whether the decrease in active RhoA level as induced by BNIP-2 and BPGAP1 concertedly will have any effect on the proliferation ability of cells, which is an important factor during initial tumor growth, the level of proliferation markers were determined by Western blot analyses using specific antibodies against the respective markers.

Single expression of either BNIP-2 or BPGAP1 resulted in a reduction in the amount of PCNA (proliferating cell nuclear antigen) and phosphorylated form of Histone H3 (residue serine10) as compared to cells transfected with only the vector controls (Figure 3.25a, first and second panel, lane 2-4). Introduction of BNIP-2 and BPGAP1 together further decreased the protein level of these markers as seen in Figure 3.25a (first and second panel, lane 1). Conversely, cells transfected with both BNIP-2 and the GAP mutant did not appear to show a similar degree of protein reduction with respect to expression of BPGAP1(R232A) alone. In all, the data derived from three or more independent sets of experiments, after normalization to tubulin as the loading control, reveal that co-expression of BNIP-2 and BPGAP1 resulted in a significantly lower level of proliferation markers including PCNA (Figure 3.25bi) and phospho-Histone H3 (Ser10) (Figure 3.25bii).

Alternatively, BrdU assay was performed to study the proliferation states of transfected cells expressing the proteins-of-interest. To do so, the cells were incubated with 5-bromo-2'deoxyuridine (BrdU), a thymine analogue that can be incorporated

into cells undergoing DNA synthesis (S phase of cell cycle). Subsequently, these cells were labeled with fluorescein-conjugated anti-BrdU monoclonal antibody as described in *Materials and Methods* to enable visualization of the incorporated BrdU. Vector control and transfected cells expressing the indicated proteins were then analyzed by wide-field fluorescence microscopy and scored for the number of transfected cells exhibiting positive BrdU staining. Interestingly, only the population of cells that were expressing both BNIP-2 and BPGAP1 differ in the level of cell proliferation as reflected by the proportion of cells undergoing DNA synthesis (Figure 3.25c). Representative fields of cells are shown in Figure 3.25d. Collectively, these data therefore indicate that BNIP-2 and BPGAP1 concertedly suppress proliferation, however through a yet unknown mechanism.

a

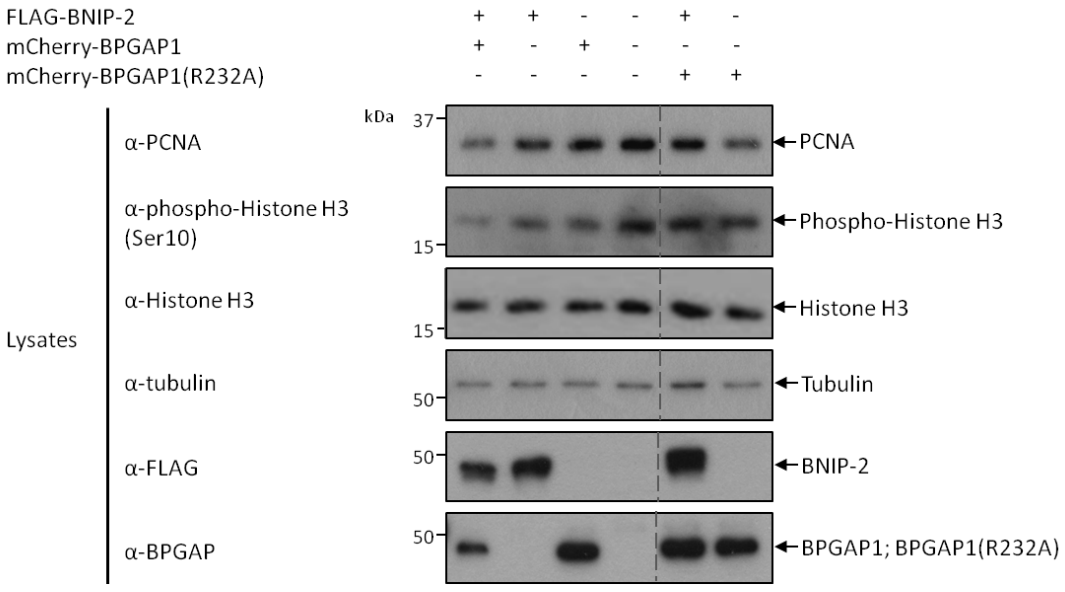

bi

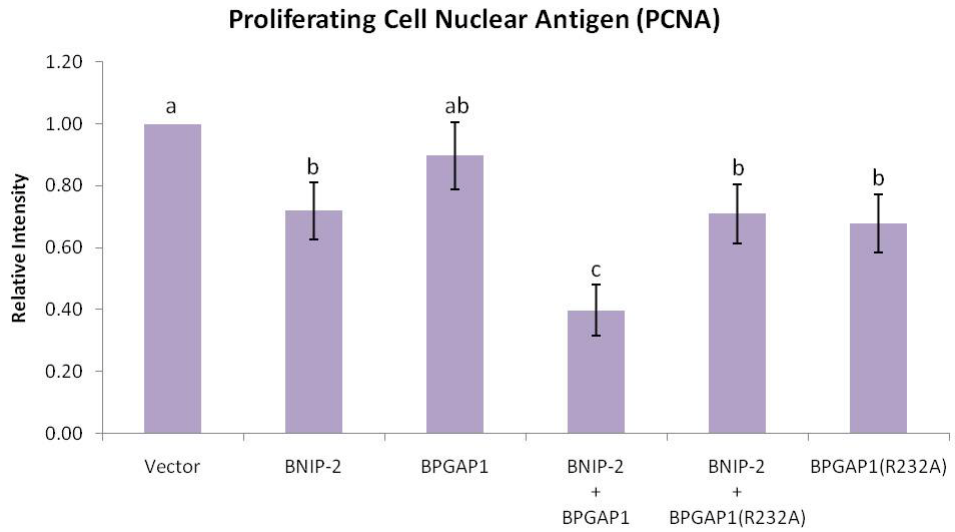
Proliferating Cell Nuclear Antigen (PCNA)
Relative Intensity
1.20
1.00
0.80
0.60
0.40
0.20
0.00
a
b
ab
c
b
b
Vector
BNIP-2
BPGAP1
BNIP-2 + BPGAP1
BNIP-2 + BPGAP1(R232A)
BPGAP1(R232A)

bii

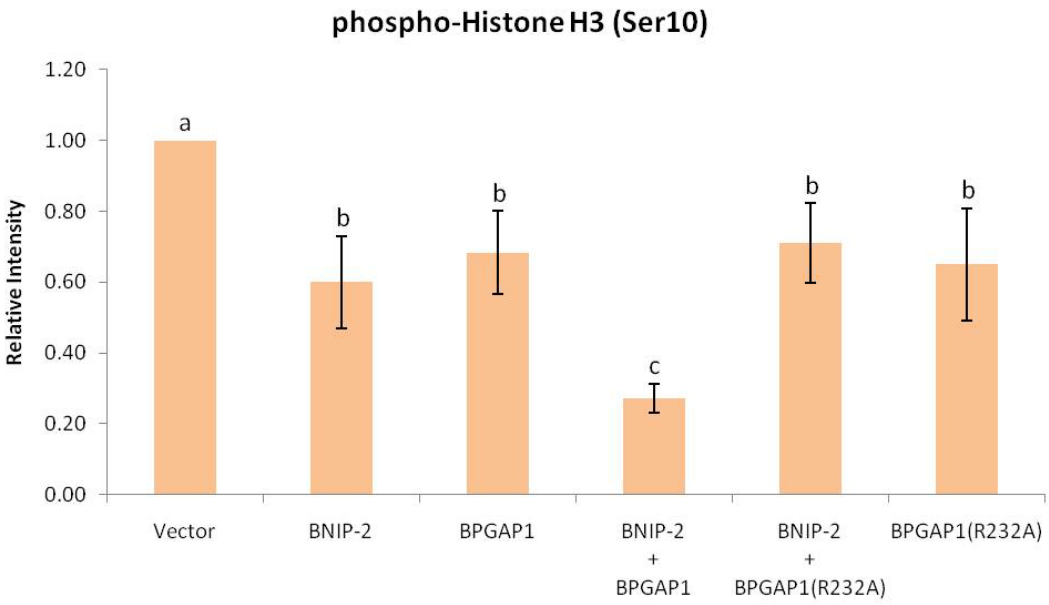
phospho-Histone H3 (Ser10)
Relative Intensity
1.20
1.00
0.80
0.60
0.40
0.20
0.00
a
b
b
c
b
b
Vector
BNIP-2
BPGAP1
BNIP-2 + BPGAP1
BNIP-2 + BPGAP1(R232A)
BPGAP1(R232A)

c

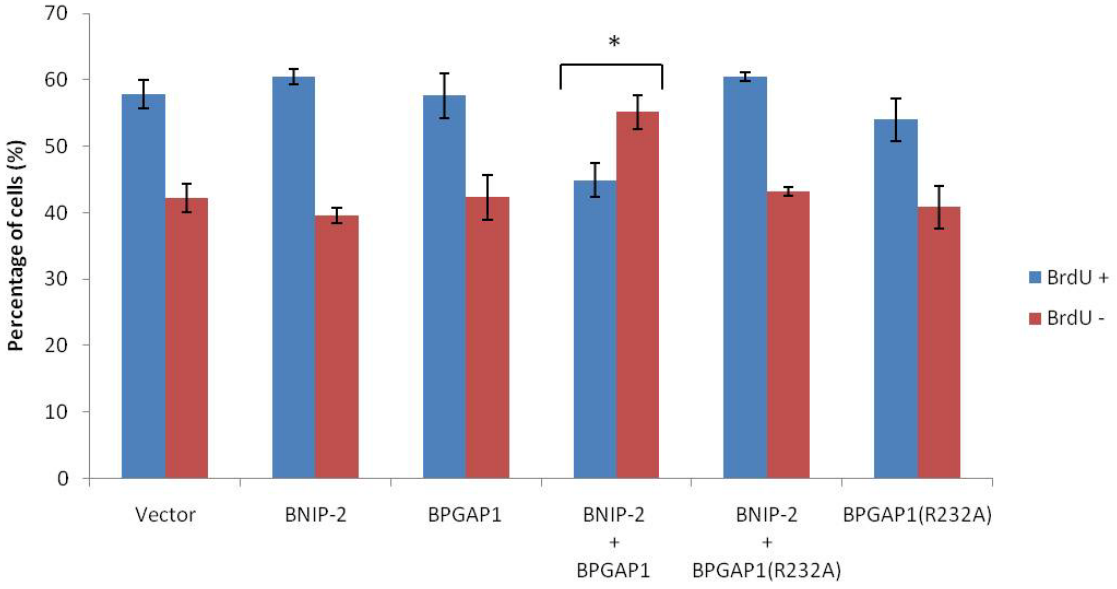
70
60
50
40
30
20
10
0
Percentage of cells (%)
*
Vector
BNIP-2
BPGAP1
BNIP-2 + BPGAP1
BNIP-2 + BPGAP1(R232A)
BPGAP1(R232A)
BrdU +
BrdU -

d

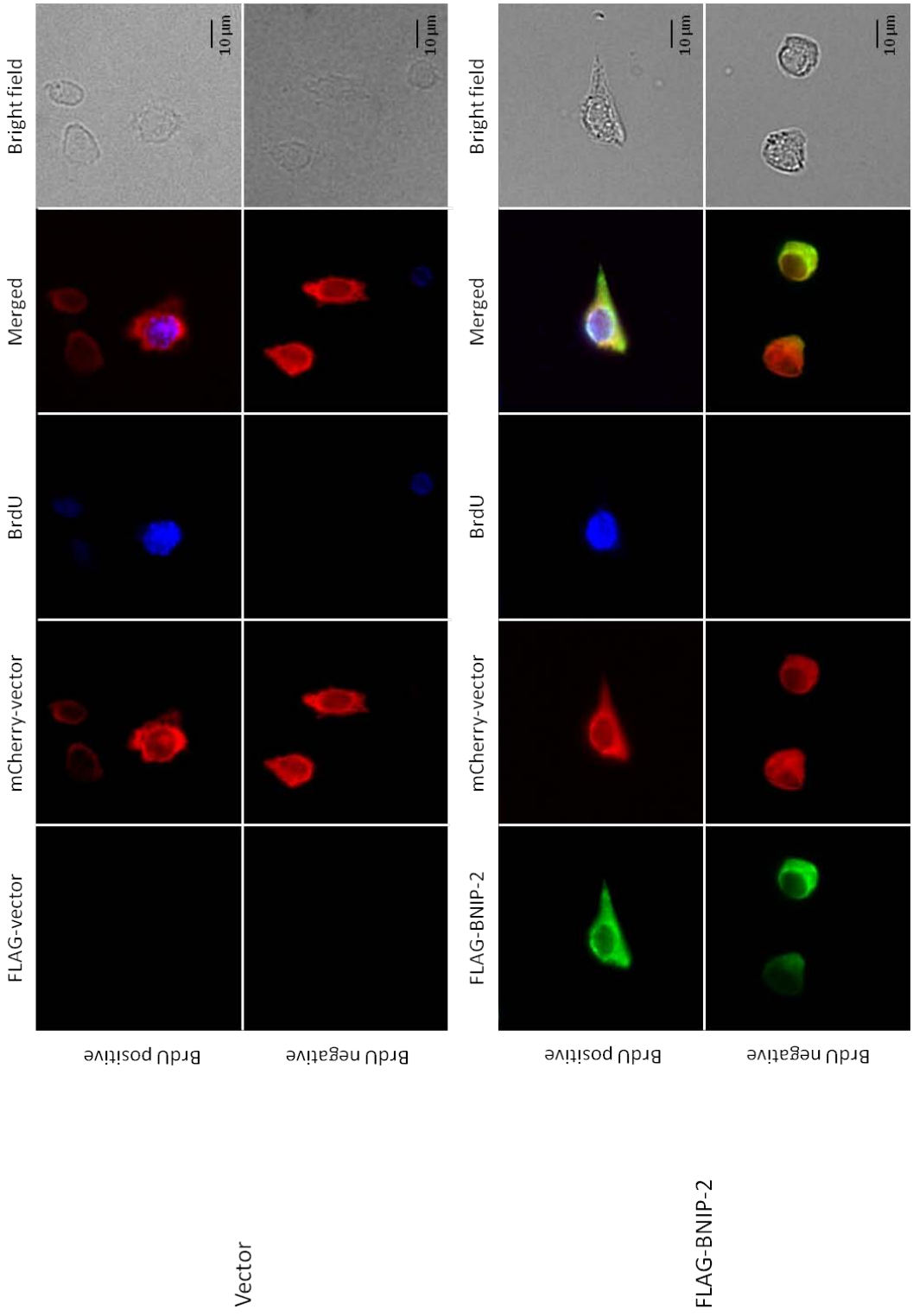
Bright field
Merged
BrdU
mCherry-vector
FLAG-vector
FLAG-BNIP-2
10 μm
BrdU positive
BrdU negative
Vector
FLAG-BNIP-2

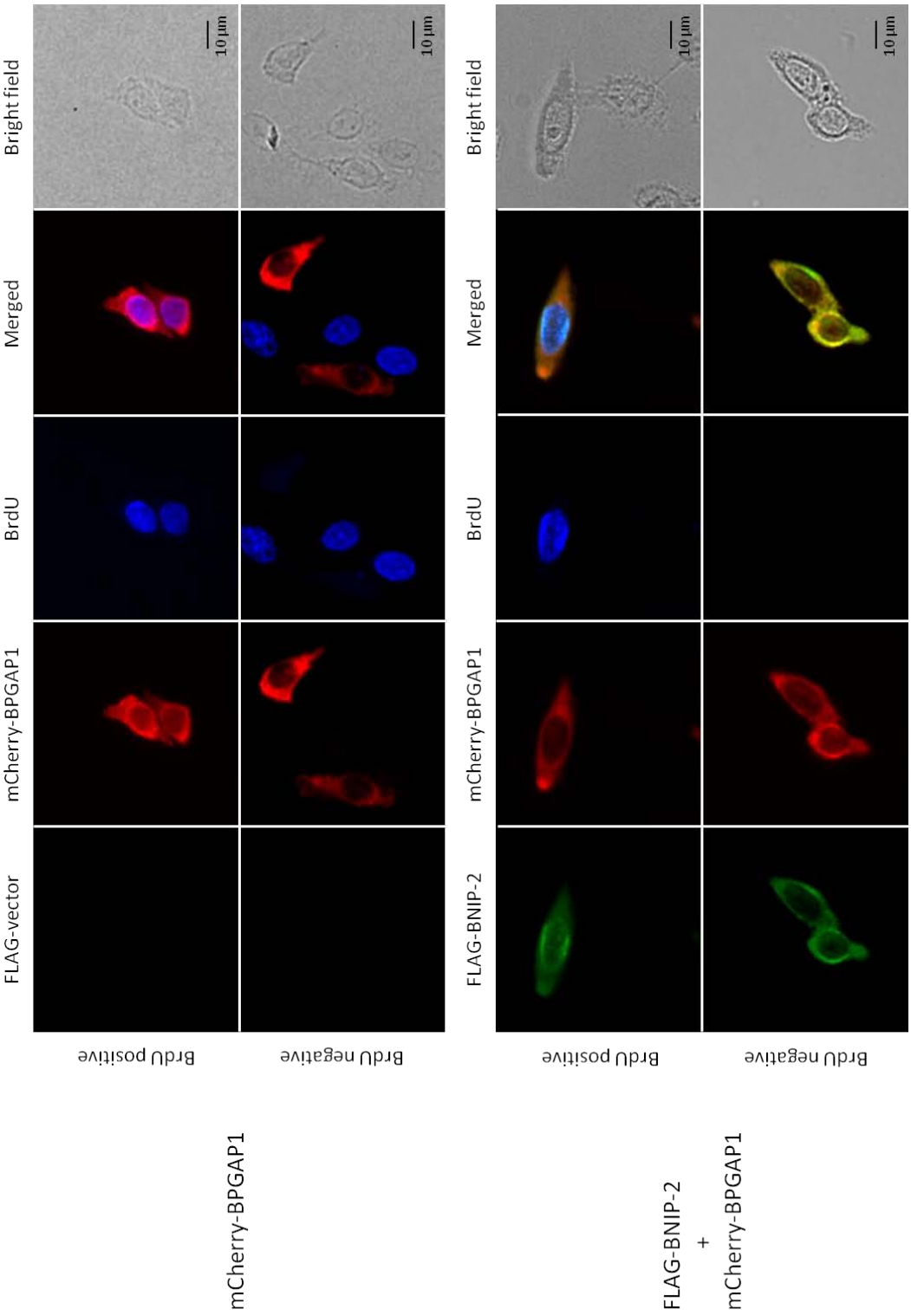
FLAG-vector
mCherry-BPGAP1
BrdU
Merged
Bright field
10 µm
BrdU positive
BrdU negative
mCherry-BPGAP1
FLAG-BNIP-2
BrdU
Merged
Bright field
10 µm
BrdU positive
BrdU negative
FLAG-BNIP-2
+
mCherry-BPGAP1

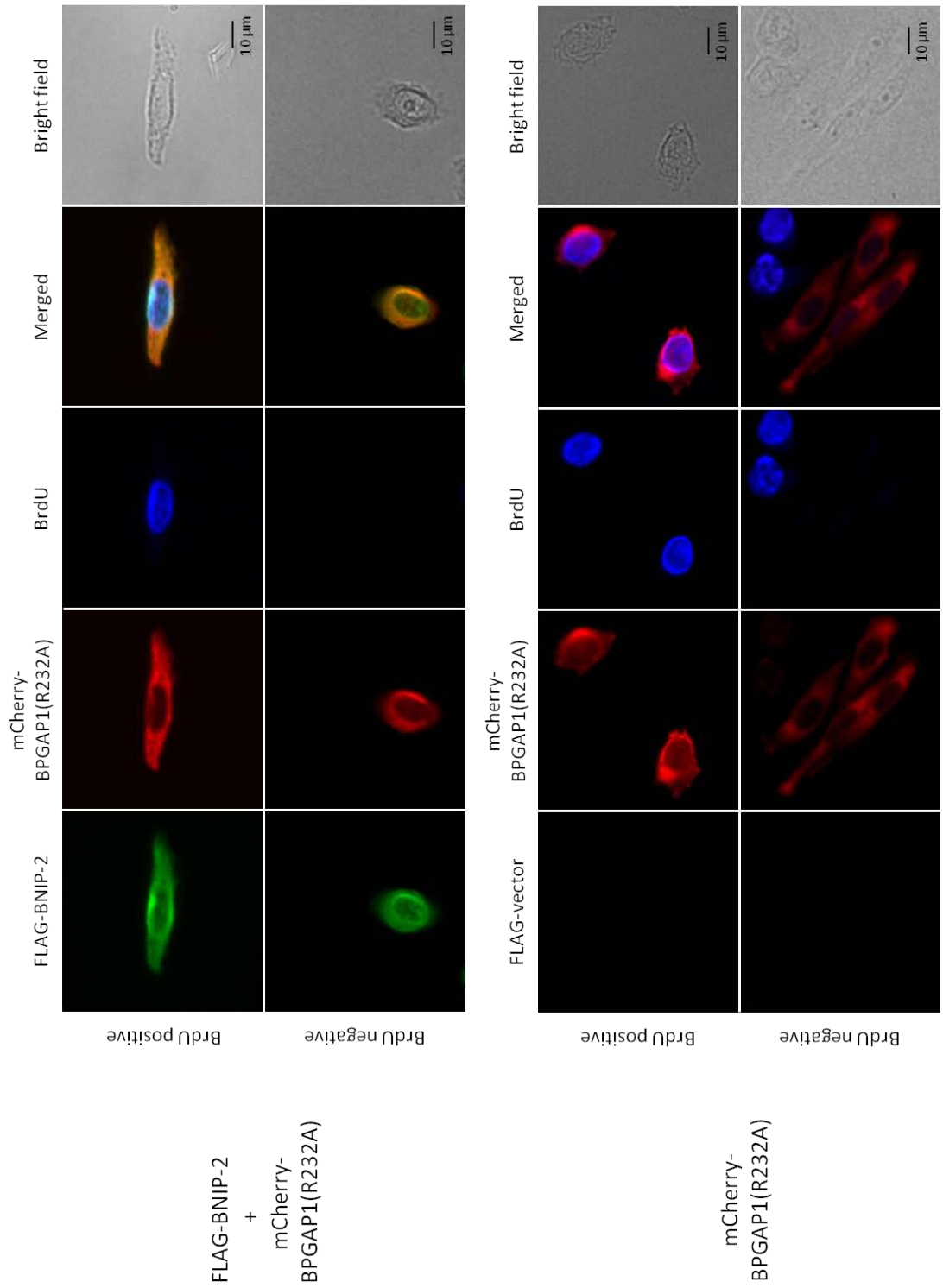
FLAG-BNIP-2
+
mCherry-
BPGAP1(R232A)
mCherry-
BPGAP1(R232A)
FLAG-BNIP-2
mCherry-
BPGAP1(R232A)
BrdU
Merged
Bright field
BrdU positive
BrdU negative
FLAG-vector
mCherry-
BPGAP1(R232A)
BrdU
Merged
Bright field
BrdU positive
BrdU negative
10 µm

Figure 3.25 BNIP-2 and BPGAP1 concertedly suppress cell proliferation. (a) CHO cells expressing BNIP-2, BPGAP1 or BPGAP1(R232A), either alone or in combination were reseeded at 24 hrs and lysed after 48 hrs. An equivalent amount of correspondingly tagged expression vectors denoted by the – sign was co-transfected to maintain a constant amount of DNA introduced into the cells. Harvested lysates of transfected cells were separated by SDS-PAGE, blotted and probed with antibodies against proliferation markers including anti-PCNA (first panel) and anti-phospho-Histone H3 (Ser10) (second panel), as well as with anti-FLAG and anti-BPGAP1 antibodies to verify the presence of overexpressed BNIP-2 (fifth panel), BPGAP1 and BPGAP1(R232A) (bottom panel). Total Histone H3 and tubulin were used as loading controls (third and fourth panel). For quantitative analysis, the amount of (b) PCNA and (c) phospho-Histone H3 (Ser10) were normalized to the level of tubulin in cell lysates and represented as relative intensity to the vector-expressing control cells (set as 1), as described in *Materials and Methods*. Data derived from three or more independent sets of experiments are expressed as mean $\pm$ standard error mean and the different letters represent differences between values that are statistically significant at $p < 0.05$, measured by two-tailed Student's t-test with unequal variance. (d) Quantitative analysis of BrdU assay. The ratio of transfected cells with and without BrdU was scored and at least 100 transfected cells were counted per sample per experiment. Data from three independent sets of experiments are presented as mean $\pm$ standard error mean and the asterisk indicates differences between values that are statistically significant at $p < 0.02$, measured by two-tailed Student's t-test with unequal variance. (e) Representative fields of CHO cells expressing vector controls, FLAG-BNIP-2, mCherry-BPGAP1 or BPGAP1(R232A) or in combination as indicated. Transiently transfected cells were incubated with BrdU, fixed and labeled with fluorescein-conjugated anti-BrdU monoclonal antibody as described in *Materials and Methods* before visualizing with wide-field fluorescence microscopy. Scale bar, 10 μm.

Chapter 4

Discussion

4 DISCUSSION

4.1 BNIP-2 acts in synergism with BPGAP1 to downregulate RhoA activity

Previous studies on characterizing the functions of various BCH domain-containing proteins have established that BCH domain mediates the diverse spectrum of cellular dynamics associated with these proteins (Figure 1.16). Notably, BCH domain has widely been implicated in small GTPases signaling, and its role as an accessory regulatory module for the small GTPases and their regulators (Soh and Low, 2008; Zhou et al., 2006) is of particular interest. In this study, endogenous BNIP-2 is confirmed as a *bona fide* interacting partner of BPGAP1, further supported by regions of co-localization of these two proteins in the cell.

With its unique localization at the leading edge of cellular protrusions, BNIP-2 induces cell elongation and protrusions through the Cdc42 signaling pathway (Low et al., 1999; Low et al., 2000a; Low et al., 2000b; Zhou et al., 2005). In addition, it contributes to both myogenic and neuronal differentiations by facilitating the integration of Cdc42 and p38α/β MAPK signaling pathways (Kang et al., 2008; Oh et al., 2009). Although previous studies on the functions of BNIP-2 are centered on its association with Cdc42, we herein focus on its effect on another Rho GTPase – RhoA, for which BPGAP1 has been demonstrated to serve as a RhoGAP specifically for RhoA *in vivo* (Shang et al., 2003). Immunoprecipitation studies using transient expression system have established that BNIP-2 could interact with RhoA specifically via its BCH domain and interestingly they co-localized predominantly at regions of cellular protrusions where BNIP-2 are concentrated. This interaction is not too unexpected given that many other BCH domain-containing proteins such as BNIP-Sα, BNIP-XL, p50RhoGAP and including BPGAP1 as shown in this study, have also

been found to interact with RhoA through their BCH domains (Soh and Low, 2008; Zhou et al., 2010; Zhou et al., 2006). Intriguingly, despite the presence of a highly conserved BCH domain, BNIP-H, a brain-specific member of the BCH domain-containing protein family, fails to interact with RhoA. This further highlights the specificity in interaction between each of the BCH domain-containing proteins with RhoA.

Results from immunoprecipitation studies have revealed that BPGAP1 is able to associate with both BNIP-2 and RhoA in the presence of each other, which could indicate independent associations of BPGAP1 with either BNIP-2 or RhoA, or association of these three proteins in a tripartite complex. Co-localization of BNIP-2, BPGAP1 and RhoA in the cells further suggests that they could exist in a functional complex. These observations are at first glance surprising given that BNIP-2 interacts with both BPGAP1 and RhoA via a common motif within its BCH domain. However, since deletion of RhoA binding region (residues 167-211) within BNIP-2 BCH domain totally abolished the interaction between BNIP-2 and RhoA but not its binding with BPGAP1, hence there is no complete overlap of the RhoA binding region with the BPGAP1 interacting site. Moreover, the extent of loss of binding between BNIP-2 and BPGAP1 was reduced when deletion mutants encompassing smaller regions within residues 167 to 211 were used, implying that the occlusion of a smaller motif will not lead to a complete loss of interaction between BNIP-2 and BPGAP1. Whether the RhoA binding region of BNIP-2, predicted using sequence alignment with the established RhoA binding motif of BNIP-Sα, constitutes the minimal region required for interaction, needs to be further elucidated using deletion mutants that cover smaller motifs. This overlapping of the RhoA binding region with BPGAP1 interactive motif on BNIP-2 BCH domain may on the other hand serves to

facilitate close association of BPGAP1 with RhoA. Indeed, a similar model of association is also observed for Myosin phosphatase-Rho Interacting Protein (M-RIP) whose RhoA binding region overlaps with the site for mediating interaction with myosin binding subunit (MBS) of myosin phosphatase, thereby bringing RhoA into close proximity with MBS for regulation of myosin phosphorylation state (Surks et al., 2003).

Besides having a highly conserved GAP domain that is required for catalyzing the GTPase activity of Rho GTPases, RhoGAPs contain multiple additional functional modules. The presence of varying combinations of these different domains allow for spatiotemporal regulation of these RhoGAPs through recruitment of other interacting partners that may serve as regulators, facilitation of crosstalk among proteins and integration of different signaling pathways, targeting to specific subcellular localization, mediating posttranslational modifications and/or removal of auto-inhibition (Bos et al., 2007; Moon and Zheng, 2003). Being multi-modular in nature, many of the characterized functions of BPGAP1 involve the concerted action of its various modules including BCH and GAP domains, as well as the proline-rich region; and are attributed to its interactions with other proteins mediated by these modules. For instance, BPGAP1 promotes cell migration through the interplay of its BCH and GAP domains to induce morphological changes and by its interaction with cortactin via the proline-rich region to translocate cortactin to the cell periphery (Lua and Low, 2004; Shang et al., 2003). It can also trigger EGF receptor endocytosis either independently or by interacting with EEN/endophilin II through the proline-rich region (Lua and Low, 2005). Moreover, BPGAP1 can induce ERK1/2 signaling via both its BCH and GAP domains (Lua and Low, 2005).

While the earlier studies uncover mainly the functions of BPGAP1, recent work has shed more light on the regulation of this protein. For example, upon the release of BPGAP1 auto-inhibition by active MEK2 that targets the proline-rich region, Pin1 functions to suppress BPGAP1-induced acute ERK activation in a GAP-independent manner and attenuate Rho signaling via stimulation of the GAP activity (Pan et al., 2010). Another protein, SmgGDS, also serves as a negative regulator by sequestering BPGAP1 through its BCH domain, thereby preventing BCH domain-mediated activation of Ras and subsequent ERK-induced differentiation (Ravichandran and Low, unpublished data). A more recent study on BPGAP1 and its interacting partner, human LanCL1, reveals that complex formation between these two proteins suppresses their individual effects on Ras and ERK activation, and delays the effect of BPGAP1 on neuronal potentiation at suboptimal level of NGF stimulation (Sharmy and Low, unpublished data). In this current study, through the employment of immunoprecipitation and immunofluorescence studies, RhoA activity assays, as well as examination of the impact of BNIP-2-BPGAP1 interaction on cell proliferation, we have further identified BNIP-2 as an accessory protein that functions as a regulator of BPGAP1.

Results from RhoA activity assays using transient RhoA overexpression demonstrate that BNIP-2 synergistically enhanced the RhoGAP activity of BPGAP1 such that the overall reduction in RhoA activity was greater than the total impact brought about by each of the two proteins alone. A similar synergistic effect on RhoA inactivation can be seen with the fast cycling mutant RhoA(F30L). By introducing a RhoGAP catalytically inactive mutant - BPGAP1(R232A), the stimulatory effect of BNIP-2 on RhoA inactivation was abolished, indicating that such effect is coupled to the GAP activity of BPGAP1. Consistently, assessment on the endogenous active

RhoA level reveals a similar activity profile in comparison to the RhoA overexpression system. Similarly, removal of the RhoGAP activity restored the level of endogenous active RhoA. These observations further support the notion that BNIP-2 synergizes with BPGAP1 to induce RhoA inactivation by coupling to the RhoGAP activity. However, due to the lack of a non-interacting mutant that is able to uncouple the binding between BNIP-2 and BPGAP1 while retaining interaction with RhoA, we can only speculate that the observed synergistic effect is brought about by the interaction between BNIP-2 and BPGAP1.

In an overexpression system, the introduced protein-of-interest is present in greater excess as compared to the endogenous level. As such, the observed effect is most likely attributed to the protein introduced. Furthermore, overexpression of the protein allows the functional effect brought about by that particular protein to be unmasked and made more pronounced by diluting the amount of endogenous regulators present. In this regard, we conclude from both RhoA overexpression and endogenous RhoA systems that BNIP-2 functions in synergism with BPGAP1 to augment RhoA inactivation by promoting the RhoGAP activity of BPGAP1.

4.2 BNIP-2 synergistically promote RhoGAP activity of BPGAP1 leading to BPGAP1-mediated loss of stress fiber and cell rounding

Typically, disruption of actin cytoskeletal structures can occur as a consequence of RhoA inactivation mediated by GAP activity and is accompanied by changes in cell morphology including cell rounding. ARAP1 (ArfGAP and RhoGAP with ankyrin repeat and PH domains), which contains both Arf and Rho GAP domains, modulates active RhoA level *in vivo* through its RhoGAP domain and causes a reduction in stress fibers. A greater degree of cell rounding also occurs upon

serum starvation in the presence of overexpressed ARAP1 but not the RhoGAP-dead [R338K]ARAP1 mutant (Miura et al., 2002). In other instances, cells overexpressing DLC1 or DLC2 (deleted in liver cancer) exhibit inhibition of LPA-induced actin stress fiber formation and altered morphology with extensive cell rounding. Such effects could be suppressed by abolishing the RhoGAP function through mutation of the conserved residue(s) crucial for catalytic activity (Leung et al., 2005; Wong et al., 2005).

By examining the morphology of transfected cells, we show that BPGAP1-expressing cells induced a marked increase in the percentage of round or retracting cells. These changes in cell morphology occur as a result of the RhoGAP activity of BPGAP1 since expression of the GAP-deficient mutant BPGAP1(R232A) did not bring about a similar extent of cell rounding or retraction/shrinkage. Indeed, a recent study has also shown that the GAP domain of p50RhoGAP confers GAP activity towards RhoA and results in extensive cell rounding, which can be blocked by either the catalytic inactive triple-point mutant or constitutive active RhoA(G14V) mutant (Zhou et al., 2010). Although the effect of BNIP-2 itself on cell rounding or retraction/shrinkage is negligible, co-expression of both BNIP-2 and BPGAP1 further promotes these morphological effects as observed, clearly demonstrating a synergistic increase in BPGAP1-mediated cell rounding or retraction/shrinkage. On the contrary, abolishment of the RhoGAP activity can abrogate this synergism. The consistency in cell rounding or retraction/shrinkage with inhibition of RhoA activity as brought about by the RhoGAP function further supports that BNIP-2 functions in synergism with BPGAP1 to augment its RhoGAP activity and consequently suppresses RhoA activity.

RhoA, amongst members of Rho GTPases that function as key regulators of cytoskeleton dynamics, induces the assembly of stress fibers by activating its downstream effectors mDia and ROCK (Bishop and Hall, 2000; Hall, 1998; Jaffe and Hall, 2005). With the positive correlation between cell rounding/retraction and reduced RhoA activity, it is highly plausible that these morphological changes are attributed to the collapse of actin cytoskeletal structures. As expected, a higher percentage of BNIP-2 and BPGAP1-expressing cells display loss of stress fibers in comparison with cells that express either BNIP-2 or BPGAP1 alone. Similarly, suppression of RhoGAP activity using the GAP-deficient mutant reduces the percentage of cells that are without stress fibers and introduction of BNIP-2 did not further promote the disruption of actin stress fibers. Together, these results imply that BNIP-2 and BPGAP1 work in concert to mediate disruption of stress fiber and this loss of actin stress fibers as induced by inactivation of RhoA correlates in part to the observed effect on cell rounding/retraction.

Intriguingly, unlike the effect observed for RhoA activity and cell rounding or retraction/shrinkage, suppressing the RhoGAP activity in this instance could not fully restore the percentage of transfected cells expressing stress fibers. This result suggests that BPGAP1 may regulate actin stress fiber within the cells via a separate mechanism independent of its functional GAP domain and its effect on RhoA inactivation. In this regard, previous study on BPGAP1 has demonstrated that in addition to its biochemical function as a negative regulator of RhoA through its GAP activity, it is also able to induce morphological changes via pathways involving other members of the Rho GTPase family including active Rac1 and Cdc42 (Shang et al., 2003). This insight thus raises our speculation that BPGAP1 may target other proteins that mediate actin stress fiber formation independently of RhoA.

To our knowledge, another member of the Rho GTPase family - Rif (Rho in filopodia), is also able to stimulate the formation of actin stress fiber. Interestingly, this Rif-induced stress fiber formation does not occur through the canonical pathway involving RhoA, but by directly interacting with mDia1, downstream of RhoA, and this process is found to be dependent on ROCK activity (Fan et al., 2010). Although the authors have reported that formation of stress fibers triggered by Rif only occurs in cells of epithelial origin but not in fibroblasts, it remains to be determined if this protein can induce stress fiber formation in the cell line used in this context and if BPGAP1 can indeed affect the activity of this particular Rho GTPase, either directly or indirectly.

4.3 BNIP-2 and BPGAP1 concertedly suppress cell proliferation

Rho GTPases, known classically for their role in modulating actin cytoskeletal dynamics, are also widely implicated in the control of signal transduction pathways for cell proliferation. Inhibition of RhoA activity with Rho inhibitor exoenzyme C3 transferase or by introducing RhoA dominant negative mutant prevents entry into cell cycle whereas microinjection of constitutive active RhoA mutant sufficiently promotes progression from G_1 to S phase in quiescent fibroblast (Olson et al., 1995; Yamamoto et al., 1993). Indeed, this growth promoting property of RhoA has subsequently been shown to associate with the regulation of several key proteins involved in cell cycle progression. Mainly, RhoA mediates anchorage-dependent cell growth by promoting sustained ERK activation to achieve an optimal level and timing of Cyclin D1 expression during mid-G_1 phase (Liberto et al., 2002; Welsh et al., 2001). Progression from G_1 to S phase is further complemented by RhoA-induced suppression of p21 transcription (Liberto et al., 2002; Olson et al., 1998; Sahai et al.,

2001). In addition, RhoA is involved in furrow formation and actomyosin ring contraction during cytokinesis (Barr and Gruneberg, 2007). This process requires active GDP/GTP cycling of RhoA (Morin et al., 2009) and is regulated spatiotemporally by RhoGEF Ect2, as well as RhoGAPs such as MgcRacGAP and p190RhoGAP (Hall, 2009; Manchinelly et al., 2010; Su et al., 2009).

Since RhoA contributes to many aspects of cell cycle progression and proliferation, downregulation of RhoA activity by RhoGAP-containing proteins should therefore contribute to the suppression of cell growth. As illustrated, DLC1, which has been demonstrated in RBD pull-down assay and RhoA biosensor analysis to decrease RhoA activity via its RhoGAP domain (Holeiter et al., 2008; Wong et al., 2003), inhibits cell proliferation and anchorage-independent growth in hepatocellular carcinoma (Wong et al., 2005). Similarly, DLC2-expressing HepG2 cells with reduced level of active RhoA exhibit lower proliferative ability (Leung et al., 2005). However, such scenario may not be absolute. Instead of suppressing cell growth, p200RhoGAP promotes cell cycle progression and proliferation by mediating crosstalk between Ras and Rho signaling pathways to stimulate activation of ERK1/2 downstream of Ras (Shang et al., 2007). In the case for BPGAP1, clues to the potential involvement of this protein in proliferation came from earlier studies in which PP mutant, a BPGAP1 mutant that has its proline residues at 184 and 186 within the proline rich region substituted with alanines, has been observed to accumulate in the cleavage furrow during cell division (Lua and Low, unpublished). Although BPGAP1 functions biochemically as a GAP to reduce level of active RhoA, surprisingly its upregulation was reported in majority of colorectal tumors and also in cervical cancer (Johnstone et al., 2004; Song et al., 2008).

In the context of this study, introduction of BNIP-2 along with BPGAP1 suppresses proliferation as reflected by the significantly lower number of cells with positive BrdU, further supported by a corresponding decrease in the level of proliferation markers. This synergism between BNIP-2 and BPGAP1 on cell proliferation is no longer observed when the GAP activity of BPGAP1 is abolished. Therefore, it is possible that the suppression on proliferative property could be linked to the reduction in RhoA activity induced by the RhoGAP domain. However, such association requires further investigation as expression of BPGAP1 alone did not appear to alter the percentage of cells undergoing proliferation even though these cells displayed modest decease in the level of proliferation marker, phospho-Histone H3.

Intriguingly, BPGAP1 interacts with all three Ras isoforms including H-Ras, K-Ras and N-Ras (Ravichandran and Low, unpublished), and is capable of inducing sustained ERK1/2 activation upon EGF stimulation (Lua and Low, 2005; Pan et al., 2010). In particular, BCH domain of BPGAP1 alone enhances K-Ras activity (Ravichandran and Low, unpublished) and triggers a more robust level of prolonged ERK activation (Soh, F.L., MSc thesis). Notably, treatment of BPGAP1-expressing PC12 cells with EGF for an extended period induces neurite protrusions, which is reminiscent of the differentiation response induced by sustained ERK activation in the presence of NGF. This result therefore indicates that BPGAP1 is able to promote prolonged ERK activation upon EGF stimulation. Prolonged activation of Ras-induced ERK/MAPK pathway in response to growth factor stimulation is essential for Cyclin D1 induction (Balmanno and Cook, 1999; Cook et al., 1999) and for subsequent S phase entry (Yamamoto et al., 2006) and this sustained level of ERK activity has been shown to be dependent on RhoA signaling (Coleman et al., 2004; Welsh et al., 2001).

Taken together, while the possible involvement of BPGAP1 in proliferation could not be undermined, the exact role of this protein and how it affects this process requires further examination under synchronized conditions. In addition, it remains to be determined on how BNIP-2 and BPGAP1 together can bring about the reduction in proliferation. Despite the above mentioned, the data presented here indicates that BNIP-2 functions in synergism with BPGAP1 to suppress cell proliferation, through a yet unknown pathway.

4.4 BNIP-2 positively regulates RhoGAP function of BPGAP1 – a conceptual framework

Functioning as key regulators that terminate Rho GTPases signaling, the RhoGAP function is often subjected to tight regulation and clearly, the multi-domain nature of RhoGAPs forms the basis by which this biochemical activity of these negative regulators of Rho GTPases can be modulated. Several mechanisms exist to regulate the function of RhoGAPs including alteration of phosphorylation states or protein-protein or protein-lipid interactions. These common mechanisms serve to directly affect the GAP activity, relieve autoinhibition or target the proteins to specific subcellular locations. Alternatively, the GAP activity of RhoGAPs may be downregulated through protein degradation.

It is worth noting that a single RhoGAP protein could be modulated in multiple ways under different cellular contexts as observed for p190RhoGAP. For example, phosphorylation of p190RhoGAP by Src family tyrosine kinases or Brk - an intracellular Src-like family of tyrosine kinases, augments its RhoGAP activity towards RhoA, as well as promotes the association between p190RhoGAP and p120RasGAP (Hu and Settleman, 1997; Roof et al., 1998; Shen et al., 2008). On the

other hand, formation of this p190RhoGAP/p120RasGAP complex, when triggered downstream of integrin signaling through Arg (Abl-related gene), would recruit p190RhoGAP to the plasma membrane where it inhibits Rho activity (Bradley et al., 2006). There are also evidences whereby the GTP binding domain (GBD) located at the N terminus of p190RhoGAP and the middle region in between the GBD and C-terminal RhoGAP domain, function to promote p190RhoGAP GAP activity through interaction with GTP and the small GTPase Rnd, respectively (Tatsis et al., 1998; Wennerberg et al., 2003). Moreover, p190RhoGAP is also implicated in the cytokinesis process such that its downregulation by an ubiquitin-proteasome pathway mediated by the GBDS1 region is essential for the successful completion of cytokinesis (Manchinelly et al., 2010; Su et al., 2003).

Amongst the various mechanisms of RhoGAP regulation, intramolecular interaction is a critical regulatory mode commonly present in the GAPs and GEFs. Frequently, the existence of intramolecular interaction serves to block access to the catalytic domain. In the case of DLC1, deletion of the SAM domain from the N-terminal substantially increases the RhoGAP activity of DLC1, suggesting that SAM domain could negatively regulate the catalytic RhoGAP domain via intramolecular interaction (Healy et al., 2008; Kim et al., 2008). The inhibition of RhoGAP activity by another region through intramolecular interaction is also observed for Oligophrenin-1 (Fauchereau et al., 2003). In another instance, binding of PH domain located at the N-terminal of p120GAP to the C terminus RasGAP domain hinders the interaction between Ras and the catalytic subunit and this interference can in turn be relieved by competitive binding of Ras (Drugan et al., 2000).

Previous findings on BPGAP1 have implied that this protein exists in a "closed" conformation held by intramolecular interaction, potentially mediated by amino acids 34 to 74 within the N-terminal BCH domain and amino acids 389 to 433, a segment located beyond the GAP domain at the C terminus (Ravichandran and Low, unpublished). The presence of a proline-rich region in between the BCH and GAP domains further supports the notion as proline residues are likely to introduce turns and kinks, and a proline-rich region may adopt an omega loop structure (Kim and Roeder, 1993; Leszczynski and Rose, 1986) that functions as a hinge for mediating associations of proteins (Bernacchi et al., 2011) or perhaps adjacent domains. Indeed, p50RhoGAP – a close relative that shares the same domain architecture as BPGAP1, exists in an autoinhibited state held by intramolecular interaction between a segment within the BCH domain and the GAP module (Moskwa et al., 2005). However, this intramolecular interaction alone does not fully account for the suppression of its RhoGAP activity and is complemented by sequestration of RhoA by the RhoA-binding motif distal to the intramolecular interaction region (Zhou et al., 2010). Intriguingly, such inhibition of the catalytic GAP activity conferred by p50RhoGAP BCH domain acts solely *in cis* but not *in trans* and the concerted action of intramolecular interaction and RhoA sequestration is necessary to restore the RhoGAP activity (Zhou et al., 2010).

In this current study, we have demonstrated that BNIP-2, when present together with BPGAP1, augments the RhoGAP activity of GAP domain towards RhoA. Consistent with the downregulation of active RhoA level, enhanced GAP activity also leads to a further loss of stress fiber, an increase in GAP-induced cell rounding and an overall decrease in cell proliferation. This synergism and the

downstream effects are however abolished upon inactivation of the RhoGAP activity with the use of BPGAP1(R232A) GAP inactive mutant.

Based on our current experimental findings and already established work in the field, it is tempting to propose the following model as shown in Figure 4.1a that BPGAP1 in its native form is held by intramolecular interaction between the BCH domain and PGAP module, which may serve to block the catalytic site of the GAP domain and hence inhibiting its GAP activity. BNIP-2, in this context, could function to relieve the autoinhibition within BPGAP1 by inducing a conformational change mediated via heterophilic interaction of their BCH domains, while acting as a scaffold to bring BPGAP1 and RhoA into close proximity through its BCH domain. Indeed, BNIP-2 has been shown previously to act as a scaffold to facilitate the integration of Cdc42 signaling and p38α/β MAPK activity during myogenic and neuronal differentiation (Kang et al., 2008; Oh et al., 2009). Upon removal of the autoinhibitory effect, this allows the catalytic module of GAP domain to act on the nearby RhoA with a higher efficiency. The BCH domain of BNIP-2 could also help in stabilizing the "open" structure of BPGAP1 for it to exert its catalytic activity on RhoA, which probably explains the interaction observed between BNIP-2 BCH domain and GAP domain of BPGAP1.

Besides regulation by autoinhibitory intramolecular interaction, suppression of the GAP activity of p50RhoGAP has been demonstrated in a recent study to involve also the sequestration of RhoA by the RhoA binding motif within the adjacent BCH domain (Zhou et al., 2010). While it remains to be determined if sequestration of RhoA by BPGAP1 BCH domain is similarly required for inhibition of its GAP activity, there is a possibility that this mode of regulation exists within BPGAP1 since p50RhoGAP and BPGAP1 are two closely related proteins that share the same

domain architecture. In the alternative model (Figure 4.1b), apart from mediating conformation changes in BPGAP1 to relieve the autoinhibition through heterophilic interaction of the BCH domains, it is conceivable that BNIP-2 could also serve to release the sequestered RhoA via simple displacement of this protein away from the RhoA binding site of BPGAP1. With the displacement, this frees the RhoA protein and allows it to be acted upon by the nearby GAP domain, while the interaction between BNIP-2 BCH domain and GAP domain of BPGAP1 serves a stabilizing purpose. This mode of regulation, as described, is not unprecedented. In one case, BNIP-Sα through its BCH domain can displace away and prevent p50RhoGAP from inactivating RhoA while separately inducing RhoA activation to mediate cell rounding and apoptosis (Zhou et al., 2006). On a similar note, BNIP-XL competes off Lbc RhoGEF from RhoA using its BCH domain to inhibit RhoA activation, thereby suppressing Lbc-induced cellular transformation (Soh and Low, 2008).

Our study herein establishes that association of BNIP-2 with BPGAP1, mediated by heterophilic interaction between BCH domains of these two proteins, as well as binding between BNIP-2 BCH domain and GAP module of BPGAP1, promotes RhoA inactivation, leading to further loss of stress fibers, enhanced cell rounding and a decrease in proliferation. This is in addition to the described examples on BNIP-Sα and BNIP-XL, another study which supports the findings that Type I BCH domain-containing proteins are involved in modulating Rho GTPases, as well as their immediate regulators.

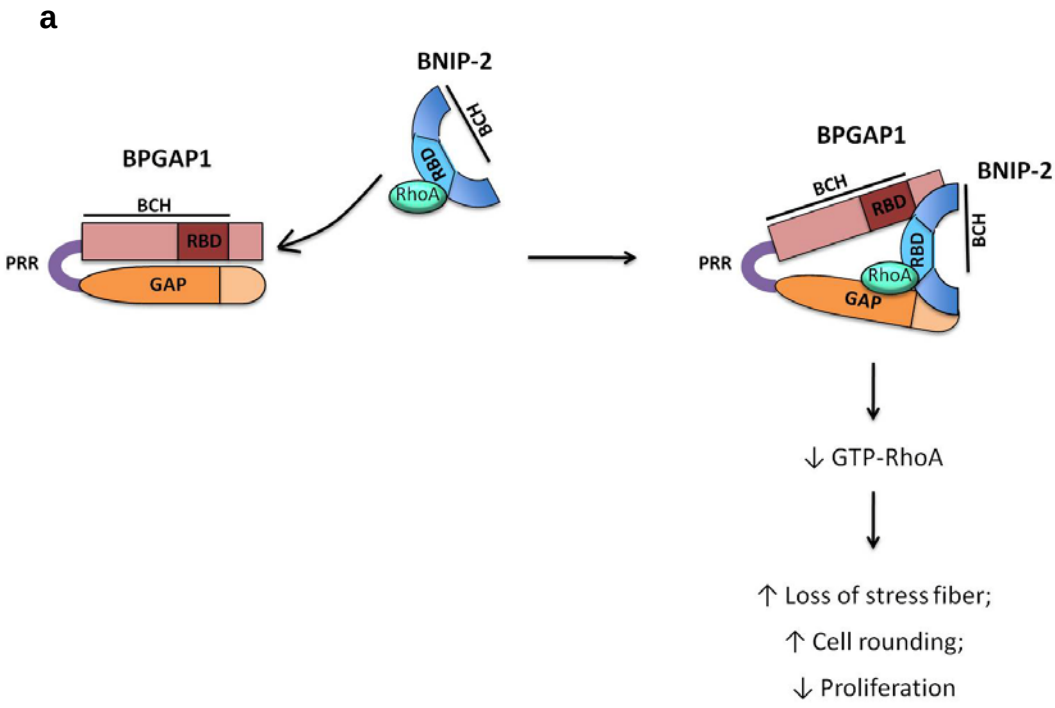
a
BNIP-2
BCH
RBD
RhoA
BPGAP1
BCH
RBD
PRR
GAP
BPGAP1
BNIP-2
BCH
RBD
RBD
BCH
PRR
RhoA
GAP
↓ GTP-RhoA
↑ Loss of stress fiber;
↑ Cell rounding;
↓ Proliferation

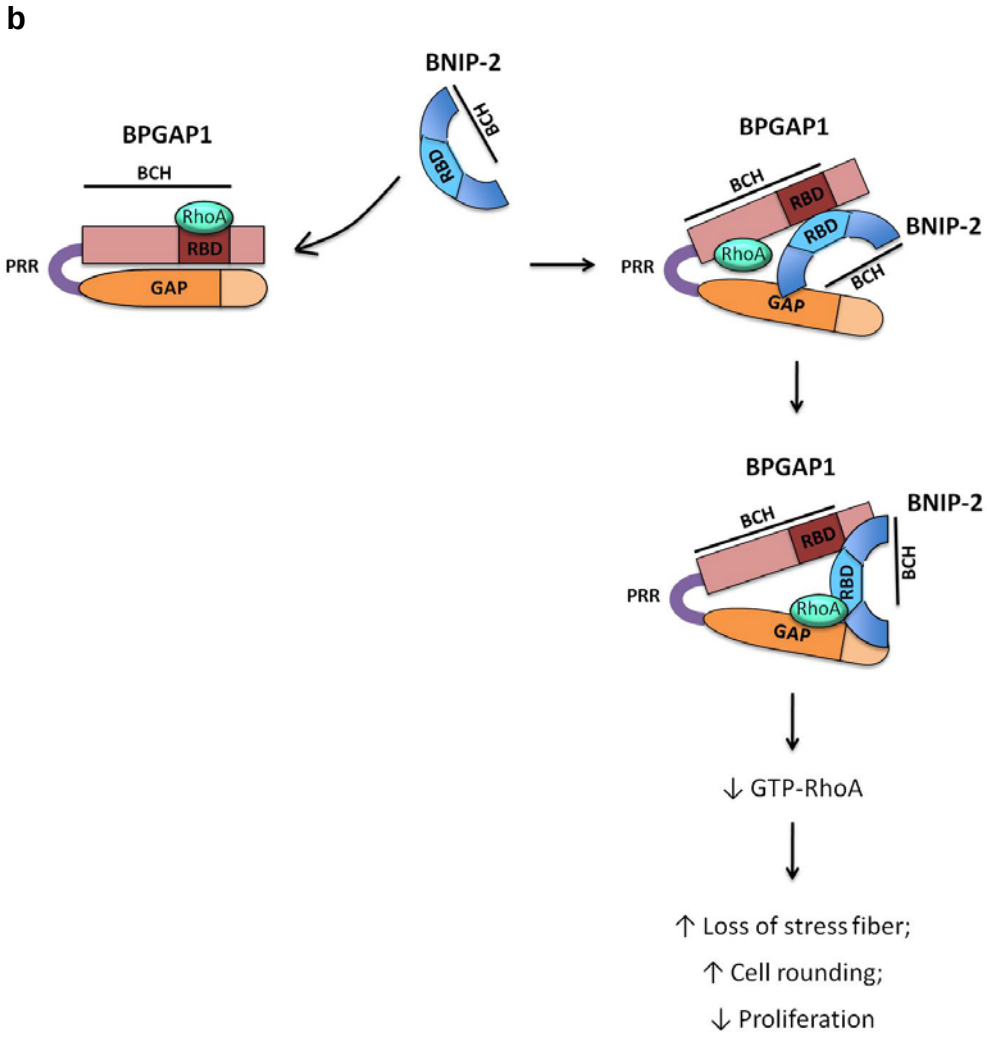
b
BNIP-2
BCH
RBD
BPGAP1
BCH
RhoA
RBD
PRR
GAP
BPGAP1
BCH
RBD
BNIP-2
RBD
RhoA
BCH
PRR
GAP
BPGAP1
BNIP-2
BCH
RBD
RBD
BCH
PRR
RhoA
GAP
↓ GTP-RhoA
↑ Loss of stress fiber;
↑ Cell rounding;
↓ Proliferation

Figure 4.1 Proposed models of synergism between BNIP-2 and BPGAP1 in regulating RhoA activity and downstream cellular effects. (a) BPGAP1, held possibly in a closed conformation by intramolcular interactions, displays marginal GAP activity towards RhoA. Through heterophilic association of the BCH domains of BNIP-2 and BPGAP1, BNIP-2 interacts and introduces a conformation change within BPGAP1 to relieve this autoinhibition, while acting as a scaffold to bring BPGAP1 and RhoA in close proximity for inactivation. (b) Alternatively, the GAP activity of BPGAP1 in its native state may be suppressed by both autoinhibitory intramolecular interaction, as well as sequestration of RhoA by the adjacent BCH domain. Through heterophilic association of the BCH domains of BNIP-2 and BPGAP1, BNIP-2 not only functions to relieve the autoinhibition via introduction of conformational change, but also aids in the displacement of RhoA to allow the GAP domain to gain access to and inactivate RhoA. In both models, interaction between BCH domain of BNIP-2 and PGAP module of BPGAP1 may serve to stabilize the resultant structure of BPGAP1 for better catalytic efficiency. Altogether, interactions between BNIP-2 and BPGAP1 allow the GAP domain to act on and promote inactivation of the nearby RhoA, thereby bringing about an increase in loss of stress fiber, alteration in cell morphology and a decrease in cellular proliferation. This study therefore adds to the mounting evidences that BCH domain-containing proteins function to modulate Rho GTPases and their immediate regulators.

4.5 BCH domain as a small GTPase regulatory domain

With the exception of the brain specific member – BNIP-H, all of the remaining BCH domain-containing proteins studied in our laboratory possess the ability to associate with RhoA via their respective BCH domains and also with other Rho GTPases such as Cdc42 or Rac1 for some of these proteins. Amongst these RhoA-interacting members of the BCH domain-containing family, BCH domain of BNIP-XL harbors multiple RhoA interacting sequences (Soh and Low, 2008), whereas BNIP-2, BNIP-Sα, p50RhoGAP and BPGAP1 each contains a specific RhoA binding motif and are aligned using multiple sequence alignment as shown in Figure 4.2. The authenticity of these motifs in binding to RhoA has been verified primarily in immunoprecipitation studies (Zhou et al., 2010; Zhou et al., 2006) and further confirmed by structure analysis at least in the case of p50RhoGAP in a current study. These results together suggest the possible existence of a consensus sequence or

critical residues for RhoA binding within the BCH domains. However, positive interactions between BCH domain-containing proteins and RhoA might not solely rely on the presence of this interacting motif but are also dependent on other spatial and temporal factors.

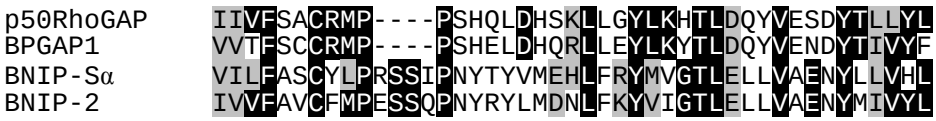

Figure 4.2 Possible existence of a consensus RhoA binding sequence within BCH domains. Multiple sequence alignment of the verified RhoA binding regions within BCH domains of *Homo sapiens* p50RhoGAP (Q07960), BPGAP1 (AAN40769), BNIP-Sα (AY078983) and BNIP-2 (U15173) using ClustalW and formatted using BOXSHADE. Identical residues are shaded black while grey shadings represent similar or conserved residues.

Intriguingly, not only does BCH domain possess the ability to target Rho GTPases per se, it is also able to alter the level of active Rho GTPases indirectly by modulating the activity of their immediate regulators RhoGAPs and RhoGEFs as seen in the many examples discussed, including BNIP-Sα, BNIP-XL and p50RhoGAP (Soh and Low, 2008; Zhou et al., 2010; Zhou et al., 2006). Our study herein has also demonstrated that BNIP-2 can function in synergism with BPGAP1 to negatively regulate RhoA activity by enhancing the GAP function of BPGAP1, thereby adding to the repertoire of evidences supporting the role of BCH domain as a regulator for both Rho GTPases and their immediate upstream activators or inactivators.

Further to regulating the Rho family of small GTPases, interestingly BCH domain can also modulate members of the Ras GTPase family. It has been demonstrated in PC12 cells that BCH domain of BPGAP1 is able to activate K-Ras, leading to formation of neurite-like protrusions (Ravichandran and Low,

unpublished). This new insight on substrates beyond the Rho GTPase family that are acted upon by the BCH domain certainly demonstrates the versatility of this highly conserved domain in mediating signaling pathways of a diverse range of small GTPases. In fact, other than Rho and Ras GTPases, ongoing work by colleagues have shown that BCH domain could also associate with members of other families under the Ras superfamily, including Rab.

Crosstalk of different small GTPase signaling pathways mediated by complex formation is not unprecedented given that p190RhoGAP associates with p120RasGAP upon phosphorylation (Roof et al., 1998) and formation of this complex can facilitate crosstalk between Rho and Ras. This crosstalk leads to an overall decrease in active RhoA and a corresponding increase in the level of activated Ras due to enhanced RhoGAP activity and suppression of RasGAP activity, respectively (Bradley et al., 2006; Moran et al., 1991; Shen et al., 2008). The presence of a conversed BCH domain within BCH domain-containing proteins that can target different families of small GTPases while at the same time modulate their respective regulators therefore would suggest that these proteins may function in concert to mediate crosstalks of the different small GTPases signaling pathways. In this regard, BCH domain could well serve as a scaffold in regulating the activity of a single small GTPase protein or in linking signaling events of multiple small GTPases and in some cases with other signaling pathways. For example, BNIP-2 BCH domain is known to function as a scaffold to connect Cdo receptor signaling to the Cdc42 signaling pathway (Kang et al., 2008).

Besides being able to interact with small GTPases, BCH domain also harbors lipid binding ability (Zhou and Low, unpublished) due to its limited homology with the Sec14p domain that is involved in phosphatidylinositol and phosphatidylcholine

transfer (Mousley et al., 2007; Saito et al., 2007; Schaaf et al., 2008). Through possible associations with lipids, BCH domain could serve to target these BCH domain-containing proteins and the bound proteins to designated subcellular compartments, thereby providing an additional form of regulation in terms of spatial regulation. Notably, substrate preference of p190GAP towards either Rho or Rac GTPases can be altered by the various physiological phospholipids (Ligeti et al., 2004; Ligeti and Settleman, 2006). This finding thus raises the possibility that other forms of lipid-mediated regulatory mechanisms could exist to modulate the functions of BCH domain-containing proteins. Further exploration on the multiple roles of this BCH domain in regulating the functions of small GTPases will therefore open up a new and exciting paradigm.

Chapter 5

Conclusions

and

Future Perspectives

5 CONCLUSIONS AND FUTURE PERSPECTIVES

5.1 Conclusions

Since the identification of BPGAP1 as a member of the *Homo sapiens* multi-modular RhoGAP family, much effort has been made to characterize this protein in terms of its GAP activity and its cellular functions conferred through associations with various interacting partners identified from proteomics pull-down. In addition to its known function as a RhoGAP protein with specificity towards RhoA *in vivo* (Shang et al., 2003), BPGAP1 was found to promote cell migration, which requires its GAP activity and the BCH domain for inducing morphological changes, as well as the proline rich region for translocation of cortactin (Lua and Low, 2004; Shang et al., 2003). Further to this role, the GAP domain is also involved in promoting ERK signaling downstream of EGF receptor endocytosis (Lua and Low, 2005). With the RhoGAP activity contributing significantly to the various functions mediated by BPGAP1, this explains the paramount importance in identifying regulators that modulate this catalytic activity and to elucidate the mechanisms behind this regulation.

In this regard, the focus in recent work has been shifted to exploring and understanding the possible ways by which BPGAP1 can be regulated while continuing to uncover more biological functions of this protein. In one such study, the evidence presented supports the role of Pin1 as a regulator of BPGAP1 such that it attenuates RhoA signaling via stimulation of the GAP activity (Pan et al., 2010).

By a candidate approach, we have identified BNIP-2 as a novel regulator of BPGAP1 and these two proteins associate through heterophilic interaction of their respective BCH domains. Interestingly, BCH domain of BNIP-2 also interacts with

the GAP module of BPGAP1, perhaps to stabilize the structure of BPGAP1 for its catalytic function. Besides being capable of mediating homophilic or heterophilic interactions with BCH domain-containing proteins, bioinformatics analyses and subsequent verification by immunoprecipitation studies have also mapped the RhoA interaction site to specific region within the BCH domain, suggesting the possibility of a consensus RhoA binding sequence within this conserved domain.

Even though RhoA and BPGAP1 share overlapping interacting sites on BNIP-2 BCH domain, BNIP-2 is able to associate with BPGAP1 in the presence of RhoA and colocalization of these three proteins further suggests that they might associate to form a tripartite complex. Consistently, results from RhoA activity assays demonstrate that BNIP-2 augments the GAP activity of BPGAP1 and promote RhoA inactivation. This reduction in active RhoA amount leads to an increase in the loss of stress fibers and GAP-induced cell rounding, as well as an overall decrease in cellular proliferation. On the contrary, synergistic effect between BNIP-2 and BPGAP1 was no longer evident once the RhoGAP activity of BPGAP1 was abolished as shown with the catalytic inactive mutant, further strengthening the positive role of BNIP-2 in GAP activity regulation.

Working on this basis, we hereby propose the model in which BPGAP1 in its native confirmation displays minimal RhoGAP activity towards RhoA due to autoinhibitory forces and/or sequestration of RhoA, as deduced from studies on p50RhoGAP (Moskwa et al., 2005; Zhou et al., 2010). By forming heterophilic interaction with BPGAP1 via the BCH domain, BNIP-2 could possibly serve to relieve the autoinhibition within BPGAP1 by introducing a conformational change that enables the GAP domain to gain access to and inactivate RhoA. In addition, BNIP-2 may function as a scaffold to bring BPGAP1 and RhoA in close proximity for

more efficient catalysis or simply as a regulator that aids in the displacement of RhoA from the Rho binding site on BPGAP1 BCH domain to allow subsequent RhoA inactivation by the adjacent GAP domain. Interaction between BCH domain of BNIP-2 and GAP module of BPGAP1 could on the other hand stabilize the resultant structure of BPGAP1. Together, these interactions function in concert to promote RhoA inactivation, thereby bringing about the observed downstream effects on stress fiber, cell morphology and proliferation. However, there exist several interesting aspects that could be further explored for a more in-depth understanding on the detailed molecular mechanism and also on other possible physiological effects conferred by this BNIP-2-BPGAP1 interaction, some of which are further discussed below.

5.2 Future work

5.2.1 Validation of molecular mechanism model

To fully comprehend the fundamental molecular mechanism that underlies the physiological outcomes observed for interaction between BNIP-2 and BPGAP1, several issues pertaining to the current proposed model remain to be addressed in greater details. Firstly, although previous work by colleagues strongly suggests the existence of autoinhibition within BPGAP1 (Pan et al., 2010; Shang et al., 2003), whether this autoinhibition is mediated by intramolecular interaction requires further validation. While the regions that could be essential for intramolecular interaction have been identified through immunoprecipiation study with deletion mutants (Ravichandran and Low, unpublished), use of fluorescence resonance energy transfer (FRET)-based analysis in live cell imaging would not only further validate the presence of intramolecular interaction within BPGAP1, but could also provide

valuable information on the exact spatial activation of this protein. In essence, both ends of the protein-of-interest are differentially tagged with either a cyan fluorescence protein (CFP) or a yellow fluorescence protein (YFP) and a basal level of FRET signal exists when the protein is in an autoinhibited state due to close proximity of the two fluorophores. An abolishment of the FRET activity will occur once these fluorophores are at a distance sufficiently far from each other, hence allowing any changes in conformation to be monitored.

Studies on p50RhoGAP have provided evidences that inhibition of the GAP activity by its adjacent BCH domain is conferred not only by intramolecular interactions but also depends greatly on RhoA sequestration by the BCH domain (Moskwa et al., 2005; Zhou et al., 2010). Unlike p50RhoGAP, BPGAP1 utilizes the same region within its BCH domain for binding to RhoA (as identified in this study) and for establishing intramolecular interaction with the C-terminal region at amino acids 389-433, beyond the GAP domain (Ravichandran and Low, unpublished). In this case, the use of a BPGAP1 deletion mutant devoid of the RhoA binding region, which is important also for intramolecular interaction, when assaying for RhoGAP activity could not effectively distinguish whether one or both mechanisms are required for autoinhibition within BPGAP1. This can ideally be overcome by using another protein, which displays a higher RhoA-binding affinity than BPGAP1 that could sequester RhoA away from the RhoA binding region and yet not disturb any intramolecular interaction. It would also be of interest to study the binding profiles of BCH and GAP domains of BPGAP1 to the nucleotide-free, GDP- or GTPγS-bound form of RhoA using in vitro GTP and GDP loading assays, for comparison with the binding profiles of the various RhoA mutants.

Next, although it has been established in this study that BCH domain of BNIP-2 could form heterophilic interaction with BPGAP1 BCH domain, whether any conformational change is introduced within BPGAP1 upon their association would require further validation from structural studies. In addition, to further substantiate the role of BNIP-2 as regulator of BPGAP1, siRNA can be designed to transiently knockdown this protein. By decreasing the amount of endogenous protein present, this abolishes the functional effect brought about by this protein and hence allows the manifestation of physiological effects, if any.

5.2.2 Spatiotemporal dynamics of RhoA activity in the presence of BNIP-2 and BPGAP1

Having shown through a biochemical approach that BNIP-2 and BPGAP1 function in synergism to perturb global level of active RhoA, it is of great interest next to dissect this change by examining the spatiotemporal dynamics of RhoA activity in living cells when BNIP-2 and BPGAP1 are introduced. Over the years, with the emergence of GFP-based FRET probes, real-time monitoring of spatiotemporal activities of Ras and Rho small GTPases has been made possible in live cell imaging (Nakamura et al., 2005; Pertz and Hahn, 2004). Continuous improvement in the design of these probes has further led to the development of single-chain biosensor that not only allows for the activity of RhoA to be monitored in terms of GDP/GTP exchange, but also enable subcellular targeting of this molecule through the C-terminal CAAX motif, as well as regulation of its membrane localization by RhoGDI (Pertz et al., 2006). Each single chain biosensor is composed of RBD of effector Rhotekin that recognizes and binds specifically to GTP-RhoA, CFP, an unstructured linker of optimized length, YFP and RhoA in tandem. In theory,

intramolecular binding of activated RhoA to RBD upon activation by GTP loading re-orientates the two fluorophores, which subsequently brings them into close proximity for increasing FRET (Nakamura et al., 2005; Pertz et al., 2006). Use of this technique along with multiple Rho biosensors has successfully demonstrated the dynamics of Rho GTPase activities including RhoA, Rac1 and Cdc42 during cell protrusion event (Machacek et al., 2009).

In future studies, we therefore aim to investigate the spatiotemporal regulation of RhoA activity by its negative regulator BPGAP1 and when in concert with BNIP-2 using live cell imaging with RhoA biosensor. This approach overcomes the limitation of current immunofluorescence study that enables only the detection of subpopulations of colocalized proteins but does not reflect their activity state in precise spatial localization and timing within the cells.

5.2.3 Role of BPGAP1 in cellular proliferation

While there have been some hints to a role of BPGAP1 in cellular proliferation, how this protein governs the process remains largely unknown. Although analyses of the proliferation status of cells transiently transfected with BPGAP1 have been carried out in this study, the lack of synchronization could potentially obscure the effect of this protein. As such, it is imperative that future studies should be performed in conjunction with cell synchronization by first subjecting the cells to either serum starvation or treatment with nocodazole.

Thus far, there have been mixed evidences in suggesting the possible involvement of BPGAP1 in different processes of cell proliferation. We therefore wish to determine the exact phase in which BPGAP1 participates during proliferation. To begin, cells transiently transfected with BPGAP1 could be assayed for DNA

content using FACS (fluorescence activated cell sorting) at various time points during cell cycle to identify any deviation in the distribution of cell populations from the control cells (Morin et al., 2009). Of note, BPGAP1 induces sustained ERK activation upon EGF stimulation (Lua and Low, 2005; Pan et al., 2010). It has yet to be ascertained if there is any perturbation in ERK activity under non-stimulated conditions in the presence of BPGAP1 and whether the change, if any, will affect the proliferation process.

Besides entry into S-phase, it is not known if BPGAP1 as a negative regulator of RhoA, is involved in the cytokinesis process. Multinucleation assay and FRET analysis in combination with time-lapse imaging as described in the studies conducted on p190RhoGAP could be similarly employed to investigate in real-time whether the RhoGAP activity of BPGAP1 is required for controlling the level of active RhoA during cytokinesis and also to define the phase of cytokinesis involved (Manchinelly et al., 2010; Su et al., 2009). Alternatively, it would be interesting to study if BPGAP1, through downregulation of RhoA, may alter the proliferation state of cells by interfering with the transcription process.

On a final note, based on the known effect of BPGAP1 on cell migration and its biochemical activity towards RhoA (Shang et al., 2003), it may be worthwhile to pursue the effect of BNIP-2 and BPGAP1 interaction on other RhoA-mediated processes such as migration and cellular transformation. Furthermore, given that RhoA and RhoC are selectively immunoprecipitated by BNIP-2 and BPGAP1, and both Rho proteins have been shown to perform distinct roles in the same processes including migration and invasion by acting through different downstream targets (Vega et al., 2011), it would be interesting to investigate if RhoC is similarly regulated by concerted action of BNIP-2 and BPGAP1, and the resulting effects.

Chapter 6

References

Arakawa, Y., Bito, H., Furuyashiki, T., Tsuji, T., Takemoto-Kimura, S., Kimura, K., Nozaki, K., Hashimoto, N., and Narumiya, S. (2003). Control of axon elongation via an SDF-1alpha/Rho/mDia pathway in cultured cerebellar granule neurons. J Cell Biol *161*, 381-391.

Aspenstrom, P., Ruusala, A., and Pacholsky, D. (2007). Taking Rho GTPases to the next level: the cellular functions of atypical Rho GTPases. Exp Cell Res *313*, 3673-3679.

Arthur, W. T., Ellerbroek, S. M., Der, C. J., Burridge, K., and Wennerberg, K. (2002). XPLN, a guanine nucleotide exchange factor for RhoA and RhoB, but not RhoC. J Biol Chem *277*, 42964-42972.

Aznar, S., and Lacal, J. C. (2001). Rho signals to cell growth and apoptosis. Cancer Lett *165*, 1-10.

Balmanno, K., and Cook, S. J. (1999). Sustained MAP kinase activation is required for the expression of cyclin D1, p21Cip1 and a subset of AP-1 proteins in CCL39 cells. Oncogene *18*, 3085-3097.

Ban, R., Irino, Y., Fukami, K., and Tanaka, H. (2004). Human mitotic spindle-associated protein PRC1 inhibits MgcRacGAP activity toward Cdc42 during the metaphase. J Biol Chem *279*, 16394-16402.

Bankaitis, V. A., Mousley, C. J., and Schaaf, G. (2010). The Sec14 superfamily and mechanisms for crosstalk between lipid metabolism and lipid signaling. Trends Biochem Sci *35*, 150-160.

Barr, F. A., and Gruneberg, U. (2007). Cytokinesis: placing and making the final cut. Cell *131*, 847-860.

Belcredito, S., Vegeto, E., Brusadelli, A., Ghisletti, S., Mussi, P., Ciana, P., and Maggi, A. (2001). Estrogen neuroprotection: the involvement of the Bcl-2 binding protein BNIP2. Brain Res Brain Res Rev *37*, 335-342.

Benitah, S. A., Valeron, P. F., Rui, H., and Lacal, J. C. (2003). STAT5a activation mediates the epithelial to mesenchymal transition induced by oncogenic RhoA. Mol Biol Cell *14*, 40-53.

Benitah, S. A., Valeron, P. F., van Aelst, L., Marshall, C. J., and Lacal, J. C. (2004). Rho GTPases in human cancer: an unresolved link to upstream and downstream transcriptional regulation. Biochim Biophys Acta *1705*, 121-132.

Bernacchi, S., Mercenne, G., Tournaire, C., Marquet, R., and Paillart, J. C. (2011). Importance of the proline-rich multimerization domain on the oligomerization and nucleic acid binding properties of HIV-1 Vif. Nucleic Acids Res *39*, 2404-2415.

Bishop, A. L., and Hall, A. (2000). Rho GTPases and their effector proteins. Biochem J *348 Pt 2*, 241-255.

Bonner, A. E., Lemon, W. J., Devereux, T. R., Lubet, R. A., and You, M. (2004). Molecular profiling of mouse lung tumors: association with tumor progression, lung development, and human lung adenocarcinomas. Oncogene *23*, 1166-1176.

Bos, J. L., Rehmann, H., and Wittinghofer, A. (2007). GEFs and GAPs: critical elements in the control of small G proteins. Cell *129*, 865-877.

Boureux, A., Vignal, E., Faure, S., and Fort, P. (2007). Evolution of the Rho family of ras-like GTPases in eukaryotes. Mol Biol Evol *24*, 203-216.

Bourne, H. R., Sanders, D. A., and McCormick, F. (1991). The GTPase superfamily: conserved structure and molecular mechanism. Nature *349*, 117-127.

Boyd (1994). Adenovirus E1B 19 kDa and Bcl-2 proteins interact with a common set of cellular proteins. Cell *79*, 1121.

Bradley, W. D., Hernandez, S. E., Settleman, J., and Koleske, A. J. (2006). Integrin signaling through Arg activates p190RhoGAP by promoting its binding to p120RasGAP and recruitment to the membrane. Mol Biol Cell *17*, 4827-4836.

Brouns, M. R., Matheson, S. F., Hu, K. Q., Delalle, I., Caviness, V. S., Silver, J., Bronson, R. T., and Settleman, J. (2000). The adhesion signaling molecule p190 RhoGAP is required for morphogenetic processes in neural development. Development *127*, 4891-4903.

Bryan, B. A., and D'Amore, P. A. (2007). What tangled webs they weave: Rho-GTPase control of angiogenesis. Cell Mol Life Sci *64*, 2053-2065.

Buchsbaum, R. J. (2007). Rho activation at a glance. J Cell Sci *120*, 1149-1152.

Burridge, K., and Wennerberg, K. (2004). Rho and Rac take center stage. Cell *116*, 167-179.

Buschdorf, J. P., Li Chew, L., Zhang, B., Cao, Q., Liang, F. Y., Liou, Y. C., Zhou, Y. T., and Low, B. C. (2006). Brain-specific BNIP-2-homology protein Caytaxin relocalises glutaminase to neurite terminals and reduces glutamate levels. J Cell Sci *119*, 3337-3350.

Buschdorf, J. P., Chew, L. L., Soh, U. J., Liou, Y. C., and Low, B. C. (2008). Nerve growth factor stimulates interaction of Cayman ataxia protein BNIP-H/Caytaxin with peptidyl-prolyl isomerase Pin1 in differentiating neurons. PLoS One *3*, e2686.

Castells, A., Gusella, J. F., Ramesh, V., and Rustgi, A. K. (2000). A region of deletion on chromosome 22q13 is common to human breast and colorectal cancers. Cancer Res *60*, 2836-2839.

Castells, A., Ino, Y., Louis, D. N., Ramesh, V., Gusella, J. F., and Rustgi, A. K. (1999). Mapping of a target region of allelic loss to a 0.5-cM interval on chromosome 22q13 in human colorectal cancer. Gastroenterology *117*, 831-837.

Cau, J., and Hall, A. (2005). Cdc42 controls the polarity of the actin and microtubule cytoskeletons through two distinct signal transduction pathways. J Cell Sci *118*, 2579-2587.

Chang, Y. W., Bean, R. R., and Jakobi, R. (2009). Targeting RhoA/Rho kinase and p21-activated kinase signaling to prevent cancer development and progression. Recent Pat Anticancer Drug Discov *4*, 110-124.

Chardin, P. (2006). Function and regulation of Rnd proteins. Nat Rev Mol Cell Biol *7*, 54-62.

Coleman, M. L., Marshall, C. J., and Olson, M. F. (2004). RAS and RHO GTPases in G1-phase cell-cycle regulation. Nat Rev Mol Cell Biol *5*, 355-366.

Colicelli, J. (2004). Human RAS superfamily proteins and related GTPases. Sci STKE *2004*, RE13.

Cook, S. J., Aziz, N., and McMahon, M. (1999). The repertoire of fos and jun proteins expressed during the G1 phase of the cell cycle is determined by the duration of mitogen-activated protein kinase activation. Mol Cell Biol *19*, 330-341.

D'Avino, P. P., and Glover, D. M. (2009). Cytokinesis: mind the GAP. Nat Cell Biol *11*, 112-114.

Debidda, M., Wang, L., Zang, H., Poli, V., and Zheng, Y. (2005). A role of STAT3 in Rho GTPase-regulated cell migration and proliferation. J Biol Chem *280*, 17275-17285.

DerMardirossian, C., and Bokoch, G. M. (2005). GDIs: central regulatory molecules in Rho GTPase activation. Trends Cell Biol *15*, 356-363.

Dovas, A., and Couchman, J. R. (2005). RhoGDI: multiple functions in the regulation of Rho family GTPase activities. Biochem J *390*, 1-9.

Drugan, J. K., Rogers-Graham, K., Gilmer, T., Campbell, S., and Clark, G. J. (2000). The Ras/p120 GTPase-activating protein (GAP) interaction is regulated by the p120 GAP pleckstrin homology domain. J Biol Chem *275*, 35021-35027.

Ellenbroek, S. I., and Collard, J. G. (2007). Rho GTPases: functions and association with cancer. Clin Exp Metastasis *24*, 657-672.

Etienne-Manneville, S., and Hall, A. (2002). Rho GTPases in cell biology. Nature *420*, 629-635.

Eva, A., and Aaronson, S. A. (1985). Isolation of a new human oncogene from a diffuse B-cell lymphoma. Nature *316*, 273-275.

Fan, L., Pellegrin, S., Scott, A., and Mellor, H. (2010). The small GTPase Rif is an alternative trigger for the formation of actin stress fibers in epithelial cells. J Cell Sci *123*, 1247-1252.

Fauchereau, F., Herbrand, U., Chafey, P., Eberth, A., Koulakoff, A., Vinet, M. C., Ahmadian, M. R., Chelly, J., and Billuart, P. (2003). The RhoGAP activity of OPHN1, a new F-actin-binding protein, is negatively controlled by its amino-terminal domain. Mol Cell Neurosci *23*, 574-586.

Garcia-Mata, R., and Burridge, K. (2007). Catching a GEF by its tail. Trends Cell Biol *17*, 36-43.

Goulimari, P., Kitzing, T. M., Knieling, H., Brandt, D. T., Offermanns, S., and Grosse, R. (2005). Galpha12/13 is essential for directed cell migration and localized Rho-Dia1 function. J Biol Chem *280*, 42242-42251.

Hakoshima, T., Shimizu, T., and Maesaki, R. (2003). Structural basis of the Rho GTPase signaling. J Biochem *134*, 327-331.

Hall, A. (1998). Rho GTPases and the actin cytoskeleton. Science *279*, 509-514.

Hall, A. (2009). The cytoskeleton and cancer. Cancer Metastasis Rev *28*, 5-14.

Healy, K. D., Hodgson, L., Kim, T. Y., Shutes, A., Maddileti, S., Juliano, R. L., Hahn, K. M., Harden, T. K., Bang, Y. J., and Der, C. J. (2008). DLC-1 suppresses non-small cell lung cancer growth and invasion by RhoGAP-dependent and independent mechanisms. Mol Carcinog *47*, 326-337.

Heasman, S. J., and Ridley, A. J. (2008). Mammalian Rho GTPases: new insights into their functions from in vivo studies. Nat Rev Mol Cell Biol *9*, 690-701.

Holeiter, G., Heering, J., Erlmann, P., Schmid, S., Jahne, R., and Olayioye, M. A. (2008). Deleted in liver cancer 1 controls cell migration through a Dia1-dependent signaling pathway. Cancer Res *68*, 8743-8751.

Hu, K. Q., and Settleman, J. (1997). Tandem SH2 binding sites mediate the RasGAP-RhoGAP interaction: a conformational mechanism for SH3 domain regulation. EMBO J *16*, 473-483.

Hwang, S. L., Hong, Y. R., Sy, W. D., Lieu, A. S., Lin, C. L., Lee, K. S., and Howng, S. L. (2004). Rac1 gene mutations in human brain tumours. Eur J Surg Oncol *30*, 68-72.

Jaffe, A. B., and Hall, A. (2005). Rho GTPases: biochemistry and biology. Annu Rev Cell Dev Biol *21*, 247-269.

Jenna, S., Hussain, N. K., Danek, E. I., Triki, I., Wasiak, S., McPherson, P. S., and Lamarche-Vane, N. (2002). The activity of the GTPase-activating protein CdGAP is regulated by the endocytic protein intersectin. J Biol Chem *277*, 6366-6373.

Johnstone, C. N., Castellvi-Bel, S., Chang, L. M., Bessa, X., Nakagawa, H., Harada, H., Sung, R. K., Pique, J. M., Castells, A., and Rustgi, A. K. (2004). ARHGAP8 is a novel member of the RHOGAP family related to ARHGAP1/CDC42GAP/p50RHOGAP: mutation and expression analyses in colorectal and breast cancers. Gene *336*, 59-71.

Kandpal, R. P. (2006). Rho GTPase activating proteins in cancer phenotypes. Curr Protein Pept Sci *7*, 355-365.

Kang, J. S., Bae, G. U., Yi, M. J., Yang, Y. J., Oh, J. E., Takaesu, G., Zhou, Y. T., Low, B. C., and Krauss, R. S. (2008). A Cdo-Bnip-2-Cdc42 signaling pathway regulates p38alpha/beta MAPK activity and myogenic differentiation. J Cell Biol *182*, 497-507.

Karlsson, R., Pedersen, E. D., Wang, Z., and Brakebusch, C. (2009). Rho GTPase function in tumorigenesis. Biochim Biophys Acta *1796*, 91-98.

Karnoub, A. E., Symons, M., Campbell, S. L., and Der, C. J. (2004). Molecular basis for Rho GTPase signaling specificity. Breast Cancer Res Treat *84*, 61-71.

Kim, T. K., and Roeder, R. G. (1993). Transcriptional activation in yeast by the proline-rich activation domain of human CTF1. J Biol Chem *268*, 20866-20869.

Kim, T. Y., Healy, K. D., Der, C. J., Sciaky, N., Bang, Y. J., and Juliano, R. L. (2008). Effects of structure of Rho GTPase-activating protein DLC-1 on cell morphology and migration. J Biol Chem *283*, 32762-32770.

Kobayashi, S. D., Voyich, J. M., Whitney, A. R., and DeLeo, F. R. (2005). Spontaneous neutrophil apoptosis and regulation of cell survival by granulocyte macrophage-colony stimulating factor. J Leukoc Biol *78*, 1408-1418.

Kozma, R., Ahmed, S., Best, A., and Lim, L. (1995). The Ras-related protein Cdc42Hs and bradykinin promote formation of peripheral actin microspikes and filopodia in Swiss 3T3 fibroblasts. Mol Cell Biol *15*, 1942-1952.

Le Roy, C., and Wrana, J. L. (2005). Clathrin- and non-clathrin-mediated endocytic regulation of cell signalling. Nat Rev Mol Cell Biol *6*, 112-126.

Leszczynski, J. F., and Rose, G. D. (1986). Loops in globular proteins: a novel category of secondary structure. Science *234*, 849-855.

Leung, T. H., Ching, Y. P., Yam, J. W., Wong, C. M., Yau, T. O., Jin, D. Y., and Ng, I. O. (2005). Deleted in liver cancer 2 (DLC2) suppresses cell transformation by means of inhibition of RhoA activity. Proc Natl Acad Sci U S A *102*, 15207-15212.

Liberto, M., Cobrinik, D., and Minden, A. (2002). Rho regulates p21(CIP1), cyclin D1, and checkpoint control in mammary epithelial cells. Oncogene *21*, 1590-1599.

Ligeti, E., Dagher, M. C., Hernandez, S. E., Koleske, A. J., and Settleman, J. (2004). Phospholipids can switch the GTPase substrate preference of a GTPase-activating protein. J Biol Chem *279*, 5055-5058.

Ligeti, E., and Settleman, J. (2006). Regulation of RhoGAP specificity by phospholipids and prenylation. Methods Enzymol *406*, 104-117.

Low, B. C., Lim, Y. P., Lim, J., Wong, E. S., and Guy, G. R. (1999). Tyrosine phosphorylation of the Bcl-2-associated protein BNIP-2 by fibroblast growth factor receptor-1 prevents its binding to Cdc42GAP and Cdc42. J Biol Chem *274*, 33123-33130.

Low, B. C., Seow, K. T., and Guy, G. R. (2000a). The BNIP-2 and Cdc42GAP homology domain of BNIP-2 mediates its homophilic association and heterophilic interaction with Cdc42GAP. J Biol Chem *275*, 37742-37751.

Low, B. C., Seow, K. T., and Guy, G. R. (2000b). Evidence for a novel Cdc42GAP domain at the carboxyl terminus of BNIP-2. J Biol Chem *275*, 14415-14422.

Lu, P. J., Zhou, X. Z., Shen, M., and Lu, K. P. (1999). Function of WW domains as phosphoserine- or phosphothreonine-binding modules. Science *283*, 1325-1328.

Lua, B. L., and Low, B. C. (2004). BPGAP1 interacts with cortactin and facilitates its translocation to cell periphery for enhanced cell migration. Mol Biol Cell *15*, 2873-2883.

Lua, B. L., and Low, B. C. (2005a). Activation of EGF receptor endocytosis and ERK1/2 signaling by BPGAP1 requires direct interaction with EEN/endophilin II and a functional RhoGAP domain. J Cell Sci *118*, 2707-2721.

Lua, B. L., and Low, B. C. (2005b). Cortactin phosphorylation as a switch for actin cytoskeletal network and cell dynamics control. FEBS Lett *579*, 577-585.

Machacek, M., Hodgson, L., Welch, C., Elliott, H., Pertz, O., Nalbant, P., Abell, A., Johnson, G. L., Hahn, K. M., and Danuser, G. (2009). Coordination of Rho GTPase activities during cell protrusion. Nature *461*, 99-103.

Madaule, P., and Axel, R. (1985). A novel ras-related gene family. Cell *41*, 31-40.

Maddox, A. S., and Burridge, K. (2003). RhoA is required for cortical retraction and rigidity during mitotic cell rounding. J Cell Biol *160*, 255-265.

Maesaki, R., Ihara, K., Shimizu, T., Kuroda, S., Kaibuchi, K., and Hakoshima, T. (1999). The structural basis of Rho effector recognition revealed by the crystal structure of human RhoA complexed with the effector domain of PKN/PRK1. Mol Cell *4*, 793-803.

Manchinelly, S. A., Miller, J. A., Su, L., Miyake, T., Palmer, L., Mikawa, M., and Parsons, S. J. (2010). Mitotic down-regulation of p190RhoGAP is required for the successful completion of cytokinesis. J Biol Chem *285*, 26923-26932.

Merajver, S. D., and Usmani, S. Z. (2005). Multifaceted role of Rho proteins in angiogenesis. J Mammary Gland Biol Neoplasia *10*, 291-298.

Merdek, K. D., Jaffe, A. B., Dutt, P., Olson, M. F., Hall, A., Fanburg, B. L., Kayyali, U. S., and Toksoz, D. (2008). Alpha(E)-Catenin induces SRF-dependent transcriptional activity through its C-terminal region and is partly RhoA/ROCK-dependent. Biochem Biophys Res Commun *366*, 717-723.

Michaelson, D., Silletti, J., Murphy, G., D'Eustachio, P., Rush, M., and Philips, M. R. (2001). Differential localization of Rho GTPases in live cells: regulation by hypervariable regions and RhoGDI binding. J Cell Biol *152*, 111-126.

Miralles, F., Posern, G., Zaromytidou, A. I., and Treisman, R. (2003). Actin dynamics control SRF activity by regulation of its coactivator MAL. Cell *113*, 329-342.

Miura, K., Jacques, K. M., Stauffer, S., Kubosaki, A., Zhu, K., Hirsch, D. S., Resau, J., Zheng, Y., and Randazzo, P. A. (2002). ARAP1: a point of convergence for Arf and Rho signaling. Mol Cell *9*, 109-119.

Moon, S. Y., and Zheng, Y. (2003). Rho GTPase-activating proteins in cell regulation. Trends Cell Biol *13*, 13-22.

Moran, M. F., Polakis, P., McCormick, F., Pawson, T., and Ellis, C. (1991). Protein-tyrosine kinases regulate the phosphorylation, protein interactions, subcellular distribution, and activity of p21ras GTPase-activating protein. Mol Cell Biol *11*, 1804-1812.

Morin, P., Flors, C., and Olson, M. F. (2009). Constitutively active RhoA inhibits proliferation by retarding G(1) to S phase cell cycle progression and impairing cytokinesis. Eur J Cell Biol *88*, 495-507.

Moskwa, P., Paclet, M. H., Dagher, M. C., and Ligeti, E. (2005). Autoinhibition of p50 Rho GTPase-activating protein (GAP) is released by prenylated small GTPases. J Biol Chem *280*, 6716-6720.

Mousley, C. J., Tyeryar, K. R., Vincent-Pope, P., and Bankaitis, V. A. (2007). The Sec14-superfamily and the regulatory interface between phospholipid metabolism and membrane trafficking. Biochim Biophys Acta *1771*, 727-736.

Nakamura, T., Aoki, K., and Matsuda, M. (2005). Monitoring spatio-temporal regulation of Ras and Rho GTPase with GFP-based FRET probes. Methods *37*, 146-153.

Narumiya, S., Tanji, M., and Ishizaki, T. (2009). Rho signaling, ROCK and mDia1, in transformation, metastasis and invasion. Cancer Metastasis Rev *28*, 65-76.

Nassar, N., Hoffman, G. R., Manor, D., Clardy, J. C., and Cerione, R. A. (1998). Structures of Cdc42 bound to the active and catalytically compromised forms of Cdc42GAP. Nat Struct Biol *5*, 1047-1052.

Nobes, C. D., and Hall, A. (1995). Rho, rac, and cdc42 GTPases regulate the assembly of multimolecular focal complexes associated with actin stress fibers, lamellipodia, and filopodia. Cell *81*, 53-62.

Nomanbhoy, T. K., Erickson, J. W., and Cerione, R. A. (1999). Kinetics of Cdc42 membrane extraction by Rho-GDI monitored by real-time fluorescence resonance energy transfer. Biochemistry *38*, 1744-1750.

Oh, J. E., Bae, G. U., Yang, Y. J., Yi, M. J., Lee, H. J., Kim, B. G., Krauss, R. S., and Kang, J. S. (2009). Cdo promotes neuronal differentiation via activation of the p38 mitogen-activated protein kinase pathway. FASEB J *23*, 2088-2099.

Olson, M. F., Ashworth, A., and Hall, A. (1995). An essential role for Rho, Rac, and Cdc42 GTPases in cell cycle progression through G1. Science *269*, 1270-1272.

Olson, M. F., Paterson, H. F., and Marshall, C. J. (1998). Signals from Ras and Rho GTPases interact to regulate expression of p21Waf1/Cip1. Nature *394*, 295-299.

Pan, C. Q., Liou, Y. C., and Low, B. C. (2010). Active Mek2 as a regulatory scaffold that promotes Pin1 binding to BPGAP1 to suppress BPGAP1-induced acute Erk activation and cell migration. J Cell Sci *123*, 903-916.

Parsons, J. T., Horwitz, A. R., and Schwartz, M. A. (2010). Cell adhesion: integrating cytoskeletal dynamics and cellular tension. Nat Rev Mol Cell Biol *11*, 633-643.

Peck, J., Douglas, G. t., Wu, C. H., and Burbelo, P. D. (2002). Human RhoGAP domain-containing proteins: structure, function and evolutionary relationships. FEBS Lett *528*, 27-34.

Pertz, O., and Hahn, K. M. (2004). Designing biosensors for Rho family proteins--deciphering the dynamics of Rho family GTPase activation in living cells. J Cell Sci *117*, 1313-1318.

Pertz, O., Hodgson, L., Klemke, R. L., and Hahn, K. M. (2006). Spatiotemporal dynamics of RhoA activity in migrating cells. Nature *440*, 1069-1072.

Piekny, A., Werner, M., and Glotzer, M. (2005). Cytokinesis: welcome to the Rho zone. Trends Cell Biol *15*, 651-658.

Raftopoulou, M., and Hall, A. (2004). Cell migration: Rho GTPases lead the way. Dev Biol *265*, 23-32.

Ren, X. D., and Schwartz, M. A. (2000). Determination of GTP loading on Rho. Methods Enzymol *325*, 264-272.

Renault, L., Guibert, B., and Cherfils, J. (2003). Structural snapshots of the mechanism and inhibition of a guanine nucleotide exchange factor. Nature *426*, 525-530.

Ridley, A. J., and Hall, A. (1992). The small GTP-binding protein rho regulates the assembly of focal adhesions and actin stress fibers in response to growth factors. Cell *70*, 389-399.

Ridley, A. J., Paterson, H. F., Johnston, C. L., Diekmann, D., and Hall, A. (1992). The small GTP-binding protein rac regulates growth factor-induced membrane ruffling. Cell *70*, 401-410.

Ridley, A. J., Schwartz, M. A., Burridge, K., Firtel, R. A., Ginsberg, M. H., Borisy, G., Parsons, J. T., and Horwitz, A. R. (2003). Cell migration: integrating signals from front to back. Science *302*, 1704-1709.

Ridley, A. J., Self, A. J., Kasmi, F., Paterson, H. F., Hall, A., Marshall, C. J., and Ellis, C. (1993). rho family GTPase activating proteins p190, bcr and rhoGAP show distinct specificities in vitro and in vivo. EMBO J *12*, 5151-5160.

Riento, K., and Ridley, A. J. (2003). Rocks: multifunctional kinases in cell behaviour. Nat Rev Mol Cell Biol *4*, 446-456.

Rittinger, K., Walker, P. A., Eccleston, J. F., Smerdon, S. J., and Gamblin, S. J. (1997). Structure at 1.65 A of RhoA and its GTPase-activating protein in complex with a transition-state analogue. Nature *389*, 758-762.

Roberts, P. J., Mitin, N., Keller, P. J., Chenette, E. J., Madigan, J. P., Currin, R. O., Cox, A. D., Wilson, O., Kirschmeier, P., and Der, C. J. (2008). Rho Family GTPase modification and dependence on CAAX motif-signaled posttranslational modification. J Biol Chem *283*, 25150-25163.

Roof, R. W., Haskell, M. D., Dukes, B. D., Sherman, N., Kinter, M., and Parsons, S. J. (1998). Phosphotyrosine (p-Tyr)-dependent and -independent mechanisms of p190 RhoGAP-p120 RasGAP interaction: Tyr 1105 of p190, a substrate for c-Src, is the sole p-Tyr mediator of complex formation. Mol Cell Biol *18*, 7052-7063.

Roovers, K., Klein, E. A., Castagnino, P., and Assoian, R. K. (2003). Nuclear translocation of LIM kinase mediates Rho-Rho kinase regulation of cyclin D1 expression. Dev Cell *5*, 273-284.

Rossman, K. L., Der, C. J., and Sondek, J. (2005). GEF means go: turning on RHO GTPases with guanine nucleotide-exchange factors. Nat Rev Mol Cell Biol *6*, 167-180.

Sahai, E., Olson, M. F., and Marshall, C. J. (2001). Cross-talk between Ras and Rho signalling pathways in transformation favours proliferation and increased motility. EMBO J *20*, 755-766.

Saito, K., Tautz, L., and Mustelin, T. (2007). The lipid-binding SEC14 domain. Biochim Biophys Acta *1771*, 719-726.

Sanz-Moreno, V., Gadea, G., Ahn, J., Paterson, H., Marra, P., Pinner, S., Sahai, E., and Marshall, C. J. (2008). Rac activation and inactivation control plasticity of tumor cell movement. Cell *135*, 510-523.

Schaaf, G., Ortlund, E. A., Tyeryar, K. R., Mousley, C. J., Ile, K. E., Garrett, T. A., Ren, J., Woolls, M. J., Raetz, C. R., Redinbo, M. R., and Bankaitis, V. A. (2008). Functional anatomy of phospholipid binding and regulation of phosphoinositide homeostasis by proteins of the sec14 superfamily. Mol Cell *29*, 191-206.

Scheffzek, K., Ahmadian, M. R., Kabsch, W., Wiesmuller, L., Lautwein, A., Schmitz, F., and Wittinghofer, A. (1997). The Ras-RasGAP complex: structural basis for GTPase activation and its loss in oncogenic Ras mutants. Science *277*, 333-338.

Schmidt, A., and Hall, A. (2002). Guanine nucleotide exchange factors for Rho GTPases: turning on the switch. Genes Dev *16*, 1587-1609.

Schwartz, M. (2004). Rho signalling at a glance. J Cell Sci *117*, 5457-5458.

Scott, G. B., Bowles, P. A., Wilson, E. B., Meade, J. L., Low, B. C., Davison, A., Blair, G. E., and Cook, G. P. (2010). Identification of the BCL2/adenovirus E1B-19K protein-interacting protein 2 (BNIP-2) as a granzyme B target during human natural killer cell-mediated killing. Biochem J *431*, 423-431.

Shang, X., Moon, S. Y., and Zheng, Y. (2007). p200 RhoGAP promotes cell proliferation by mediating cross-talk between Ras and Rho signaling pathways. J Biol Chem *282*, 8801-8811.

Shang, X., Zhou, Y. T., and Low, B. C. (2003). Concerted regulation of cell dynamics by BNIP-2 and Cdc42GAP homology/Sec14p-like, proline-rich, and GTPase-activating protein domains of a novel Rho GTPase-activating protein, BPGAP1. J Biol Chem *278*, 45903-45914.

Shen, C. H., Chen, H. Y., Lin, M. S., Li, F. Y., Chang, C. C., Kuo, M. L., Settleman, J., and Chen, R. H. (2008). Breast tumor kinase phosphorylates p190RhoGAP to regulate rho and ras and promote breast carcinoma growth, migration, and invasion. Cancer Res *68*, 7779-7787.

Sit, S. T., and Manser, E. (2011). Rho GTPases and their role in organizing the actin cytoskeleton. J Cell Sci *124*, 679-683.

Soh, U. J., and Low, B. C. (2008). BNIP2 extra long inhibits RhoA and cellular transformation by Lbc RhoGEF via its BCH domain. J Cell Sci *121*, 1739-1749.

Song, J. Y., Lee, J. K., Lee, N. W., Jung, H. H., Kim, S. H., and Lee, K. W. (2008). Microarray analysis of normal cervix, carcinoma in situ, and invasive cervical cancer: identification of candidate genes in pathogenesis of invasion in cervical cancer. Int J Gynecol Cancer *18*, 1051-1059.

Sotiropoulos, A., Gineitis, D., Copeland, J., and Treisman, R. (1999). Signal-regulated activation of serum response factor is mediated by changes in actin dynamics. Cell *98*, 159-169.

Su, L., Agati, J. M., and Parsons, S. J. (2003). p190RhoGAP is cell cycle regulated and affects cytokinesis. J Cell Biol *163*, 571-582.

Su, L., Pertz, O., Mikawa, M., Hahn, K., and Parsons, S. J. (2009). p190RhoGAP negatively regulates Rho activity at the cleavage furrow of mitotic cells. Exp Cell Res *315*, 1347-1359.

Surks, H. K., Richards, C. T., and Mendelsohn, M. E. (2003). Myosin phosphatase-Rho interacting protein. A new member of the myosin phosphatase complex that directly binds RhoA. J Biol Chem *278*, 51484-51493.

Takaesu, G., Kang, J. S., Bae, G. U., Yi, M. J., Lee, C. M., Reddy, E. P., and Krauss, R. S. (2006). Activation of p38alpha/beta MAPK in myogenesis via binding of the scaffold protein JLP to the cell surface protein Cdo. J Cell Biol *175*, 383-388.

Tatsis, N., Lannigan, D. A., and Macara, I. G. (1998). The function of the p190 Rho GTPase-activating protein is controlled by its N-terminal GTP binding domain. J Biol Chem *273*, 34631-34638.

Tcherkezian, J., and Lamarche-Vane, N. (2007). Current knowledge of the large RhoGAP family of proteins. Biol Cell *99*, 67-86.

ten Klooster, J. P., and Hordijk, P. L. (2007). Targeting and localized signalling by small GTPases. Biol Cell *99*, 1-12.

Thomas, C., Fricke, I., Scrima, A., Berken, A., and Wittinghofer, A. (2007). Structural evidence for a common intermediate in small G protein-GEF reactions. Mol Cell *25*, 141-149.

Tsuji, T., Ishizaki, T., Okamoto, M., Higashida, C., Kimura, K., Furuyashiki, T., Arakawa, Y., Birge, R. B., Nakamoto, T., Hirai, H., and Narumiya, S. (2002). ROCK and mDia1 antagonize in Rho-dependent Rac activation in Swiss 3T3 fibroblasts. J Cell Biol *157*, 819-830.

Valencia, C. A., Cotten, S. W., and Liu, R. (2007). Cleavage of BNIP-2 and BNIP-XL by caspases. Biochem Biophys Res Commun *364*, 495-501.

Vega, F. M., and Ridley, A. J. (2008). Rho GTPases in cancer cell biology. FEBS Lett *582*, 2093-2101.

Vega, F. M., Fruhwirth, G., Ng, T., and Ridley, A. J. (2011). RhoA and RhoC have distinct roles in migration and invasion by acting through different targets. J Cell Biol *193*, 655-665.

Vetter, I. R., and Wittinghofer, A. (2001). The guanine nucleotide-binding switch in three dimensions. Science *294*, 1299-1304.

Vigil, D., Cherfils, J., Rossman, K. L., and Der, C. J. (2010). Ras superfamily GEFs and GAPs: validated and tractable targets for cancer therapy? Nat Rev Cancer *10*, 842-857.

Villalonga, P., and Ridley, A. J. (2006). Rho GTPases and cell cycle control. Growth Factors *24*, 159-164.

Wadsworth, P. (2005). Cytokinesis: Rho marks the spot. Curr Biol *15*, R871-874.

Wei, Y., Zhang, Y., Derewenda, U., Liu, X., Minor, W., Nakamoto, R. K., Somlyo, A. V., Somlyo, A. P., and Derewenda, Z. S. (1997). Crystal structure of RhoA-GDP and its functional implications. Nat Struct Biol *4*, 699-703.

Welsh, C. F. (2004). Rho GTPases as key transducers of proliferative signals in g1 cell cycle regulation. Breast Cancer Res Treat *84*, 33-42.

Welsh, C. F., Roovers, K., Villanueva, J., Liu, Y., Schwartz, M. A., and Assoian, R. K. (2001). Timing of cyclin D1 expression within G1 phase is controlled by Rho. Nat Cell Biol *3*, 950-957.

Wennerberg, K., and Der, C. J. (2004). Rho-family GTPases: it's not only Rac and Rho (and I like it). J Cell Sci *117*, 1301-1312.

Wennerberg, K., Forget, M. A., Ellerbroek, S. M., Arthur, W. T., Burridge, K., Settleman, J., Der, C. J., and Hansen, S. H. (2003). Rnd proteins function as RhoA antagonists by activating p190 RhoGAP. Curr Biol *13*, 1106-1115.

Wennerberg, K., Rossman, K. L., and Der, C. J. (2005). The Ras superfamily at a glance. J Cell Sci *118*, 843-846.

Werner, M., and Glotzer, M. (2008). Control of cortical contractility during cytokinesis. Biochem Soc Trans *36*, 371-377.

Wheeler, A. P., and Ridley, A. J. (2004). Why three Rho proteins? RhoA, RhoB, RhoC, and cell motility. Exp Cell Res *301*, 43-49.

Wittmann, T., and Waterman-Storer, C. M. (2001). Cell motility: can Rho GTPases and microtubules point the way? J Cell Sci *114*, 3795-3803.

Wong, C. M., Lee, J. M., Ching, Y. P., Jin, D. Y., and Ng, I. O. (2003). Genetic and epigenetic alterations of DLC-1 gene in hepatocellular carcinoma. Cancer Res *63*, 7646-7651.

Wong, C. M., Yam, J. W., Ching, Y. P., Yau, T. O., Leung, T. H., Jin, D. Y., and Ng, I. O. (2005). Rho GTPase-activating protein deleted in liver cancer suppresses cell proliferation and invasion in hepatocellular carcinoma. Cancer Res *65*, 8861-8868.

Yamada, T., Sakisaka, T., Hisata, S., Baba, T., and Takai, Y. (2005). RA-RhoGAP, Rap-activated Rho GTPase-activating protein implicated in neurite outgrowth through Rho. J Biol Chem *280*, 33026-33034.

Yamamoto, M., Marui, N., Sakai, T., Morii, N., Kozaki, S., Ikai, K., Imamura, S., and Narumiya, S. (1993). ADP-ribosylation of the rhoA gene product by botulinum C3 exoenzyme causes Swiss 3T3 cells to accumulate in the G1 phase of the cell cycle. Oncogene *8*, 1449-1455.

Yamamoto, T., Ebisuya, M., Ashida, F., Okamoto, K., Yonehara, S., and Nishida, E. (2006). Continuous ERK activation downregulates antiproliferative genes throughout G1 phase to allow cell-cycle progression. Curr Biol *16*, 1171-1182.

Yasuda, S., Oceguera-Yanez, F., Kato, T., Okamoto, M., Yonemura, S., Terada, Y., Ishizaki, T., and Narumiya, S. (2004). Cdc42 and mDia3 regulate microtubule attachment to kinetochores. Nature *428*, 767-771.

Zarrinpar, A., Bhattacharyya, R. P., and Lim, W. A. (2003). The structure and function of proline recognition domains. Sci STKE *2003*, RE8.

Zheng, Y., and Quilliam, L. A. (2003). Activation of the Ras superfamily of small GTPases. Workshop on exchange factors. EMBO Rep *4*, 463-468.

Zhou, Y. T., Chew, L. L., Lin, S. C., and Low, B. C. (2010). The BNIP-2 and Cdc42GAP homology (BCH) domain of p50RhoGAP/Cdc42GAP sequesters RhoA from inactivation by the adjacent GTPase-activating protein domain. Mol Biol Cell *21*, 3232-3246.

Zhou, Y. T., Guy, G. R., and Low, B. C. (2005). BNIP-2 induces cell elongation and membrane protrusions by interacting with Cdc42 via a unique Cdc42-binding motif within its BNIP-2 and Cdc42GAP homology domain. Exp Cell Res *303*, 263-274.

Zhou, Y. T., Guy, G. R., and Low, B. C. (2006). BNIP-Salpha induces cell rounding and apoptosis by displacing p50RhoGAP and facilitating RhoA activation via its unique motifs in the BNIP-2 and Cdc42GAP homology domain. Oncogene *25*, 2393-2408.

Zhou, Y. T., Soh, U. J., Shang, X., Guy, G. R., and Low, B. C. (2002). The BNIP-2 and Cdc42GAP homology/Sec14p-like domain of BNIP-Salpha is a novel apoptosis-inducing sequence. J Biol Chem *277*, 7483-7492.

7 Appendix

a BNIP-2

```
  1 MEGVELKEEWQDEDFPIPLPEDDSIEADILAITGPEDQPGSLEVNGNKVRKKLMAPDISL 60
    ---EEE-------------------------------------------EEEE----EE

 61 TLDPSDGSVLSDDLDESGEIDLDGLDTPSENSNEFEWEDDLPKPKTTEVIRKGSITEYTA 120
    E------EE-----------------------------------------------------H

121 AEEKEDGRRWRMFRIGEQDHRVDMKAIEPYKKVISHGGYYGDGLNAIVVFAVCFMPESSQ 180
    HHHHH----HHEEE-----------------EEEEE---------EEEEEE---------

181 PNYRYLMDNLFKYVIGTLELLVAENYMIVYLNGATTRRKMPSLGWLRKCYQQIDRRLRKN 240
    ----HHHHHHHHHHHHH-------EEEEEE-----------HHHHHHHHHH-HHHHHH

241 LKSLIIVHPSWFIRTLLAVTRPFISSKFSQKIRYVFNLAELAELVPMEYVGIPECIKQVD 300
    HHEEEEE---HHHHHHHHHHH--------EEEEEE--HHHHHHH---------HHHHHHH

301 QELNGKQDEPKNEQ
    HHHHH---------
```

Key: Regions deleted in BNIP-2 mutants: Δ(167-184); Δ(185-211)

b BPGAP1

```
  1 MAGQDPALSTSHPFYDVARHGILQVAGDDRFGRRVVTFSCCRMPPSHELDHQRLLEYLKY 60
    ------------HHHHHH--EEEEEEE-----EEEEEE-----------HHHHHHHHHH

 61 TLDQYVENDYTIVYFHYGLNSRNKPSLGWLQSAYKEFDRKYKKNLKALYVVHPTSFIKVL 120
    HHHH------EEEEEE----------HHHHHHHHHHHHHHHHHHHHHEEEE--HHHHHHH

121 WNILKPLISHKFGKKVIYFNYLSELHEHLKYDQLVIPPEVLRYDEKLQSLHEGRTPPPTK 180
    HHHH----------EE----HHHHHHHH---------------HHHH----------

181 TPPPRPPLPTQQFGVSLQYLKDKNQGELIPPVLRFTVTYLREKGLRTEGLFRRSASVQTV 240
    -----------------EE----------HHHHHHHHHHHH-------EEE----HHHH

241 REIQRLYNQGKPVNFDDYGDIHIPAVILKTFLRELPQPLLTFQAYEQILGITCVESSLRV 300
    HHHHHHH-------------HHHHHHHHHHHH---------HHHHHHHH-----HHHH

301 TGCRQILRSLPEHNYVVLRYLMGSLHAVSRESIFNKMNSSNLACVFGLNLIWPSQGVSSL 360
    HHHHHHHHH--HHHHHHHHHHHHHHHHH---------HHHHHHH------------HH

361 SALVPLNMFTELLIEYYEKIFSTPEAPGEHGLAPWEQGSRAAPLQEAVPRTQATGLTKPT 420
    HHHHHHHHHHHHHHHHH-------------------------------------------

421 LPPSPLMAARRRL
    -------------
```

Key: Regions in BPGAP1 PGAP mutants - PGAP (168-281) (Bright green region); PGAP (168-310) (Bright green and green regions)

Figure S1 Secondary structure predictions of BNIP-2 and BPGAP1. The predicted secondary structures of (a) BNIP-2 (U15173) and (b) BPGAP1 (AAN40769) were obtained using secondary structure prediction server - Jpred (http://www.compbio.dundee.ac.uk/www-jpred/). Letters H and E represent the residues predicted as a part of α-helices and β-sheet, respectively. The regions deleted in BNIP-2 are highlighted as follow: 167-184 (magenta) and 185-211 (cyan), while the regions covered in PGAP truncation mutants are highlighted in either bright green alone (168-281) or both bright green and green (168-310) as indicated.

a

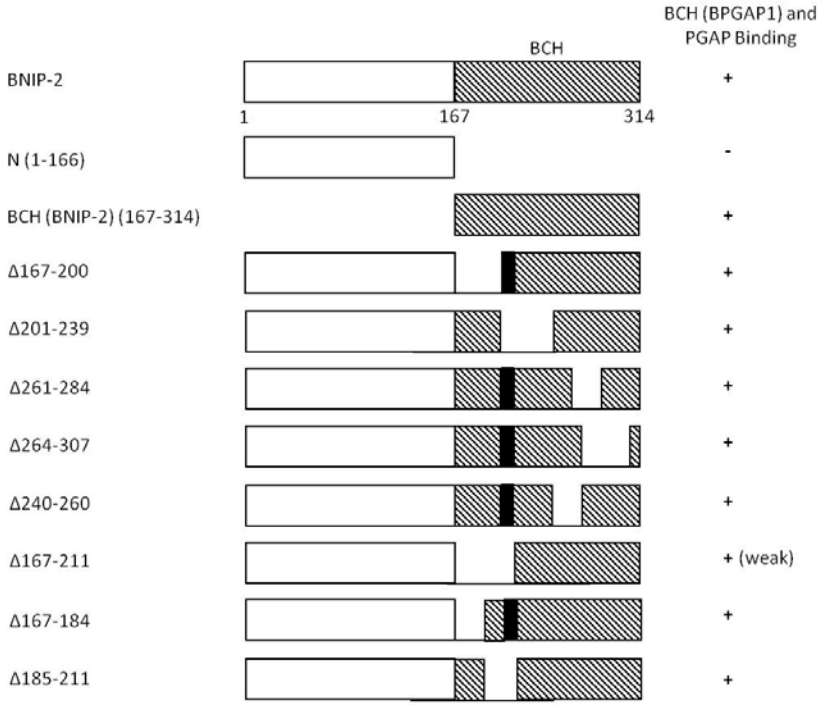

bi

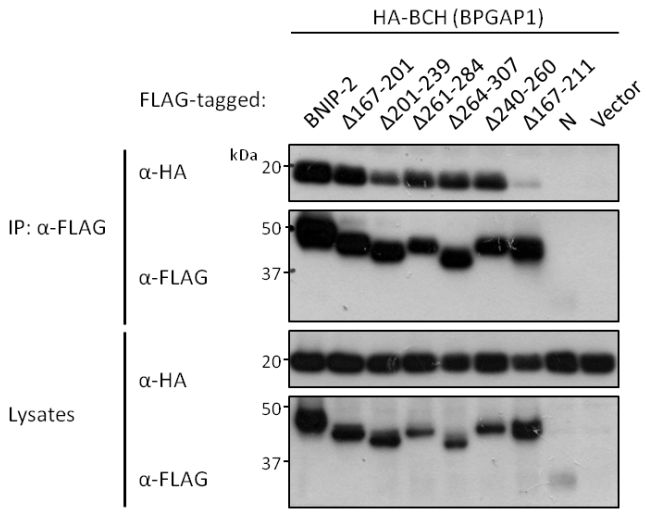

bii

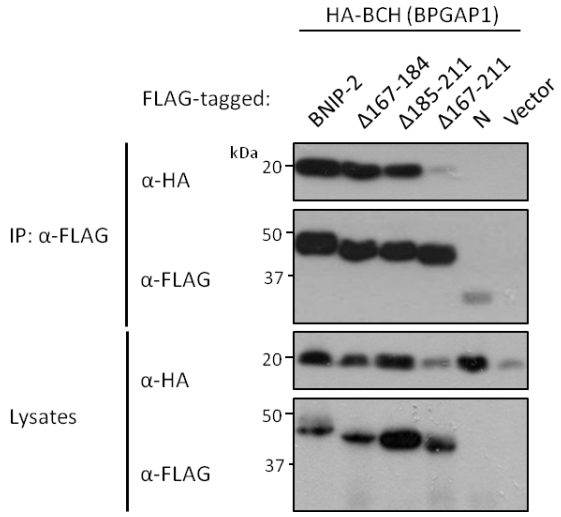
HA-BCH (BPGAP1)
FLAG-tagged:
BNIP-2
Δ167-184
Δ185-211
Δ167-211
N
Vector
kDa
IP: α-FLAG
α-HA
α-FLAG
Lysates
α-HA
α-FLAG
20
50
37
20
50
37

ci

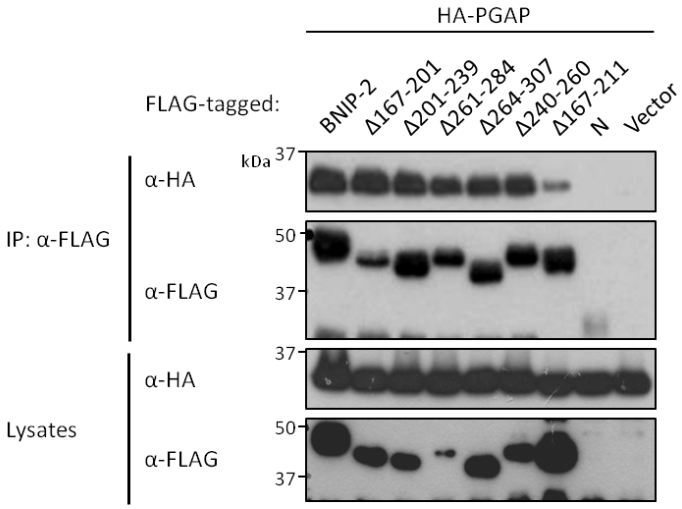
HA-PGAP
FLAG-tagged:
BNIP-2
Δ167-201
Δ201-239
Δ261-284
Δ264-307
Δ240-260
Δ167-211
N
Vector
kDa
IP: α-FLAG
α-HA
α-FLAG
Lysates
α-HA
α-FLAG
37
50
37
37
50
37

cii

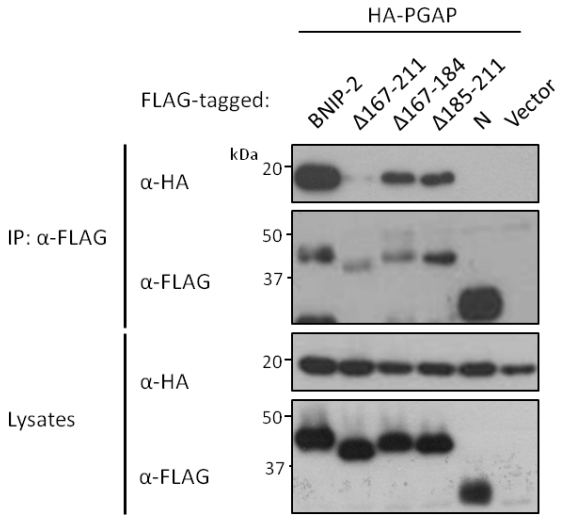
HA-PGAP
FLAG-tagged:
BNIP-2
Δ167-211
Δ167-184
Δ185-211
N
Vector
kDa
IP: α-FLAG
α-HA
α-FLAG
Lysates
α-HA
α-FLAG
20
50
37
20
50
37

Figure S2 Residues 167-211 within BNIP-2 BCH domain mediate interactions with BPGAP1 BCH domain and PGAP module. (a) Schematic diagram of BNIP-2 and its deletion mutants. Binding abilities of BNIP-2 BCH domain deletion mutants to BPGAP1 BCH domain and PGAP module were summarized and as indicated by the positive (+) or negative (-) sign. (b) HA-BCH domain (BPGAP1) or (c) PGAP region of BPGAP1, along with each of the FLAG-tagged BNIP-2 deletion mutants, were introduced into 293T cells as indicated before subjecting the harvested lysates to immunoprecipitation with anti-FLAG M2 beads. Co-transfection of HA-tagged BCH (BPGAP1) or PGAP module with FLAG-tagged full length BNIP-2, N terminal or expression vector was used as controls. To detect the associated proteins, immunoprecipitated lysates were separated on SDS-PAGE, blotted and probed with anti-HA (first panel), before stripping and re-probing with anti-FLAG antibodies (second panel). WCL were also analyzed by Western blot to verify the presence of the proteins introduced (third and fourth panel).

a

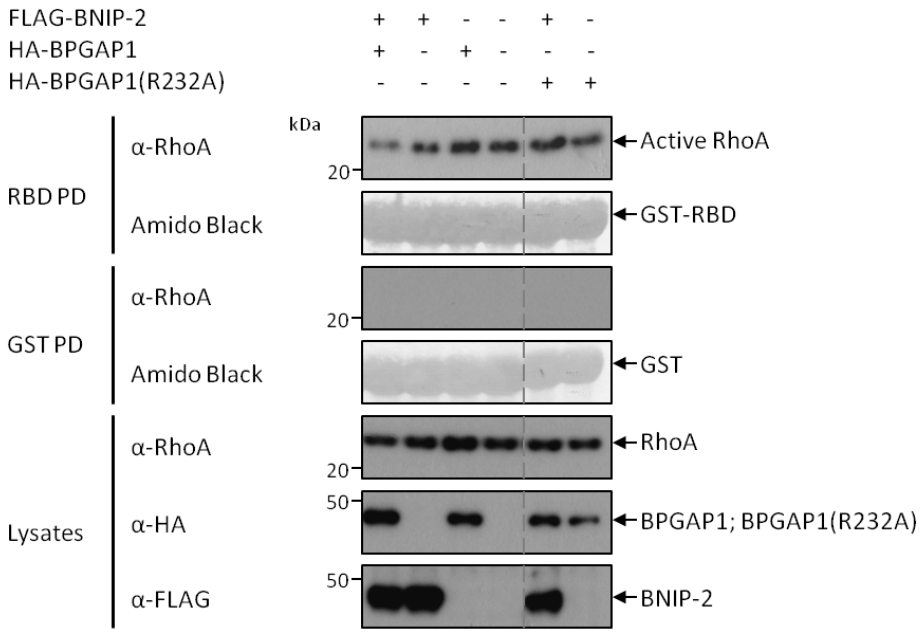

b

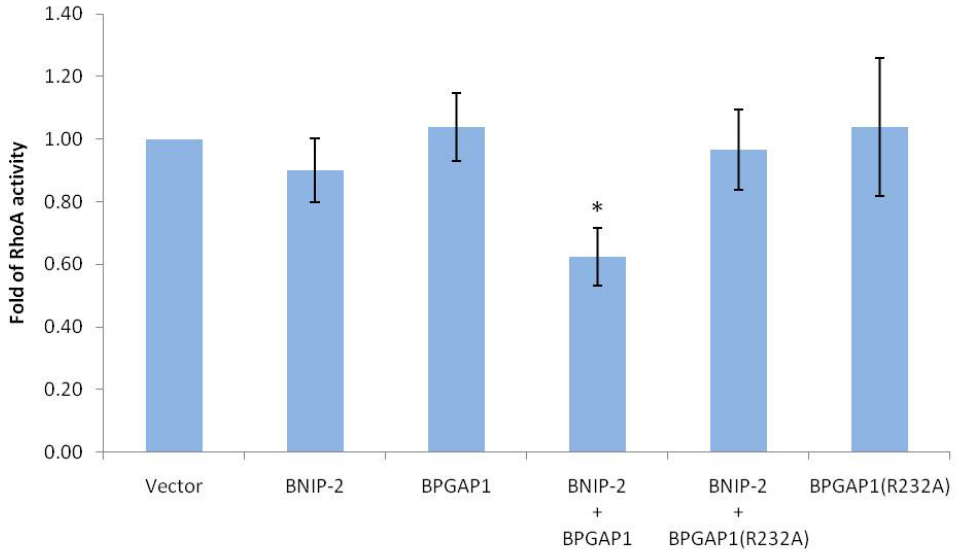

Figure S3 RhoA activity assay for endogenous active RhoA level in CHO cells. (a) To assay the endogenous active RhoA level, FLAG-BNIP-2, HA-tagged BPGAP1 or BPGAP1(R232A) were expressed alone or co-expressed as indicated in CHO cells. An equivalent amount of correspondingly tagged expression vector control denoted by the – sign was transfected to maintain a constant amount of DNA introduced into the cells. After 20-24 hours, the lysates were collected and incubated with either GST fusion of Rho-binding domain of Rhotekin immobilized on glutathione sepharose beads or with GST proteins as controls. Subsequently, active RhoA proteins captured on GST-RBD beads and WCL were resolved on SDS-PAGE, blotted and probed with anti-RhoA antibody to detect the amount of bound RhoA protein (first panel) and endogenous level of total RhoA protein (fifth panel). Similarly, protein expression of HA-tagged BPGAP1, BPGAP1(R232A) and FLAG-BNIP-2 were verified by Western blot analyses of the WCL using anti-HA (sixth panel) or anti-FLAG antibodies (bottom panel). Equal loading of GST fusion proteins and GST proteins were shown using amido black staining in the second and fourth panel, respectively. Blots separated by the dotted line are from the same blot with same exposure time. PD: Pull-down. (b) For quantitative analysis, amount of active RhoA captured by GST-RBD beads was normalized to the total level of endogenous RhoA proteins in the cell lysates and represented as fold of active RhoA relative to the vector-expressing control cells (set as 1), as described in *Materials and Methods*. Data derived from three or more independent sets of experiment are expressed as mean $\pm$ standard error mean and the asterisk indicates differences between values that are statistically significant at $p < 0.05$, measured by two-tailed Student's t-test with unequal variance.